Plasma Polymerization

Mitchel Shen and
Alexis T. Bell, EDITORS
University of California, Berkeley

Based on a symposium
sponsored by the
ACS Division of Polymer Chemistry
at the 176th Meeting of the
American Chemical Society,
Miami Beach, Florida,
September 15–16, 1978.

ACS SYMPOSIUM SERIES 108

AMERICAN CHEMICAL SOCIETY
WASHINGTON, D. C. 1979

Library of Congress CIP Data

Symposium on Plasma Polymerization, Miami Beach, Fla., 1978.
Plasma polymerization.
(ACS symposium series; 108 ISSN 0097-6156)

Includes bibliographies and index.

1. Polymers and polymerization—Congresses. 2. Plasma chemistry—Congresses.
I. Shen, Mitchel C., 1938– . II. Bell, Alexis T., 1942– . III. American Chemical Society. Division of Polymer Chemistry. IV. Title. V. Series: American Chemical Society. ACS symposium series; 108.

QD380.S938 1978 547'.84 79–15252
ISBN 0-8412-0510-8 ACSMC8 108 1-344 1979

ACS Symposium Series

M. Joan Comstock, *Series Editor*

Advisory Board

In Plasma Polymerization; Shen, M., et al.;
ACS Symposium Series; American Chemical Society: Washington, DC, 1979.

FOREWORD

The ACS SYMPOSIUM SERIES was founded in 1974 to provide a medium for publishing symposia quickly in book form. The format of the Series parallels that of the continuing ADVANCES IN CHEMISTRY SERIES except that in order to save time the papers are not typeset but are reproduced as they are submitted by the authors in camera-ready form. Papers are reviewed under the supervision of the Editors with the assistance of the Series Advisory Board and are selected to maintain the integrity of the symposia; however, verbatim reproductions of previously published papers are not accepted. Both reviews and reports of research are acceptable since symposia may embrace both types of presentation.

In Plasma Polymerization; Shen, M., et al.;
ACS Symposium Series; American Chemical Society: Washington, DC, 1979.

PREFACE

Although the formation of high-molecular-weight materials through the use of ionized gaseous plasma has been known for many years, the detailed mechanism of the process is still not fully understood. It is obviously quite different from conventional polymerization since for plasma polymerization monomers need not contain particular functional groups, and the polymers usually do not bear a simple stoichiometric relation to the starting monomers. For example, ethane can be plasma polymerized, but the resulting polymer has a chemical formula closer to C_2H_3. Plasma polymerization has been further classified into "plasma-state polymerization" and "plasma-induced polymerization." More recently, a hybrid type of polymerization using a plasma to initiate conventional polymerizations has been discovered. These diverse and interesting phenomena, as well as the properties and characteristics of the materials produced therefrom, are fully discussed in this Symposium.

The twenty chapters included in this volume can be conveniently divided into the following groups: review; plasma polymerization of hydrocarbons; plasma polymerization of fluorocarbons; plasma polymerization of organometallic systems; plasma-initiated polymerization; and applications of plasma polymerization. Though the emphasis of this Symposium is on the fundamental aspects of plasma polymerization, we should not lose sight of the fact that it is the potential applications of this technique that has stimulated the efforts in basic research. Potential applications for plasma-polymerized films include membranes for reverse osmosis, protective coatings for optical components, and insulating layers for semiconductors.

We should like to take this opportunity to thank the contributors to this volume for their efforts, and the expert referees whose anonymity did not interfere with their conscientious and objective judgment in upholding the standards of scholarship.

MITCHEL SHEN
ALEXIS T. BELL

University of California
Berkeley, California
April 9, 1979

A Review of Recent Advances in Plasma Polymerization

MITCHEL SHEN and ALEXIS T. BELL

Department of Chemical Engineering, University of California, Berkeley, CA 94720

A plasma is a partially ionized gas composed of ions, electrons and neutral species. It is a state of matter that can be created by such diverse techniques as flames, electrical discharges, electron beams, lasers or nuclear fusion. The technique of most interest to plasma polymerization is the glow discharge, in which free electrons gain energy from an imposed electrical field, and subsequently loses it through collisions with neutral molecules in the gas. The transfer of energy to gas molecules leads to the formation of a host of chemically reactive species, some of which become precursors to the plasma polymerization reaction.

The plasma created by a glow discharge possesses average electron energies in the range of 1-10 ev and electron densitites of 10^9 - 10^{12}/c.c. In addition, the electron temperature (T_e) of the plasma is not equal to the gas temperature (T_{gas}) but has a T_e/T_{gas} ratio of 10 - 100. It is therefore possible for plasma polymerization to proceed at near ambient temperatures in the presence of electrons to rupture covalent bonds in the gas molecules. Thus plasmas produced by the glow discharge are called non-equilibrium plasmas, in contradistinction to equilibrium plasmas created by arcs or plasma jets where $T_e = T_{gas}$. The very high temperatures in these plasmas (in thousands of degrees Kelvin) render them unsuitable for plasma polymerizations, since polymers produced under these conditions will be rapidly degraded.

Since de Wilde (1) and Thenard (2) first reported the formation of solid products in a plasma of organic vapor more than a centrury ago, many workers in the field of plasma organic chemistry have observed the presence of high molecular weight materials as reaction by-products. These materials adhered tightly

0-8412-0510-8/79/47-108-001$08.25/0

to the walls of reaction vessels, and were insoluble in most solvents. They were considered a nuisance until Goodman (3) demonstrated that a 1 mm thick plasma polymerized styrene film deposited on titanium foil made a satisfactory dielectric for a nuclear battery. Since that time plasma-derived polymers have been suggested for numerous applications because of their unique physical properties, ease of preparation, and propensity for the formation of thin pinhole-free films.

A wide variety of organic and organometllic compounds can be polymerized to form a thin film on a substrate placed in a glow discharge. Although the rate at which a monomer will polymerize depends on a large number of parameters, one of the most unique features of plasma polymerization is that monomers need not possess such reactive functional groups as double bonds to be polymerizable. For instance, ethane and benzene have been readily polymerized in the plasma. Furthermore, polymers have also been prepared from inorganic starting materials. Hollahan and McKeever (4) reported that polymers were formed in an electrodeless discharge sustained in mixtures of CO, H_2, and N_2. The structure of those materials was found to resemble that of proteins.

The purpose of this paper is to discuss some of the recent advances in our understanding of the kinetics and mechanism of plasma polymerization, the structure and properties of plasma polymers and some of their potential applications. It is not intended to be exhaustive, as earlier reviews (5-10) are already available. Interested readers are referred to the literature cited for further details.

Kinetics

The rate of plasma polymerization depends on the nature of the monomer gas. In addition, such parameters as flow rate, pressure, power, frequency, electrode gap and reactor configuration also strongly influence the polymerization rate for a given monomer. Generally at low flow rates there is an abundance of reactive species so the polymerization rate is limited only by the availability of monomer supply. At high flow rates, however, there is an overabundance of monomer concentration and the polymerization rate now depends on the residence time. At intermediate flow rates these two competing processes result in a maximum. This behavior is illustrated in Figure 1 for ethane, ethylene, and acetylene (11). These data also demonstrate the effect of increased unsaturation in

In Plasma Polymerization; Shen, M., et al.;
ACS Symposium Series; American Chemical Society: Washington, DC, 1979.

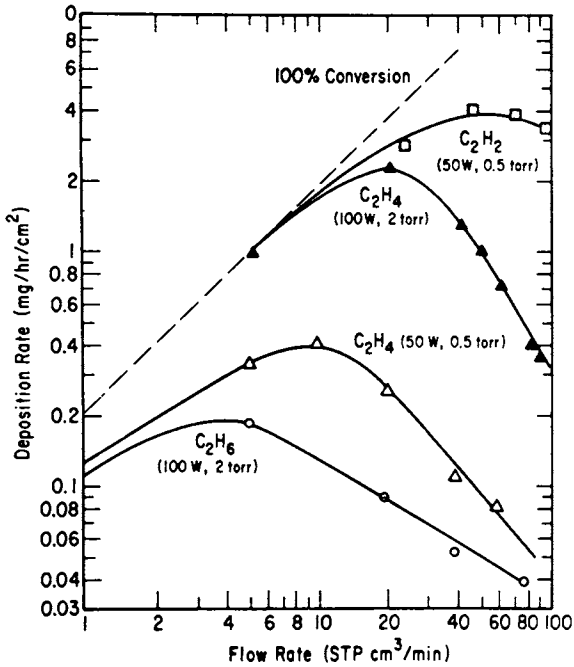

Figure 1. Rates of plasma polymerization of acetylene, ethylene, and ethane as a function of monomer flow rate (11)

In Plasma Polymerization; Shen, M., et al.;
ACS Symposium Series; American Chemical Society: Washington, DC, 1979.

monomers on the polymerization rate. At comparable reaction conditions, acetylene with a triple bond polymerizes an order of magnitude faster than ethylene which has a double bond; while ethylene in turn is much more reactive than the saturated ethane.

The polymerization rates for three olefinic hydrocarbons (11) are shown in Figure 2. Isobutylene is seen to polymerize more slowly than propylene, while ethylene polymerizes faster than either isobutylene or propylene by an order of magnitude. These data indicate that in a given homologous series of hydrocarbons, higher polymerization rates are favored by lower molecular weights. Figure 3 compares three monomers containing four carbon atoms. Here butadiene with two double bonds polymerizes substantially faster than either cis-2-butene or isobutylene with one double bond (11).

Yasuda (12) surveyed 28 monomers and found that monomers containing aromatic groups, nitrogen (e.g., -NH, $-NH_2$, -CN), silicon and olefinic double bonds are more polymerizable while those containing oxygen (e.g. -C=O,-O-,-OH), chlorine, aliphatic hydrocarbon and cyclic hydrocarbons tend to decompose. Brown (13) reported in his studies of a series of vinyl halides that the dihaloethylenes polymerize more rapidly than the corresponding monohalides and that chlorides and bromides polymerize more rapidly than the fluorides. Kobayashi, et. al. (14) found that the additons of certain halogenated compounds to hydrocarbon monomer streams often dramatically increases the polymerization rate. Thus, these halogenated compounds may be considered to act as gas phase catalysts for the plasma polymerization of hydrocarbons.

The rate of plasma polymerization generally increases with increasing power, until at high power densities when it becomes nearly independent of power. This is illustrated in Figure 4 for tetrafluoroethylene (14). The interelectrode gap also exerts a similar effect. Figure 5 shows that as the gap is narrowed (higher electron density) the rate increases. For small electrode gaps there is significant powder formation, which is typical of the product formed at high polymerization rates (15). The effect of increased pressure is to decrease the rate of polymerization (15,16) as shown in Figure 6 for styrene (16). The kinetics of plasma polymerization is often affected by the reactor configuration (9,17,18). Kobayashi, et. al. (17) showed that under otherwise identical conditions, the polymerization rates of ethylene are not the same for those using tubular type and bell-jar type reactors.

In Plasma Polymerization; Shen, M., et al.;
ACS Symposium Series; American Chemical Society: Washington, DC, 1979.

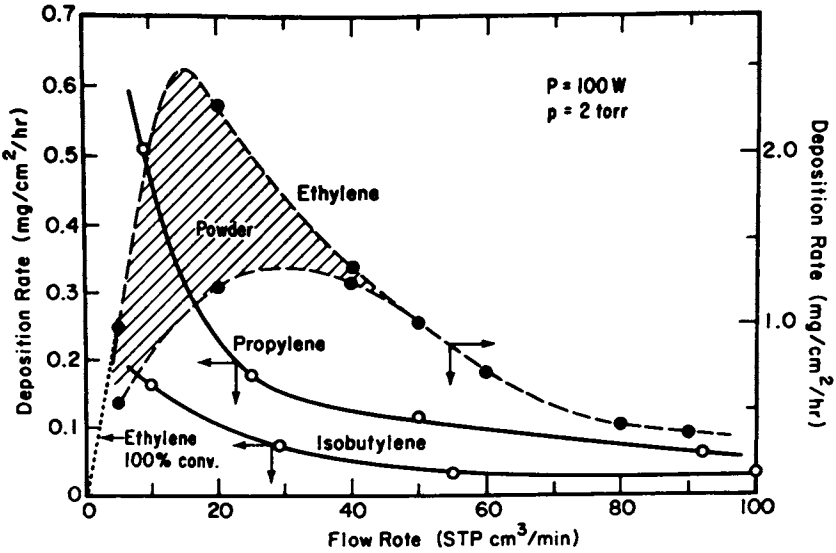

Figure 2. Rates of plasma polymerization of ethylene, propylene, and isobutylene as a function of monomer flow rate (11)

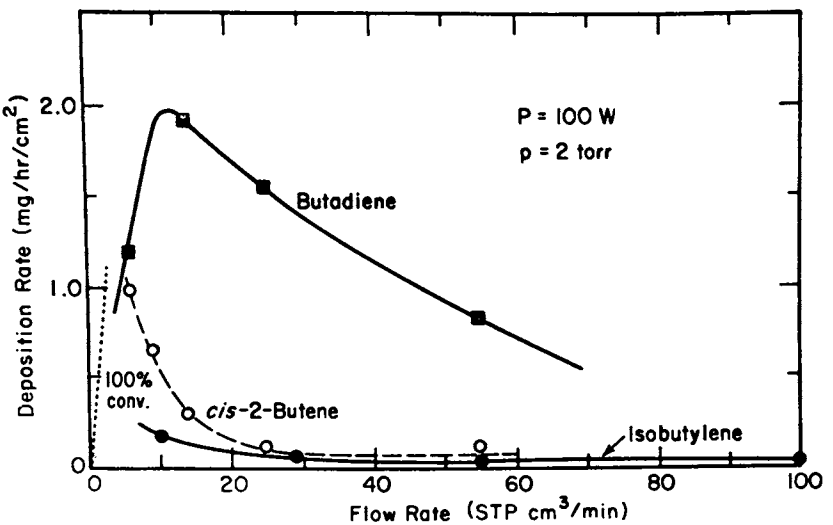

Figure 3. Rates of plasma polymerization of butadiene, cis-2-isobutylene, and isobutylene as a function of monomer flow rate (11)

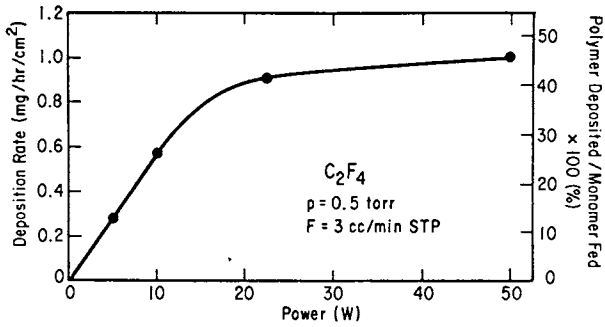

Journal of Macromolecular Science, Chemistry

Figure 4. The rate of plasma polymerization of tetrafluoroethylene as a function of power (14)

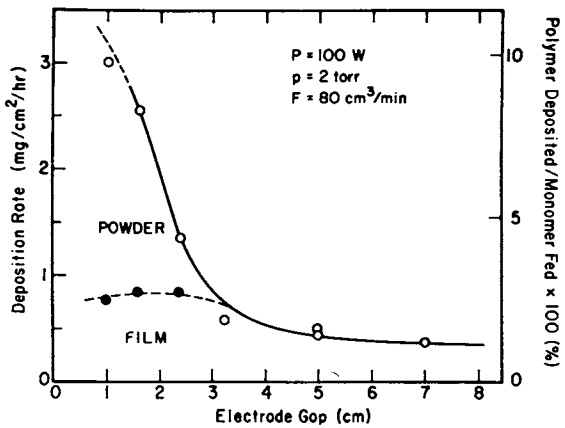

Journal of Macromolecular Science, Chemistry

Figure 5. The rate of plasma polymerization of ethylene as a function of electrode gap (15)

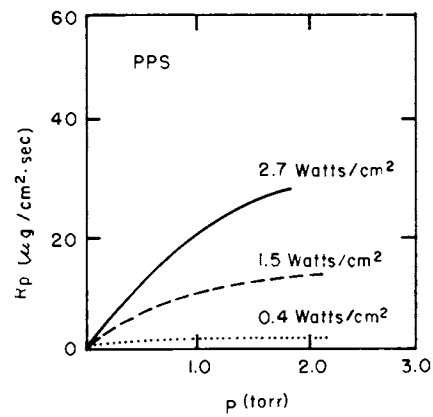

Figure 6. Rates of plasma polymerization of styrene as a function of pressure for various power inputs (16)

In addition, the use of electrodless glow discharge will produce different results than those with internal electrodes. In the former case, rare gases such as He, Ar was introduced from one end of the tubular reactor and the plasma was sustained by a rf coil outside the reactor. Gaseous monomer was fed into the afterglow of a rare gas and polymer film deposited on the substrate placed downstream. Yasuda, et. al. (18) observed that the deposition rate in electrodeless discharge was independent of the power input and increased in proportional to the square of the monomer pressure.

Plasma polymerization can be carried out in either dc or ac discharge at various frequencies. In a dc discharge, the movement of the larger positive ions is much slower than that of the electrons, consequently a concentration of charge is built up in front of the anode which opposes the applied field and thereby inhibits excitation. It has been found (8), however, that the reproducibility of films deposited from dc glow discharge is generally poor, and there is often the danger of contamination of the polymer from sputtering. Thus, dc discharges are not frequently used. In an ac glow discharge, the field is reversed periodically. These space charges are dissipated at each half cycle to promote chemical reaction. At lower frequencies this effect is significant. Morita, et. al. (19) has found that the rate of polymerization increases with increasing frequency up to about 5 kHz (Figure 7). Below this frequency surface-free radicals are generated by the impact of energetic ions accelerated through the cathode fall. Gas phase free radicals are concentrated near the cathode dark space because of the higher field strength, and the radical concentration will increase with increasing frequency. This accounts for the observed polymerization rate increase. Above 5 KHz, however, the inertial effects of the ions prevent them from reaching the electrodes. The immobilization of the ionic species leads to a decrease in the polymerization rate (13,19,20).

As the frequency now is increased above 50 kHz, there is another increase in polymerization rate. Here the excess space charge near the electrodes may have recombined with the opposite charges on the electrodes at increased rates with increasing frequency. This increase leads to a second maximum in polymerization rate at 0.6 MHz, above which there is a precipitous drop by nearly an order of magnitude until it levels off around 6 MHz (19,21). The low polymerization rate in the megahertz region is most likely due to the immobilization of electrons between the

In Plasma Polymerization; Shen, M., et al.;
ACS Symposium Series; American Chemical Society: Washington, DC, 1979.

electrodes as a consequence of their inertial effects. In this region the polymerization proceeds mainly via free radicals diffused from the plasma to the electrodes, or by ion-electron pairs through ambipolar diffusion or vacuum ultraviolet radiation from the plasma.

The effect of pulsed discharges on the rate of plasma polymerization at a fixed excitation frequency has been investigated for in-electrode (22) as well as electrodeless discharges (23). Generally, it was found that the rate of polymerization is lower for reactions carried out in pulsed discharges in comparison with continuous-wave discharges under similar plasma conditions. Some exceptions to this trend were noted by Yasuda and Hsu (23), notably for monomers of acrylic acid and tetrafluoroethylene (Table 1). Although the pulsed discharge technique is reminiscent of the rotating sector method in photopolymerization (24) for the determination of absolute rate constants, the theoretical treatment developed for the latter cannot be applied to the pulsed plasma polymerization because of the essential differences in mechanisms of polymerization.

Mechanism

Since ions, free radicals, electrons as well as excited molecules are present in a plasma, it is important to identify the dominant species that control the mechanism of plasma polymerization. Westwood (25) first suggested that positive ions from the plasma cause the polymerization reaction to occur. The suggestion is based on the observation of plasma polymerization in d.c. discharge in which the polymer is deposited almost exclusively on the cathode (26). This fact implies that direct bombardment of electrodes by electrons have no significant role but rather that positive ions figure prominantly in the production of polymer. Thompson and Mayhan (27,28) later also support a cationic mechanism based on the result of a series of free-radical scavenger and ion deflection experiments. More recently, Smolinsky and Vasile (28,30) carried out a series of experiments in direct sampling of ionic and neutral species from rf discharges of organic and organometallic vapors, and concluded that highly unsaturated ions play a predominant role.

Denaro, et. al. (16) on the other hand, favored a free radical mechanism, based on the observation that significant amount of free radicals are trapped in

In Plasma Polymerization; Shen, M., et al.;
ACS Symposium Series; American Chemical Society: Washington, DC, 1979.

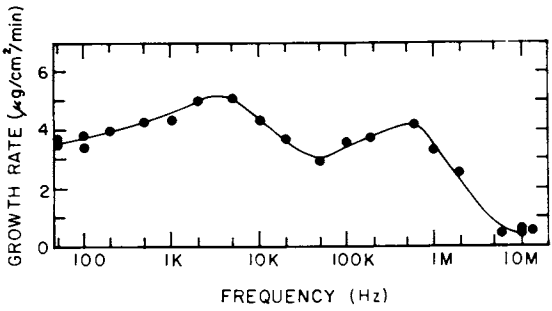

Figure 7. The rate of plasma polymerization of ethane as a function of discharge frequency (19)

Table 1. Rate of Plasma Polymerization of Various Monomers in Continuous Wave and the Pulsed R.F. Discharges (23)

	Deposition Rate x 10^8 ($g/cm^2 \cdot min$)			
Monomer	Continuous	Pulsed	Change*	
Acetylene	31	24	-7	(-23%)
Benzene	110	101	-9	(-8%)
Hexafluorobenzene	190	149	-41	(-22%)
Styrene	173	145	-28	(-16%)
Ethylene	42	43	+1	(+2%)
Tetrafluoroethylene	18	37	+19	(+110%)
Cyclohexane	92	9	-83	(-90%)
Ethylene oxide	15	14	-1	(-7%)
Acrylic Acid	28	61	+33	(+120%)
Propionic Acid	7	15	+8	(+110%)
Vinyl Acetate	31	16	-15	(-48%)
Methylacrylate	32	33	+1	(+3%)
Hexamethyldisilane	251	65	-186	(-74%)
Tetramethyldisiloxane	191	102	-89	(-47%)
Hexamethyldisiloxane	233	43	-190	(-82%)
Divinyltetramethyl-disiloxane	641	277	-364	(-57%)

*Based on values of continuous wave discharge.

the film. The presence of large concentrations of free radicals has also been detected by e.s.r. technique (15,31,32). Although no experimental data are available for organic plasmas, it has been shown that in inorganic systems free radicals are present to the extent of 10^{-2} to 10^{-1} of the neutral species whereas ions are present to the extent of 10^{-6} to 10^{-5} of the neutrals (33). The observation is reasonable since the energy (34) required to form free radicals (3-4 eV) is considerably less than that required to form ions (9-13 eV). The former is in the range of the average electron energy in low pressure discharges, thus a substantially higher concentration of radicals than ions may be expected (35).

A number of workers have reported on kinetic models for plasma polymerization. Williams and Hayes (36) first suggested that the reaction occurred exclusively on solid surfaces within the reaction zone. Initially, monomer is adsorbed onto the electrode surface, where a portion is converted to free radical species after bombardment by ions and electrons produced in the plasma. Surface radicals then polymerize with adsorbed monomer to yield the thin film product. Based on this scheme, Denaro, et. al. derived a simple rate expression which showed reasonably good agreement with deposition rate data at various pressures and power levels (16). It is, however, unrealistic to assume that the plasma polymerization reactions occur exclusively on the surface. A more likely mechanism is that both gas phase and surface reactions proceed simultaneously in plasma polymer formation.

More recently, quantitative treatments of plasma polymerization kinetics have become available. Carchano (37) interpreted the results of organic vapor polymerization in a dc discharge using the surface polymerization mechanism. Assuming that initiation, reaction and termination occur only on the surface, he showed that the inverse of reaction rate is directly proportional to the inverse of system pressure provided that adsorbed monomer concentration is proportional to gas pressure. This relationship agrees well with his experimental data. However, this model is not valid at discharge frequencies above 10^{5} Hz, when active species will oscillate in the interelectrode space and lead to gas phase polymerization.

Morita, et. al. (38) suggested that the polymerization mechanism may be different at high and low frequencies. They believe that polymerization through radical intermediates is the predominant mechanism at discharge frequencies higher than a few MHz, but that

In Plasma Polymerization; Shen, M., et al.;
ACS Symposium Series; American Chemical Society: Washington, DC, 1979.

substrate reaction initiated by ionic species predominates at low discharge frequencies. Under low frequency conditions, they found that the film growth rate is directly proportional to the product of the number of monomer units polymerized per incident ion and the number of incident ions per unit area and unit time (N). The value of N is determined by the rate of transport of ions to the surface, which is controlled by ambipolar diffusion, recombination of charges in the ion sheath, and the effect of stray capacity (39).

Lam and coworkers (40) developed kinetic models in which initiation of monomer by electron impact is followed by propagation and termination. They showed that activation of monomer in the gas phase followed by propagation and termination on the electrode surface gave an excellent description of the plasma polymerization process. The predicted functional dependence of deposition rate on pressure (p) and current density (J) is $R \propto p^{1/2} J^{1/2}$.

Tibbitt, et. al. (41) wrote the following kinetic scheme for the plasma polymerization of hydrocarbons:

$$e + M_g \xrightarrow{k_i} 2R_g\cdot + e \qquad \text{(Initiation)}$$

$$S + R_{g_n}\cdot \xrightarrow{k_{pg}} R_{s_n}\cdot \qquad \text{(Radical Adsorption)}$$

$$R_{g_n}\cdot + M_g \xrightarrow{k_{pg}} R_{g_{n+1}}\cdot \qquad \text{(Homogeneous propagation)}$$

$$R_{s_n}\cdot + M_g \xrightarrow{k_{ps}} R_{s_{n+1}}\cdot \qquad \text{(Heterogeneous propagation)}$$

where e, M and R refer to electrons, monomers and radicals, and s and g designate substrate and gas respectively. The expression for the rate of plasma polymerization was written as:

$$r_p = \left(\frac{d}{2} k_{pg} + k_{ps} K_R\right) [M_g][R_g] \qquad (1)$$

where d is the space between the electrodes, and K_R is the adsorption coefficient of the radicals on the electrode surface:

$$[R_s] = K_R[R_g] \qquad (2)$$

To compute r_p, the concentrations of monomer and free radicals in the gas phase must be determined. Solution of the appropriate species conservation equations and substitution of the solutions into eq. 1 leads to:

$$r_p = [M_g]_o^2 \, 2ac[1-e^{-(a-b)\tau}]/(a-b)e^{(a+b)\tau}] \qquad (3)$$

where $a=k_i[e]$, $b=(2/d)k_a[S]$, $c=(d/2)k_i+k_{ps}$, and $\tau=V/Q$.

By adjusting the magnitudes of the rate coefficients appearing in the model, good agreement was obtained between polymerization rates predicted by the model and those measured experimentally for a variety of unsaturated monomers (Figure 8). The magnitudes of the fitted rate coefficients describing the initiation of polymerization and gas phase oligomerization were found to be in good quantitative agreement with independently observed rated coefficients.

Structure

Variations in the plasma parameters often produce significant changes in the structure and properties of the plasma polymerized materials. For a given monomer polymerized in a reactor at a fixed frequency, a "characteristic map" may be constructed (11,15,42). Figure 9 shows that for ethylene polymerized at a frequency of 13,56 MHz, both powder and film are formed at low pressure and low monomer flow rates (42). At high pressures and high flow rates, an oily product is produced. Only at low pressure and high flow rate can a solid, pinhole-free film be obtained. If the pressure in the reactor is high and the monomer flow rate is low, then the discharge becomes unstable. Figure 9 also shows that decreased power renders it possible to produce a film at lower flow rates. For conditions near the vicinity of the powder-film borderline, the films are not transparent because of the incorporation of very fine powder particles (43,44,45, 46). Upon further increase in flow rate, however, a transparent film can be formed indicating that pow-

In Plasma Polymerization; Shen, M., et al.;
ACS Symposium Series; American Chemical Society: Washington, DC, 1979.

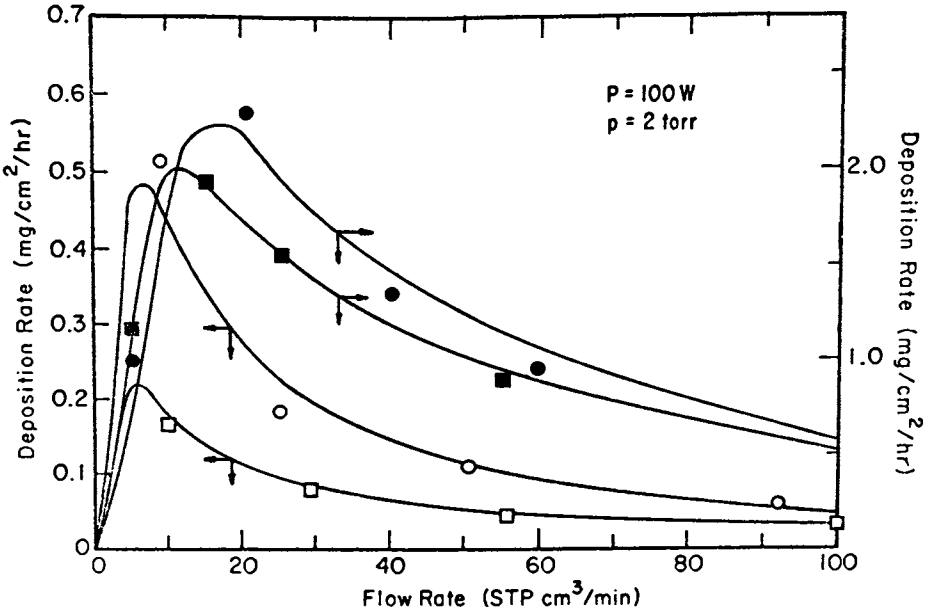

Figure 8. Computed and experimental rates of plasma polymerizations for olefins as a function of monomer flow rate (41). (●) Ethylene, (■) butadiene, (○) propylene, (□) isobutylene.

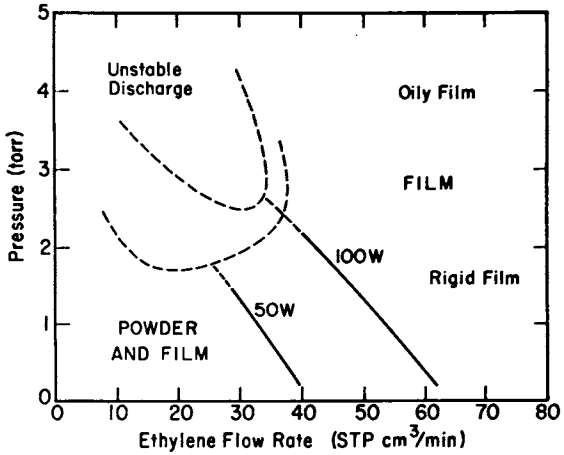

Journal of Macromolecular Science, Chemistry

Figure 9. Characteristic map for the plasma polymerization of ethylene (15)

ders trapped in the film must now be smaller than the wavelength of the visible light.

The formation of powder is attributed to the homogeneous reactions in the gaseous phase. Here the reactive species in the plasma polymerize faster than the rate of diffusion of these species to the substrate. As a consequence macroscopic particles are formed while suspended in the gaseous phase until gravitational force eventually causes the powder to precipitate onto the substrate surface. We recall that acetylene undergoes plasma polymerization at a much higher rate than ethylene. Figure 10 shows in fact that for this monomer only powdery products are formed. On the other hand, ethane polymerizes slower than ethylene by an order of magnitude under comparable conditions (11). In this instance we note that the film formation region is much greater than those for powder and oil formation (Figure 11). Duval and Theoret (47) envision the growing chains to be initiated in the gas phase and subsequently deposited on the electrode surface as oligomers. They suggest that at high reaction pressure (>1 torr) there is sufficient monomer on the surface to dissolve the reactive chain and limit the degree of polymerization, thus explaining the formation of low molecular weight oily products at high reaction pressures. At low pressures, the surfaces are deficient in monomer and the reactive oligomers continue to grow yielding high molecular weight solid products. These authors used gel permeation chromatography to evaluate gross structural changes in polymer form resulting from changes in reaction pressure and power level. The molecular weight distributions obtained in this study indicate that higher molecular weight is favored by low pressure and high power, which was later verified by Kobayashi, et. al. (42). Duval and Theoret also found that at a given pressure and power level, polymer deposited on the electrode surface has a higher molecular weight than that formed on a substrate placed in the interelectrode gap.

The morphology of the plasma polymerized films has been examined by electron microscopy by a number of workers (43,44,45,46,48). Figure 12 shows the replica electron micrograph of plasma polymerized ethylene deposited on chromium substrate at several gas pressures (46). The presence of powder particles is clearly evidenced in Figures 12a-c. The size and density of the powdery products decrease with increasing pressure until at a pressure of 3 torr when the polymer is mainly film and contains very few particles.

In Plasma Polymerization; Shen, M., et al.;
ACS Symposium Series; American Chemical Society: Washington, DC, 1979.

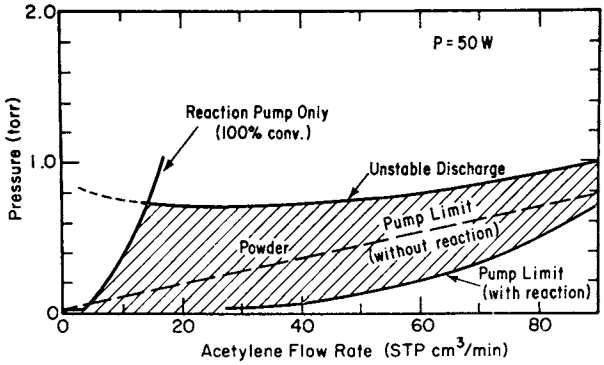

Figure 10. Characteristic map for the plasma polymerization of acetylene (11)

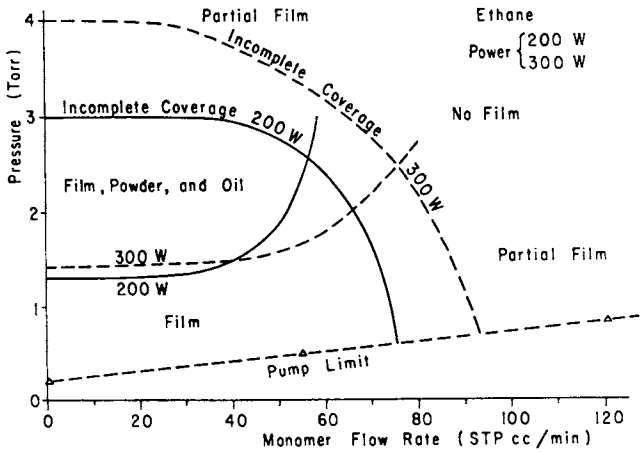

Figure 11. Characteristic map for the plasma polymerization of ethane (102)

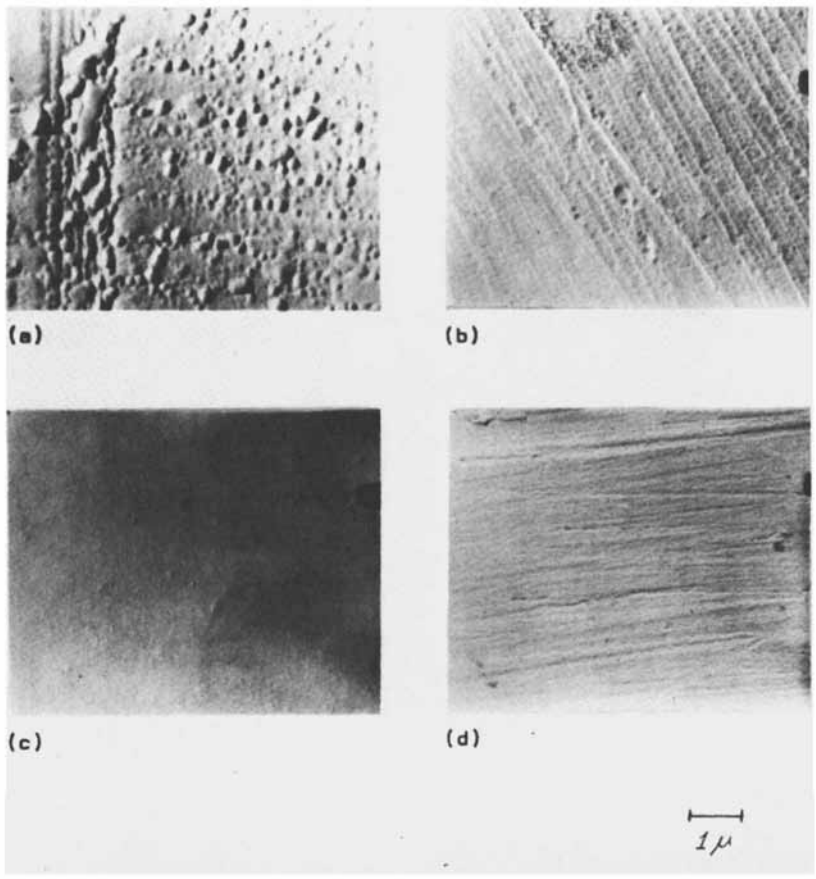

Figure 12. Transmission electron micrographs of plasma-polymerized ethylene on chromium substrate at 80 mL/min, 100 W, and (a) 0.7 torr, (b) 1.5 torr, (c) 3 torr, and (d) substrate alone (46)

The effect of monomer flow rate on the film appearance is similar. At low flow rates (high polymerization rate), particles are buried inside the film. As the flow rate is increased, both the size and the density of the particles decrease to yield a smoother film.

Figures 13 and 14 compare the surface structures of the plasma polymerized ethylene on Teflon, and cleaved mica (46). Because of the rougher initial surface on Teflon, there is a greater concentration of powder on that surface. The mica surface is smooth before polymer deposition. The polymer films are also very smooth and featureless, indicating the strong dependence of morphology of plasma polymerized films on the surface roughness of the substrates.

Plasma polymerized films are thin (from hundreds of angstroms to several microns) and pinhole-free. The absence of pinholes was determined by Lee and co-workers (49,50) using hydrogen gas evolution and electrophoretic decoration techniques. X-ray diffraction studies show the complete absence of crystallinity (42). Both films and powders are insoluble in convential organic solvents, indicating the highly cross-linked nature of the polymer. Oily products, on the other hand, are completely soluble. These are generally branched oligomers. Gel permeation chromatography (27) and vapor phase osmometry (15) determinations show that the molecular weights of the oils are of the order of a few thousand grams per mole. The chemical composition of the polymer generally bear no simple relation to that of the starting monomer. For instance, the carbon to hydrogen ratio is about 2/3 for plasma polymerized ethylene, in contradistinction to that of the conventional polyethylene which is 1/2(15,42,51,52). However, the stoichiometric ratio of the polymer may vary with the condition under which the polymerization reaction was carried out (15).

Differential scanning calorimetry and thermal gravimetric analysis have been used by several authors (27,53) to show that plasma-derived polymers have no phase transitions until decomposition occurs. The remarkable thermal stability of these materials is evidenced by data which show that 80 wt.% of a film prepared from methyl chloride remains at 800°C and that 40 wt.% of a styrene derived film remains at 700°C.

Infrared spectroscopy has been extensively used in elucidating the microstructure of plasma-polymerized materials. Earlier works (54,55) have shown that short alkane segments and various types of vinyl groups are the predominant structural groups observed.

In Plasma Polymerization; Shen, M., et al.;
ACS Symposium Series; American Chemical Society: Washington, DC, 1979.

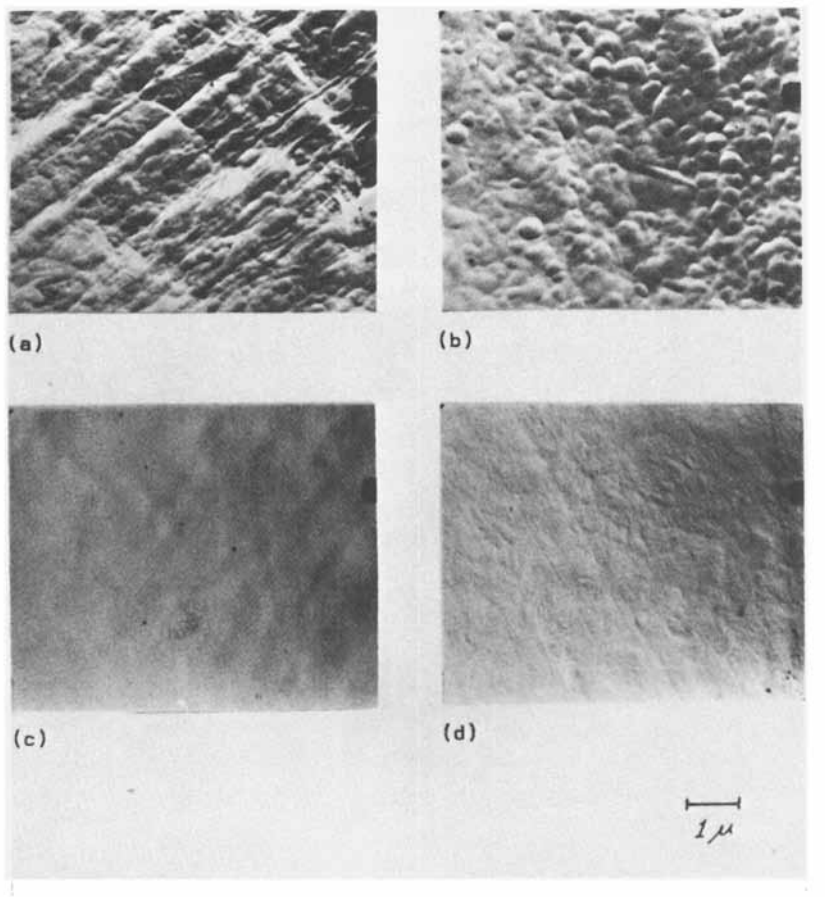

Figure 13. Transmission electron micrographs of plasma-polymerized ethylene on Teflon substrate. Polymerization conditions are the same as in Figure 12 (46).

In Plasma Polymerization; Shen, M., et al.;
ACS Symposium Series; American Chemical Society: Washington, DC, 1979.

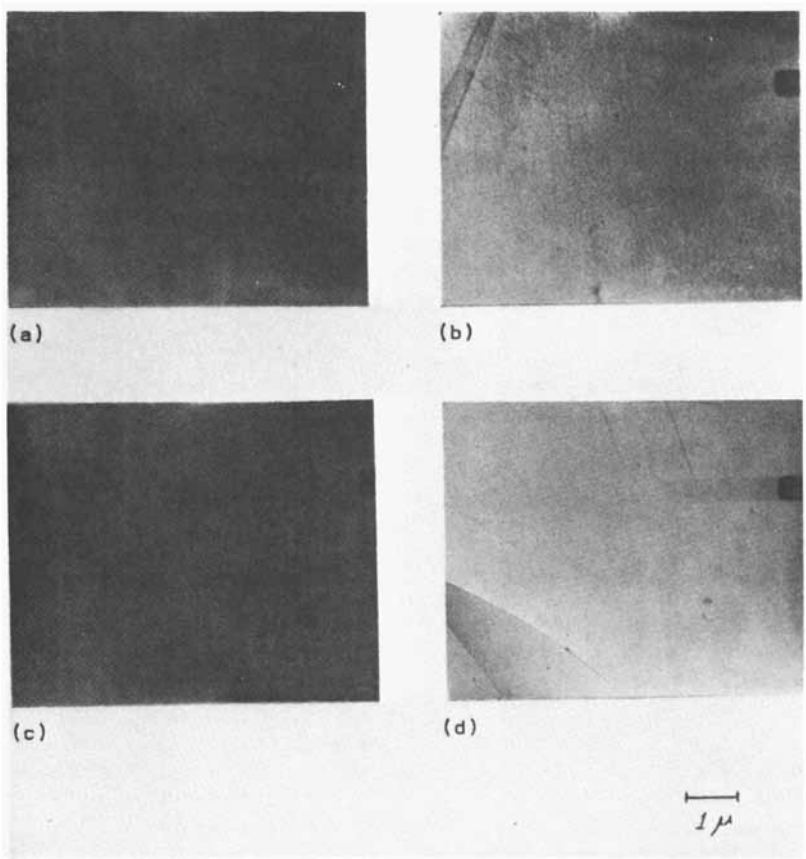

Figure 14. Transmission electron micrographs of plasma-polymerized ethylene on cleaved mica. Polymerization conditions are the same as in Figure 12 (46).

There is no evidence of long alkane segments in the products. These data support the hypothesis that plasma-derived polymers have a mesh structure, with only short chain segments between branch and crosslink points. This structural description has also been supported by NMR (56) and mass spectral (27,38) studies.

More recently Tibbitt, Bell and Shen (56,57) carried out quantitative determinations of the structure of plasma polymerized hydrocarbons by infrared spectroscopy. Typical spectra of films deposited on sodium chloride substrates are shown in Figure 15. Absorptions peaks were identified to be associated with various group frequencies, corroborated with the findings from NMR spectra of dilute solutins of the oily products. From the knowledge of the extinction coefficients, concentrations of the functional groups in the plasma polymerized materials were determined. A postulated molecular model for the plasma polymerized ethylene is shown in Figure 16 (56). The polymer does not contain regular repeating units of methylene groups, as in conventional polyethylene. Rather it has numerous unsaturated groups, aromatic groups, and side branches. In addition, the polymer is very highly crosslinked, with about one crosslink per six to ten chain carbon atoms. These structural units combine to render the final polymer uncrystallizable. Not included in the postulated structure are the tetrafunctional crosslinks, which are no doubt present, because these groups are not amenable to detection by the infrared technique.

Pyrolysis/gas chromatography (P/GC) has been used also to investigate the structure of the plasma polymerized materials (58,59). Figure 17 shows a comparison of the P/GC pyrograms of plasma polymerized ethylene (PPE) and conventional polyethylene (PE). It is seen that the methane (C_1) peak is very pronounced for PPE but appears only as a shoulder in the pyrogram of conventional PE. The implication is that PPE is highly branched and crosslinked compared to PE. The isoalkanes/n-alkanes ratio is lower for PE, but is rather high for PPE, indicating the irregularity of structure in the latter material. Table 2 gives the sums of the heights of all isoalkane peaks and the "7F peak," the P/GC data for plasma polymerized ethylene, butadiene and benzene. The 7F peak is characteristic of aromatic fragments in the structure, while the isoalkane content is related to the concentration of tertiary carbons. Also included in the table are the functional group concentrations of tertiary carbon atoms and phenyl groups as well as the crosslink densities

In Plasma Polymerization; Shen, M., et al.;
ACS Symposium Series; American Chemical Society: Washington, DC, 1979.

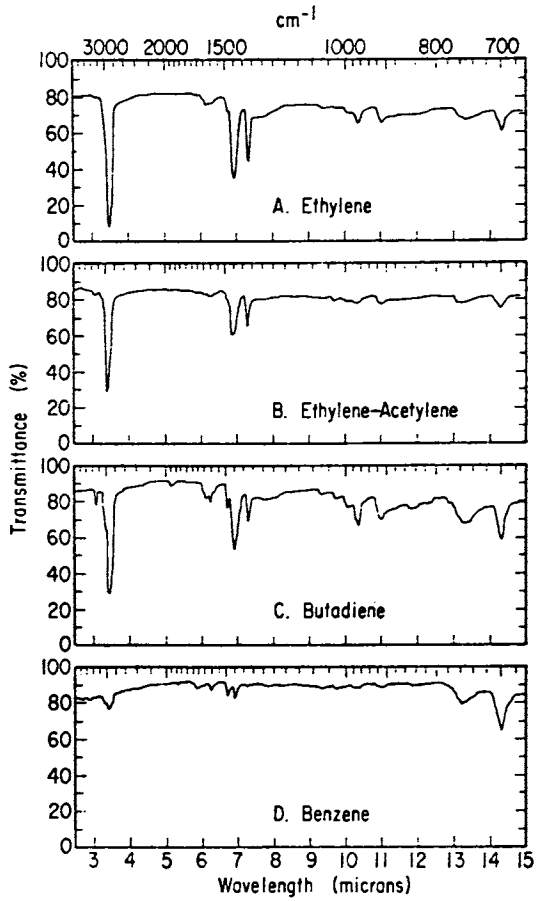

Journal of Macromolecular Science, Chemistry

Figure 15. IR spectra of plasma-polymerized films on sodium chloride substrate (56).

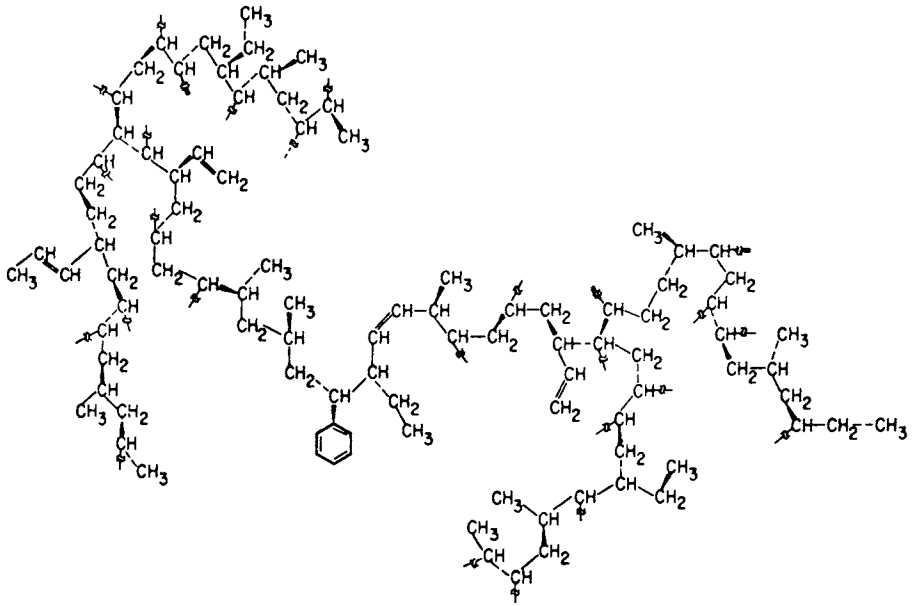

Figure 16. Postulated model of plasma-polymerized ethylene film (56)

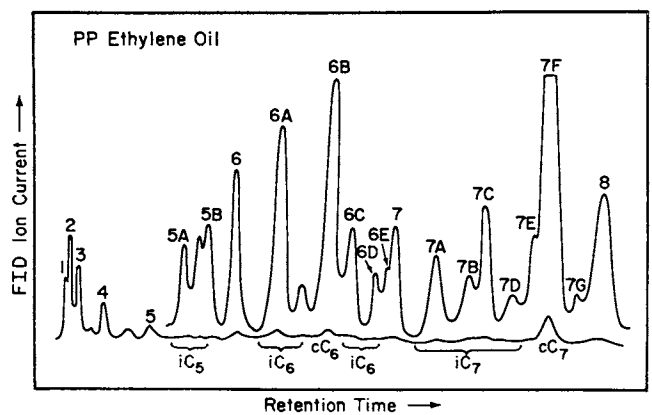

Figure 17. Pyrolysis/gas chromatography pyrogram of plasma-polymerized ethylene oil (59)

determined from infrared spectra (56,57). There is qualitative agreement between the data determined by these two techniques, thus reinforcing the postulated structure of the plasma polymerized hydrocarbons.

Electron spectroscopy (ESCA) has been found to be particularly useful for the structural analysis of plasma polymerized film surfaces. Most of the applications are directed to fluorocarbon polymers because of the large chemical shifts in the binding energies of C(1s) electrons caused by fluorines bonded to carbon. As a result CF_3, CF_2, CF and tetrafunctional carbons can be distinguished (60,61,62,63,64). Knowing the relative electron line positions of the various groups, the C(1s) spectra can be deconvoluted and the group concentrations determined. The application of ESCA is not limited to plasma polymers containing fluorine atoms. Oxygen and nitrogen containing polymers have also been successfully analyzed (60,65,66).

Another important characteristic of plasma-polymerized films is the existence of trapped free radicals. These active sites are probably formed both through incorporation of free radicals from the gas phase and by the impingement of active plasma species and radiation onto the depositing film. Due to the highly crosslinked structure, trapped radicals have low mobility and do not recombine rapidly. Upon exposure to the atmosphere, these trapped radicals react with oxygen and infrared measurements (42,67) demonstrate that carbonyl and hydroxyl groups are formed in the polymer. Denaro (16) has shown by titration of plasma-polymerized styrene with DPPH that one in twenty polymer molecules is a radical. Electron spin resonance spectroscopy has been used to determine the spin densities in plasma polymerized materials (15, 31,32). These radicals were found to possess a long half-life, and has been known to be responsible for polymerization to continue after the plasma has been turned off. The reduction of radical concentration can be achieved either by the use of lower power, or by pulsed plasma (23) as shown in Figure 18.

Properties

There has been a great deal of interest in the study of the electrical properties of plasma polymerized films. Early data on the dielectric and conductivity of the films has been reviewed by Mearns (8). More recently, the dielectric properties of plasma polymerized styrene (69-71), acrylonitrile (72), hexamethyldisiloxane (73-75), tetrafluoroethylene

In Plasma Polymerization; Shen, M., et al.;
ACS Symposium Series; American Chemical Society: Washington, DC, 1979.

Table 2. Functional Group Characterizations of Plasma-Polymerized Products Deduced from IR Spectroscopy, NMR and P/GC

Monomer	Functional Group Concentration (mole/gm polym) $[R_3CH]$	$[\phi]$	Apparent Crosslink Density backbone carbons / crosslink	Isoalkane Relative Peak Height (% of C_2 Peak Height)	7F Relative Peak Height (% of C_2 Peak Height)
Ethylene	18.0	0.39	6.4	82	10
Butadiene	12.0	1.2	9.6	66	20
Benzene	26.0	7.9	6.9	20	83

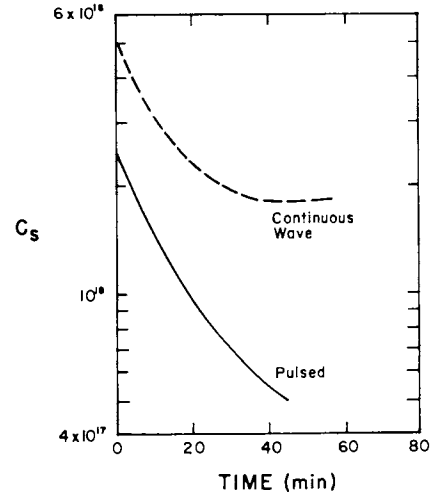

John Wiley and Sons

Figure 18. Electron spin concentrations of plasma-polymerized hexamethyldisilane as a function of time after removal from plasma (23)

and hydrocarbons (76) have been reported. Sawa, et.al. (70,71) noted two major peaks in the dielectric loss spectra of plasma polymerized styrene, a low temperature relaxation which is ascribed to the motion of short chain segments and a higher temperature process related to the motion of pendant phenyl groups. The authors observed a shift of the peak maxima to higher temperatures as the material was formed at lower pressures. They explained the peak temperature shift as a result of increased crosslinking at low reaction pressure.

Mann (73) and Tuzov, et. al. (74,75) studied the dielectric properties of plasma polymerized silicone films, and found that there is an increase in dielectric constant and loss tangent upon exposure to air. These workers attributed the changes to the absorption of the water vapor which increases the polarity of the films. Recently Tibbitt, et. al. (76) carried out parallel infrared measurements with dielectric experiments on plasma polymerized hydrocarbons and a fluorocarbon before and after significant oxidation has taken place. The dielectric spectra of plasma polymerized ethylene shows that the as-polymerized film shows little change in loss tangent as a function of temperature, except at higher temperatures where dc conductivity effects sets in (Figure 19). Upon oxidation in the atmosphere, however, there is a relaxation peak centered at -50°C (100 Hz), which is shifted to higher temperatures with increasing frequency (Activation energy is 13.8 kcal/mole). The peak is attributed to the local mode motion of several molecular segments. Oxidation of the trapped free radicals introduces carbonyl groups that act as "tracers" to render the molecular motion observable by dielectric experiments. The carbonyl concentrations determined by infrared spectroscopy are shown to bear a linear relationship with the strengths of dielectric loss (Figure 20).

The conductivity and capacitance of plasma polymerized films has also been reported by numerous workers (72,77-81). Morita, et. al. (81) found that the dc conduction current decreases when exposed to oxygen, and attributed the decrease to the disappearance of space charge on exposure to oxygen. Harai and Nakada (72) suggested that the dc conductivity effects of plasma polymerized acrylonitile can be adequately interpreted by the field assisted ionization of impurity levels first enunciated by Poole and Frenkel (82).

Recently Hetzler and Kay (8) studied the ac-

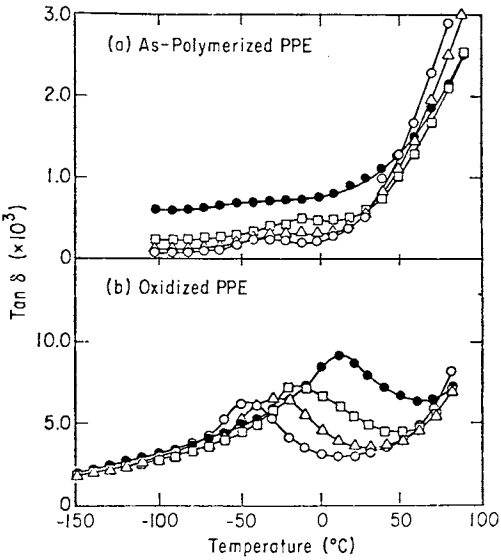

Journal of Macromolecular Science, Chemistry

Figure 19. Dielectric loss tangent as a function of temperature for plasma-polymerized ethylene at four frequencies (76). (○) 10^2Hz, (△) 10^3Hz, (□) 10^4Hz, (●) 10^5Hz.

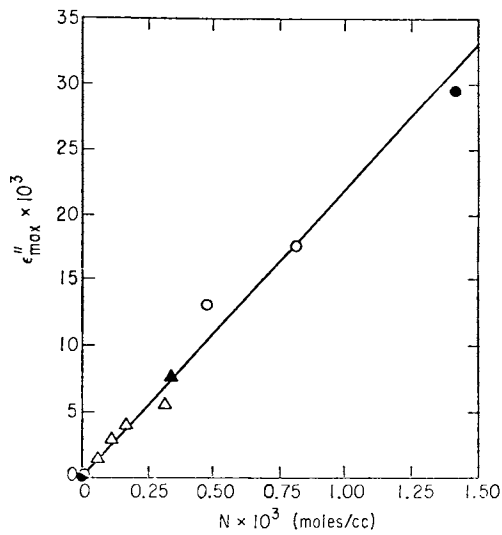

Journal of Macromolecular Science, Chemistry

Figure 20. Dielectric loss constant of plasma-polymerized (○) PPE, (△) PPEA, (●) PPEVC, (▲) PPTFE.

conductivity of plasma polymerized tetrafluoroethylene, and showed that at high requeencies and low temperatures the mechanism of hopping conductivity dominates, at low frequencies and high temperatures, a dipole orientation process is operative. On the basis of ir and esr measurements, these authors concluded that the carbonyl groups formed by oxidation are responsible for the observed effect.

Photoconductive properties of plasma polymerized films have been studied. Bradley and co-workers (77) observed negative short circuit current in the direction of illumination for several plasma polymerized films on aluminum electrode. Guastavino, et. al. (83) found positive short circuit current for plasma polymerized styrene (PPS) on gold electrodes. Morita, et. al. (84) showed that the photoconductive behavior of PPS depends on the nature of the electrodes. If both electrodes are gold, the photocurrent threshold energy is around 1.6 ev, and is attributable to the energy of hole generation in bulk with residual free radicals acting as acceptors. If the gold/aluminum electrodes are used, then the electron injection from aluminum is the more likely mechanism, with a barrier height of 2.6 ev.

Applications

For quite some time, the potential use of plasma polymerized thin films as membranes, coatings and as insulating layers in microelectronic components has generated much industrial interest. It is recognized though, that despite the significant research effort, few plasma polymerization processes have reached the stage of commercial development. Yet plasma polymers still generate a significant amount of application oriented research because of their unique physical properties and ease of preparation.

The application of plasma polymerized thin films as reverse osmosis membranes has received considerable attention. Yasuda and his co-workers (85-87) have demonstrated that reverse osmosis membranes prepared from nitrogen containing monomers can yield up to 98% salt rejection with a flux of 6.4 gallons/ft^2 day (85). More recent experiments indicate that membranes formed from a mixture of acetylene, carbon monoxide and water vapor exhibit reverse osmosis properties similar to the nitrogen containing materials, yet have the added advantage of being chlorine resistant (87). Reverse osmosis membranes prepared from allylamine by the plasma polymerization

In Plasma Polymerization; Shen, M., et al.;
ACS Symposium Series; American Chemical Society: Washington, DC, 1979.

process also gave excellent results (65,66,88,89).

Stancell et. al. (90) reported the possible use of ultrathin films deposited onto relatively permeable substrates as permselective membranes. Ultrathin and highly crosslinked coatings effectively distinguish between molecules of different sizes and increase the permselectivity of the substrate film. Chang et. al. (91) demonstrated that the permeability coefficient of silicone rubber to oxygen decreased noticeably after depositing a plasma-polymerized ethylene film on the surface. Colter, et. al. (92,93) found similar effects of plasma polymerized films as diffusion barriers in controlled-released drug delivery systems.

The use of plasma-polymerized films to protect or modify the surface of an existing material has also been explored. The deposition of protective coatings (94,95) for juice cans and steel panels have been investigated, but the necessity of operating batchwise in a vacuum has impeded the rapid implementation of such processes. Byrne and Brown (96) studied the treatment of various fabrics in a glow discharge of argon containing various vinyl monomers. They found that changes in soil release, water repellency, and dyeability, were accomplished in a very short time. The use of plasma grafting of synthetic polymers on wool for shrink-proofing has also been extensively investigated (97,98).

Plasma-polymerized materials can also be used for their unique optical properties. For example a laser lightguide film has been prepared by plasma-polymerization of hexamethyl disiloxane (99). An excellent lightguide must exhibit extremely low scattering losses. Films produced in a glow discharge are amorphous, smooth relative to the wavelength of light, and do not contain inclusions which can scatter light nor does it have regions with abrupt difference in refractive index.

The use of thin films derived from chlorotrifluoroethylene as optical device protective coatings has been reported (100,101). Not only do the films protect the moisture sensitive substrates from atmospheric humidity but they also exhibited antireflection properties. Reis, et. al. (102) and Hiratsuka, et. al. (103) explored the use of plasma polymerized ethane as protective coatings for laser windows. The absorption and antireflection characteristics of these coatings were reported.

In Plasma Polymerization; Shen, M., et al.;
ACS Symposium Series; American Chemical Society: Washington, DC, 1979.

Acknowledgement

This work was supported by a grant from the National Science Foundation.

Abstract

Polymers can be obtained by subjecting an organic or organometallic vapor to the plasma created in an electrical glow discharge. By varying the plasma conditions such as pressure, monomer flow rate, power etc., not only films but also powder and oil are formed. In this paper we shall consider both the mechanism of polymerization and the influence of reaction conditions upon the rates of polymerization. A kinetic model will be presented, which appears to be in good agreement with experiments. The plasma polymerized materials can be characterized by IR, NMR, ESCA and other analytical techniques. It has been found that the polymer is highly crosslinked, amorphous and often contains functional groups not originally present in the monomer. The electrical properties of these films will also be discussed. Some of the potential applications of plasma polymerized films will be pointed out.

Literature Cited

1. DeWilde, P., Ber., (1874), 7, 352.
2. Thenard, P., Thenard, A., Compt. Rend., (1874), 78, 219.
3. Goodman, J., J. Polymer Sci., (1960), 44, 551.
4. Hollahan, J. R., McKeever, R. P., Adv. Chem. Ser., (1969), 80, 272.
5. Allam, D. S., Stoddard, C. T. H., Chem. Beit., (1965), 1, 410.
6. Gregor, L. V., in Thun, R. E., Hass, G., eds., "Physics of Thin Films," Vol. 3, p. 61, Academic Press, New York, 1966.
7. Kolotyrkin, V. M., Gilman, A. B., Tsapuk, A. K., Russ. Chem. Revs., (1967), 36, 579.
8. Mearns, A. M., Thin Solid Films, (1969), 3, 201.
9. Millard, M., in Hollahan, J. R., Bell, A. T., eds., "Techniques and Applications of Plasma Chemistry," p. 177, Wiley, New York, 1974.
10. Yasuda, H., in Shen, M., ed., "Plasma Chemistry of Polymers," p. 15, Dekker, New York, 1976.
11. Kobayashi, H., Bell, A. T., Shen, M., Macromol., (1974), 7, 277.
12. Yasuda, J., Lamaze, C. E., J. Appl. Polymer Sci., (1973), 17, 1533.

13. Brown, K. C., Europ. Polymer J., (1972), 8, 117.
14. Kobayashi, H., Shen, M., Bell, A. T., J. Macromol. Sci.-Chem., (1974), 8, 1345.
15. Kobayashi, H., Shen, M., Bell, A. T., J. Macromol. Sci.-Chem., (1974), 8, 373.
16. Denaro, A. R., Owens, P. A., Crawshaw, A., Europ. Polymer J., (1968), 4, 93.
17. Kobayashi, H., Bell, A. T., Shen, M., J. Macromol Sci.-Chem., (1976), 10, 491.
18. Yasuda, H., Lamaze, C. E., J. Appl. Polymer Sci., (1971), 15, 2277.
19. Morita, S., Bell, A. T., Shen, M., to be published.
20. Taniguchi, I., IEE-Japan, Report of Study Meeting on Insulating Materials, EI-42-8, 1967.
21. Brown, K. C., Copsey, M. J., Europ. Polymer J., (1972), 8, 129.
22. Vinzant, J. W., Bell, A. T., Shen, M., this issue.
23. Yasuda, H., Hsu, T., J. Polymer Sci., Polymer Chem. Ed., (1977), 15, 81.
24. Burnett, G. M., "Mechanism of Polymer Reactions," Interscience, New York, 1954.
25. Westwood, A. R., Europ. Polymer J., (1971), 7, 363.
26. Tickner, A. W., Can. J. Chem., (1961), 39, 87.
27. Thomson, L. F., Mayhan, K. G., J. Appl. Polymer Sci., (1972), 16, 2291.
28. Thomson, L. F., Mayhan, K. G., J. Appl. Polymer Sci., (1972), 16, 2317.
29. Vasile, M. J., Smolinsky, G., J. Electrochem. Soc., (1972), 119, 451.
30. Smolinsky, G., Vasile, M. J., J. Macromol. Sci.-Chem., (1976), 10, 473.
31. Morita, S., Mizutani, T., Ieda, M., Jap. J. Appl. Phys., (1971), 10, 1275.
32. N. Morosoff, N., Crist, B., Bumgarner, M., Hus, T., Yasuda, H., J. Macromol. Sci.-Chem., (1976), 10, 451.
33. Benson, S. W., O'Neal, H.E., "Kinetic Data, on Gas Phase Unimolecular Reactions, NSRDS-NBS21, U.S., Department of Commerce, Washington, D.C., 1970.
34. Brown, S. C., "Introduction to Electrical Discharges in Gases," Wiley, New York, 1966.
35. Brown, L. C., Bell, A. T., Ind. Eng. Chem., (1974), 13, 210.
36. Williams, T., Hayes, M. W., Nature, (1966), 209, 769.
37. Carchano, H., J. Chem. Phys., (1974), 61, 3634.
38. Morita, S., Sawa, G., Ieda, M., J. Macromol. Sci., (1976), 10, 501.

In Plasma Polymerization; Shen, M., et al.;
ACS Symposium Series; American Chemical Society: Washington, DC, 1979.

39. Poll, H. V., Z. Angew. Phys., (1970), 29, 260.
40. Lam, D. K., Baddour, R. F., Stancell, A. F., J. Macromol. Sci.-Chem, (1976), 10, 421.
41. Tibbitt, J. M., Jensen, R., Bell, A. T., Shen, M., Macromol., (1977), 10, 647.
42. Kobayashi, H., Shen, M., Bell, A. T., J. Appl. Polymer Sci., (1973), 18, 885.
43. Thompson, L. F., Smolinsky, G., J. Appl. Polymer Sci., (1972), 16, 1179.
44. Hafer, D., Tiller, H. J., Meyer, K., Plaste und Kautschuk, (1972), 5, 354.
45. Tiller, H. J., Breitbarth, F., Kuhn, W., Meyer, K., Z. Chem., (1972), 12, 456.
46. Niinomi, M., Kobayashi, H., Bell, A. T., Shen, M., J. Appl. Phys., (1973), 44, 4317.
47. Duval, M., Theoret, A., J. Appl. Polymer Sci., (1973), 17, 527.
48. Niinomi, M., Kobayashi, H., Bell, A. T., Shen, M., J. Appl. Polymer Sci., (1974), 18, 2199.
49. Lee, S. M., McCloskey, Licari, J. J., Insulation, (1969), 5, 40.
50. Lee, S. M., Eisenberg, P. H., Insulation, (1969), 5, 97.
51. Vastola, F. J., Wightman, J. P., J. Appl. Chem., (1964), 14, 69.
52. McTaggart, F. K., "Plasma Chemistry in Electrical Discharges," Elsevier, New York, 1967.
53. Wightman, J. P., Johnson, N. J., Adv. Chem. Ser., (1969), 80, 322.
54. Jesch, K. F., Bloor, J. E., Kronick, P. L., J. Polymer Sci., Part A-1, (1966), 4, 1487.
55. Kronick, P. L., Jesch, K. F., J. Polymer Sci., Part A-1, (1969), 7, 767.
56. Tibbitt, J. M., Shen, M., Bell, A. T., J. Maxromol. Sci.-Chem., (1976), 10, 1623.
57. Tibbitt, J. M., Bell, A. T., Shen, M., J. Macromol. Sci.-Chem., (1977), 11, 139.
58. Seeger, M., Barrell, E. M., Shen, M., J. Polymer Sci., Polymer Chem. Ed., (1975), 13, 1541.
59. Seeger, M., Gritter, R. J., Tibbitt, J. M., Shen, M., Bell, A. T., J. Polymer Sci., Polymer Chem., ed., (1977), 15, 1403.
60. Clark, D. T. in Ivin, K. J., ed., "Structural Studies of Macromolecules by Spectroscopic Methods," p. 111, Wiley, New York, 1976.
61. O'Kane, D. F., Rice, D. W., J. Macromol. Sci.-Chem., (1976), 10, 567.
62. Millard, M. M., Pavalath, A. E., J. Macromol. Sci.-Chem., (1976), 10, 579.
63. Nakajima, K., Bell, A. T., Shen, M., Millard, M., to be published in J. Appl. Polymer Sci.

64. Pender, M., Shen, M., Bell, A. T., this issue.
65. Bell, A. T., Wydeven, T., Johnson, C. C., J. Appl. Polymer Sci., (1975), 19, 1911.
66. Peric, D., Bell, A. T., Shen, M., J. Appl. Polymer Sci., (1977), 21, 2661.
67. Neiswender, Adv. Chem. Ser., (1969), 80, 338.
68. Stuart, M., Nature, (1963), 199, 59.
69. Bagirov, M. A., Abasov, S. A., Malin, V. P., Angew. Makromol. Chem., (1970), 12, 137.
70. Sawa, G., Ito, O., Morita, S., Ieda, M., J. Polymer Sci., Polymer Phys. Ed., (1974), 12, 1231.
71. Sawa, G. Suzuki, K., Morita, S., Ieda, M., J. Polymer Sci., Polymer Phys. Ed., (1976), 14, 173.
72. Hirai, T., Nakada, O., Jap. J. Appl. Phys., (1968), 7, 112.
73. Mann, H. T., J. Appl. Phys., (1964), 35, 55.
74. Tuzov, L. S., Gilman, A. B., Shchurov, A. N., Kolotyrkin, V. M., Vysokomol. Soed., (1965), 7, 1802.
75. Tuzov., L. S., Kolotyrkin, V. M., Tuniskii, N. N. Int'l Chem. Eng., (1971), 11, 60.
76. Tibbitt, M. M., Bell, A. T., Shen, M., J. Macromol. Sci.-Chem., (1976), 10, 519.
77. Bradley, A., Hammes, J. P., J. Electrochem. Soc., (1969), 110, 15.
78. Bashara, N. M., Doty, C. T., J. Appl. Phys., (1964), 35, 3498.
79. Carchano, H., Valentin, E., Thin Solid Films, (1975), 30, 335.
80. Kay, E., Hetzler, U., to be published in J. Appl. Phys.
81. Morita, S., Sawa, G., Ieda, M., J. Appl. Phys., (1973), 44, 2435.
82. Frenkel, J., Phys. Rev., (1938), 54, 647.
83. Guastavino, J., Carchano, H., Bui, A., Thin Solid Films, (1972), 27, 225.
84. Morita, S., Shen, M., Ieda, M., J. Polymer Sci., Polymer Phys. Ed., (1977), 15, 981.
85. Yasuda, H., Lamaze, C. E., J. Appl. Polymer Sci., (1973), 17, 201.
86. Yasuda, H., Appl. Polymer Symp., (1973), 22, 241.
87. Yasuda, H., Marsh, H. C., J. Appl. Polymer Sci., (1975), 19, 2981.
88. Hollohan, J. R., Wydeven, Science, (1973), 179, 500.
89. Hinman, P. V., Bell, A. T., Shen, M., to be published in J. Appl. Polymer Sci.
90. Stancell, A. F., Spencer, A. T., J. Appl. Polymer Sci., (1972), 16, 1505.

In Plasma Polymerization; Shen, M., et al.;
ACS Symposium Series; American Chemical Society: Washington, DC, 1979.

91. Chang, F. Y., Shen, M., Bell, A. T., J. Appl. Polymer Sci., (1973), 17, 2915.
92. Colter, K. D., Bell, A. T., Shen, M., Biomat. Med. Dev. Art. Org., (1977), 5, 1.
93. Colter, K. D., Shen, M., Bell, A. T., Biomat. Med. Dev. Art. Org., (1977), 5, 13.
94. Brick, R. M., Knox, J. R., Modern Packaging, (1965), 123.
95. Williams, T., J. Oil Color Chem. Assoc., (1965), 48, 936.
96. Byrne, G. A., Brown, K. C., J. Soc. Dyers Colorists, (1972), 88, 113.
97. Millard, M., Lee, K. S., Pavlath, A. E., Textile Res. J., (1972), 42, 307.
98. Pavlath, A. E., Lee, K. S., J. Macromol. Sci., Chem., (1976), 10, 619.
99. Tien, P. K., Smolinsky, G., Martin, R. J., Appl. Opt., (1972), 11, 637.
100. Hollahan, J. R., Wydeven, T., Johnson, C. C. Appl. Optics, (1974), 13, 1844.
101. Wydeven, T., Kubadhi, Appl. Optics, (1976), 15, 132.
102. Reis, T. A., Hiratsuka, H., Bell, A. T., Shen, M., NBS Special Publ. No. 462, p. 230, Washington, D.C., 1976.
103. Hiratsuka, H., Vinzant, J. W., Bell, A. T., Shen, M., "Proc. High Power Laser Opt. Comp. Mtg.," p. 419, Boulder, CO, 1977.

RECEIVED March 29, 1979.

Competitive Ablation and Polymerization (CAP) Mechanisms of Glow Discharge Polymerization

H. K. YASUDA

Graduate Center for Materials Research, University of Missouri–Rolla, Rolla, MO 65401

The formation of a polymer in a glow discharge is a complex phenomenon, and the interpretation of the formation mechanism is not at all clarified by the misapplication of the term "polymerization". The term "polymerization" is generally accepted to mean that the molecular units (monomers) are linked together by the "polymerization" process. Consequently, the resultant polymer is conventionally named by using the prefix "poly" plus the name of the monomer. For instance, the polymer formed by the polymerization of styrene is referred to as polystyrene. In other words, "polymerization" conventionally refers to molecular polymerization; that is, the chemical structure of a polymer can be derived from the chemical structure of the monomer.

Strictly speaking, "polymerization" in the conventional sense does not represent the process of polymer formation that occurs in a glow discharge, because in glow discharge atomic polymerization may take place instead of molecular polymerization. Because of this atomic polymerization, some of the elements or fractions of the monomer are not incorporated into the polymer that is deposited but play an important role in sustaining the glow discharge of the polymer-forming plasma.

Although the individual steps or reactions that are involved in the process of polymer formation in a glow discharge are extremely complex and are dependent on the system, several important types of phenomena can be identified for the purpose of constructing a general picture of the glow discharge polymerization. This process is represented by the Competitive Ablation and Polymerization (CAP) mechanism schematically shown in Figure 1. The direct route shown in the Figure is referred to as plasma-induced polymerization; the indirect route as plasma state polymerization.

0-8412-0510-8/79/47-108-037$05.00/0

In Plasma Polymerization; Shen, M., et al.;
ACS Symposium Series; American Chemical Society: Washington, DC, 1979.

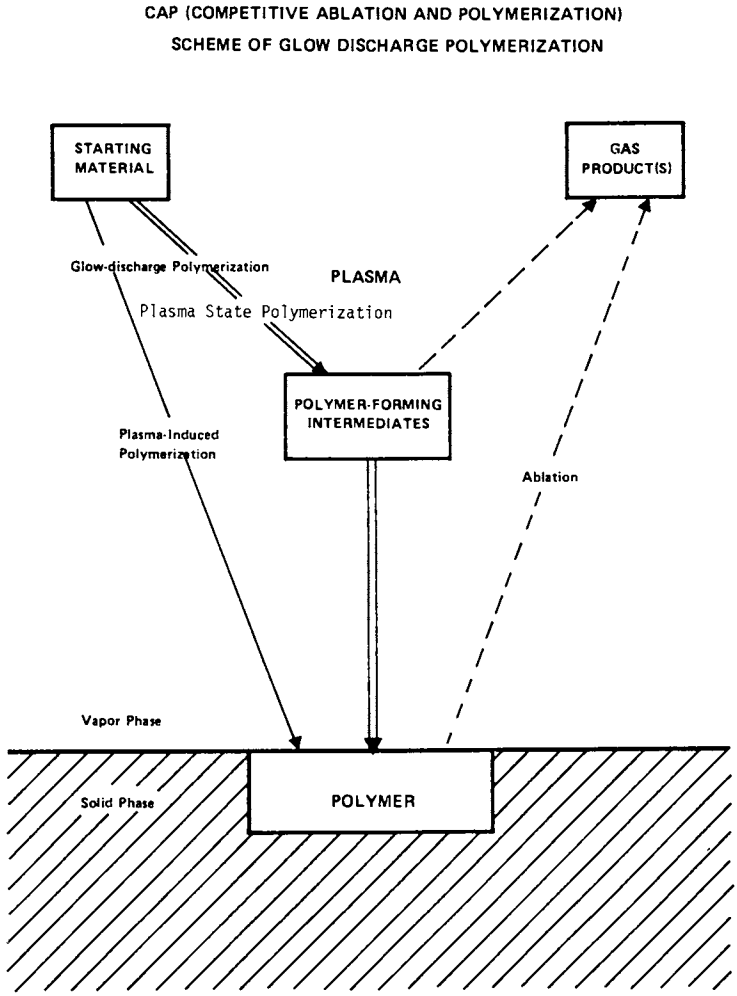

Figure 1. Overall mechanism of glow discharge polymerization

Plasma-induced polymerization is essentially conventional (molecular) polymerization that is triggered by a reactive species created in an electric discharge. In order for one to form polymers by plasma-induced polymerization, the starting material must contain polymerizable structures, such as olefinic double bonds, triple bonds, or cyclic structures.

Plasma state polymerization is an atomic process, which occurs only in a plasma state. This type of polymerization can be represented by the statements

Initiation or Reinitation

$$M_i \rightarrow M_i^*$$

$$M_k \rightarrow M_k^*$$

Propagation and Termination

$$M_i^* + M_k^* \rightarrow M_i\text{-}M_k$$

$$M_i^* + M_k \rightarrow M_i\text{-}M_k$$

in which i and k are the numbers of repeating units (i.e., i = k = 1 for the starting material), and M* represents a reactive species, which can be an ion of either charge, an excited molecule, or a free radical produced by M but not necessarily retaining the molecular structure of the starting material. That is, M can be a fragment or even an atom detached from the original starting material.

In plasma state polymerization, the polymer is formed by the repeated stepwise reaction described above. It should be noted that plasma-induced polymerization does not produce a gas phase by-product, because the polymerization proceeds via the utilization of a polymerizable structure. The process can be schematically represented by the following chain propagation mechanism:

$$\left.\begin{aligned} M^* + M &\rightarrow MM^* \\ M_i^* + M &\rightarrow M_{i+1}^* \end{aligned}\right\} \text{ Propagation}$$

$$M_i^* + M_k^* \rightarrow M_i\text{-}M_k \quad \text{Termination}$$

It should be emphasized that polymerization in a glow discharge consists of both plasma-induced polymerization and plasma state polymerization. Which of these two mechanisms plays the predominant role depends not only on the chemical structure of the starting material but on the condition of the discharge.

Nonpolymer-forming gas products are produced where reactive

In Plasma Polymerization; Shen, M., et al.;
ACS Symposium Series; American Chemical Society: Washington, DC, 1979.

(polymer-forming) intermediates are formed when the polymer deposit or the substrate material is decomposed (etched). Because polymer-forming species leave the gas (plasma) phase as the polymers are deposited, the major portion of the gas consists of the product gas when a high conversion ratio of a starting material to a polymer is obtained. Although this is an extremely important factor, it has been dealt with lightly or neglected in most of the articles appearing in the literature.

The characteristics of the product-gas plasma are the predominant factors in determining the extent of the ablation process, which is shown in Figure 1. Because much of the work in glow discharge polymerization that appears in the literature deals with hydrocarbons, which produce hydrogen as the main product gas, the effect of ablation is not great. Consequently, the complete neglect of ablation does not make a significant difference in the overall picture of glow discharge polymerization; however, when a fluorine- or oxygen-containing compound is used as the starting material, the extent of ablation becomes the dominant factor, and the extent of polymer formation depends entirely on the extent of the product gas formation.

Perhaps the most dramatic ablation effect for the glow discharge polymerization of CF_4 was recently demonstrated by Kay (1). It had been thought that CF_4 was one of the very few organic compounds that does not polymerize in a glow discharge. On the other hand, CF_4 had been used as one of most effective gases in plasma etching. Kay observed that no polymer deposition occurs under normal conditions in spite of the fact that C-F bonds are broken in the glow discharge, a fact which has been confirmed by mass-spectroscopic analysis of the gas phase. However, when a small amount of hydrogen is introduced into the discharge, a polymer is deposited. When the hydrogen flow is stopped, the polymer deposit ablates.

The situation observed in the above example may be visualized by comparing bond energies. It should be noted that the energy level involved in a glow discharge is high enough to break any bond (2,3), i.e., C-F is broken, although C-F is stronger than C-H. The important fact is the stability of the product gas. The bond energy for F-F is only 37 kcal/mol, whereas H-F is 135 kcal/mol, which is higher than 102 kcal/mol for a C-F bond. The introduction of H_2 into the monomer flow evidently produces HF and removes F from the discharge system. This reduces the etching effect of the product gas (F_2) plasma and shifts the balance between polymerization and ablation to polymerization. Although the term F_2 plasma is used to describe the effect of the detached F in plasma, F_2 is not detected in the plasma state, perhaps because of its extremely high reactivity (4).

It is interesting to note that F and O are the two elements that reduce the rate of polyer formation of compounds containing one or the

In Plasma Polymerization; Shen, M., et al.;
ACS Symposium Series; American Chemical Society: Washington, DC, 1979.

other of these elements. These two elements are the most electronegative of all elements, but the bond energy itself is not a measure of the etching effect of the plasma. For instance, the N-N bond is only 32 kcal/mol, and the N_2 plasma does not etch polymer surfaces. Instead, the incorporation of N into the surface predominates (5). Nevertheless, the importance of the ablation process shown in Figure 1 seems to be well demonstrated by the paucity of the polymer formation in the glow discharge polymerization of CF_4 and of oxygen-containing compounds (6).

The polymer formation and properties of polymers formed by glow discharge polymerization are controlled by the balance among plasma-induced-polymerization, plasma state polymerization, and ablation. That is, polymer formation is a part of the CAP scheme shown in Figure 1. Because of this CAP scheme, gas evolved from substrate materials also plays an important role, particularly at the early stage of coating. It has been noticed that the deposition of a polymer from the glow discharge of styrene onto plyoxymethylene, which is an oxygen-containing, plasma labile substrate, is significantly different from the deposits on more stable substrates and depends greatly on the condition of the glow discharge (7).

A study of the properties of polymers formed by glow discharge polymerization from tetrafluoroethylene and investigated by electron spectroscopy for chemical analysis (ESCA) provides further evidence for the importance of the CAP mechanism (8).

The ESCA C1s spectrum of commercially prepared polytetrafluoroethylene (Teflon) shows a single intense peak about 291 eV that corresponds to $-CF_2-$ carbons. The ESCA C1s spectrum of glow discharge polymerized tetrafluoroethylene is significantly different from that of Teflon and contains many peaks corresponding to $-CF_3$, >CF-, -C-, and carbons bonded to other substituents, which includes nitrogen- and oxygen-containing groups, depending on the condition of glow discharge.

If a polymer is formed through plasma-induced polymerization from tetrafluoroethylene, the ESCA C1s spectrum should be identical to that of Teflon. Therefore, the fact that the ESCA C1s peaks are significantly different from those in the spectrum of Teflon indicates that a major portion of the glow discharge polymerization is not plasma-induced polymerization. How the balance between plasma state polymerization and plasma-induced polymerization is influenced by the conditions of glow discharge and the location of polymer deposition within a reactor can be seen by comparing the ESCA C1s spectra shown in Figures 2-4.

The characteristic shapes of the C1s peaks shown in Figure 2 indicate that the polymers formed at locations on the upstream side and downstream side of the rf coil are quite different when a relatively low discharge power is used. The polymer formed on the upstream side contains considerable amounts of CF_3 (about 293 eV) and CF (about 289

In Plasma Polymerization; Shen, M., et al.;
ACS Symposium Series; American Chemical Society: Washington, DC, 1979.

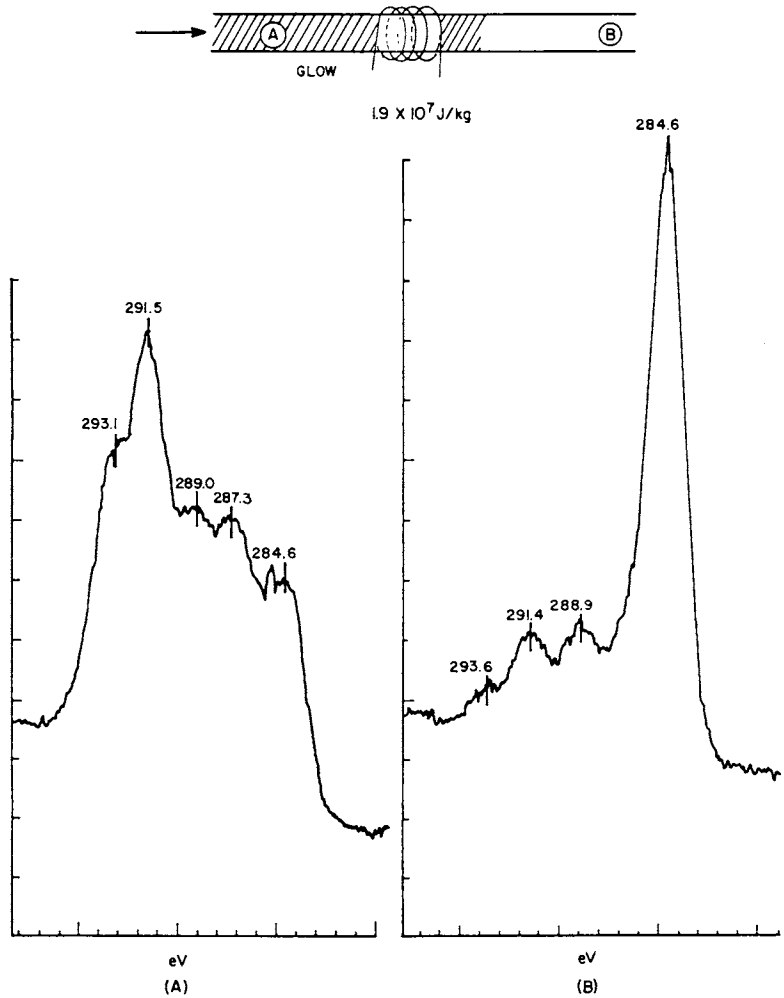

Figure 2. Dependence of the ESCA C(1s) peaks of glow discharge polymers of tetrafluoroethylene on discharge conditions and the location of polymer deposition. Polymer deposits occur at two locations (a) before the rf coil and (b) after rf coil. Discharge power level is 1.9 × 10⁷ J/kg.

In Plasma Polymerization; Shen, M., et al.;
ACS Symposium Series; American Chemical Society: Washington, DC, 1979.

eV) besides the expected CF_2. This is undoubtedly due to the atomic nature of glow discharge polymerization rather than conventional molecular polymerization.

The polymer formed on the downstream side of the rf coil at this low discharge power contains much less F, i.e., much smaller peaks for a higher binding energy, and the peak of 284.6 eV (carbon which is not attached to F) becomes the major peak. This is a dramatic display of the effect of the energy input zone, where the tube is directly inside of the rf coil, on the properties of glow discharge polymers. As the discharge power is increased, this severe effect of the energy input zone expands eventually to the entire length of the tube, and at a high discharge power, the polymer formed on the upstream side of the rf coil becomes similar to the polymer formed on the downstream side, as can be seen in Figure 3.

When a system in which the flow does not pass through the energy input zone and glow discharge polymerization is carried out in the tail-flame portion of the glow discharge, the polymer formed at the downstream end of a reactor is not necessarily the same as that formed at the downstream end of a straight tube. The results depicted in Figure 4 show that the polymer formed in the nonglow region, although located at the downstream end of a reactor, is nearly identical to conventional polytetrafluoroethylene. This means that polymers formed under such conditions are formed mainly by plasma-induced polymerization.

With regard to the CAP mechanisms of glow discharge polymerization, it is important to recognize the following aspects that are inevitably involved.

1. The rate of polymer deposition as well as the rate of ablation vary according to the location of deposition within the reactor.
2. The properties of the polymer deposits are also different depending on the location of their deposition within the reactor.
3. The materials that are used in a reactor, such as the vessel walls and substrates, influence the glow discharge polymerization, i.e., the rate of polymer deposition and the properties of the polymer deposits.

Because polymer formation can proceed through more than one major type of reaction, i.e., plasma-induced polymerization and plasma state polymerization, depending on the chemical structure of the monomer and also on the conditions of discharge, such as discharge wattage, flow rate, type of discharge, and geometrical factors of the reactor, the balance between polymer formation (polymerization) and ablation is for most cases extremely complicated.

An attempt, the details of which are presented below, has been made to demonstrate the balance between polymerization and ablation by selecting a monomer system that can be manipulated to shift the balance.

In Plasma Polymerization; Shen, M., et al.;
ACS Symposium Series; American Chemical Society: Washington, DC, 1979.

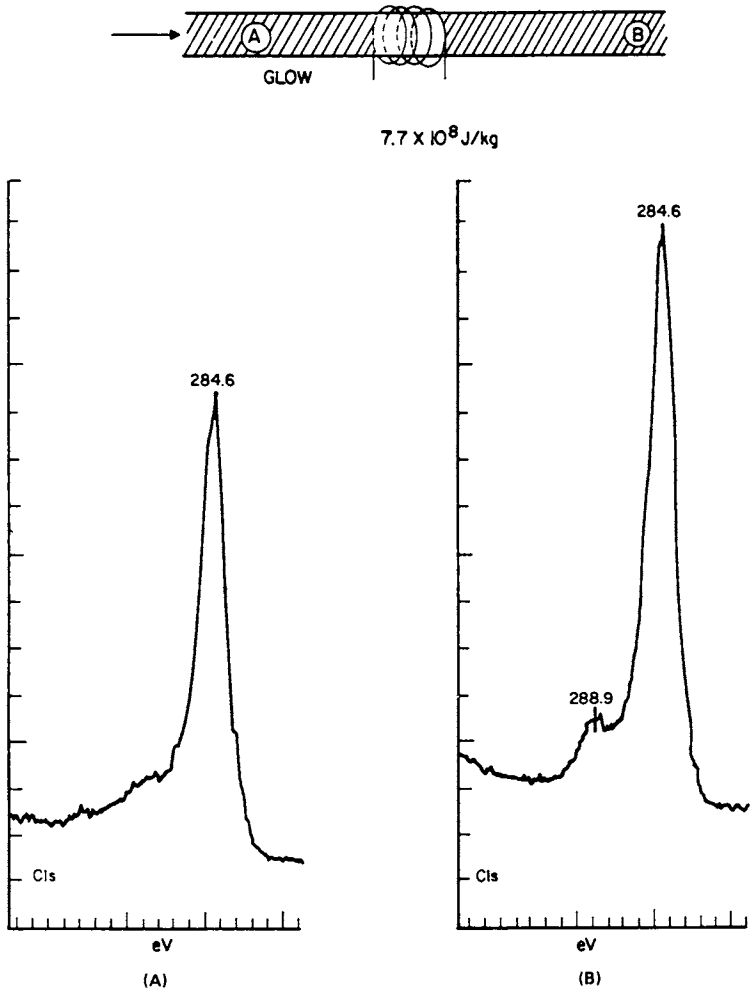

Figure 3. ESCA C(1s) peaks of glow discharge polymers of tetrafluoroethylene in the same reactor shown in Figure 2 but at the higher discharge power level of 7.7×10^8 *J/kg*

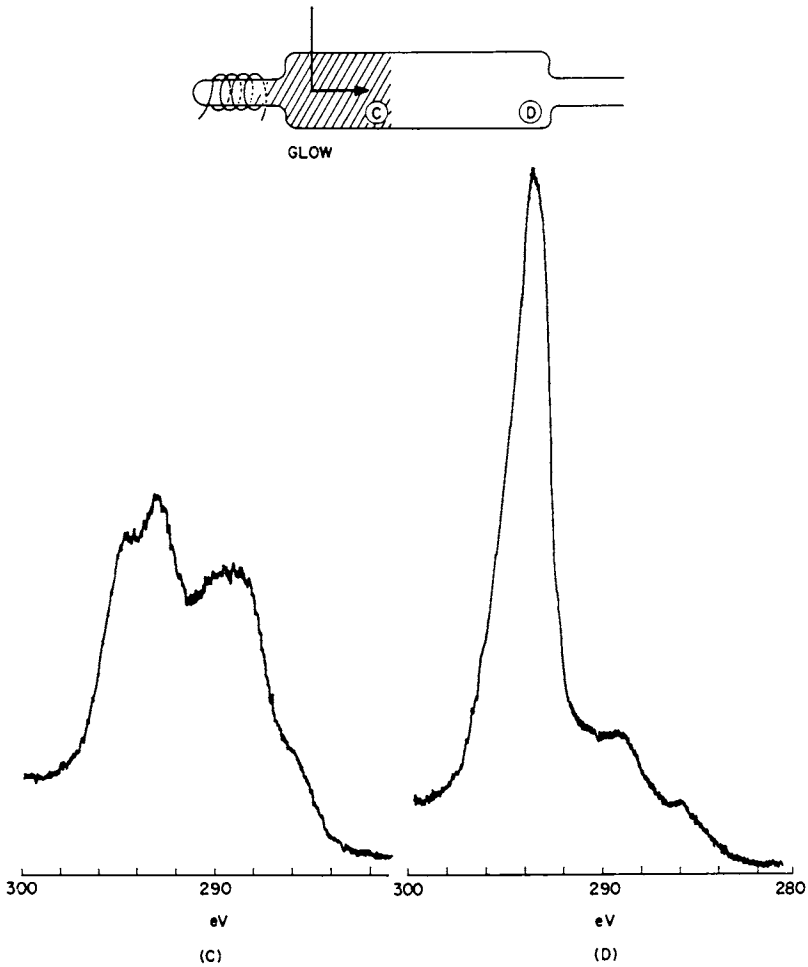

Figure 4. ESCA C(1s) peaks of glow discharge polymers of tetrafluoroethylene prepared in the reactor shown in the insert: (c) at the end of the glow region, and (d) at the end of the tube in the nonglow region.

In Plasma Polymerization; Shen, M., et al.;
ACS Symposium Series; American Chemical Society: Washington, DC, 1979.

The monomer chosen is hexafluoroethane, which cannot be polymerized by plasma-induced polymerization and which cannot be polymerized in a glow discharge under ordinary conditions presumably because the ablation process associated with the glow discharge is excessive. Attempts have been made to supress the ablation process and to shift the balance between plasma state polymerization, which is assumed to be present, and ablation. However, it has been observed that polymer formation for hexafluoroethane does occur when polyethylene is used as substrate. On the other hand, no polymer formation can be observed either with ESCA or by surface energy analysis when glass is used as a substrate.

In an earlier study of glow discharge polymerization of ethylene in a magnetically enhanced discharge by a 10 kHz power source, the distribution of polymer deposition on the surfaces of electrodes and on an aluminum plate inserted between two electrodes was investigated (10). In a magnetically enhanced discharge, the power density or the intensity of glow is not uniform, because an intense glow occasioned by the magnetic field occurs near the surfaces of electrodes. This uneven distribution can be utilized to investigate how the formation of a polymer in a glow discharge is related to power density. In this study, the distribution of polymer deposition was compared for ethylene and hexafluoroehtane in identical systems with the addition of various amounts of H_2. The contributions of the component mechanisms, which are part of the CAP mechanism for these two monomers, are summarized in Table I.

Table I

Contributions of Different Mechanisms in Glow Discharge Polymerization

Monomer		Plasma-Induced Polymerization	Plasma State Polymerization	Ablation
Ethylene	$CH_2=CH_2$	Occurs	Occurs	Minimal
Hexafluoroethane	CF_3-CF_3	None	Increases as a function of H_2 concentration	Decreases as a function of H_2 concentration

The distribution of polymer deposition from the glow discharge of ethylene is shown in Figure 5. In this figure, the deposition rate is plotted against the distance from the center of the electrode. The deposition rate profile shows a strong peak at a location that corresponds with the intense glow. A much sharper peak occurs at the position of the electrode surface. The peaks for the deposition on an aluminum plate substrate placed between electrodes is much less pronounced (Fig.

In Plasma Polymerization; Shen, M., et al.;
ACS Symposium Series; American Chemical Society: Washington, DC, 1979.

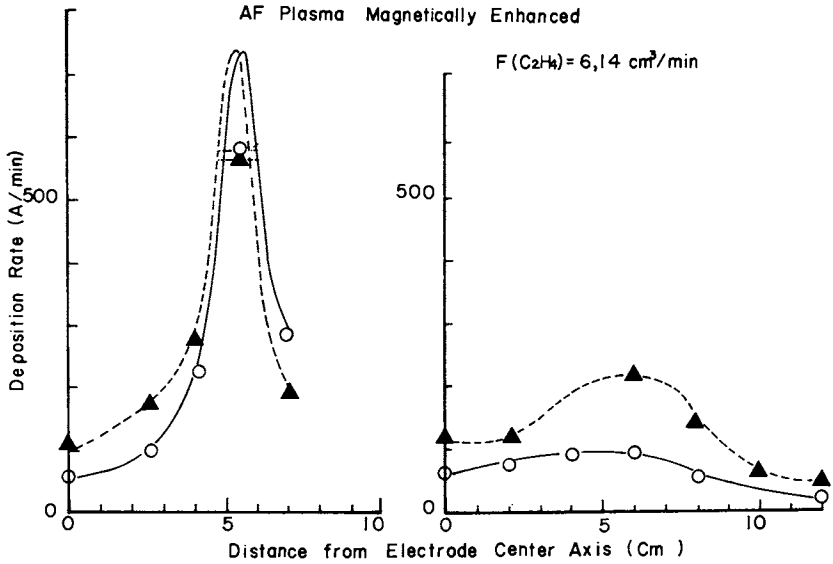

Figure 5. Deposition rate profile on the electrode and substrate for a glow discharge polymerization of ethylene activated at a frequency of 10 kHz with magnetic enhancement. The system pressure is 20 μm Hg. (○) 60 mA, (▲) 200 mA.

5). The sharp increase at the position of the intense glow indicates that the polymer formation from ethylene is proportional to the extent of ionization caused by electron bombardment.

The deposition rate profile for hexafluoroethane is quite different as shown in Figures 6 and 7. The positive peak observed for ethylene at the location of the intense glow appears as a negative peak for hexafluoroethane. As indicated in a previous study for tetrafluoroethylene (11), the ablation effect of tetrafluoroethylene depends on the energy density of the glow discharge. It has been observed that when the energy density increases above a certain critical value, ablation becomes the predominant process, and a drastic decrease in polymer formation occurs.

Therefore, the negative peak in the deposition profile can be explained by extensive ablation in the high energy density region. The relatively high deposition rates at the substrate surface, as compared to those at the electrode surface, can also be explained by the lower energy density in the middle of two electrodes, i.e., less ablation.

As the concentration of H_2 is increased to the stoichiometric equivalent of the numbers of F atoms (H_2/H F E = 3), the negative peak observed without H_2 (Fig. 6) is changed to the positive peak (Fig. 7). This indicates that ablation is no longer dominant, and polymer formation prevails. This phenomenon can be explained by postulating that H_2 reacts with F atoms emanating from the fluorine containing compound in the glow discharge and forms the more stable HF, which reduces the ablation in a dramatic manner. Because hexafluoroethane does not form a polymer by plasma-induced polymerization, the overall effect can be explained by the balance between plasma state polymerization and ablation.

This postulate of glow discharge polymerization can be extended to a case in which a fluorine containing compound is added to a hydrocarbon monomer. Kobayashi et al. (12) demonstrated that the addition of small amounts of Freon increases the deposition rate of ethylene and ethane in a glow discharge, and they reasoned that the increase is due to the enhanced abstraction of hydrogen from the monomers. However, when a similar experiment is conducted under the conditions in which plasma state polymerization rather than plasma-induced polymerization predominates and a very high yield of monomer to polymer is obtained, no such dramatic increase can be observed (13). Therefore, it can be stated that the addition of a fluorine containing compound enhances plasma state polymerization, which probably does not play a major role under the conditions employed in the experiment conducted by Kobayashi et al. (12).

The above results demonstrate that CAP mechanisms may provide a reasonable explanation for glow discharge polymerization. Which reac-

In Plasma Polymerization; Shen, M., et al.;
ACS Symposium Series; American Chemical Society: Washington, DC, 1979.

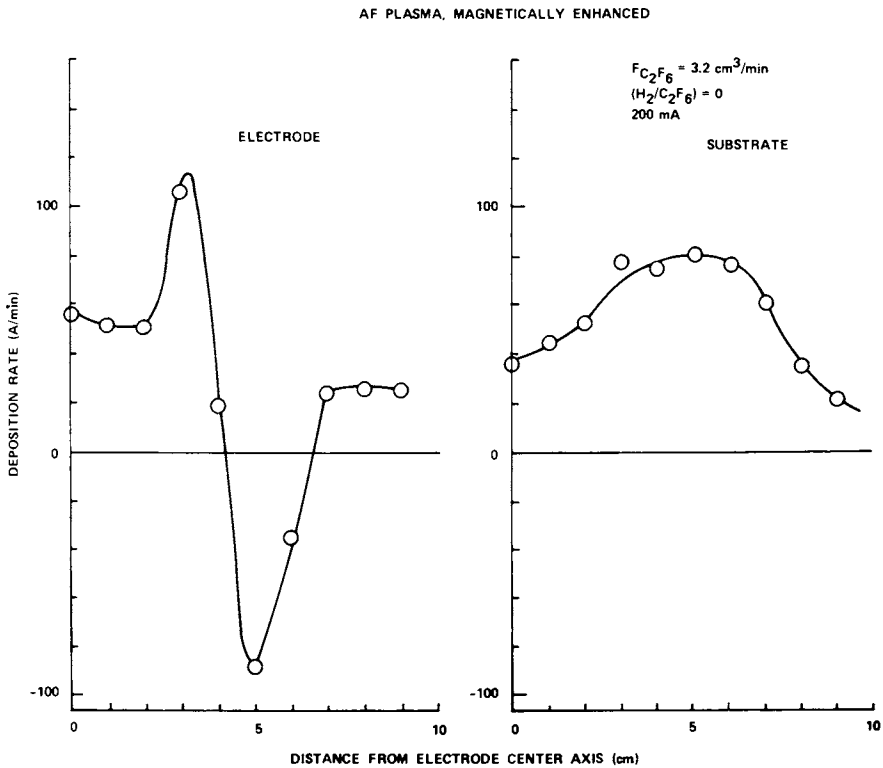

Figure 6. Deposition rate profile on the electrode and substrate for a glow discharge polymerization of tetrafluoroethane activated at a frequency of 10 kHz with magnetic enhancement. The system pressure is 20 μm Hg.

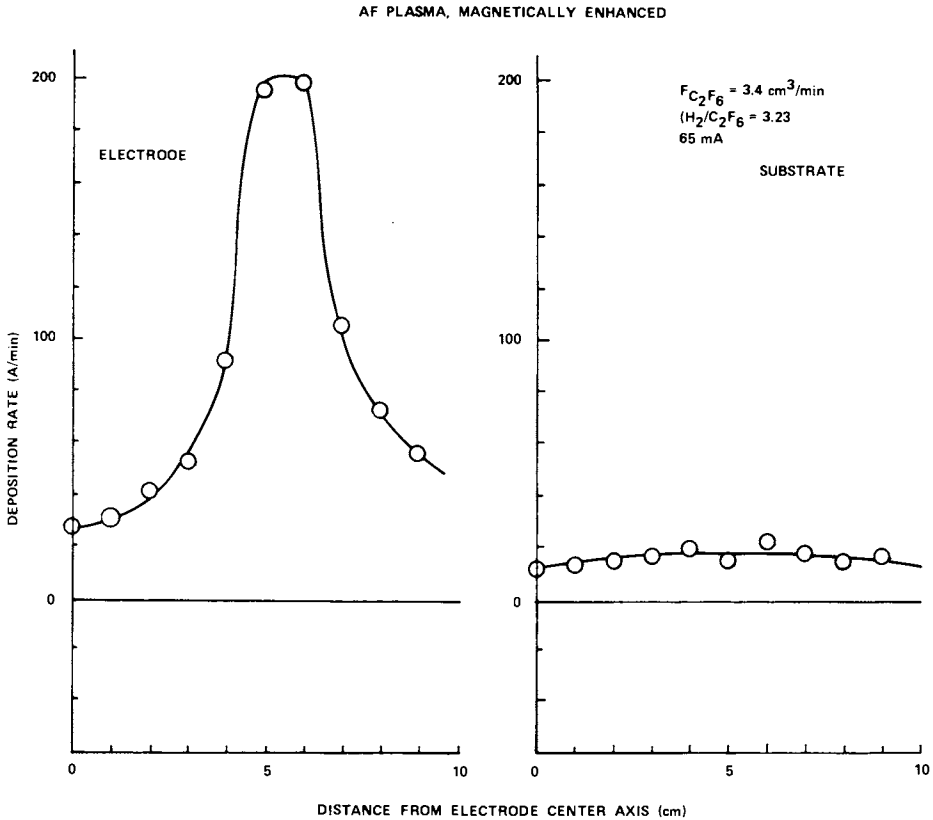

Figure 7. Deposition rate profile on the electrode and substrate for a glow discharge polymerization of tetrafluoroethane with H_2 activated at a frequency of 10 kHz with magnetic enhancement. System pressure is 50 μm Hg.

tion predominates in the glow discharge polymerization of a particular monomer depends not only on the chemical structure of the monomer but also on the conditions of the discharge, particularly the energy density at the location of deposition.

Synopsis

The formation of polymers in the glow discharge of an organic compound may be explained by Competitive Ablation and Polymerization (CAP) mechanisms. According to this postulate, polymer formation competes with ablation in the presence of nonpolymer-forming gases, which emanate from the monomer in the glow discharge. The polymerization process is not the same as conventional molecular polymerization. It is an atomic polymerization, in which the molecular structure of the monomer is not retained. This can be determined by using electron spectroscopy for chemical analysis data of the glow discharge polymer of tetrafluoroethylene for various discharge conditions, and by deposition rates of polymers formed from mixtures of hexafluoroethane and hydrogen.

Acknowledgments

This work was supported in part by the Office of Water Research and Technology of the U. S. Department of the Interior under Contract No. 14-34-001-7537 and the National Heart, Lung, and Blood Institute under Contract No. NIH-NO1-HV-3-2913.

References

1. Kay, E., paper presented at International Round Table on Plasma Polymerization and Treatment, IUPAC Symp. on Plasma Chem., Limoges, France, July 13-19, 1977.
2. Clark, D. T. and Dilks, A., Characterization of Metal on Polymer Surfaces, in "Polymer Surfaces", Academic Press, New York, 1977.
3. Wehner, G. K. and Anderson, G. S., in "Handbook of Thin Film Technology", Maissel, L. I. and Glang, R., eds., McGraw-Hill, New York, 1970.
4. Smolinsky, G., Bell Telephone Laboratories, private communication, August 1977.
5. Yasuda, H., Marsh, H. C., Brandt, E. S.., and Reilley, C. N., J. Poly. Sci., Poly. Chem. Ed. (1977) 15 991.
6. Yasuda, H., paper presented at International Round Table on Plasma Polymerization and Treatment, IUPAC Symp. on Plasma Chem., Limoges, France, July 13-19, 1977.

7. Yasuda, H., Lamaze, C. E., and Sakaoku, K., J. Appl. Poly. Sci., (1973) 17, 137.

8. Yasuda, H. and Hirotsu, T., Surf. Sci. (1978) 76, 232.

9. Yasuda, H. and Hsu, T. S., J. Poly. Sci., Poly. Chem. Ed. (1977) 15, 2411.

10. Morosoff, N., Newton, W., and Yasuda, H., J. Vac. Sci. Tech. (March 1978) (submitted).

11. Yasuda, H. and Hsu, T. S., J. Poly. Sci., Poly. Chem. Ed. (1978) 16, 415.

12. Kobayashi, H., Bell, A. T., and Shen, M., J. Macromol. Sci. Chem. (1976) A10 (3), 491.

13. Yasuda, H. and Hirotsu, T., J. Poly. Sci., Poly. Chem. Ed. (1978) 16, 229.

RECEIVED April 10, 1979.

Propylene Glow Discharge Polymerization in the Presence of Bromotrichloromethane

ASHOK K. SHARMA, FRANK MILLICH, and ECKHARD W. HELLMUTH

Polymer Division, Department of Chemistry, University of Missouri–Kansas City, Kansas City, MO 64110

The use of low pressure electric discharges (plasma) for the polymerization of organic compounds has attracted much attention in the past few years (1, 2, 3, 4). But, the lack of sufficient information about the nature of organic glow discharges has very often surprised the polymer chemist and led to controversial statements. One such subject is the reaction mechanism - specifically, the type of active species involved. Some workers regard free radicals to be the predominant active species (5 - 11) while others consider ions to be the major species (12, 13, 14, 15). Perhaps the greatest difficulty in elucidating a reaction mechanism has been in devising tools and techniques to probe for clues within the plasma itself. In the present study multiple evidence for the involvement of free radicals in the glow discharge polymerization of propylene is provided. Bromotrichloromethane, a free radical generator and a potential chain transfer agent, has been employed to interact in the polymerization. Interactions of $BrCCl_3$ with freshly polymerized propylene films on aluminum were also studied.

Experimental

An electromagnetically-coupled tubular reactor (1000 mm long and 75 mm in diameter) operating at a radiofrequency of 27·1 MHz was used for polymer deposition (Fig. 1). Power to the reactor (at current density setting of 125 mA, 100 W listed by distributor of the source) was supplied from a Tomac Diathermy unit Model 1505 and was kept at this level for all the polymerizations conducted during this study. RF coupling is inductive perpendicular to the reactor. The reactor was attached to a monomer mixing systems (MMS) (Fig. 2) carrying 3 reservoirs specifically designed to formulate custom tailored feed mixtures. A secondary inlet system provided with the reactor was used for introducing less volatile reactants into the reactor. The reactor could accept 5 glass

0-8412-0510-8/79/47-108-053$05.00/0

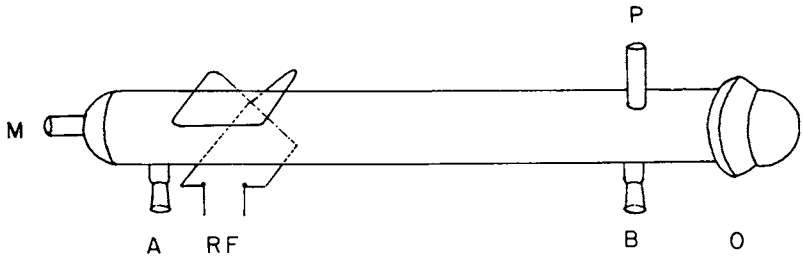

Figure 1. Polymerization reactor (1 m long and 75 mm in diameter): (M) leads to monomer mixing system and (P) to pumps; (O) is a #75 O-ring joint; (A) and (B) are 24/40 ground glass joints, (A) connects to a secondary inlet system and (B) to a pressure guage; and, (RF) is the 27.1 MHz radio frequency source.

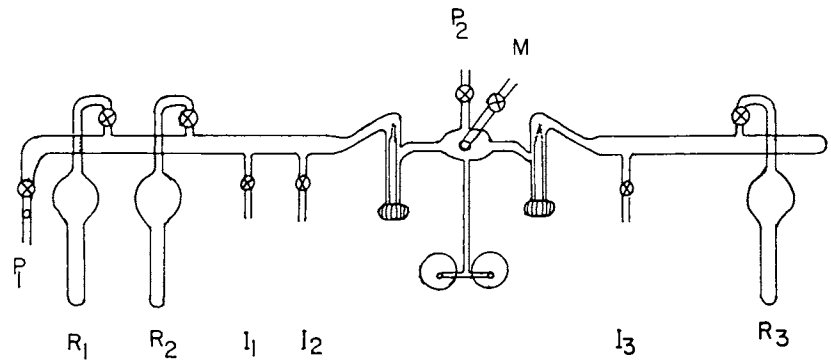

Figure 2. Monomer mixing system: R_1, R_2, and R_3 are reservoirs; I_1, I_2, and I_3 are monomer inlets. P_1 and P_2 connect monomer mixing system to the reactor, P_2 through a cold trap; M is a connection to the mechanical roughing pump.

In Plasma Polymerization; Shen, M., et al.;
ACS Symposium Series; American Chemical Society: Washington, DC, 1979.

sleeve inserts each 200 mm in length and 65 mm in outer diameter. The sleeves were used to protect the reactor from permanent deposition of polymer on its wall and also served as rigid markers for substrate position. The pressure in the reactor was monitored at the downstream end by a thermistor vacuum guage (General Electric Co.); the pressure in the monomer mixing system was controlled by a set of mechanical absolute pressure guages (Pennwalt, Wallace & Tiernan Division - Belleville Division N.J.). All operations were conducted at low pressures (25 Pa maximum) maintained by a combination of liq. N_2 cold trap, M2 NRC oil diffusion pump and a Duoseal roughing pump.

Micro glass slides, dimensions 60 x 25 x 1.02 mm (Corning glass works) and aluminum foil (Reynold's Metal Co.) were used as substrates for polymer deposition. The cleaning of the glass substrate was performed in two steps. A glass slide was first etched for 3 minutes in 10% hydrofluoric acid (HF) followed by a thorough washing in boiling distilled H_2O. It was then dried in an oven at 110°C for a minimum of 12 hours. The second step of the cleaning operation consisted of argon sputtering and was performed in the reactor itself just before the polymerization. The HF-cleaned glass slide was mounted vertically (and parallel to the flow of gas) within one of the removable sleeves of the reactor at a desired position. Argon was admitted through the monomer mixing system at a reactor pressure of 4.6 ± 0.6 Pa and sputtering was performed at a power of 140 watt (current density setting of 175 ± 5 MA) for a period of 20 minutes. The only cleaning operation performed on the Al substrate was by argon sputtering and was done under the same conditions as on the glass substrate. For this, the clean unwrinkled aluminum foil was carefully wrapped over one side of the clean glass slide in such a way that the glazed side of the aluminum foil faced the glass slide. It was determined gravimetrically that argon sputtering under the above discussed conditions does not lead to any significant weight loss of aluminum foil.

After the argon sputtering operation the entire reactor assembly was re-evacuated; and a certain pressure of monomer or feed mixture was built up in the monomer mixing system. The volume of the MMS system used as monomer reservoir was 2.3 liter, a pressure of 300-800 torr (depending on the length and condition of polymerization) was found to be high enough to ensure a constant monomer flow rate throughout a run. For long term high flow rate experiments refilling and minor readjustment of flow was required. When $BrCCl_3$ was used in the feed mixture, the component with the lower mole fraction (i.e. $BrCCl_3$) was admitted first followed by the other component. Enough time (2-8 hrs.) was provided for the mixing of the components of feed mixture. The process of mixing could be accelerated by developing thermal convection currents in the MMS. The polymerization was started by slowly diffusing the reactants into the reactor at a desired flow rate and turning on the diathermy

In Plasma Polymerization; Shen, M., et al.;
ACS Symposium Series; American Chemical Society: Washington, DC, 1979.

unit. The monomer flow rate was computed from a knowledge of the rate of pressure decrease in the MMS during the polymerization. The "partial" flow rate, i.e. the absolute flow rate of one component of a mixture, is calculated from the component composition and the flow rate of the mixture. Since all the experiments reported in this work were conducted at a constant pumping speed, the monomer flow rate was directly related to the pressure in the reactor.

At the end of the experiment; the usual procedure was to turn off the diathermy unit and record monomer mixing system pressure and reactor pressure. The reactant gas in the reactor was left flowing for another 5 minutes after which it was stopped and the reactor evacuated.

The initiation of glow discharge in the reactor was normally accompanied with a change in original reactor pressure. The pressure changes were precisely recorded for all the experiments.

The mass of the deposited polymer on Al-substrate was determined by weighing with a "Cahn Gram Electrobalance" (Cahn Instrument Co., Paramount, California). Infrared spectra of polymers were also recorded, using a Perkin-Elmer Spectrophotometer.

The presence of trapped free radicals in the freshly synthesized polymer films was ascertained by reaction with 1,1,diphenyl-2-picrylhydrazyl(DPPH) (6), by dark interaction with $BrCCl_3$ vapors and by ageing of polymers on exposure to atmosphere. For DPPH interaction the glass and aluminum slides carrying the deposited film were dropped separately in closed containers carrying 1.5×10^{-5} M solution of DPPH in C_6H_6. The transmittance of the resulting solution was measured at 522 nm using a Bausch and Lomb Spectronic-20 photometer. For dark interaction with $BrCCl_3$ the evacuated reactor after polymerization was completely isolated from the rest of the assembly and flushed with $BrCCl_3$ vapors through the secondary inlet system attached to the reactor. An equilibrium pressure of about 30 torr was normally built during this operation. $BrCCl_3$ was kept degassed and frozen in liq. N_2 before it was passed into the reactor. The interaction was continued for a period of about 24 hrs., after which the reactor was again evacuated, and samples examined. The increase in mass of glow discharge polymers on exposure to atmosphere was followed at a relative humidity of $52 \pm 1\%$ (maintained in a desiccator by a saturated solution of $Na_2Cr_2O_7 \cdot 2H_2O$).

Supply of Chemicals: Monomer propylene (CP grade) was purchased from Matheson Gas Products and was used as received. Argon was obtained from Airco Inc. The reagent bromotrichloromethane (99%) was obtained from Aldrich Chemical Company.

In Plasma Polymerization; Shen, M., et al.;
ACS Symposium Series; American Chemical Society: Washington, DC, 1979.

Results and Discussion

The effect of incorporating 0.05 mole fraction of $BrCCl_3$ vapors with propylene in the feed mixture on the rate of polymer deposition at different propylene partial flow rates is illustrated in Fig. 3 and 4. The dashed curve represents the polymer deposition in the absence of $BrCCl_3$ vapors. Increased rate of polymer deposition in the presence of $BrCCl_3$ is observed at all flow rates irrespective of substrate position. The data obtained in Fig. 3 were obtained by putting substrate into the center of the discharge (O-position) and at 13.5 cm. from the O-position. At high flow rates an increase in the rate as high as 400% is observed. The color of the polymer obtained in the presence of $BrCCl_3$ varied from deep yellow to reddish brown in contrast to an almost colorless polymer obtained from pure propylene at high flow rates. The adhesion of polymer (obtained in presence of $BrCCl_3$) to the glass substrate is poor at all flow rates which is in accord with our experience (17) that the best quality of adhesion is achieved only under conditions where the deposition rate decreases with increase in flow rate. Since there is no negative slope observed in the deposition curve in the presence of $BrCCl_3$, the adhesion remains poor and the film peels off in a short time.

Fig. 4 shows the variation of deposition rate as a function of $BrCCl_3$ concentration in the feed mixture. The monomer partial flow rate (325 ± 5 μmol/min) substrate position and time of polymerization were kept constant. A linear relationship is observed up to a $BrCCl_3$ concentration of 7% by volume when the substrate is kept right underneath the electrode. As the substrate is moved from the center of the electrode the effect of $BrCCl_3$ concentration on the rate is less and progressively falls away from a linear dependence, apparently approaching a limiting value.

Since $BrCCl_3$ itself shows no tendency to polymerize in the glow discharge, the above results show that $BrCCl_3$ acts as a gas phase initiator for the glow discharge polymerization of propylene. The diminution of deposition rate as the substrate is moved away from the electrode suggests radical termination processes that lower the concentrations of some of the actual species in the gas phase. The production of resonance stabilized trichloromethyl radicals and bromine atoms by the photodecomposition of $BrCCl_3$ is a well documented process (ΔH=49.5 kcal/mole) (18). The formation of α-bromoalkyl benzene on UV irradiation of a mixture of $BrCCl_3$ and alkylbenzene has been found to proceed by a free radical mechanism (19). The increased rate of propylene polymer deposition in the presence of $BrCCl_3$ may therefore be due to the following radical reactions occuring in glow discharge:

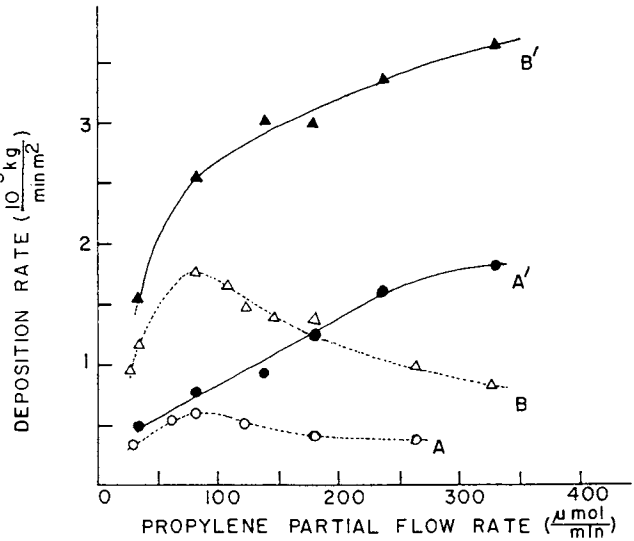

Figure 3. Variation of polymer deposition rate as a function of monomer partial flow rate: Curves A and B represent pure propylene polymerization and curves A′ and B′ refer to polymerization of propylene in the presence of 5 mol % $BrCCl_3$. Substrate positions 0 cm (Curves B and B′) and 13.5 cm (Curves A and A′) from electrodes were used and the time of polymerization was 90 min.

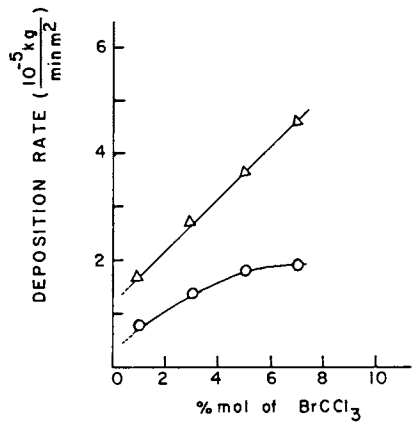

Figure 4. Effect of $BrCCl_3$ concentration in feed mixture on the rate of propylene polymer deposition: (△) refers to the substrate at 0 position and (○) refers to substrate 13.5 cm away from electrodes. Propylene partial flow rate was 325± μmol/min, and time of polymerization was 90 min.

In Plasma Polymerization; Shen, M., et al.;
ACS Symposium Series; American Chemical Society: Washington, DC, 1979.

$$BrCCl_3 \longrightarrow Br^{\cdot} + {}^{\cdot}CCl_3$$

$$Br^{\cdot} \text{ or } CCl_3^{\cdot} + CH_3CH{=}CH_2 \longrightarrow C_3H_5^{\cdot} + \begin{matrix} HBr \\ \text{or} \\ CHCl_3 \end{matrix} \quad \text{etc.}$$

It is believed that the hydrogen abstraction from monomer resulting in the formation of C_3H_5 radicals is a vital step in the propylene glow discharge polymerization, which is facilitated by the presence of Br and CCl_3 radicals. The chain transfer reactions of $BrCCl_3$ would be less frequent than the propagation reactions at the used concentration of $BrCCl_3$, which is relatively low in the feed mixture compared to the monomer. A similar enhancement in polymer deposition by including halogens or halogen-containing compounds has been reported by other workers (9, 10, 11).

While the assumption that $BrCCl_3$ performs in the glow discharge polymerization in the same manner as in conventional chemistry is questionable. The more important evidence in favor of a radical mechanism was provided by the dark (in the absence of glow discharge) interaction of $BrCCl_3$ vapors with freshly polymerized propylene sample. The mass of the deposited polymer (4.95 mg/cm^2) on Al-substrate after $BrCCl_3$ interaction was about 100 times more than the expected amount of polymer at the polymerization condition of the experiment (propylene flow rate 57 μmol/min, reactor pressure 20±2 mtorr, substrate position at center of electrodes, and time 4 hours). It was visually noticed (by the color change of film) that the interaction starts almost instantaneously developing brown deposits at the surface of aluminum. The mass of interacted polymer kept increasing at a very fast rate even after it was removed from the reactor and left in air. In a period of about 24 hours the increase in mass was more than its original value. The mass of the polymer reached a saturation value of about 11 mg/cm^2 in a period of 1 week. The Al-foil slowly became corroded at reaction sites. Attempts to remove brown polymeric material often resulted in cracking the Al-substrate. Similar results were observed on interaction of a low flow rate polymerized ethylene sample with $BrCCl_3$ (20). Since no such interaction of Al-substrate itself with $BrCCl_3$ liquid and even $BrCCl_3$ glow discharge was observed the following mechanism involving chain transfer reactions(21) may account for the increase in mass of the polymer:

In Plasma Polymerization; Shen, M., et al.;
ACS Symposium Series; American Chemical Society: Washington, DC, 1979.

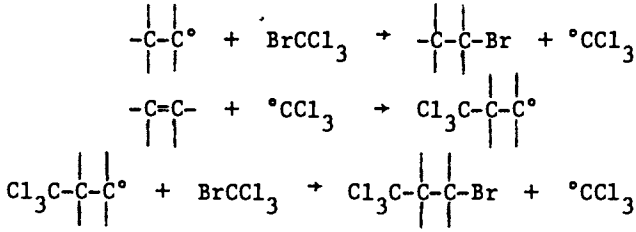

Surprisingly it was noticed that high flow rate polymerized propylene (flow rate 231 μmol/min) which had an excellent adhesion to Al-substrate did not show any significant dark interaction with $BrCCl_3$. While the surface study of the polymer obtained under different reaction conditions is in progress it is reasonable to assume that the high flow rate-obtained glow discharge polymer has reached a certain degree dimensional and chemical stability. The results with ethylene parallels propylene. Under the conditions leading to excellent polymer adhesion to the Al-substrate (high monomer flow rate 516 μmol/min) no dark interaction with $BrCCl_3$ was observed.

The residual free radical activity in glow discharge polymers is also indicated by DPPH measurements, IR spectroscopy and by mass increase of glow discharge polymers on standing in air. The slow increase in transmittance of the DPPH solution on interaction with all samples indicates that the free radicals are not all available at the surface of polymer but are encaged in the body of crosslinked structure. However, the results cannot be considered as conclusive since a blank DPPH/C_6H_6 solution also showed an increase in transmittance (although at a slower rate). Such an increase in transmittance may also be expected by greater solubility of oxygen in the polymer.

Infrared spectra of all glow discharge polymers developed broad absorption bands corresponding to -OH and -C=O functional groups as storage time elapsed. All polymeric samples, irrespective of the conditions of polymerization showed an increase in mass on exposure to air (which sometimes rises to 25% over a period of 3 months). These results have been discussed in detail elsewhere (20).

Rates of polymer deposition of monomers propane and propyne (both purchased from Matheson Gas Products) at a reactor pressure of 44 ± 2 mtorr (time 1 hour) were compared with that of propylene under identical conditions. The following observed relation is in accordance with a free radical mechanism and is similar to the ranking published in

In Plasma Polymerization; Shen, M., et al.;
ACS Symposium Series; American Chemical Society: Washington, DC, 1979.

the literature (5) for ethane, ethylene and acetylene series: propyne > propylene > propane, in rate of deposition.

The exact mechanism of propylene glow discharge polymerization is not known. The presence of a terminal acetylene (presumable propyne) in the gaseous products of propylene polymerization was indicated by the interaction of the cold trap gaseous condensates with 1% alcoholic or ammoniacal $AgNO_3$sol.(22) after the polymerization was over. An immediate formation of an explosive silver acetylide was detected. Intermediate formation of propyne is also indicated by the IR spectra of the yellow relatively less volatile liquid left in the cold trap after the polymerization was over. Sharp but weak absorptions at 3310 cm^{-1} and 1270 cm^{-1} are indications of a substituted acetylenic compound. The IR spectra of the yellow liquid also points to the presence of mono, di- and tri-substituted aromatic compounds in the mixture (i.e. sharp absorption bands at 3080 cm^{-1}, 1640 cm^{-1}, 920 cm^{-1}, 810 cm^{-1} and a multiple band in the 1000-1120 cm^{-1} region are observed). The NMR spectra in deuterated acetone indicated the presence of an aromatic nucleus in the yellow liquid obtained from the cold trap. The formation of aromatic compounds can be explained if a propynylic intermediate is involved.

It was also observed that the walls of a cold trap cooled with liquid nitrogen develops a black or highly reflective metal-like mirror coating during polymerization. The mirror formation is very sensitive to reaction conditions but is accelerated when $BrCCl_3$ is present in the feed mixtures. Slow evaporation of the cold trap condensate content (as the liq. N_2 level goes down) due to continuous mechanical pumping results in the mirror forming just above the liquid nitrogen level. The coating which remains shiny even after exposure to air is insoluble in all common solvents and dissolves only slightly in warm concentrated H_2SO_4.

The formation of the propynylic intermediate is also indicated by the fact that polymerization of gaseous products (obtained during prior propylene polymerization) in the cold trap give deposition rates which are greater than that of the pure propylene.

It seems reasonable to assume that the propylene polymerization proceeds via the formation of propyne and H_2 is the uncaptured gas product. The change in the reactor pressure (ΔP) often encountered on initiation of glow discharge during polymerization depends on the original reactor pressure, but more important on the position of the pressure guage used for monitoring the reactor pressure. In the vicinity of RF source the pressure change (ΔP) is mostly positive while at the farthest end of the reactor tube it passes from a negative to a positive value with increasing flow rate. The magnitude of the pressure change depends on monomer flow rate and other reactor conditions. Presence of absorbed vapor leads to a change in magnitude of ΔP..

In Plasma Polymerization; Shen, M., et al.;
ACS Symposium Series; American Chemical Society: Washington, DC, 1979.

Presence of $BrCCl_3$ in the feed mixture, which promotes polymerization, gave a negative value of pressure change at all the flow rates when measurements were done at the farthest end of the reactor. These results vitiate the proposed classification (16) of monomers based on the direction of pressure change on initiation of glow discharge, since both propylene and ethylene were found to show increase as well as decrease in reactor pressure on initiation of glow discharge depending on polymerization conditions.

Summary

Glow discharge polymerization of propylene in an electromagnetically coupled tubular reactor, operating at a radio-frequency of 27·1 MHz, is described. Evidence for a free radical polymerization mechanism is given which also includes the interaction of bromotrichloromethane with a freshly polymerized propylene sample during the dark period after glow discharge operation. An analysis of the gaseous product of polymerization indicates that the glow discharge polymerization of propylene most probably proceeds via a propynylic intermediate.

Acknowledgements

The work was partly supported by a University of Missouri-Kansas City Faculty Research Grant (E.W.H.).

"Literature Cited"

1. Kolotyrkin, V. M., A.B. Gilman, and A. K. Taspuk, Russian Chemical Reviews, (1967), 36 (8), 579.

2. Mearns, A.M., Thin Solid Films, (1969), 3 (3), 201.

3. Mayhan, K. G., M. E. Biolsi, and M. R. Havens, J. Vac. Sci. Technol., (1976), 3 (2), 575.

4. Yasuda, H., J. Macromol. Sci.-Chem., (1976), A10 (3), 383.

5. Kobayashi, H., A. T. Bell and M. Shen, Macromol. (1974), 7, 277.

6. Denaro, A. R., P. A. Owens, and B. Crashaw, Eur. Polym. J., (1968), 4, 93.

7. Yasuda, H., M. O. Bumgarner, H.C. March, and N. Morosoff, J. Polym. Sci. Polym. Chem., Ed., (1976), 14, 195.

8. Stille, J. K., R. L. Sung, and J. Vander Kooi, J. Org. Chem., (1965), 30, 3116.

9. Hays, P. M., Advan. Chem. Ser. (1969), 80, 350.

10. Brown, K.C., Eur. Polym. J., (1971), 7, 363.

11. Kobayashi, H., M. Shen, and A. T. Bell, J. Macromol. Sci.-Chem., (1974), A8 (8), 1345.

12. Brown, K. C. and M. J. Copsey, Eur. Polym. J., (1972), 8, 129.

13. Smolinsky, G. and M. J. Vosile, Int. J. Mass Spectrom. Ion Phys., (1973), 12, 133.

14. Westwood, A. R., Eur. Polym. J., (1971), 7, 363.

15. Thompson, L. F. and K. G. Mayhan, J. Appl. Polym. Sci., (1972), 16, 2317.

16. Yasuda, H. and C. E. Lamaze, J. Appl. Polym. Sci., (1973), 17, 1519.

17. Sharma, A. K., Frank Millich, and Eckhard W. Hellmuth, J. Appl. Phys., (1978), 49, 5055.

In Plasma Polymerization; Shen, M., et al.;
ACS Symposium Series; American Chemical Society: Washington, DC, 1979.

18. Sharma, A. K., A. Hahn, F. Millich, and E. W. Hellmuth, Bull. Am. Physical Soc., (1978), 23, 267.

19. Stirling, C. J. M., "Radicals in Organic Chemistry", Oldbourne Press, London, 1965.

20. Sharma, A. K., Frank Millich and Eckhard W. Hellmuth, ACS Polymer Preprints (1978), 19 (2), 435.

21. Skinner, W. A., E. Bishop, D. Teiszen, and J. D. Johnston, J. Org. Chem., (1958), 23, 1710.

22. Kleinberg, J. (Editor), "Organic Experiments," 31, D.C. Heath and Co., London, 1974.

RECEIVED April 27, 1979.

The Formation Mechanism of Styrene Polymer Film by Glow Discharge Direct Method

K. TSUNETO and I. TANIGUCHI

Department of Electronics, Doshisha University, Kyoto, Japan

A wide variety of organic polymer thin films have been formed in a glow discharge. In 1960, Goodman described the formation of films in a glow discharge from hydrocarbon vapors (1). In 1963, Bradley et al. described films produced from many organic substances in a glow discharge (2).

Polymerized thin films have been formed by several methods such as glow discharge, photolysis, electron bombardment and vacuum evaporation. The films formed in a glow discharge are pinhole free and possess a number of unique and desirable properties. The glow discharge methods are also simpler than the other methods from a processing point of view.

Two different methods are used to form thin films in a glow discharge method, an a.c. or d.c. glow discharge is initiated between the electrodes, and the electrodes serve as the substrate for film formation. In the indirect method, the substrate is placed in the plasma formed by two electrodes or by an electrodeless discharge, and the polymerized film is formed on the substrate. The growth rate of film is greater with the direct method, and it is easier to control the film thickness with the direct method. On the other hand, insulator materials can be used as substrates only in the indirect method. Also the bombardment of charged particles affects the film formation less in the indirect method than in the direct method.

The general properties of polymer films formed in glow discharges have gained much attention, but rather few investigations of the formation mechanism have been made. It is desirable to understand the mechanism of film formation in order to improve film properties and stabilize film formation.

Christy's theory of polymerization by electron bombardment contains an important idea which can be applied to the theory of direct glow discharge polymerization (3). Williams and Hayes emphasized the importance of monomer adsorption to the electrode in the direct method (4). Poll also described the process of film formation in the direct method (5). Yasuda et al. employed the indirect method, using an electrodeless discharge, and the results

0-8412-0510-8/79/47-108-065$05.00/0

showed that polymerization in the vapor phase was important (6). Morita et. al proposed a formation mechanism in both the direct and indirect methods using Poll's model (7).

The conclusions of previous investigations of the polymerization mechanism are:
1) Organic monomer is adsorbed on the surface of an electrode, and polymerization proceeds by bombardment of positive ions.
2) Polymerization occurs in the gas phase and polymerized particles deposits on the substrate surface.
In general the two mechanisms described above coexist in a glow discharge. The former mechanism predominates in the direct method and the latter predominates in the indirect method.

This paper is primarily concerned with the direct method of glow discharge polymerization. The bombardment of positive ions plays an important role in film formation by the direct method as mentioned above, but the bombarding ion itself and the reactive species in the gas phase may contribute to film formation. The relative importance of these factors depends on the discharge conditions. A theoretical equation for the growth rate of film will be presented from a phenomenological point of view and compared with experimental results. The theory takes into account bombardment by ions and transport of ions.

Theory of film growth rate

This theory is an extension of Christy's model, which takes electron bombardment in the account. The bombarding electrons do not contribute to film formation. His experiments were done at a vapor pressure of about 10^{-5} Torr so reactions in the vapor phase were insignificant. However, the bombardment of positive ions at the cathode plays a leading role and the bombarding ions themselves possibly contribute to film formation. It is possible that ions combine with other particles or grow into large ions. Electron bombardment at the anode is unimportant because the film is formed mainly on the cathode, as shown by d.c. glow discharge experiments.

The equation for film growth rate must include the effects of ion bombardment and ion transport. Let P be the number of molecules per unit area which have been polymerized. The time variation of these molecules is given by

$$\frac{dP}{dt} = \sigma N i_p + \beta i_p \qquad (1)$$

where N is the number of adsorbed molecules on the electrode surface per unit area, i_p is the flux of ions, σ is the collision cross section for polymerization, β is the rate of polymerization by transport of one ion. The behavior of the adsorbed molecules on the electrode surface is given by

$$\frac{dN}{dt} = \gamma F - \frac{N}{\tau} - \frac{dp'}{dt} \qquad (2)$$

In Plasma Polymerization; Shen, M., et al.;
ACS Symposium Series; American Chemical Society: Washington, DC, 1979.

where F is the number of molecules per unit area per unit time striking the electrode surface, γ is the sticking coefficient of molecules to the electrode surface, τ is the mean life time of adsorption, P' is the number of molecules per unit area polymerized by ion bombardment. In Eq. (2), β is not included in dP'/dt since dN/dt is not influenced by the transport of ions.

From Eq. (1) and Eq. (2) we get N and dP'/dt(τ<<t) and by adding βi_p to dP'/dt we get dP/dt. Defining the growth rate of film we have

$$R = V \cdot dP/dt \tag{3}$$

$$R = \left(\frac{\gamma \cdot F}{1+1/\sigma \cdot \tau \cdot i_p} + \beta \cdot i_p\right)V \tag{4}$$

$$N = \frac{\gamma F \cdot \tau}{1+\sigma \cdot \tau \cdot i_p} \tag{5}$$

where V is the volume of one polymer molecule. The growth rate of film and the number of density adsorbed monomer for various discharge conditions are shown in Table I, assuming that α, β and γ are constant. Table I suggests the following observations:

Table I. Theoretical equations for growth rate.

	$\sigma\tau i_p < 1$	1	$\sigma\tau i_p > 1$
$N < \frac{1}{A}$	$R \simeq (\gamma F \sigma\tau + \beta) V i_p$ $N \simeq \gamma F \tau$ (a)		$R \simeq (\gamma F + \beta i_p) V$ $N \simeq \frac{\gamma F}{\sigma i_p}$ (c) $\left(\frac{\gamma F}{i_p} \leq \frac{\sigma}{A}\right)$
$N \geq \frac{1}{A}$	$R \simeq \left(\frac{\sigma}{A} + \beta\right) V i_p$ $N \simeq \frac{1}{A}$	(b)	$R \simeq \left(\frac{\sigma}{A} + \beta\right) V i_p$ $N \simeq \frac{1}{A}$

1) In cases of high substrate temperature or low vapor pressure at low current density, i.e. $\sigma\tau i_p$ <<1, as shown in Table I(a), the growth rate of film depends on the temperature and the vapor pressure. At a very high temperature, when $\gamma F\sigma\tau$<<β, the growth rate does not depend on temperature.

2) At a low substrate temperature or high vapor pressure, as shown in Table I(b), the number of adsorbed monomers on the substrate increases. When the surface is covered uniformly with a monolayer of monomer, the number of adsorbed monomers N reaches 1/A, where A is the geometrical cross section of monomer. The

In Plasma Polymerization; Shen, M., et al.;
ACS Symposium Series; American Chemical Society: Washington, DC, 1979.

growth rate does not depend on the vapor pressure or the temperature.
3) At high current density i.e. $\sigma\tau i_p >> 1$, which as shown in Table I(c), all the adsorbed monomer is polymerized. Change in the growth rate of film is due only to the transport term.

Experimental

Our experiments were carried out in a bell jar under controlled pressures of organic monomer. A schematic diagram of the apparatus is shown in Fig. 1. Styrene gas was used as the monomer. The vapor pressure was determined by a Pirani guage which was calibrated by the saturated vapor pressure to temperature the characteristics of the organic monomer source. When the discharge contained a mixed gas, first styrene monomer and then Ar or He was introduced into the bell jar. Glass coated slides with evaporated aluminum were used as substrates. The film thickness was measured by multiple beam interferometry. The mean value of the discharge current was measured by a frequency calibrated d.c. am meter. A quartz crystal deposition monitor was used to measure the adsorption of styrene monomer. The quartz crystals were heat treated prior to experiments, in order to avoid errors due to the adsorption of water or other condensibles. The first half of our experiments were performed at a frequency of 1 KHz, with a guard electrode placed around a 1 cm^2 substrate. In some experiments, the quartz crystal was used as a substrate. In the experiments which measured the growth rate of film vs. frequency, the substrate area was 5 cm^2 and no guard electrode was used. The aluminum coated plate used to measure film thickness was 0.5 cm wide and was placed on the substrate. In most experiments the spacing between electrodes was 1 cm. Other electrode spacings are noted in the results. Values of the cross section of styrene monomer and the volume of styrene polymers were calculated from the specific gravity of styrene.

Results and Discussion

The adsorption isotherm of styrene monomer is shown in Fig. 2. The result is similar to a BET isotherm. At room temperature and a styrene vapor pressure of $0.3 \sim 0.4$ Torr the electrode surface is covered with a monolayer of styrene.

Fig. 3 shows the growth rate of film as a function of styrene vapor pressure for the conditions described in Table I(a). In this experiment the quartz crystal is used as the discharge electrode. The equation in Table I(a) is rewritten:

$$\frac{R}{Vi_p} = \gamma \cdot \sigma \cdot \tau F + \beta \qquad (6)$$

If R/Vi_p is plotted against F ($\propto P$), the value of β can be determined from the intercept at P=0. The value of $\beta=2.2$ is obtained from Fig. 3 by a least squares fit.

Fig. 4 the effect of substrate temperature is shown. The

In Plasma Polymerization; Shen, M., et al.;
ACS Symposium Series; American Chemical Society: Washington, DC, 1979.

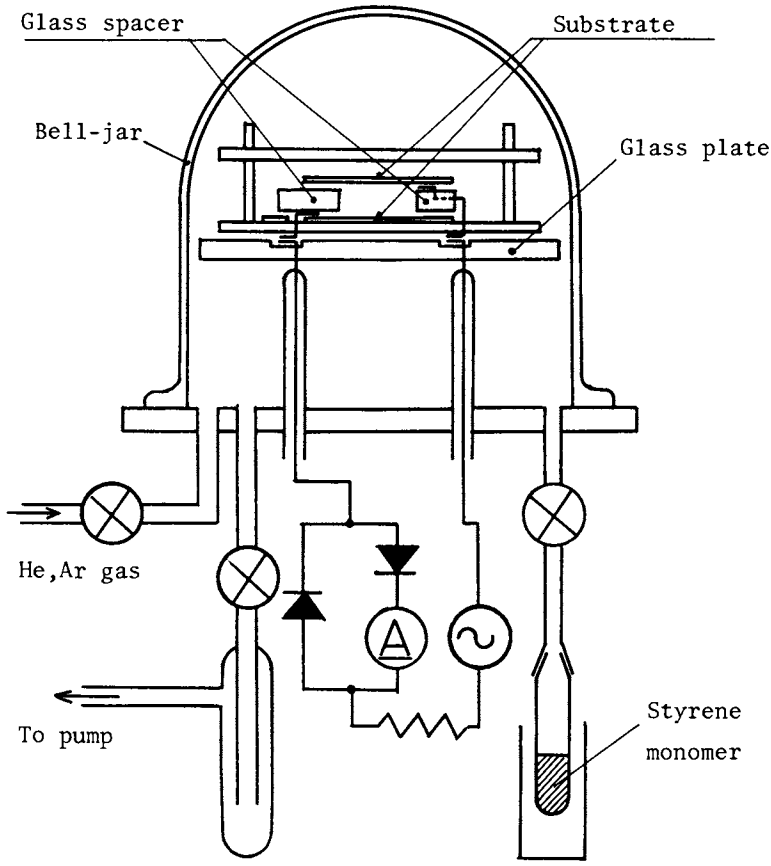

Figure 1. Schematic of the apparatus

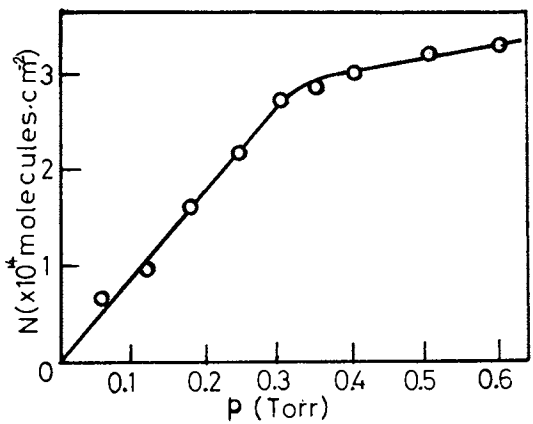

Figure 2. Relationship between the number of adsorption monomers (N) and the vapor pressure of styrene (P)

In Plasma Polymerization; Shen, M., et al.;
ACS Symposium Series; American Chemical Society: Washington, DC, 1979.

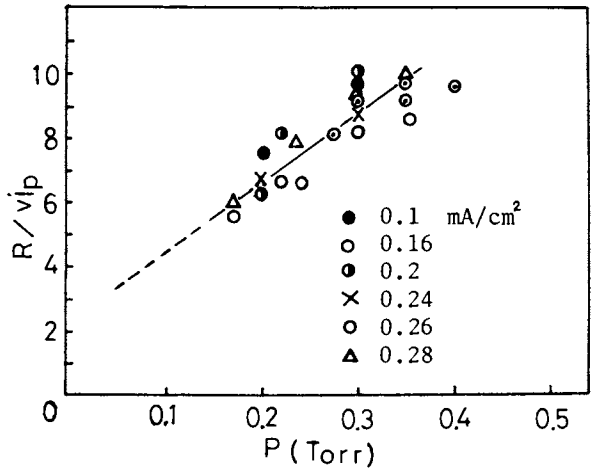

Figure 3. Relationship between the growth rate (R) *and styrene vapor pressure* (p)

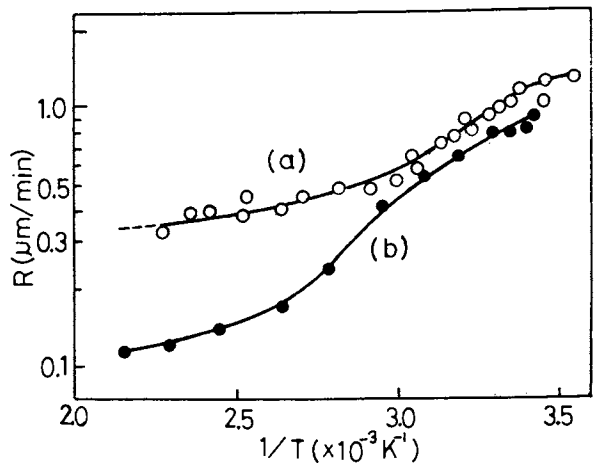

Figure 4. Relationship between the growth rate (R) *and reciprocal temperature of the substrate. (a) Styrene: 0.5 torr, (b) styrene: 0.17 torr + He 3 torr; 0.5 mA/cm².*

In Plasma Polymerization; Shen, M., et al.;
ACS Symposium Series; American Chemical Society: Washington, DC, 1979.

region of the constant film growth rate at low temperatures is assumed to occur for a monolayer coverage of styrene monomer. This is explained by the equation indicated in Table I(b). As substrate temperature is increased monomer adsorption decreases and the growth rate of film also decreases. This is predicted by the equation in Table I(a). At still higher substrate temperatures, the growth rate of film becomes constant as only the β term remains in Eq. (4). A value of $\beta=2.4$ was obtained from Fig. 4. A value of $\sigma=230$ A^2 was obrained from the value of β and the constant growth rate at the low substrate temperature. Consequently, it is shown that the bombardment of one ion corresponds to the polymerization of about 5 to 6 monomer units, in the case of styrene.

When $\beta=1$, the ions which bombard the electrode are incorporated into the film. When $\beta>1$ the existence of other mechanism in the vapor phase is suggested, for example, the formation of ion clusters. If the reaction in the vapor phase is rapid, powder particles may form, which can incorporate into the film making it cloudy.

Williams and Hayes (4) have described a method for preventing species which are produced in the negative glow from being incorporated into the film. This may be achieved by working in an atmosphere of monomer and inert gas; the monomer being present at very low partial pressure.

The effect of the substrate temperature for a discharge containing a mixture of styrene and helium is shown in Fig. 4. The fact that $\beta\simeq0.4$ in this case indicates that the influence of vapor phase polymerization decreases as was expected.

The activation energy obtained from the decreasing region of the growth rate curve in Fig. 4 is about 6 Kcal/mol. This is an appropriate value for the energy of physical adsorption of styrene monomer.

In Fig. 5 the film growth rate is plotted against discharge current in order to obtain a value for the sticking coefficient γ. Argon was mixed with styrene to obtain a stabilized discharge. The intercepts of the assymptotic part of R in Fig. 5 give a value of $\gamma=2\times10^{-4}$.

Poll obtained a value for γ the same order of magnitude using tetrafluoroethylene (C_2F_4). We also obtained a value of $\tau=10^{-2}$ sec from the values of β, γ and σ at room temperature.

From the calculated value of the constants β, γ and σ, it is concluded that under the discharge conditions shown in Fig. 5, about 3/4 of the film volume is formed by ion bombardment and about 1/4 of the film volume is formed by ion transport.

Fig. 6 shows the dependence of film growth rate on discharge frequency. The growth rate increases with increasing frequency in the low frequency region and reaches a maximum beyond which the growth rate decreases with increasing frequency. Moreover, it is observed that the position of the maximum shifts as the electrode spacing vapor pressure and discharge current density are changed.

In Plasma Polymerization; Shen, M., et al.;
ACS Symposium Series; American Chemical Society: Washington, DC, 1979.

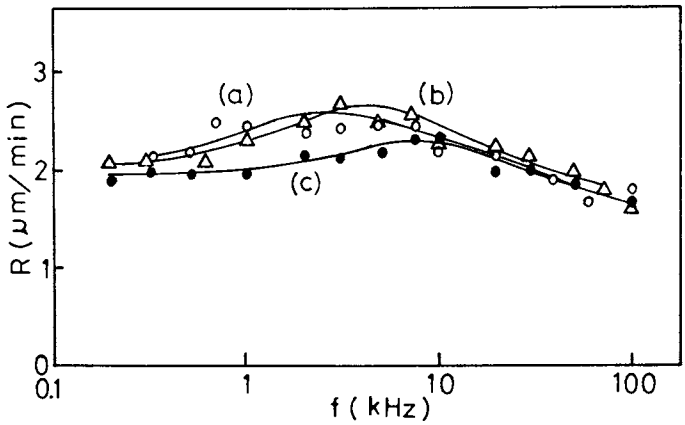

Figure 5. Relationship between the growth rate (R) *and the discharge current* (i_p). *(a) Styrene 0.4 torr + Ar 3 torr, (b) styrene 0.3 torr + Ar 3 torr, (c) styrene 0.13 torr + Ar 3 torr.*

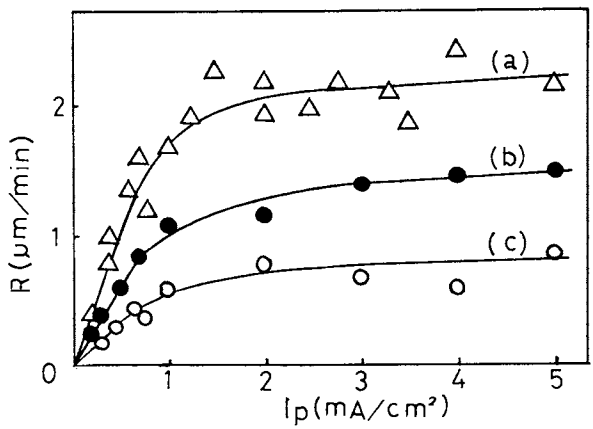

Figure 6. Relationship between the growth rate (R) *and the frequency* (f). *Styrene: 0.9 torr. The distance of electrodes: (a) 1 cm, (b) 0.7 cm, (c) 0.5 cm. 0.4 mA/cm².*

In Plasma Polymerization; Shen, M., et al.;
ACS Symposium Series; American Chemical Society: Washington, DC, 1979.

In Fig. 6 the position of the maximum shifts for different electrode spacings. As the spacing between electrodes decreases, the maximum occurs at higher frequencies. For each electrode spacing shown in Fig. 6, the length of the cathode fall was almost the same. Therefore the frequency at which the growth rate is maximized is inversely proportional to the transit time for ions in the region exclusing the cathode fall.

The films formed at frequencies higher than the maximum became cloudy and appeared different from those formed at lower frequencies. The aluminum plated substrates used for measuring film thickness may have increased the strength of the electric field around the substrate, affecting the size of styrene ion clusters formed in the vapor phase. The growth rate in this case decreased at higher frequency because the larger clusters could not reach the substrate. This explains the gradual decrease in film growth rate (in Fig. 6(a)) at frequencies above 1 KHz. At frequencies above about 10 KHz, the growth rate decreased more rapidly. This is explained by the rapid decrease in the numbers of ions which reached the electrode. The appearance of the film was different from that formed at frequencies less than 10 KHz. Near the corner or side of the substrate a substance like viscous powder was deposited. This powder could be removed easily and little film was formed under this powder. It was also observed that a mist occurred in the discharge and the polymerization in the vapor phase became more vigorous at higher frequencies.

Fig. 7 shows the dependence of film growth rate on frequency for mixtures of argon and helium containing about 5% styrene vapor. In the case of argon, the growth rate was nearly constant and the film was apparently formed by the bombardment of argon ions only. In the case of helium, the variation of the growth rate was similar to that of pure sytrene. It seems that the styrene monomer is more easily ionized in helium than in argon. The discharge in argon is more stable though than in helium.

The decrease in ion current in the high frequency region can be treated analytically (see Appendix). We assume that the discharge current, which is a sum of ion current and electron current, is constant. The results are shown in Fig. 8. From this figure we set the relative ion current at 1 KHz equal to 1. In the case of styrene, the tendency for the ion current to decrease is similar to the results of the experiment shown in Fig. 6. The change in electrode spacing is inversely proporational to the change in frequency.

In order to get desirable films, it is necessary to choose carefully discharge conditons in the direct method as follows. The discharge frequency must be below the maximum in the frequencies, however, ion cause film damage by the occurrence of spark discharges. It is desirable to have the electrode spacing as narrow as possible. If possible, the discharge should be limited to the cathode fall region. This also helps to prevent the occurrence of spark discharges.

In Plasma Polymerization; Shen, M., et al.;
ACS Symposium Series; American Chemical Society: Washington, DC, 1979.

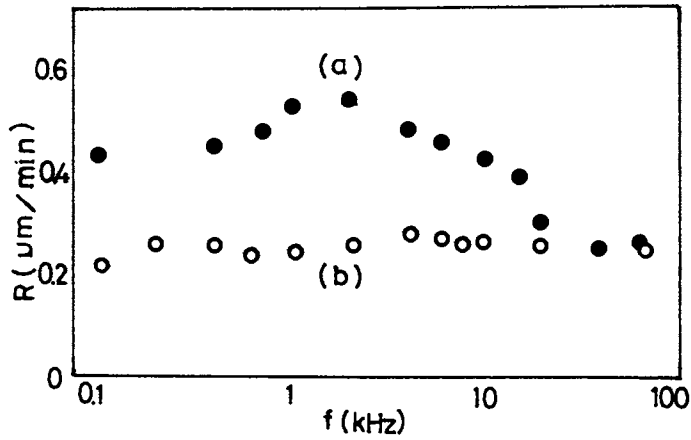

Figure 7. Relationship between the growth rate (R) and the frequency (f) in the case of mixed gas. (a) Styrene 0.17 torr + He 3 torr, (b) styrene 0.17 torr + Ar 3 torr. 0.2 mA/cm².

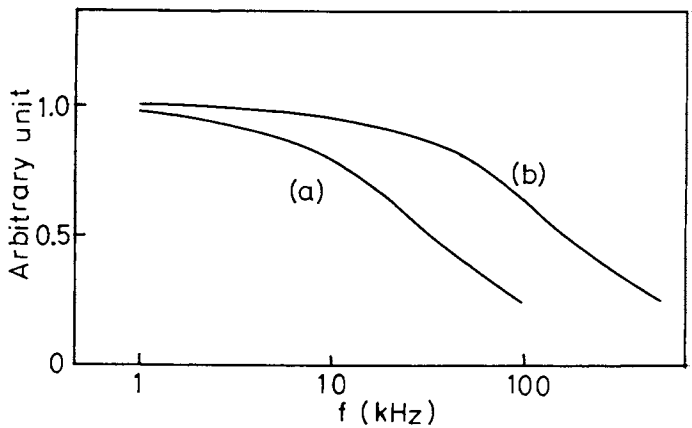

Figure 8. The calculated ion current. The distance of electrodes: (a) 1 cm, (b) 0.2 cm.

In Plasma Polymerization; Shen, M., et al.;
ACS Symposium Series; American Chemical Society: Washington, DC, 1979.

As vapor pressure increases, the length of the cathode fall region decreases. The effect is the same as increasing the electrode spacing. At low vapor pressure, the electrode surface is covered with a monolayer of monomer. Therefore, a change in substrate temperature causes a change in film thickness. The appropriate vapor pressure in our experiment was about 0.5 to 1 Torr.

On the other hand, it is known that the state of the film changes with vapor pressure. At high vapor pressure, the film becomes soft and viscuous, since unreacted monomer is incorporated into the growing film. At low vapor pressure, the film becomes hard and brittle since the number of bombarding ions is in excess of that required to make every adsorbed monomer react. From this point of view, it is desirable to maintain high discharge current density within the limit of damage or degradation of the film. The increase in discharge current density also decreases the number of residual ions between the two electrodes.

In our experiment glass spacers were used to support the electrodes, but it is desirable to avoid their use because the surface of film formed near the spacer sometimes became cloudy.

Conclusions

The growth rate of film formed by the direct glow discharge method has been explained on the basis of Christy's theory, taking into account the effect of ion transport. In the direct method the film is formed mostly by the bombardment of positive ions. The variation in the film growth rate for various discharge conditions can be associated with the variation in monomer adsorption. The effect of ion transport can not be neglected. In our experiment at 1 KHz, about 1/4 of the film volume could be attributed to ion transport. The effect of the discharge frequency on film growth rate and film appearance was significant. This is closely related to the number of residual ions between the electrodes and the degree of polymerization in the vapor.

Appendix

The basic equations are:

$$i_i = q\bar{n}_i v_i \qquad \text{(A-1)}$$

$$m_i\left(\frac{dv_i}{dt}\right) + \nu_i v_i = qE \qquad \text{(A-2)}$$

$$\bar{n}_i = \bar{Z}t - \frac{1}{qd}\int i_i dt \qquad \text{(A-3)}$$

i_i: the ion current density.

q : the ion charge.

$\bar{n}_i$: the space average ion density.

In Plasma Polymerization; Shen, M., et al.;
ACS Symposium Series; American Chemical Society: Washington, DC, 1979.

v_i: the ion velocity.

ν_i: the ion collision frequency.

m_i: the ion mass.

E : the field strength (except for cathode fall).

D : the distance between electrodes (except cathode fall).

$\bar{z}$: the average value of the number of ionizations per unit time per unit volume.

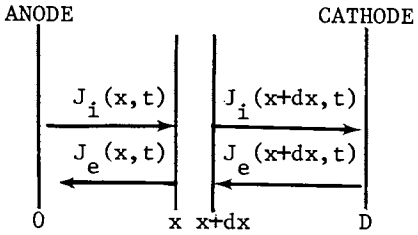

Fig. (A-1) Diagram illustrating the flux density of ions and electrons at x and x+dx.

Eq. (A-3) is given by the following treatment. In Fig. A-1, the number of electrons and ions generated between x and x+dx is given by

$$\frac{\partial}{\partial t}(n_i(x,t))dx = -\frac{\partial}{\partial x} J_i(x,t)dx + Z(x)dx \qquad (A\text{-}4)$$

where $J_i(x,t)$ is the flux density of ions, $n_i(x,t)$ is the ion density, $z(x)$ is the number of ionizations per unit time per unit volume. On integrating Eq. (A-4) we get

$$\frac{\partial}{\partial t}\int_0^D n_i(x,t)dx = -J_i(D,t) + \int_0^D Z(x)dx \qquad (A\text{-}5)$$

where Eq. (A-6) is used as a general property for glow discharges.

$$J_i(0,t) = 0 \qquad (A\text{-}6)$$

If we use the defining expressions given by Eq. (A-7), (A-8) and (A-9), then

$$J_i(D,t) = J_i(t) \qquad (A\text{-}7)$$

$$\frac{1}{D}\int_D^0 n_i(x,t)dx = \bar{n}_i(t) \qquad (A\text{-}8)$$

$$\frac{1}{D}\int_D^0 z(x)dx = \bar{Z} \qquad (A\text{-}9)$$

Eq. (A-3) may be obtained upon changing the flux density of ions to the ion current density.

In Plasma Polymerization; Shen, M., et al.;
ACS Symposium Series; American Chemical Society: Washington, DC, 1979.

From Eq. (A-1), Eq. (A-2) and Eq. (A-3), we get

$$i_i dt = \left[\frac{A\bar{Z}}{\alpha} \; t(1-\frac{\alpha}{\alpha-\nu} \; e^{-\nu t})-(\frac{1}{\alpha} - \frac{\alpha}{(\alpha-\nu)^2} \; e^{-\nu t}) \right.$$

$$\left. + (\frac{1}{\alpha} - \frac{\alpha}{(\alpha-\nu)^2} \;)e^{-\alpha t} \right] \exp(-\alpha_o e^{-\nu t}) \qquad \text{(A-10)}$$

where

$$A = \frac{q^2 E}{m_i \nu_i} \qquad \alpha = \frac{qE}{m_i \nu_i D} \qquad \alpha_\bullet = \frac{qE}{m_i \nu_i^2 D}$$

If we assume that the discharge current is given by Eq. (A-11), then we get Eq. (A-12)

$$i_i = \frac{1}{T} \int_o^T i_i dt \qquad \text{(A-11)}$$

$$= qD\bar{Z} \left[1 + \alpha_\bullet e^{-\nu T} - \frac{1}{\alpha T}(1-e^{-\alpha T})\right] \exp(-\alpha_o e^{-\nu_i t}) \qquad \text{(A-12)}$$

The electron current I_e is given by the same treatment described above.

The results shown in Fig. 8 are calculated for a condition of constant discharge current. The values used in the calculations are as follows:

$E = 3000$ V/m

$D = 0.01$ and 0.002 m

$\nu_e = \frac{V_e}{\lambda_e} = 3 \times 10^8$ sec

$\nu_i = \frac{v_i}{\lambda_i} = 10^7$ sec

$m_i = 1.7 \times 10^{-25}$ kg

References

1. Goodman, J., J. Polym. Sci., (1960), 44, 551.
2. Bradley, A., and Hammes, J.P., J. Electrochem. Soc., (1963), 110, (No. 1), 15.
3. Christy, R.W., J. Appl. Phys., (1960), 31, 1680.
4. Williams, T. and Hayes, M.W., Nature, (1966), 209, 769.
5. Poll, H.U., Z. Angew. Phys., (1970), 29, 260.
6. Yasuda, H., and Lamaze, C.E., J. Appl. Polym. Sci., (1971) 15, 2277.
7. Morita, S., Sawa, G., and Ieda, M., J. Macromol. Sci.-Chem., (1976), A10(3), 501.

RECEIVED May 9, 1979

5

Polymerization of Hydrocarbons in a Pulsed Plasma

J. W. VINZANT, M. SHEN, and A. T. BELL

Department of Chemical Engineering, University of California, Berkeley, CA 94720

Most studies of plasma polymerization have been conducted in continuous wave rf plasmas. The effects of pulsed mode operation have received only limited attention. In a recent study, Yasuda et al. (1) found that while the polymerization rate of most monomers decreased when polymerization was carried out in a pulsed versus continuous plasma, the polymerization rate of a few monomers was enhanced. The present study was undertaken to determine the effects of pulsed operation on the plasma polymerization of ethylene and ethane. These monomers were selected because their behavior in continuous wave plasmas had been examined extensively in previous investigations (2-5).

Experimental

Films were deposited on aluminum foil using the tubular flow reactor shown schematically in Fig. 1. The shell of this reactor is a 50 cm long glass tube with an inside diameter of 8 cm. The reactor end plates are lucite and are sealed with O-rings to the glass tube. Two parallel plate copper electrodes, having exposed surfaces of 6.5 cm by 15 cm and separated by a gap of 3.5 cm, are located in the center of the glass tube. The lower electrode is water cooled and is grounded. Teflon inserts upstream and downstream of the electrodes create a smooth flow path across the electrodes and minimize boundary layer separation near the reaction zone.

Power to sustain the plasma was supplied by a pulsed rf generator (Tegal Corp.) operating at 13.56 MHz. The generator is capable of delivering up to 100 W in pulses 0.2 to 2.0 msec long, separated by

0-8412-0510-8/79/47-108-079$05.00/0

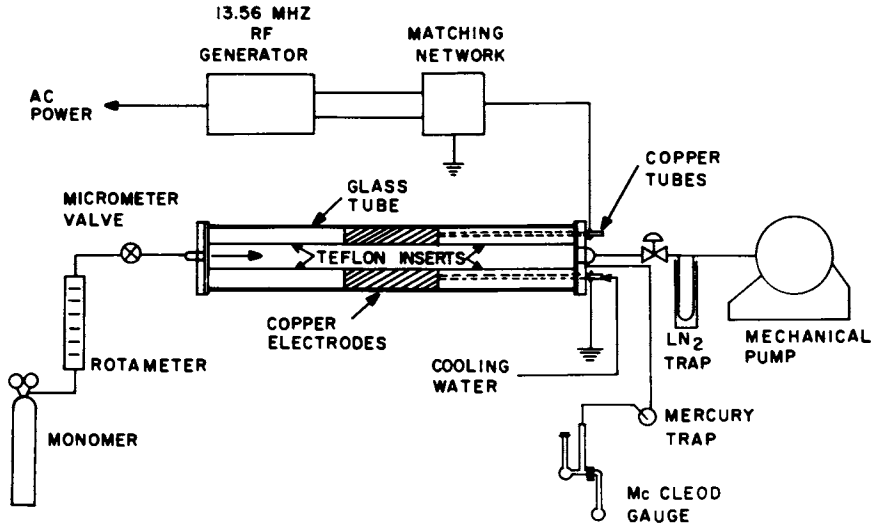

Figure 1. Schematic of tubular flow reactor

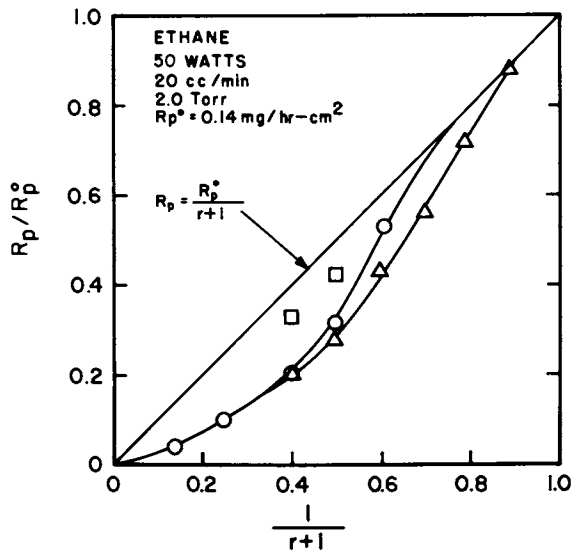

Figure 2. Effect of duty cycle on the normalized polymer deposition rate for ethane. (□) t_{ON} = 0.2 msec, (○) t_{ON} = 0.3 msec, (△) t_{ON} = 1.5 msec.

periods of 0.2 to 2.0 msec. The power level was monitored by an in-line watt meter (Bird Electronics). During pulsed operation the peak power was maintained at constant level. The pulse width, t_{on}, and pulse interval, $(t_{on} + t_{off})$, were adjusted using an oscilliscope. The duty cycle during pulsed operation is given by $(1+r)^{-1}$, where $r = t_{off}/t_{on}$.

C.P. grade ethane and ethylene were used as monomers. The flow rate of monomer was measured by a rotameter and the monomer pressure in the reactor was determined with a McLeod gauge.

Results and Discussion

Figures 2 and 3 illustrate the effect of pulse duty on the normalized polymer deposition rates for ethane and ethylene respectively. For a fixed value of t_{on} the data in both figures are seen to fall below the diagonal representing $R_p/R_p = (1+r)^{-1}$. The extent of deviation from the diagonal is the same for both monomers.

The effect of t_{on} on the normalized polymer deposition rate for a fixed duty cycle is shown in Figs. 4,5, and 6. The data show that the normalized rate is nearly constant for small values of t_{on}. A change to a new plateau occurs for t_{on} between 0.2 and 0.5 msec. For t_{on} longer than 0.5 msec, the normalized rate again remains constant but at a lower level than that observed for t_{on} less than 0.2 msec. At 2.0 torr the plateaus and the point of transition between them are identical for ethane and ethylene. When the pressure is increased to 2.5 torr the plateau levels remain the same as at 2.0 torr, but the transition point between plateaus shifts to longer t_{on}.

The results presented in Figs. 2 through 6 demonstrate that the rate of polymer deposition depends upon both r and t_{on}. These data may be discussed in terms of the expected effects of the two parameters. We begin by considering the case where t_{on} is long relative to the time constants for achieving steady state polymerization and relaxing from the steady state. For this case the relationship between R_p and R_p^o should be

$$R_p/R_p^o = 1/(1+r) \qquad (1)$$

As t_{on} is reduced at a fixed value of r, a point is finally achieved at which the time to establish and collapse a steady-state plasma become comparable to t_{on}. Under this condition, the concentrations of

In Plasma Polymerization; Shen, M., et al.;
ACS Symposium Series; American Chemical Society: Washington, DC, 1979.

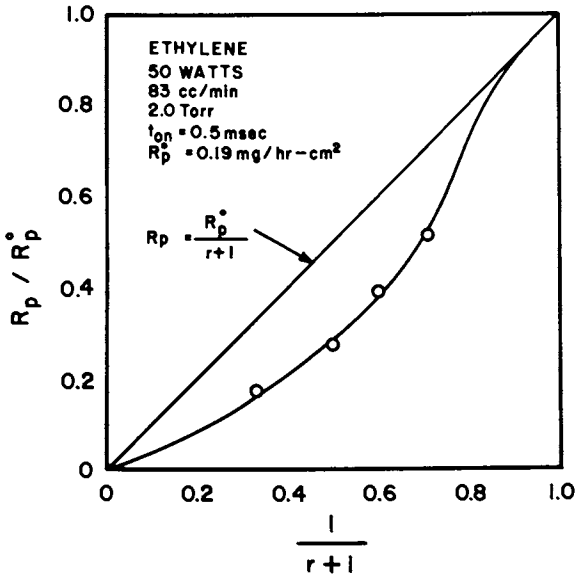

Figure 3. Effect of duty cycle on the normalized deposition rate for ethylene

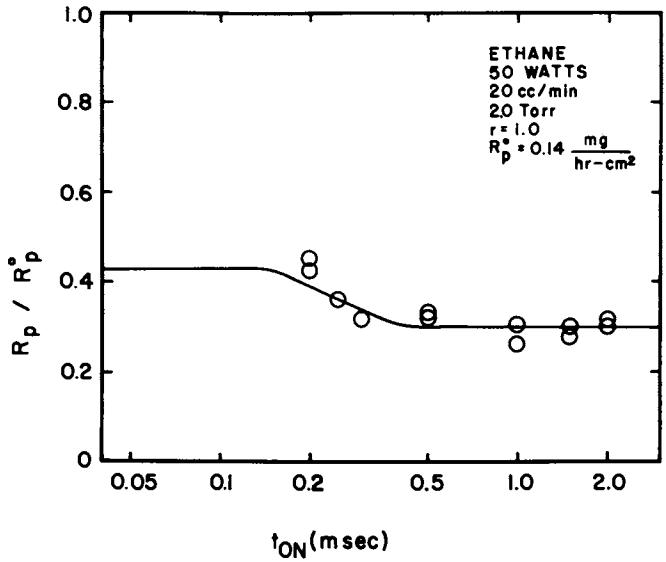

Figure 4. Effect of pulse width on the normalized deposition rate for ethane. p = *2.0 torr.*

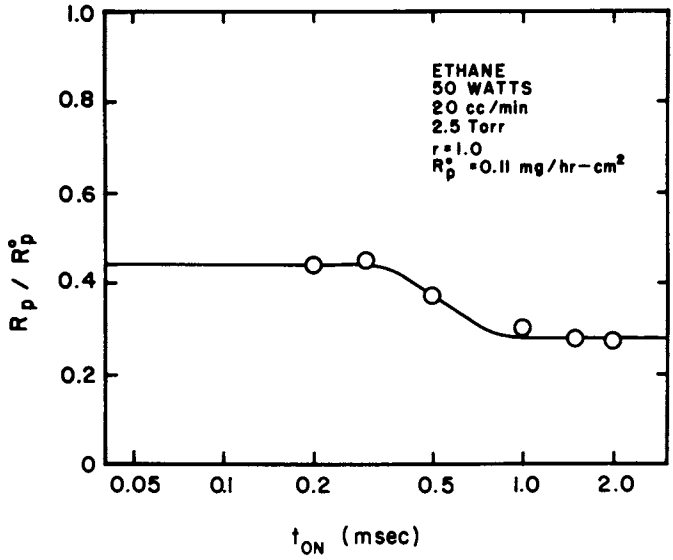

Figure 5. Effect of pulse width on the normalized deposition rate for ethane. p = *2.5 torr.*

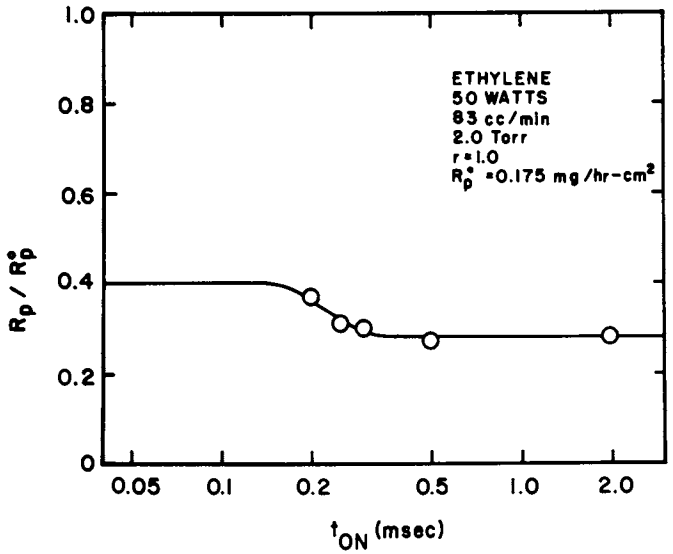

Figure 6. Effect of pulse width on the normalized deposition rate for ethylene: p = *2.0 torr.*

active species responsible for polymerization [e.g., gas phase free radicals (5)] will vary rapidly with time but not achieve steady-state levels within t_{on}. Such situations are well known, for example, in photopolymerization using a pulsed light source (6). The time average concentration of active species is then equivalent to that for a steady-state condition maintained with a source intensity of $I/(1+r)$ where I is the intensity for r = 0. The relationship between R_p/R_p^o and $(1+r)^{-1}$ can be established once it is known how the concentration of active species depends upon the source intensity and the rate of polymerization on the concentration of active species. For example, in the case of photopolymerization these relationships are given by

$$[R\cdot] = a(I)^{0.5}/(1+r)^{0.5} \qquad (2)$$

$$R_p = k[M][R\cdot] \qquad (3)$$

and thus we conclude that

$$R_p/R_p^o = 1/(1+r)^{0.5} \qquad (4)$$

Based upon the arguments just presented, we would expect a plot of R_p/R_p^o versus t_{on}, for a fixed value of r, to be sigmoidal in shape. While the data in Fig. 4 exhibit this general shape, the observed magnitudes of R_p/R_p^o at the two plateaus are quite different from those predicted. One might expect that the reason R_p/R_p^o is not equal to $(1+r)^{0.5}$ for the smallest values of t_{on} is because the polymerization mechanism used to interpret photopolymerization is not applicable to plasma polymerization. However, an investigation of more realistic mechanisms, such as those given by Tibbitt et al. (5) for example, still lead to the same relationship. Likewise, none of the polymerization mechanisms examined explain why R_p/R_p^o is not equal to $(1+r)^{-1}$ at large values of t_{on}. One reason why theory fails to explain the experimental results may lie in the assumption that the plasma characteristics during pulsed operation are essentially the same as during steady-state operation. To explore this possibility would require a more detailed characterization of the properties of the pulsed plasma, a subject which was outside the scope of the present investigation.

Acknowledgment

This work was supported by the Defense of Advanced

Research Projects Agency and monitored by the Air Force Cambridge Research Laboratories.

Abstract

The plasma polymerization of ethane and ethylene were investigated in a capacitatively coupled, pulsed radiofrequency plasma. The pulse width (t_{on}) and pulse spacing (t_{off}) could be varied independently between 0.2 and 2.0 msec. For both monomers it was observed that the polymerization rate increased with pulse duty cycle. It was also observed that for a fixed duty cycle the polymerization rate went through a sigmoidal increase with increasing pulse width. The qualitative features of the data are discussed in the light of available theory.

References

1. Yasuda, H. and Hsu, T., J. Polym. Sci., Polymer Chem. Ed., (1977) 15, 81.

2. Kobayashi, H., Bell, A. T., and Shen, M., J. Appl. Polym. Sci. (1973) 17, 885.

3. Kobayashi, H., Shen, M., and Bell, A. T., J. Macromol. Sci. Chem. (1974) A8, 373.

4. Tibbitt, J. M., Bell, A. T., and Shen, M., J. Macromol. Sci. Chem. (1977) A11, 139.

5. Tibbitt, J. M., Jensen, R., Bell, A. T., and Shen, M., Macromol. (1977) 10, 647.

6. Rodriguez, F., "Principles of Polymer Chemistry", McGraw Hill, New York, 1970.

RECEIVED March 29, 1979.

Plasma Diagnostics of Polymerizing Benzene Plasma

Plasma Diagnostics of a Tool for Controlling Plasma Reaction

MASAHIRO NIINOMI and KENJI YANAGIHARA

Japan Synthetic Rubber Co., Ltd., Tokyo Research Laboratory, 7569 Ikuta, Tama-ku, Kawasaki, Japan

ABSTRACT

The electron temperature (T_e), electron density (n_e) and electron energy distribution function for a plasma sustained in an argon/benzene mixture were measured by double and triple plasma-probe methods. Each probe was heated up to 1000 K with a sheathed heater, which was inserted into the probe, in order to prevent polymer film from depositing on the surface of the probe. T_e and n_e were very sensitive to the state of plasma, and were thus useful for detecting an occurrence of abnormal reaction and/or deviation of the polymerization reaction from the standard route. By using the method as a monitoring tool, control of plasma polymerization reaction can be performed during reaction with high reliability.

Benzene was plasma-polymerized in order to prepare a reverse osmosis (RO) membrane on a porous membrane filter for separation of various mixtures of organic solvents. Based upon thermodynamic estimates, a pressure resistance of more than 100 kg/cm^2 is necessary in many cases. Under optimum reaction conditions of the plasma, a polymer film with the required pressure resistance could be prepared. Although the reactions were controlled by monitoring macroscopic reaction conditions such as pressure of the system, monomer flow rate and electric power supply, the properties of the polymer film sometimes deteriorated significantly. Polymer deterioration may be attributed to mixing of impurities such as air into the monomer, and/or variation of monomer/carrier-gas composition in the reactor during reaction. The conventional monitoring method could not detect an occurrence of such unfavorable reactions. A more sensitive monitoring method for controlling the plasma reaction was required.

In the case of a non chemical-reaction plasma, the state of the plasma can be described by the electron energy distribution function, $f(\varepsilon)$ (1). In the case of a polymerizing plasma, however, $f(\varepsilon)$ may not be sufficient. In other words, the structure of the

0-8412-0510-8/79/47-108-087$06.75/0

plasma-polymerized polymers may not always be the same even if $f(\varepsilon)$ is kept constant, since various kinds of reactive species other than electrons are present and take part in the plasma polymerization process. It is not clear at present which of these species controls the polymerization reaction and determines the characteristics of the reaction product.

The plasma reaction is, however, initiated by generation of electrons and positive ions, followed by their collision with monomer molecules. The distribution of first-generation reactive species, which governs the successive process of the polymerization reaction, is determined by the distribution of electron energies in the system. Electrons are more significant than ions for chemical reaction because of their extremely high average energy. It may be said that a plasma reaction process (or at least its first step) can also be characterized by the characteristics of the plasma electrons. Thus, the present study was undertaken to see if the electron characteristics of the plasma could be used as a monitoring parameter for controlling the plasma polymerization reaction.

EXPERIMENTAL

Polymerization

The apparatus and the electric power supply system used in this study were essentially the same as those of Yasuda and Lamaze (2). A Pyrex glass reactor, as shown in Fig. 1, is composed of a discharge chamber (diameter 2.5 cm, length 14 cm) and a reaction chamber (diameter 6.5 cm, length 31 cm): the former was equipped with an argon gas inlet, an rf coil and a mass sampling port; and the latter, a benzene inlet, a connection to a Pirani gauge, a substrate stage, two sets of plasma probes at different positions, and another mass sampling port. Nuclepore ^{R} membrane filters of 0.03 μm pore-diameter were used as substrate material on which polymer film was deposited. Vacuum dried filters were placed on the substrate stage at two different positions, 10 cm and 15 cm downstream from the end of the rf coil (Position 10 and Position 15, respectively).

Monomer feed line and evacuation lines of the reactor are shown in Fig. 2. Distilled benzene was transferred into a flask with a ground-glass joint (1 in Fig. 2). After connecting the flask to the monomer feed line, the whole line (1-5) was evacuated, by a rotary pump (6) to less than 10^{-2} Torr as measured with a Pirani gauge (5), while keeping the benzene frozen with a liquid nitrogen bath. Benzene in the flask was then allowed to evaporate slowly, keeping all the stopcocks closed except for that to the monomer-gas reservoir (3). Since the bottom part of the reservoir had been cooled with another cryogen, benzene was transferred into, and solidified in the reservoir. About one third of the benzene was left in flask (1), and discarded. By similar operation, one third of the original amount of benzene was transferred into flask (2) and was discarded as a pre-cut distillate. As a result, one

In Plasma Polymerization; Shen, M., et al.;
ACS Symposium Series; American Chemical Society: Washington, DC, 1979.

third of the original amount of benzene was stored in the reservoir (3) under vacuum, and was used as monomer. It was found necessary for steady feed of the monomer vapor into the reactor to keep the vapor pressure in the feed line constant. This was attained by keeping the temperature of the reservoir constant with an ice-water/ NaCl bath, and by using a large volume reservoir (about 4 liters).

The reactor (9) containing degassed Nuclepore filters (10) was evacuated, prior to reaction, to less than 10^{-5} Torr by an oil diffusion pump. The vacuum was measured with an ionization gauge (11). As soon as dry argon was fed into the reactor through a rotameter (8), the evacuation of the system was switched to a second rotary pump (12). The vacuum in the reactor was now measured with a second Pirani gauge (13). The use of ground-glass joints and Kover-to-glass seals between parts enabled maintenance of a high vacuum.

The monomer vapor was then fed through rotameter (7). The total pressure in the reactor was controlled with a bellows-sealed vacuum valve (14) and monitored with a Pirani gauge (13).

An rf power at 13.56 MHz was supplied to the coil (15) by a crystal controlled generator with a power amplifier (Electronic Navigation Ind., A-300) through an LC parallel-resonance type impedance matching network. The power and SWR were monitored with a through-line wattmeter (Leader Test Instrument, LPN-885).

Pressure resistance of polymer films prepared under various reaction conditions were examined by using a batch-wise reverse osmosis apparatus. Hydrostatic pressure was applied by using a mixture of toluene/methanol as a pressure medium.

Fourier Transformation IR spectra of the polymer film were recorded on a Digilab FTS-20BD. An ATR spectrum was obtained by accumulating 100 scans of an interferogram with a resolution of 8 cm^{-1} for each specimen. Since the recorded spectrum included the spectrum of the Nuclepore filter, it was necessary to subtract the latter from the former.

Probe Experiments

The electron temperature (T_e) and electron density (n_e) of the plasma were measured by a heated double probe method (DPM). A conventional DPM (3) could not be used in a polymerizing plasma system since the surface of the probe was covered with depositing polymer film which prevented plasma electrons from flowing to the probe. To cope with this problem, all the probes were heated up to about 1000 K by sheathed tungsten heaters which were inserted into the cylindrical probes as shown in Fig. 3. The probes (15 mm length, 500 μm diameter) were made of Ni since it does not emit electrons at this temperature (see Appendix). The heater was 7 Ω, and 6 V (DC) was applied to maintain the temperature. The sheath (Al_2O_3, 200 μm dia.) was necessary to prevent electrons, emitted from the heater, from flowing into the probe. Using this device, a probe measurement could be performed on a polymerizing plasma. The wiring diagram for the probe system is shown in Fig. 3.

In Plasma Polymerization; Shen, M., et al.;
ACS Symposium Series; American Chemical Society: Washington, DC, 1979.

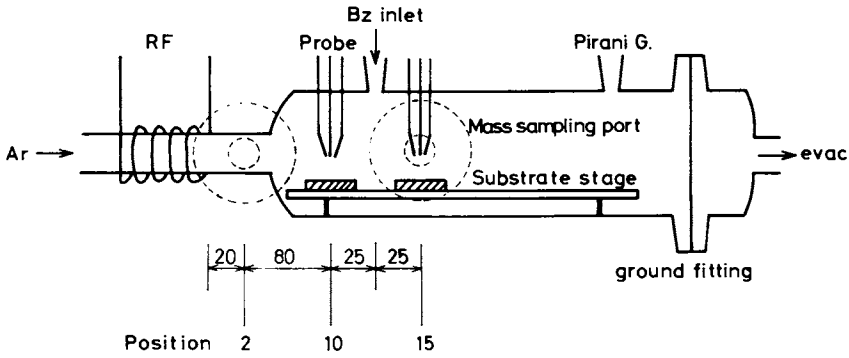

Figure 1. Schematic of electrodeless plasma reactor

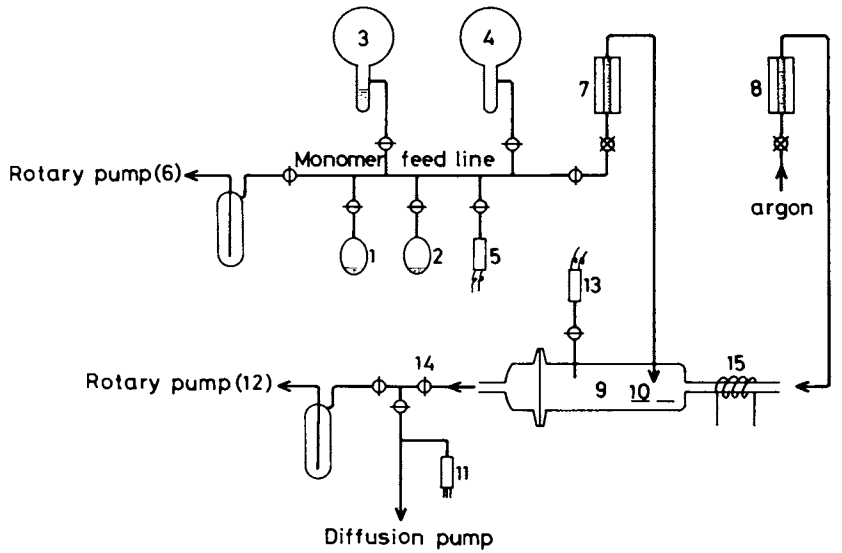

Figure 2. Schematic of monomer feed line, reactor, and evacuation system. See *text for details.*

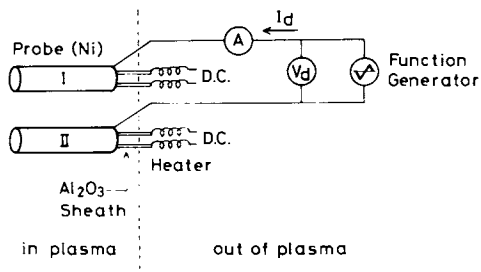

Figure 3. Wiring diagram for a heated double probe

In Plasma Polymerization; Shen, M., et al.;
ACS Symposium Series; American Chemical Society: Washington, DC, 1979.

After the probes were set in the plasma (at Position 10 and/or 15 in Fig. 1), an triangular A.C. (V_d, 20V p-p, 0.01 to 0.1 Hz) voltage was applied between the probes. The circuit current (I_d) as well as the voltage between probes (V_d) were then recorded. T_e and n_e were calculated from the relation between V_d and I_d according to the equivalent resistance method developed by Dote (4), in which it is assumed that the electron energy distribution is Maxwellian. The value of n_e was calculated according to Malter and Webster (5).

Actually, $f(\varepsilon)$ of a polymerizing plasma is expected to be non-Maxwellians, and it is thus necessary to measure the exact form $f(\varepsilon)$ in order to estimate the true values of T_e and n_e. Determinations of $f(\varepsilon)$ were carried out through the floating asymmetrical triple probe method (ATPM) developed by Okuda and Yamamoto (6). The circuit for this method is shown in Fig. 4. Although each of the three probes was again equipped with a sheathed heater, the dimensions of probes I and II were different from those shown in Fig. 3. Probe I (30 mm length, 1 mm dia.) in Fig. 4 was much larger than probe II (1 mm tip length, 5 μm tip dia.).

The ATPM allowed us to measure $f(\varepsilon)$ from a low energy level without causing a significant disturbance to the plasma. A triangular A.C. voltage (V_d) was applied between probes I and II. Adjusting a slide resistor (SR) to keep the electron current into the probe III zero, the values of I_d, V_d and d^2I_d/dV_d^2 were recorded. The second derivative gives the exact form of $f(\varepsilon)/\sqrt{V}$. The derivative was obtained directly by taking the second harmonic of I_d. For this purpose V_d (0.01 Hz, 20V p-p) was modulated at 400 Hz A.C. (lower than 4V), and the second harmonic of Id, which is proportional to the second derivative, was detected with a lock-in amplifier (Princeton Applied Research Corp., Model 5204), as shown in Fig. 4.

Mass spectroscopy

Ionic and neutral species in the benzene plasma were analyzed directly with a quadrupole mass spectrometer (ULVAC Corp, MSQ-500) equipped with an electrostatic sampling assembly (7). This assembly serves to focus the ion collected from the plasma into the quadrupole structure of the mass spectrometer and is needed to achieve a measureable ion signal. The assembly was composed of an orifice, a set of electrostatic lenses and a differential pumping system as shown in Fig. 5. The sampling orifice was a 30 μm diameter hole which was chemically machined in a 30 μm thick 18 Cr - 8 Ni stainless steel sheet. The lenses were made of 2.5 cm diameter 18-8 stainless steel tubing and were supported by open Teflon bushings. The size of the lenses were the same as those reportedly Vasile and Smolinsky (7). The electric potential of the orifice was the same as the floating potential, which was estimated at about -10V from the plasma potential. Potentials on the cylinder lenses were adjusted to obtained maximum signal intensity, i.e. about -340V on the first lens, -50V on the second, and -80V on the third. The electric lines of force generated in this case are also shown in Fig. 5. It is seen that the electrostatic lens system forms an imaginary convex

In Plasma Polymerization; Shen, M., et al.;
ACS Symposium Series; American Chemical Society: Washington, DC, 1979.

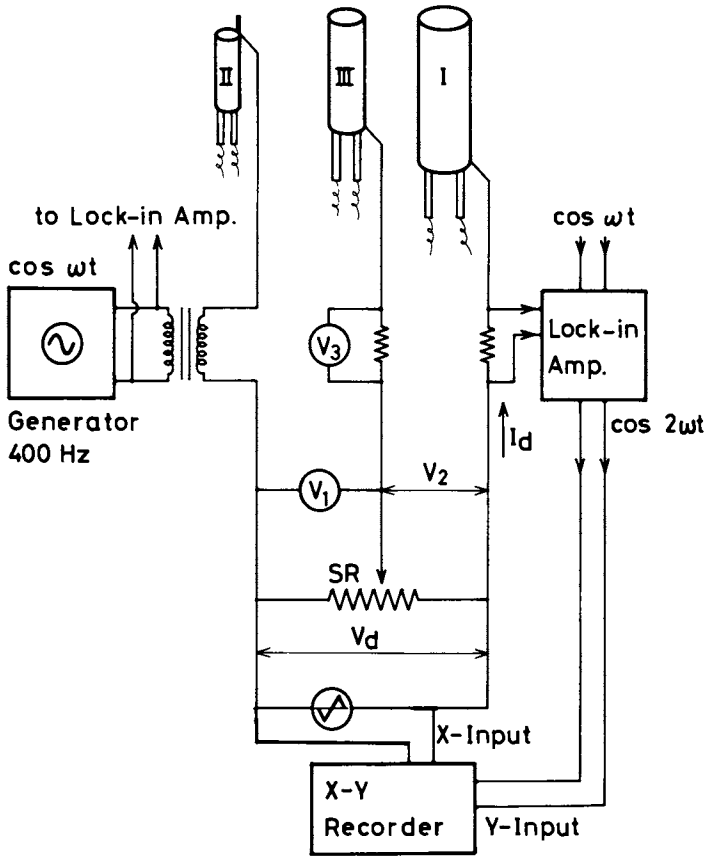

Figure 4. Wiring diagram for a heated asymmetrical triple probe. See *text for details.*

In Plasma Polymerization; Shen, M., et al.;
ACS Symposium Series; American Chemical Society: Washington, DC, 1979.

lens for positive ions. Thus, positive ions at the orifice were accelerated toward, and focused on the entrance to the mass spectrometer.

Neutral species in the plasma was analyzed by usual operation of the mass spectrometer, in which the species were ionized at the ionization chamber. The electron energy in the ionization chamber was sometimes lowered to 10V in order to reduce the fragmentation. Mass analysis was carried out up to 500 AMU for all the species.

RESULT AND DISCUSSION

Reaction condition and plasma characteristics

As in the case of ethylene and acetylene (8), plasma polymerization of benzene produced either a powder or film depending on reaction conditions. A typical condition in which thin film with the required property was produced (the RO membrane condition) is shown in Table 1, coded as Condition B, while that for poor quality film formation is designated A. Conditions for powder formation are designated C and E in the table. Generally speaking, film formation was observed at high benzene flow rates, and powder formation was observed at low pressures and low benzene flow rates, as in the case of ethylene and acetylene (8). However, the RO membrane conditions do not correspond to either a unique point on the pressure (P) versus benzene flow rate (Q(Bz)) plane nor do they correspond to the conditions in which a lot of polymer was produced. This means that the quality of the film cannot be correlated directly to the macroscopic reaction conditions.

T_e, n_e and $f(\varepsilon)$ were measured under various reaction conditions. Figs. 6, 7, 8 and 9 show $f(\varepsilon)$ for typical plasma conditions as well as argon plasma. All the data in this section were collected at Position 15 in the reactor. In each figure, Maxwell and Druyvesteyn distributions are shown for comparison. They were obtained mathematically assuming that they have the same total number of electrons (N) and total kinetic energy (E) as those of the corresponding observed distribution. Namely, N and E are expressed as follows in the case of Maxwell distribution:

$$N = \int_0^\infty C \cdot \varepsilon^{1/2} \exp(-\varepsilon/kT_e) d\varepsilon = (C\pi^{1/2}/2)(kT_e)^{3/2}$$

$$= 0.886C(kT_e)^{3/2}$$

$$E = \int_0^\infty C \cdot \varepsilon^{3/2} \exp(-\varepsilon/kT_e) d\varepsilon = C \cdot \Gamma(5/2)(kT_e)^{5/2}$$

$$= 1.33C(kT_e)^{5/2}$$

In Plasma Polymerization; Shen, M., et al.;
ACS Symposium Series; American Chemical Society: Washington, DC, 1979.

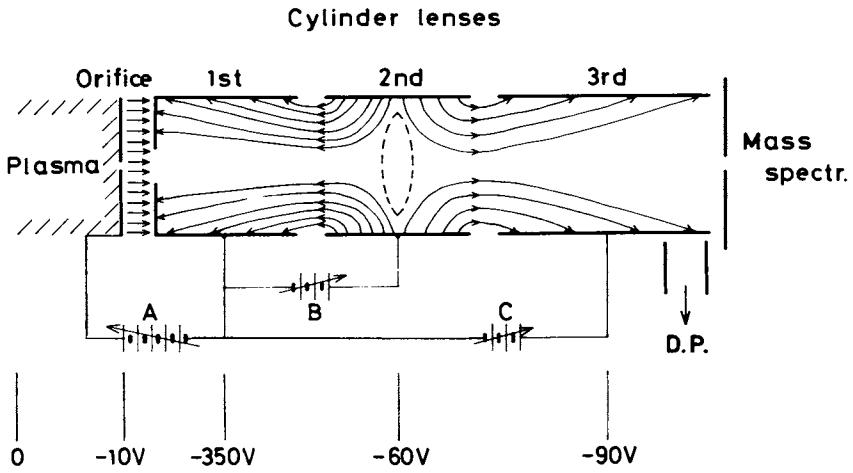

Figure 5. Schematic of ion sampling unit, composed of a sampling orifice, a set of electrostatic lenses, and a differential pumping system. The electric lines of force under the applied potential are drawn schematically together with an imaginary convex lens.

Table 1. Typical Reaction Conditions for Polymer Formation

Code	Pressure (Torr)	Flow rate[1] benzene	Flow rate[1] argon	Product
A	0.5	250	500	Film
B	0.5	500	150	Film[2]
C	1.0	250	150	Powder
E	0.2	150	150	Powder

1) STP cc/min

2) Excellent pressure resistibility

In Plasma Polymerization; Shen, M., et al.;
ACS Symposium Series; American Chemical Society: Washington, DC, 1979.

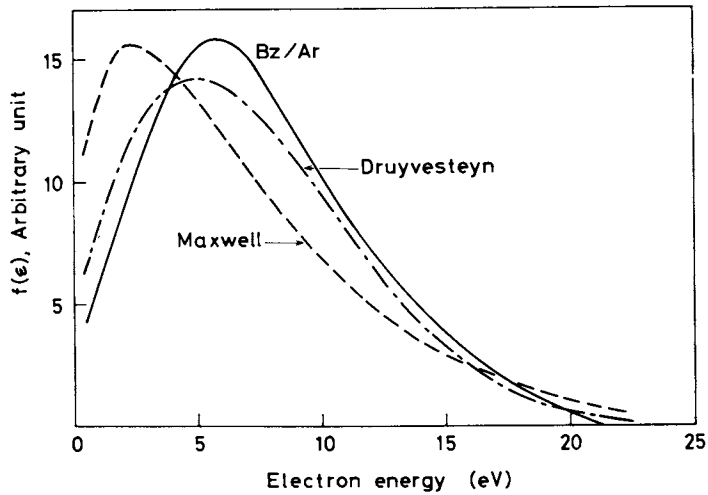

Figure 6. Electron energy distribution function in a plasma generated under Condition A (see Table 1). Maxwell and Druyvesteyn distributions were calculated under the assumption that the total energy and the total electron density were the same as those observed.

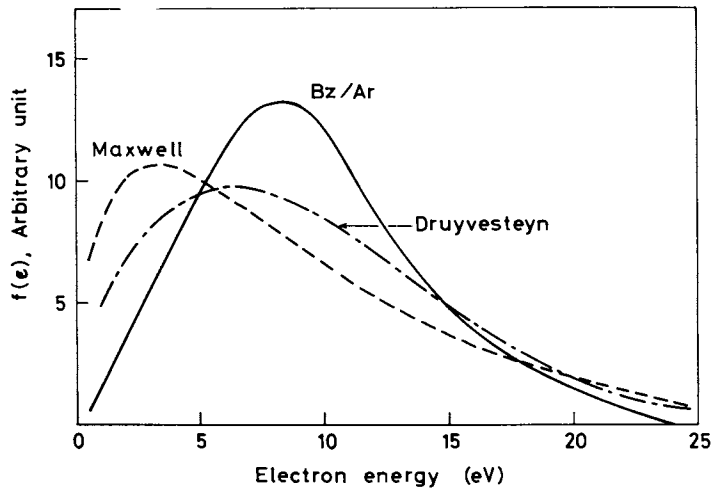

Figure 7. Electron energy distribution function of a plasma under Condition B (see Table 1)

In Plasma Polymerization; Shen, M., et al.;
ACS Symposium Series; American Chemical Society: Washington, DC, 1979.

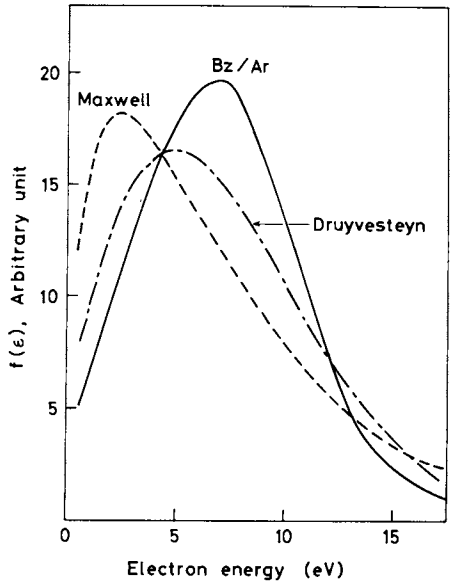

Figure 8. Electron energy distribution function of a plasma under Condition E (see Table 1)

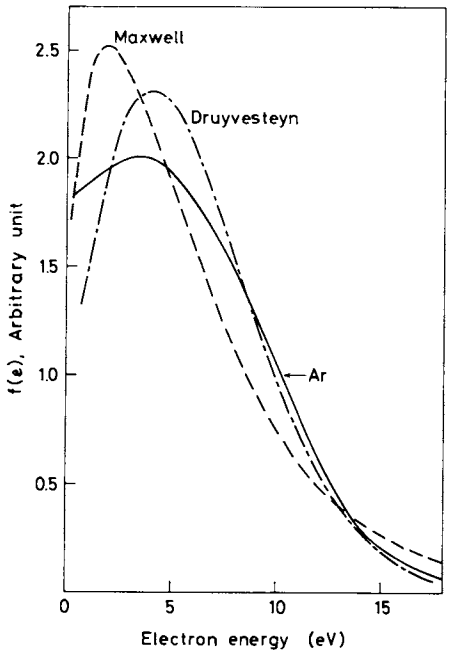

Figure 9. Electron energy distribution function of an argon plasma under the condition of 0.5 torr, 40 W, 500 STP mL/min

In Plasma Polymerization; Shen, M., et al.;
ACS Symposium Series; American Chemical Society: Washington, DC, 1979.

where C is a constant; ε is electron energy: T_e is electron temperature and Γ is gamma function. N and E of the observed $f(\varepsilon)$ were obtained by a graphic integration method, and equated to those of the Maxwell distribution to evaluate C and T_e in the equations. By using these values, $f(\varepsilon)$ of Maxwell distribution was calculated mathematically, where

$$f(\varepsilon) = C\varepsilon^{1/2} \exp(-\varepsilon/kT_e) .$$

In the case of a Druyvesteyn distribution, N and E are expressed as:

$$N = \int_0^\infty C \cdot \varepsilon^{1/2} \cdot \exp(-\varepsilon^2/kT_e) d\varepsilon = (C/2) \cdot \Gamma(3/4) \cdot (kT_e)^{3/4}$$

$$= 0.613C(kT_e)^{3/4}$$

$$E = \int_0^\infty C \cdot \varepsilon^{3/2} \exp(-\varepsilon^2/kT_e) d\varepsilon = (C/2) \cdot \Gamma(5/4) \cdot (kT_e)^{5/4}$$

$$= 0.453C(kT_e)^{5/4}$$

A procedure similar to that described above is then followed to evaluate $f(\varepsilon)$ for the Druyvesteyn distribution.

It is seen from Figs. 6, 7, 8 and 9, that $f(\varepsilon)$ of the polymerizing plasma as well as the argon plasma is neither Maxwellian nor Druyvesteyn. This is reasonable since the inelastic collisions of electrons and molecules are not taken into account in the ideal cases. Thus, T_e obtained through the double probe method cannot be defined thermodynamically in an actual plasma system. Only $f(\varepsilon)$ has physical meaning. There are, however, two reasons to justify the adoption of T_e and/or n_e as monitoring parameters for controlling a plasma reaction. The first is that both parameters are very sensitive to a change in plasma conditions, and are thus suitable for detecting the deviation of the reaction from a predetermined standard. The other is that T_e is closely related to the profile of $f(\varepsilon)$ near the floating potential of the plasma. The latter was estimated to be about 10 eV in our plasma as will be seen below. It is electrons with large energy (10-15 eV or more) that govern the polymerization process. Thus, only the profile at the high energy part of $f(\varepsilon)$ is responsible for the reaction, and it is well characterized by T_e. By the two reasons, T_e and n_e will be used as practical monitoring parameters for controlling plasma reaction in this section.

In Plasma Polymerization; Shen, M., et al.;
ACS Symposium Series; American Chemical Society: Washington, DC, 1979.

Figs. 10, 11 and 12 show contour maps of n_e as a function of volumetric flow rate and pressure (P) at fixed power of 40 W. It is seen from Fig. 10 that n_e of argon plasma shows only a slight change with plasma condition. The change is also small in the case of pure benzene plasma shown in Fig. 11, making a remarkable contrast to that of plasma of Ar/Bz mixture in which the change is drastic, especially at low flow rates of benzene, and low P, as seen in Fig. 12. The tendency is more evident in Fig. 13 in which the effect of Q_{Bz} on n_e at fixed Q_{Ar} of 150 STP cc/min. is demonstrated. The value of n_e decreases by four decades when a small amount of benzene (100 to 200 STP cc/min.) is added to the Ar plasma. However, it increases by three decades with increasing Q_{Bz} up to 400 STP cc/min. The reaction conditions for the lowest value of n_e correspond to those producing a lot of powder. It may be said that a gas phase reaction in which electrons play a significant role dominates the polymerization reaction in this region.

Except for the abrupt change, a general tendency can be observed that the higher the pressure, the lower the n_e.

The reaction conditions, where high quality polymer film formed on the substrate such as Condition B, correspond to a plateau region of high Q_{Bz} and low P (Fig. 12) where n_e shows little change with reaction conditions. Concerning Fig. 11 and 12, there were unstable plasma regions at high P and low Q_{Bz} where no probe measurement could be performed. The regions are enclosed with broken lines in each figure.

Corresponding T_e contour maps are shown in Fig. 14, 15 and 16. The change of T_e with the reaction conditions is mild in the case of an argon plasma (Fig. 14). It is seen that the lower the pressure, the higher the value of T_e; and that the smaller Q_{Ar}, the higher T_e. By comparison, the contour lines show complicated changes with reaction condition in the cases of plasma of pure benzene (Fig. 15) and Ar/Bz mixtures (Fig. 16). The location of the valley and the plateau in the map seems to closely related to that of the n_e-map. The relation between T_e and Q_{Bz} at a fixed Q_{Ar} and electric power supply is shown in Fig. 17. It is seen that T_e shows a similar Q_{Bz} dependency to that of n_e, although not on a logarithmic scale. The reason for the abrupt decrease in T_e might be elucidated as the result of a rapid gas phase reaction which decreases the number of electrons having large kinetic energy.

Mass spectroscopy

The most direct method of controlling the plasma reaction is to monitor the concentration of active species which rule the reaction. Although it is uncertain whether positive ions in plasma play the principal role in polymerization reactions, the relation between reaction conditions and distribution of ionic species was investigated. The purpose of these studies was to see whether the latter can be adopted as a monitoring parameter for reaction. A mass spectrum of ionic species under a RO membrane condition is shown in Fig. 18. Measurement was carried out at three different

In Plasma Polymerization; Shen, M., et al.;
ACS Symposium Series; American Chemical Society: Washington, DC, 1979.

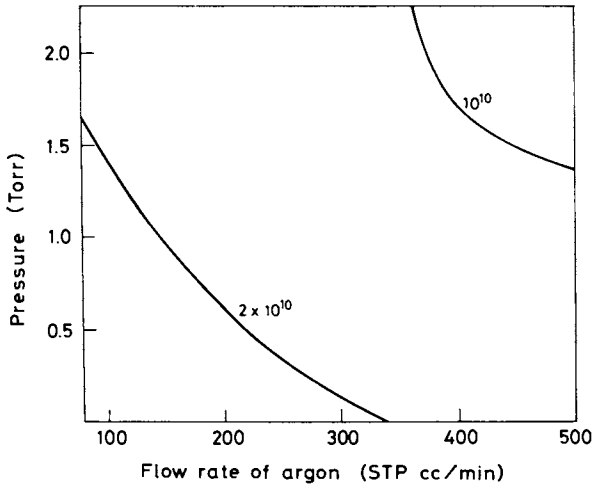

Figure 10. Contour map of $n_e(cm^{-3})$ of an argon plasma as a function of pressure and flow rate

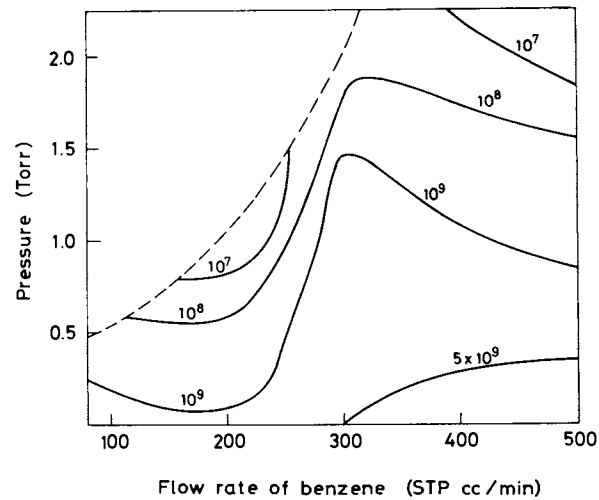

Figure 11. Contour map of $n_e(cm^{-3})$ of a benzene plasma as a function of pressure and flow rate

In Plasma Polymerization; Shen, M., et al.;
ACS Symposium Series; American Chemical Society: Washington, DC, 1979.

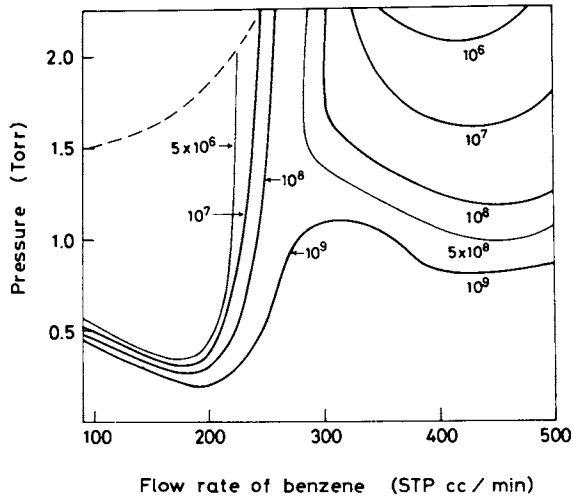

Figure 12. Contour map of $n_e(cm^{-3})$ for an argon–benzene plasma as a function of total pressure and flow rate of benzene. A flow rate of argon was fixed to 300 STP mL/min.

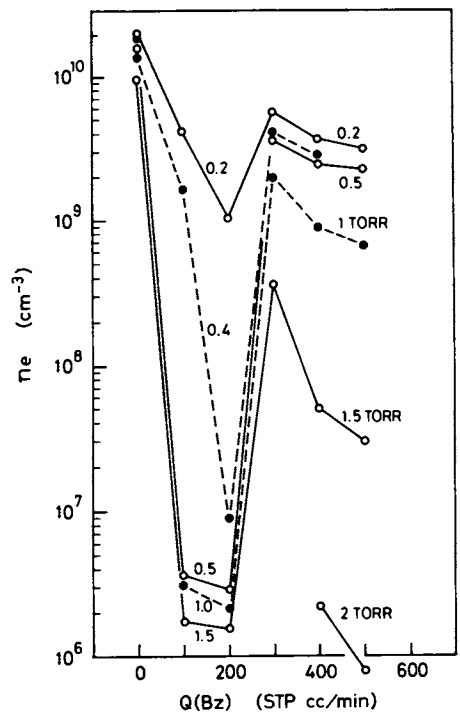

Figure 13. Relationship between n_e and benzene flow rate at a fixed argon flow rate of 150 STP mL/min

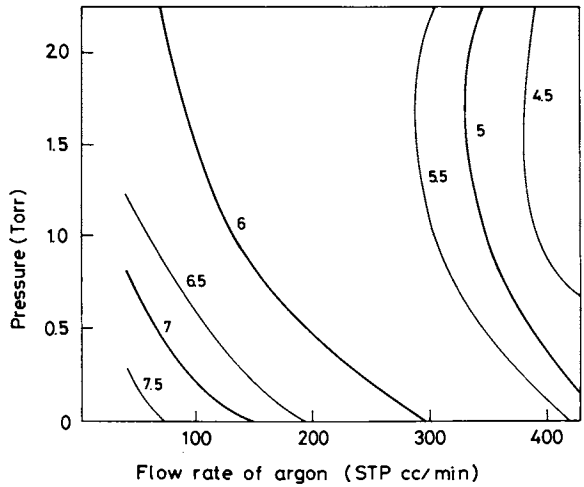

Figure 14. Contour map of $T_e(10^4K)$ for an argon plasma as a function of pressure and flow rate

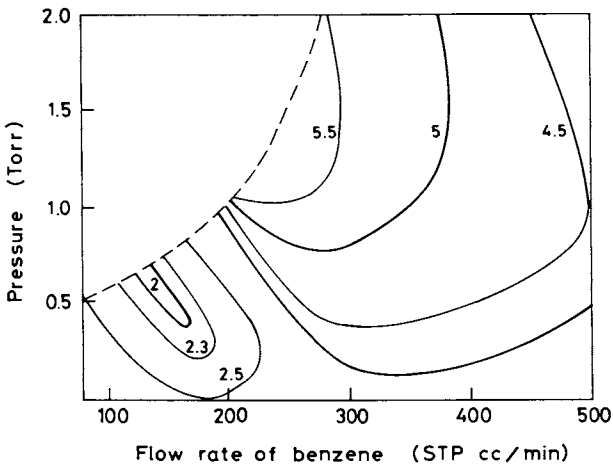

Figure 15. Contour map of $T_e(10^4K)$ for a benzene plasma as a function of pressure and flow rate

In Plasma Polymerization; Shen, M., et al.;
ACS Symposium Series; American Chemical Society: Washington, DC, 1979.

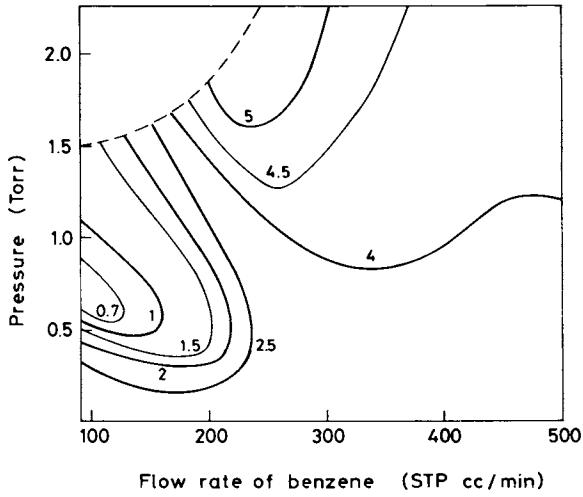

Figure 16. Contour map of $T_e(10^4K)$ for an argon–benzene plasma as a function of total pressure and flow rate of benzene at a fixed argon flow rate of 300 STP mL/min

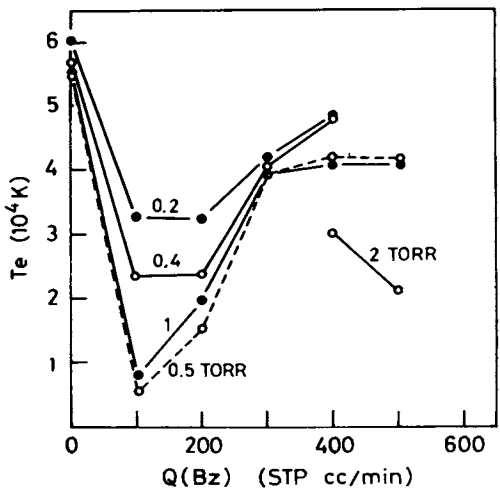

Figure 17. Relationship between T_e and benzene flow rate at a fixed argon flow rate of 150 STP mL/min

In Plasma Polymerization; Shen, M., et al.;
ACS Symposium Series; American Chemical Society: Washington, DC, 1979.

mass ranges; low mass range (m/e=1 to 50), medium mass range (m/e = 40 to 200) and high mass range (m/e = 100 to 500). These ranges are designated as L, M or H in Fig. 18. Sensitivity of the detector is also cited in terms of the reading of the electrometer of the mass spectrometer. In addition to the argon m/e = 40 and benzene ions m/e = 78, varioud kinds of fragment and oligomer ions were observed. It must be kept in mind that the ions observed were not formed by fragmentation in the mass spectrometer, but actually existed in the plasma. Principal fragment ions are listed in the first column of Table 2. Compared to the standard mass spectrum obtained at the 70 eV ionization condition, intensities of $C_2H_2^+$, $C_2H_3^+$, $C_5H_4^+$ are prominent. Some of the large peaks of oligomer are listed also in Table 2. The ion formula in the table is not definitive, but assigned for convenience from the observed m/e value. Formulae other than the listed ones are possible. For example, in the case of m/e = 499 (the highest m/e observed with our mass spectrometer), $C_{38}H_{43}^+$, $C_{37}H_{55}^+$, $C_{36}H_{67}^+$, $C_{40}H_{19}^+$ or $C_{41}H_7^+$ are possible in addition to $C_{39}H_{31}^+$. The listed formulae were assigned so that the C/H ratio is close to that of the experimental value of elementary analysis of plasma polymerized benzene, i.e., 1.0. The results of FT-IR spectra also proved that the structure of the polymer is close to polysytrene (see below), and support the formulae in Table 2.

Although the mechanism of the formation of the observed ionic species is uncertain, it is interesting to note that the formula of C_7 to C_{12} oligomers (the second column, coded as 1st Additives) can be made up by simply adding C_6H_6 to corresponding fragment formula, which was found in abundance in the plasma; e.g.

$$C_6H_5^+ + C_6H_6 \rightarrow C_{12}H_{11}^+$$

This process is remeniscent of an ion-molecule reaction of benzene (9). For oligomers of C_{13} to C_{18} as seen in the third column, a similar mechanism seems to be valid. Thus, the oligomer ions of low molecular weight seem to form a homologous series. For high molecular weight homologs, this tendency deviates. It is likely that the homolog has to split out hydrogen for structual stabilization. The observed fact that the peak intensities of low molecular weight homolog ions are always much higher than those of the higher favors the mechanism. There is, however, no evidence that the mechanism of the formation of thin polymer film on a substrate is the same as that occurs in the gas phase. It has to be said, though, that an ion-molecule reaction plays some role in polymerization in the gas phase.

The ions in a plasma under a powder forming condition, shown in Fig. 19, exhibit a clear contrast with those shown in Fig. 18. Few oligomer ion peaks and many fragment peaks are seen in this case. It may be considered that a powder forming reaction occurs very rapidly, thus a small amount of oligomer ions are left in the gas phase. In a plasma forming a membrane of an inferior quality

In Plasma Polymerization; Shen, M., et al.;
ACS Symposium Series; American Chemical Society: Washington, DC, 1979.

Table 2. Typical Positive Plasma-ions Under the RO Membrane Condition. *See* Text for Details

Fragment	Oligomer ions					
	1st Additives	2nd Additives	3rd	4th	5th	6th
		$C_{13}H_{12}^+$			$C_{31}H_{22}^+$	$C_{37}H_{34}$
CH_2^+	$C_7H_8^+$	$C_{13}H_{14}^+$		$C_{25}H_{19}^+$		
	$C_7H_{10}^+$					
	$C_8H_7^+$					$C_{38}H_{36}^+$
$C_2H_2^+$	$C_8H_8^+$	$C_{14}H_{14}^+$				
$C_2H_3^+$	$C_8H_9^+$	$C_{14}H_{15}^+$		$C_{26}H_{25}^+$		
		$C_{14}H_{16}^+$				
					$C_{33}H_{23}^+$	$C_{39}H_{31}^+$
$C_3H_2^+$	$C_9H_8^+$	$C_{15}H_{14}^+$	$C_{21}H_{18}^+$			
$C_3H_3^+$	$C_9H_9^+$		$C_{21}H_{21}^+$			
		$C_{16}H_{10}^+$				
$C_4H_2^+$		$C_{16}H_{12}^+$				
$C_4H_3^+$	$C_{10}H_9^+$	$C_{16}H_{15}^+$	$C_{22}H_{20}^+$	$C_{28}H_{20}^+$		
$C_4H_4^+$	(L)					
					$C_{35}H_{23}^+$	
		$C_{17}H_8^+$	$C_{23}H_{16}^+$			
$C_5H_3^+$			$C_{23}H_{18}^+$			
$C_5H_4^+$	$C_{11}H_{10}^+$	$C_{17}H_{16}^+$	$C_{23}H_{21}^+$	$C_{29}H_{29}^+$		
					$C_{36}H_{24}^+$	
$C_6H_3^+$		$C_{18}H_{15}^+$	$C_{24}H_{15}^+$			
$C_6H_4^+$		$C_{18}H_{16}^+$	$C_{24}H_{24}^+$			
$C_6H_5^+$	$C_{12}H_{11}^+$	$C_{18}H_{17}^+$ (L)		$C_{30}H_{29}^+$		
$C_6H_6^+$ (VL)	(VL)					
$C_6H_7^+$						

In Plasma Polymerization; Shen, M., et al.;
ACS Symposium Series; American Chemical Society: Washington, DC, 1979.

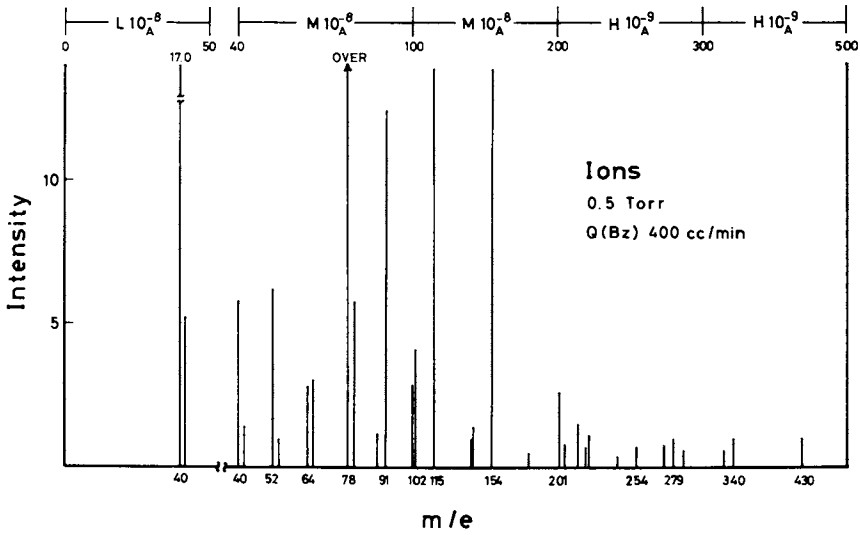

Figure 18. Mass spectrum of positive plasma-ions under the condition of 0.5 torr, Q_{Bz} = 400 STP mL/min, Q_{Ar} = 300 STP mL/min, 40 W. See *text for details.*

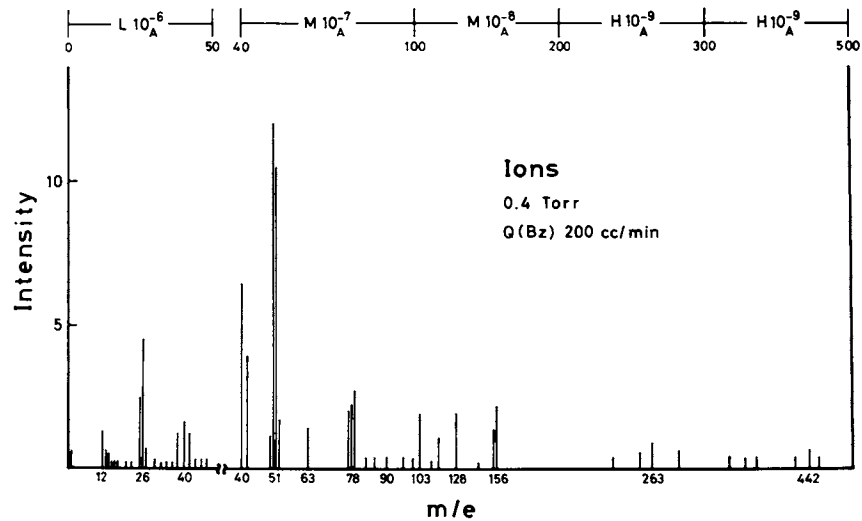

Figure 19. Mass spectrum of positive plasma-ions under the condition of 0.4 torr, Q_{Bz} = 200 STP mL/min, Q_{Ar} = 300 STP mL/min, 40 W

In Plasma Polymerization; Shen, M., et al.;
ACS Symposium Series; American Chemical Society: Washington, DC, 1979.

(Condition A), peaks of fragment ions prevail in the spectrum, though small peaks of oligomer coexist.

The mass spectra of neutral species present in the plasma are shown in Figs. 20 and 21 and exhibit almost the same trends shown in Figs. 18 and 19. Under condition B (Fig. 20), both fragment and oligomer peaks were found in abundance. The peaks at m/e = 26, 78 and 154 were very large, similar to those of ions. Under condition E (Fig. 21), only a few fragment and oligomer peaks were observed. It is quite striking that a monomer peak is not observed at all, indicating rapid consumption of it in the gas phase. Again, this coincides with the general tendency of ions. Generally, the peak intensity of neutral species was very large compared to that of ions.

In conclusion, the mass spectra of ionic or neutral species changes with the reaction conditions, although the correlation is confined to a qualitative level.

Variation of plasma characteristics with sampling position

It is expected that plasma characteristics are different from position to position in a flow reactor. Thus, densities of active species and/or composition of monomer and argon differ with position as a result of competition between diffusion and consumption. Variation of T_e and n_e with position of the probe under typical conditions is shown in Table 3. The change is significant in most cases. It explains the fact that a polymer film with excellent properties can be obtained only in a limited region of the reactor under fixed conditions. T_e and n_e showed their maximum at the rf coil position and decreased monotonically along the downstream direction. The pattern of decrease depends on the reaction conditions.

Under Condition E, T_e and n_e decreased abruptly; T_e decreased by 2.0×10^4 K, while n_e decreased by an order of magnitude. This means that few electrons were left at Position 15 in this case, owing to rapid gas phase polymerization. Under Condition B, on the contrary, the change was exceptionally small. The plasma at various positions in the reactor could thus be characterized using the probe.

Mass spectra of both ionic and neutral species also differ with position in a reactor. Intensities of high molecular weight oligomers were very small at Position 2, adjacent to the rf coil. Only fragment (especially m/e = 26), monomeric m/e = 78 and dimeric m/e = 154 species were found in abundance at this position under all the reaction conditions. This is in contrast to the spectra at Position 15, in which many high molecular weight peaks were observed.

Plasma diagnostics as a tool for controlling plasma reaction

Abnormal plasma reactions often damage the quality of polymer films. Other than the deviation of the reaction conditions from the standard, there are some factors which affect the quality of product significantly.

In Plasma Polymerization; Shen, M., et al.;
ACS Symposium Series; American Chemical Society: Washington, DC, 1979.

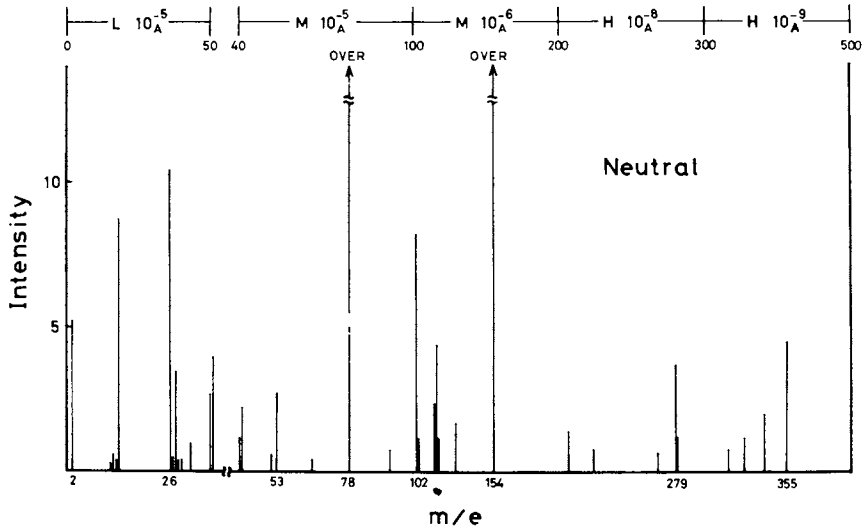

Figure 20. Mass spectrum of neutral species in a plasma under Condition B (see Table 1)

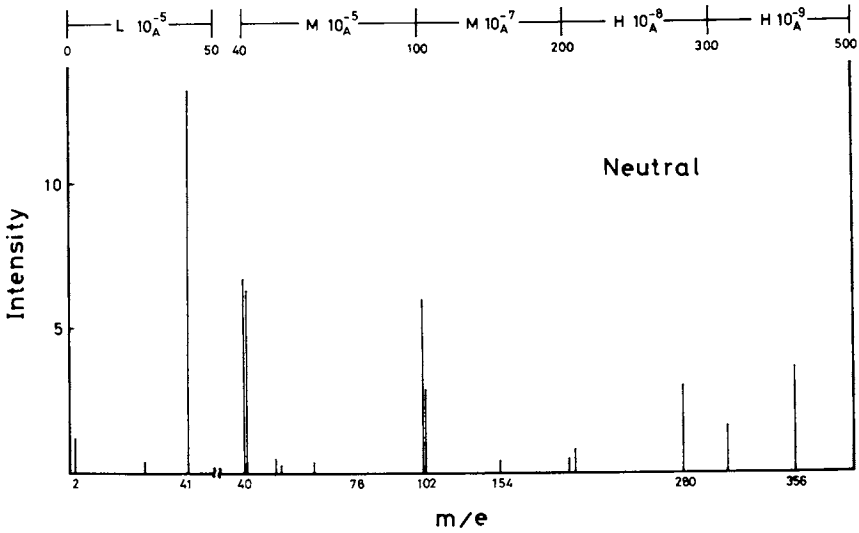

Figure 21. Mass spectrum of neutral species in a plasma under Condition E (see Table 1)

In Plasma Polymerization; Shen, M., et al.;
ACS Symposium Series; American Chemical Society: Washington, DC, 1979.

The most probable trouble is mixing of air into the reactor. The effect of mixing of O_2 and H_2O on T_e was examined. In the case of a pure Ar plasma, T_e suffered little change by the introduction of such impurities. T_e of polymerizing benzene plasma, on the contrary, was decreased about 8000 K by presence of small amounts of O_2. A mass spectrometer connected to the reactor was able to identify gaseous impurities in the reactor and could also be used to find leaks.

In a multi-component system such as was used in this study, plasma characteristics varied with the elapsed time after the reaction was initiated. The variation was remarkable especially at an early stage of the reaction, as shown in Fig. 22. T_e, for example, fluctuated about 8000 K during a reaction under the condition B. The variation in T_e was ascribed to changes in the monomer/gas composition. The latter was inevitable since the reaction of benzene was very rapid, and the time constant for restoring a disturbance in composition was large for our reactor. By using the available diagnostics it was possible to maintain the optimum monomer/gas composition during reaction.

T_e and n_e were very sensitive to small changes in reactor geometry. Two kinds of benzene inlet nozzles (Fig. 1) were used. The difference was the length of the nozzle; one leads benzene into the center of argon flow while the other is at the wall as shown in Fig. 1. The value of T_e when the latter was used higher by about 5000 K. This difference may be the result of incomplete mixing of benzene with argon in the former nozzle. Since the flow in the reactor was laminar at the conditions studied, the flow rate was fast at the center of argon flow while zero at the wall. Therefore, most of the benzene was carried away before completely mixing with the argon. Even such a small variation of reactor geometry affects the flow pattern, i.e., the distribution of gas composition in the reactor, and therefore the yield, composition and properties of reaction products. Plasma diagnostics are again capable of detecting such variation.

The effect of reactor type on the quality of polymer film deposited is important to know. Use of the plasma probe could detect differences, although these were not investigated systematically. T_e decreased about 2×10^4 K in an internal electrode type reactor (compared to the electrodeless one). The geometry and size was close to that used by Kobayashi et al. (8). In the former case, it was found that T_e remained essentially unchanged when the probes were placed at the center of the two disk electrodes and scanned across the diameter.

Reverse osmosis membranes suffered a significant deterioration in their pressure resistance when they were prepared by using a new reactor made of quartz glass. T_e in the quartz reactor was about 3×10^4 K, while 5×10^4 K in the pyrex reactor under the same reaction condition. A polymerization reaction was performed keeping T_e at 5×10^4 K by raising the electric power supply from 40 W to 52 W in the quartz reactors. The product thus obtain showed the required pressure resistance. One of the reasons for the difference

In Plasma Polymerization; Shen, M., et al.;
ACS Symposium Series; American Chemical Society: Washington, DC, 1979.

Table 3. Variation of T_e and n_e with the Position of Probe Measurement

Reaction Condition	T_e (10^4K)		n_e (10^7/cc)	
Position	10	15	10	15
A	4.5	1.3	2200	5
B	4.4	4.1	250	200
C	4.6	3.0	340	7
E	4.4	1.0	2200	0.4

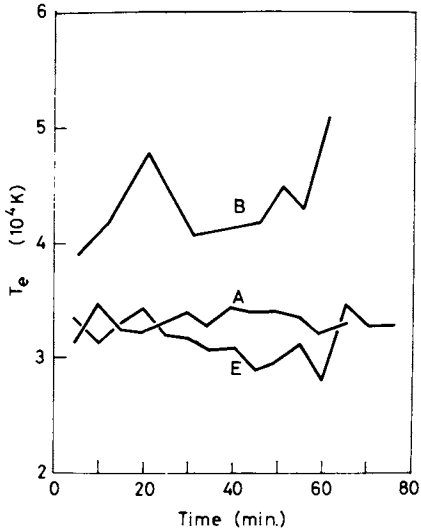

Figure 22. Variation of T_e with the elapsed time after the reaction was initiated. A, B and E stand for reaction conditions listed in Table 1.

in T_e with reactor material may be a difference in the recombination coefficient of electrons and ions on the wall, although some unnoticed factors may also contribute.

FT-IR spectra

The IR spectrum of the polymer film prepared under Condition B is shown in Fig. 23. A structure close to polystyrene is revealed as evidenced by peaks at 540, 700, 760, 840, 1070, 1450, 1490 and 1600 cm^{-1}. Solubility tests with various solvents proved that the polymer was highly cross-linked. The spectrum of the polymer powder is quite different from that of the film. Peaks assignable to acrylic ester and/or epoxy groups (3400, 1720, 1600, 1500, 1200 and 820 cm^{-1}) prevail in that spectrum together with that of polystyrene as shown in Fig. 24. Oxidation of the polymer may be the result of reaction with oxygen in the air after the polymer was taken out from the reactor, as pointed out by several authors (8). It suggests that the powder contains many more active sites, e.g. radicals, than the film. The spectrum corresponding to Condition A is shown in Fig. 25, and is seen to have features similar to both of the previous spectra. Thus, it is seen that the structure of the plasma-polymer depends on the polymerization conditions.

CONCLUSIONS

A heated plasma-probe method was found to be useful for measuring plasma parameters such as T_e, n_e and $f(\varepsilon)$ of a polymerizing plasma. The parameters were very sensitive to the state of plasma, and thus capable of detecting the occurrence of abnormal plasma reaction caused by accidental mixing of gaseous impurities, changes in reaction conditions, reactor geometry etc. By using the method as a monitoring tool, control of polymerization reactions could be performed during the reaction with high reliability.

ACKNOWLEDGMENT

The authors are much indebted to Japan Synthetic Rubber Co. Ltd. for generous permission to publish this work. The authors also wish to thank T. Katsuta and F. Shimizu for their assistance in performing the experimental work.

APPENDIX
Necessary Condition for Heated Probe

The condition necessary for our heated probe is that the emission current be small compared to the probe current. Thermionic emission from a metal is given by

$$i_s = A\,T^2 \exp\,(-e\phi/kT)$$

where, i_s is thermionic emission current, ϕ is the work function, e is elementary electric charge, k is Boltzmann's constant, T is

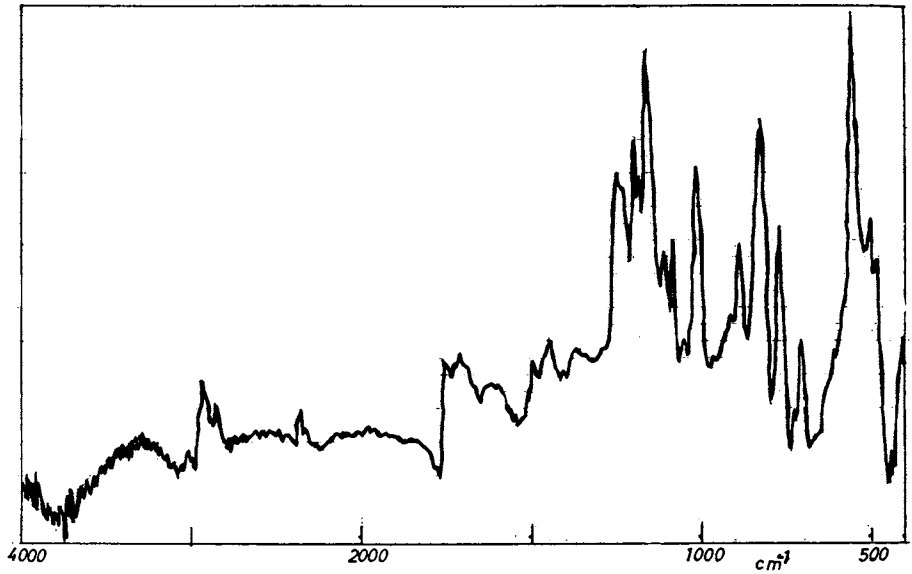

Figure 23. FTIR (ATR) spectrum of benzene polymer prepared under Condition B (see Table 1)

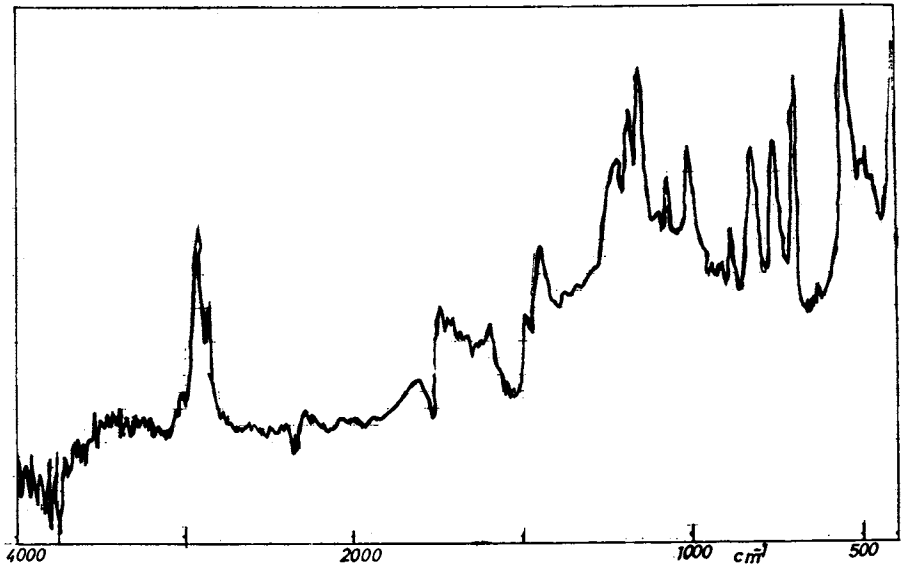

Figure 24. FTIR (ATR) spectrum of benzene polymer prepared under condition E (see Table 1)

In Plasma Polymerization; Shen, M., et al.;
ACS Symposium Series; American Chemical Society: Washington, DC, 1979.

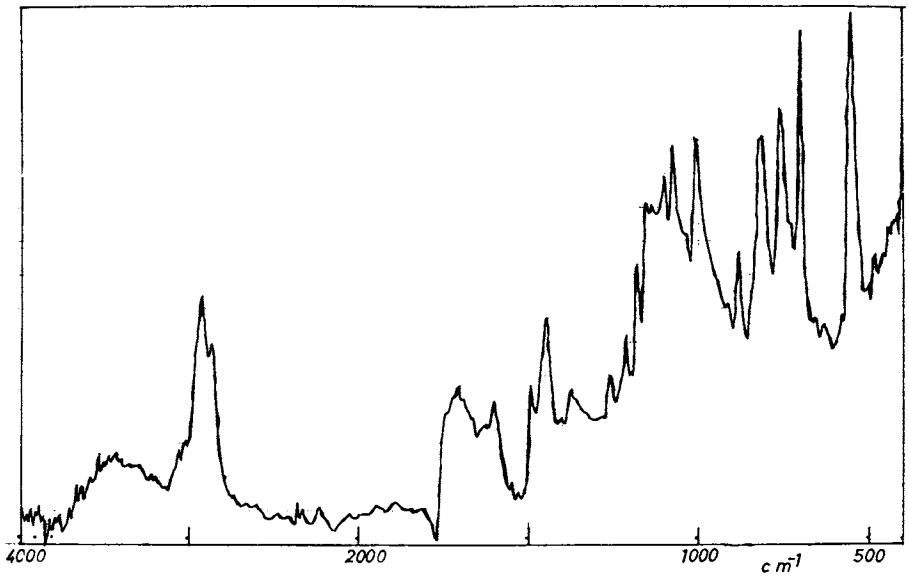

Figure 25. FTIR (ATR) spectrum of benzene polymer prepared under Condition A (see Table I)

Table 4. Electron Emission Current from Metals at Elevated Temperatures

		Emission current (A/cm^2)			
Metal	ϕ (eV)	773K	1273K	1773K	2000K
Ni	5.0	1.9×10^{-25}	3.2×10^{-12}	2.3×10^{-6}	1.2×10^{-4}
W	4.5	3.3×10^{-22}	3.0×10^{-10}	6.2×10^{-5}	2.2×10^{-3}
Pt	6.3	6.1×10^{-34}	2.2×10^{-17}	4.7×10^{-10}	6.4×10^{-8}
Mo	4.4	1.6×10^{-21}	7.8×10^{-10}	1.2×10^{-4}	4.1×10^{-3}

In Plasma Polymerization; Shen, M., et al.;
ACS Symposium Series; American Chemical Society: Washington, DC, 1979.

the absolute temperature, h is Plank constant, and m is electron mass.

Value of i_s were calculated for various metals and are shown in Table 4. The electron current flowing into the probe from the plasma is generally between 1 μA and 1 mA. The surface area of the probe was 0.01 cm^2 so that the probe current density is more than 100 $\mu A/cm^2$. Therefore the thermionic emission current is far less than the probe current at 1000 K.

LITERATURES CITED

1. Bell, A. T., "Fundamentals of Plasma Chemistry" in "Techniques and Applications of Plasma Chemistry," Hollahan, J.R. and Bell, A.T. ed., Wiley-Interscience, New York, 1974.

2. Yasuda, H. and Lamaze, C. E., J. Appl. Polymer Sci., (1971), 15, 2277.

3. Johnson, E. O. and Malter, L., Phys. Rev., (1950), 80, 58.

4. Dote, T., Japan. J. Appl. Phys., (1968), 7, 964.

5. Malter, L. and Webster, W. M., RCA Rev., (1951), 12, 191.

6. Okuda, T. and Yamamoto, K., J. Appl. Phys., (1960), 31, 158.

7. Vasile, M. J. and Smolinsky, G., Intl. J. Mass Spectr. Ion Phys., (1973), 12, 133.

8. Kobayashi, H., Bell, A. T., and Shen, M., J. Appl. Polymer Sci., (1973), 17, 885.

9. Lifshitz, C. and Reuben, B. G., J. Chem. Phys., (1969), 50, 951.

RECEIVED March 29, 1979.

Effects of Plasma-Polymerized Film on the Current-Voltage Characteristics of Single Probe

SHINJI YAMAGUCHI
Department of Electrical Engineering, Suzuka College of Technology, Suzuka, Mie, Japan
GORO SAWA
Department of Electronic Engineering, Mie University, Tsu, Japan
MASAYUKI IEDA
Department of Electrical Engineering, Nagoya University, Nagoya, Japan

It was found many years ago that a glow discharge in various organic vapors results in the formation of insulating films on surfaces exposed to the discharge.[1] Since Goodman[2] first applied this technique to the formation of insulating films, much work has been carried out on the relation between the deposition rate and the experimental discharge condition, such as discharge current, gas pressure, electric power and gas flow rate.[3-14] It is also necessary to clarify the plasma polymerization process in terms of basic quantities of organic gas plasma such as temperatures and densities of ions and electrons. However, because of the inherent complexities associated with plasma measurements in organic vapors, little work has been done on the deposition rate in relation to these quantities. For instance, in the probe measurements, the current-voltage characteristics are distorted by the polymerized film which is deposited on the probe surface during the measurement; this determination of the plasma parameters is difficult. On the one hand, the effects of the surface contamination on the probe characteristics have recently posed an annoying problem in connection with the ionospheric measurements.[15] Various techniques have been presented to overcome these contamination effects.[15,16] A polymerized film on the probe surface can be regarded as a kind of so called "contamination" for the probe. The authors have carried out measurement of the electron temperature in glow discharges of organic vapors by means of the double probe method with the aid of quick performance for minimizing the contamination.[17] During the course of the double-probe measurements, a decrease was found in the ion current flowing into the probe which was evaluated from the probe characteristics as the thickness of the polymerized film deposited on the probe surface was increased. If a decrease in the real ion current to the probe with the contamination layer is confirmed, the probe characteristic would give new information about the polymerization process. In an attempt to clarify the effects of the contamination layer on the real ion current, the current-voltage characteristics

0-8412-0510-8/79/47-108-115$05.00/0

of the single probe covered with the glow-discharge polymerized film were studied in a nitrogen gas glow discharge, in which little or no polymerization occurs. An additional experiment was also made by using the equivalent circuit model consisting of a parallel combination of C and R for the polymerized film. A comparison between two types of experiments was made in an attempt to elucidate whether or not the change in ion current with the contamination layer is due merely to the variation of electric potential on the probe surface.

Deposition Rate

First, the deposition rate of polystyrene in a dc glow discharge was reproduced.[17] A flat glass substrate(20mm×10mm×0.7mm) covered with a gold-evaporated film as shown in Fig.1, was set at the same position as the single probe, in a positive column 1.4 cm apart from the anode. After evacuation of the chamber to 10^{-5}Torr, styrene monomer gas was introduced into the discharge tube to a pressure of 1 Torr. A dc voltage was then applied to the electrodes to initiate and sustain a glow discharge with a discharge current of 2 mA. The thickness d of the polymerized film deposited on the substrate for the polymerization period t was measured with an interference microscope and the results are shown in Fig.2. If the polymerization period was less than 1.5 min., the thickness was so small that the thickness measurement was difficult. The thickness for the period t in such a small range was therefore estimated from extrapolation of the curve in Fig.2. The thickness of the film on the single probe corresponding to the polymerization period t was evaluated as shown in Table I.

Table I Thickness d of the film on the single probe corresponding to the polymerization period t evaluated from the extrapolation of the curve in Fig.2.

Polymerization period t (sec.)	1	3	5	10	20	30	40
Thickness d of the film on the probe (Å)	17	40	57	95	160	220	280

It can be seen from Fig.2 that the thickness d rises sharply at first, but tends to have a constant rate. The deposition rate R was calculated from a slope of the curve in Fig.2 and is shown as a function of the period t in Fig.3. To date, ion or radical reactions have been proposed for the glow-discharge polymerization processes, but the predominant process is not clear. If ions play an important role in the polymerization, it is anticipated from the R-t curve in Fig.3 that an ion current flowing into the floating substrate decreases to a constant value with the polymeriza-

In Plasma Polymerization; Shen, M., et al.;
ACS Symposium Series; American Chemical Society: Washington, DC, 1979.

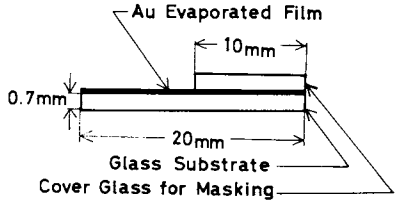

Figure 1. Au evaporated glass substrate for estimating the polymerized film thickness on the single probe

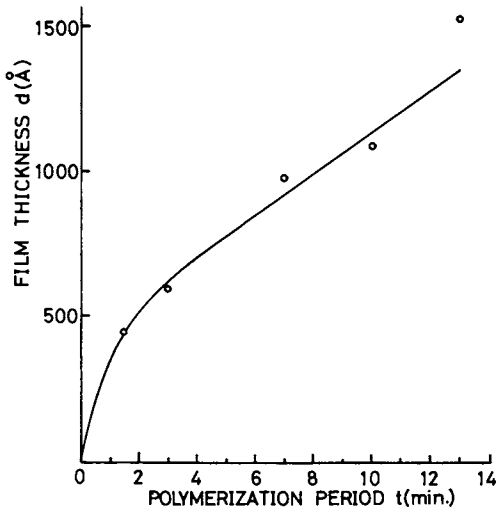

Figure 2. Thickness (d) of styrene polymerized film as a function of polymerization period (t)

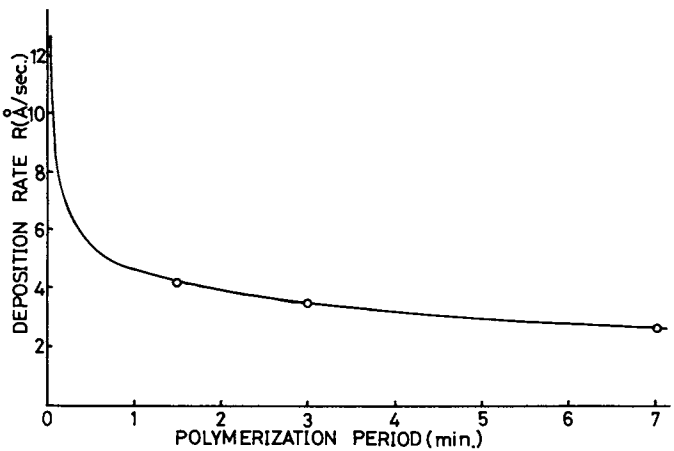

Figure 3. Polymerization rate (R) evaluated from the slope of the curve in Figure 2

In Plasma Polymerization; Shen, M., et al.;
ACS Symposium Series; American Chemical Society: Washington, DC, 1979.

tion period t and the film thickness d.

This expectation will be examined in the following section in which the I-V characteristics of the single probe covered with a glow discharge polymerized film of various thicknesses are presented.

Experimental Method

A schematic diagram of the apparatus used for the single probe measurement is illustrated in Fig.4. A pair of 3-cm-diameter stainless-steel plates were set 5 cm apart in a 6-cm-diameter glass tube. A dc glow discharge was ignited at a nitrogen gas pressure of 5 Torr and kept at a discharge current of 12 mA. Unless otherwise stated, the C-R equivalent circuit was usually removed in the circuit shown in Fig.4. Repetitive sawtooth pulses(-90 V$\sim$26 V) as shown in Fig.5, with a frequency f were applied between the anode and the single probe of 1.3-cm-long, 0.05-cm-diameter, platinum wire. The pulse frequencies were 100.0, 75.0, 47.6, 37.0, 20.0, 11.9, 6.1, 2.1, 1.0 and 0.5 Hz. The I-V curves were obtained with the clean surface single probe at various frequencies.

Second, the probe measurements were made in the nitrogen gas at the same conditions as before but with the probe contaminated with an insulating film of various thicknesses deposited in the glow discharge of styrene vapor. The procedure for coating the probe surface by the polymerized film was as follows. The clean probe, which was concealed with a glass cover removable by external manipulation, was set in the same position as that at which a flat glass substrate had been placed. Styrene monomer vapor was introduced at 1 Torr into the tube previously evacuated at 10^{-5} Torr and a dc glow discharge was ignited and maintained with a discharge current of 2 mA. The concealing glass cover was removed and the probe surface was exposed to the plasma for a definite period t corresponding to the polymerization period. Then the probe was concealed again. This operation could be controlled to an accuracy of a fraction of 1 sec. Since polymerized films were also formed on the discharge electrodes, the films were scraped off after every end of the film deposition on the probe surface.

Finally, an experiment with the C-R parallel circuit was carried out, the details of which will be described in later section.

Experimental Results

As a typical experimental result, the I-V curves of the single probe at 47.6 Hz are shown in Fig.6. An apparent current I_{ai} on the single probe characteristic is defined as given in Fig.7. Data scatter was examined by repeating the measurements several times. In one case, the glow discharge was extinguished and the discharge electrode system refabricated. The root-mean-square error in I_{ai} with the clean probe was about 0.3 μA. I_{ai} estimated from

In Plasma Polymerization; Shen, M., et al.;
ACS Symposium Series; American Chemical Society: Washington, DC, 1979.

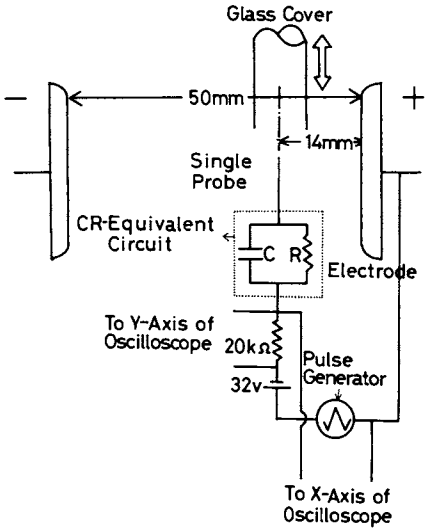

Figure 4. Schematic for the single probe measurement: the C–R circuit usually is omitted unless otherwise described.

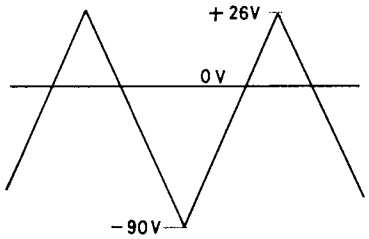

Figure 5. Repetitive sawtooth pulses applied to the single probe

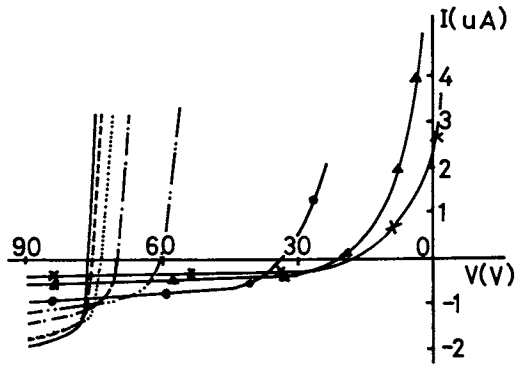

Figure 6. The I–V characteristic of the single probe without and with the styrene film cover: t *is the polymerization period; the curve for* t = *0 was obtained with no apparent contamination; the probe measurements were performed in the dc glow discharge in nitrogen gas at 5 torr and 12 mA; the frequency of sawtooth pulses applied to the probe was 47.6 Hz and their peak values were 26 V and −90V with respect to the anode: (——)* t = *0 sec; (—·—)* t = *1 sec; (· · ·)* t = *3 sec; (– · –)* t = *5 sec; (– · · –)* t = *10 sec; (●)* t = *20 sec; (▲)* t = *30 sec; (×)* t = *40 sec; f = 47.6 Hz.*

In Plasma Polymerization; Shen, M., et al.;
ACS Symposium Series; American Chemical Society: Washington, DC, 1979.

the I-V curves is shown in Fig.8 as a function of d which is estimated at 17, 40, 57, 95, 160, 220 and 280 Å at the polymerization periods t of 1, 3, 5, 10, 20, 30 and 40 respectively. It can be seen that I_{ai} decreases with increasing thickness d. In the case of the polymerized film of a fixed thickness, the variation of I_{ai} with the frequency is not yet clear, though a decrease of I_{ai} with decreasing frequency was occasionally observed. When the repetitive sawtooth pulses (illustrated in Fig.5) are applied to the contaminated single probe, the I-V curves exhibit a hysteresis as shown in Fig.9. We will here confine ourselves to the part of the curve observed when V is increased.

Discussion

It was found that the apparent ion current I_{ai} decreases with an increase in the film thickness d. A question arises as to whether the decrease in I_{ai} is an apparent phenomenon due merely to variation of potential on the probe surface or a real phenomenon based on the direct contact of polymer instead of metal with plasma.

To solve this problem, the following experiment was made: The polymerized film was replaced by a C-R parallel circuit in the external measuring circuit and the probe surface was kept clean. The I-V characteristics were obtained under the same discharge condition as before with various combination of R, C and time constant τ(=CR) as shown in Table II.

Table II A parallel combination of C and R for the polymerized film. (τ in msec.)

C(μF) \ R(kΩ)	2	10	50	250	1250	6250	∞
0.005	τ=0.01	0.05	0.25	1.25	6.25	31.3	—
0.025	0.05	0.25	1.25	6.25	31.3	156	—
0.125	0.25	1.25	6.25	31.3	156	781	—
0.625	1.25	6.25	31.3	156	781	3900	*1.25×10^{6}

*τ is estimated from the leakage resistance of the capacitor employed.

If the relative dielectric constant ε_r is assumed to be 3.0 for polystyrene films polymerized in glow discharges,(3) an equivalent capacitance C of the polystyrene film ranges between 0.019 μF and 0.32 μF, since the thickness d is between 17 Å and 280 Å, and the effective area of the probe surface is 0.2 cm^2. The values of capacitance used in the C-R circuit cover those of capacitors equivalent to the polystyrene film.

On the other hand, the volume resistivity ρ of the styrene

In Plasma Polymerization; Shen, M., et al.;
ACS Symposium Series; American Chemical Society: Washington, DC, 1979.

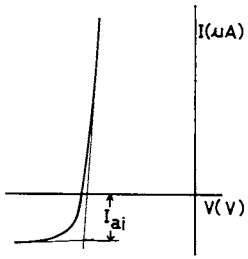

Figure 7. Definition of the apparent ion current I_{ai} on the I–V curve

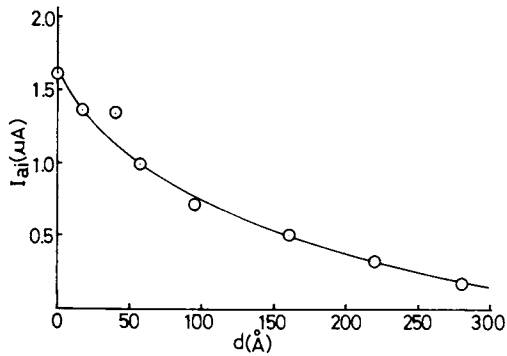

Figure 8. Apparent ion current I_{ai} as a function of d

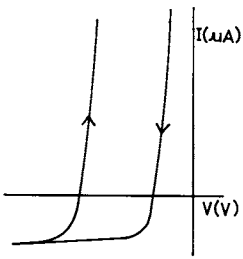

Figure 9. Hysteresis phenomenon of I–V characteristic by the contaminated single probe

In Plasma Polymerization; Shen, M., et al.;
ACS Symposium Series; American Chemical Society: Washington, DC, 1979.

polymerized film could not be specified, since ρ depends on the thickness of the film, applied voltage, polymerization conditions and atmosphere. Furthermore, the polymerized film is too thin to allow direct measurement of the resistivity. Therefore, R was varied in as wide a range as possible. Values of R in Table II correspond to equivalent resistivities ρ from 10^7 to 10^{13} Ω-cm since time constant τ (=CR) is equal to $\varepsilon_o\varepsilon_r\rho$, where ε_r is assumed to be 3.0. Figure 10(a),(b) and 11 show the change in apparent ion current I_{ai} with values of R and a parameter of C. Little change in I_{ai} was found within the present experimental conditions, while the voltage giving zero probe current (I=0) shifts with changing R and/or C. It can be thus concluded that the decrease in I_{ai} with the existence of polymerized film on the probe surface is not due to the variation of potential on the film surface, but due to some physical processes arising from the direct contact of polymerized film with plasma. No satisfactory explanation of these results can be given at this stage, but possible processes are presented. The adsorption of styrene monomer gas and the deposition of polymerized film will cause a change in electronic states around the probe surface. Neutralization processes of incident ions on the surface may be modified.[18,19,20,21] As a result, a considerable portion of the incident positive ions is probably accumulated around the probe surface and this accumulated ion layer in gaseous space would limit the ion current, resulting in the decrease in ion current.

Conclusion

The effects of glow-discharge polymerized polystyrene films on the I-V characteristics of single probe were studied in nitrogen gas, where no polymerization occurs. It was found that the apparent ion current I_{ai} flowing into the single probe decreases inversely with the film thickness as was previously reported with the double probe.

A comparison of these results with the data with the C-R parallel circuit model reveals that the decrease in I_{ai} is not caused by the potential change on the probe surface, but is related to the physical process arising from the interaction between the plasma and the polymerized film. A decrease in real ion current into the probe with an increase in the film thickness was confirmed. This fact is interesting from the point of view of the deposition rate which was also found to decrease to a constant value with the growth of film in styrene vapor. The close parallelism of the changes in ion current and polymerization rate with film thickness suggests that ions play an important role in the glow-discharge polymerization process under the present experimental conditions.

In Plasma Polymerization; Shen, M., et al.;
ACS Symposium Series; American Chemical Society: Washington, DC, 1979.

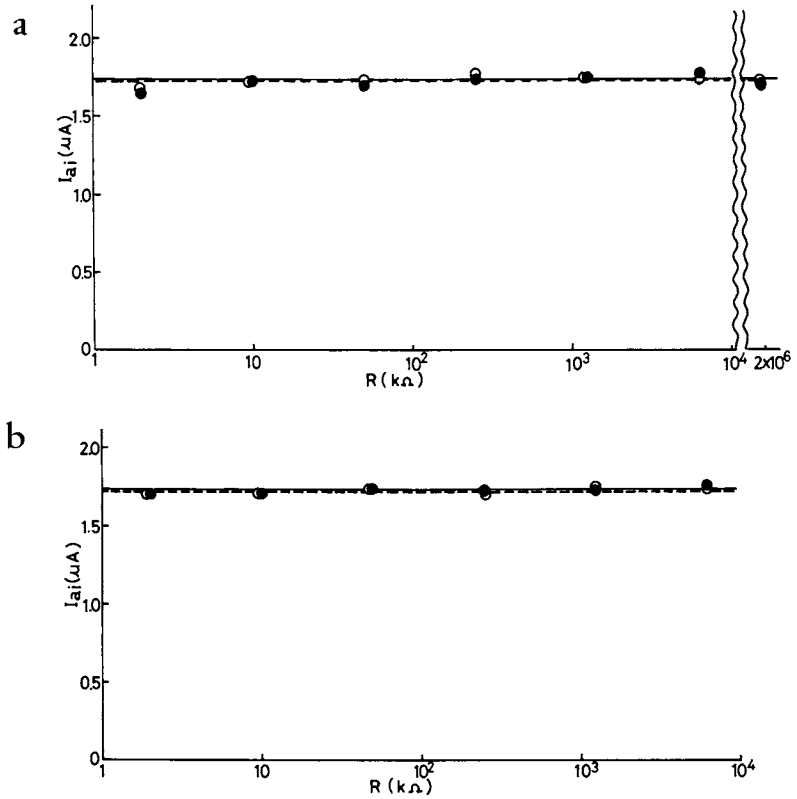

Figure 10. The apparent ion current I_{ai} *as a function of* R *with a fixed capacitance of 0.625 μF(a) and 0.005 μF(b). The measurements were made with no apparent contamination, but with C–R circuit substituted in place of the contamination layer. (●) 100 Hz, (○) 0.5 Hz.*

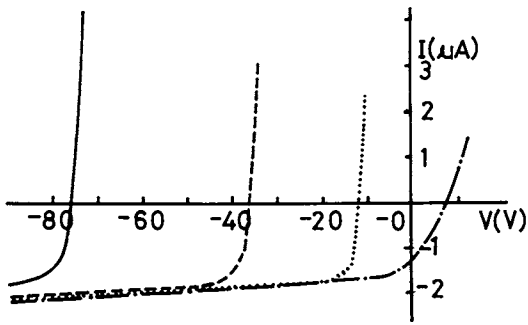

Figure 11. The I–V characteristic of the single probe obtained with C–R circuit: (——) C = 0.625 μF, R = 2 kΩ; (– – –) C = 0.625 μF, R = 250 kΩ; (· · ·) C = 0.625 μF, R = 1250 kΩ; (– · – ·) C only.

In Plasma Polymerization; Shen, M., et al.;
ACS Symposium Series; American Chemical Society: Washington, DC, 1979.

Acknowledgment

The authors wish to express their thanks to Dr.S.Morita, Meijo University,for valuable discussions.

Abstract

Current-voltage characteristics of single probes covered with plasma polymerized films were studied in a nitrogen gas glow discharge in order to clarify the plasma polymerization process. A decrease in ion current flowing into the probe was found as the thickness of polymerized film deposited on the probe surface increased. If a decrease in real ion current to the probe with contamination layer is confirmed, the probe characteristic would give new information about the polymerization process. Another experiment was made using an equivalent model consisting of a parallel combination of C and R for polymerized films.

A comparison between the two experiments was made in an attempt to elucidate whether the observed change in ion current with contamination layer can be explained by the variation of electric potential on the probe surface or not.

In Plasma Polymerization; Shen, M., et al.;
ACS Symposium Series; American Chemical Society: Washington, DC, 1979.

Literature Cited

1 E.G.Linder and A.P.Davis, J. Phys. Chem., (1931) 35 3649
2 J.Goodman, J. Poly. Sci., (1960) 44 552
3 T.Williams and M.W.Hayes, Nature (1966) 209 769
4 A.R.Denaro, P.A.Owens and A.Crawshaw, Eur. Polym. J.(1968) 4 93
5 A.R.Denaro, P.A.Owens and A.Crawshaw, Eur. Polym. J.(1969) 5 471
6 H.U.Poll, Z. Angew. Phys. (1970) 29 260
7 A.R.Westwood, Eur. Polym. J. (1971) 7 363
8 K.C.Brown and M.J.Copsey, Eur. Polym. J. (1972) 8 129
9 K.C.Brown, Eur. Polym. J. (1972) 8 117
10 H.Yasuda and C.E.Lamaze, J. Appl. Polym. Sci. (1971) 15 2277
11 H.Yasuda and C.E.Lamaze, J. Appl. Polym. Sci. (1973) 17 1519
12 H.Kobayashi, A.T.Bell and M.Shen, J. Appl. Polym. Sci. (1973) 44 4317
13 M.Niinomi, H.Kobayashi, A.T.Bell and M.Shen, J. Appl. Phys. (1973) 44 4317
14 M.M.Millard, J.J.Windle and A.E.Pavlath, J. Appl. Polym. Sci. (1973) 17 2501
15 P.M.Chung, L.Talbot and K.J.Touryan, Electric Probes in Stationary and Flowing Plasmas: Theory and Application. (Springer-Verlag, Berlin·Heidelberg·New York, 1975)
16 J.C.Holmes and E.P.Szuszczewinz, Rev. Sci. Instrum. (1975) 46 592
17 S.Yamaguchi, G.Sawa and M.Ieda, J. Appl. Phys. (1977) 48 2363
18 H.D.Hagstrum, Phys. Rev. (1954) 96 336
19 H.D.Hagstrum, Phys. Rev. (1956) 104 672
20 H.D.Hagstrum and G.E.Becker, Phys. Rev. (1973) B8 107
21 H.D.Hagstrum, Phys. Rev. (1966) 150 495

RECEIVED March 29, 1979.

Fourier Transform Infrared Analysis of Plasma-Polymerized 2-Vinylpyridine Thin Films

K. W. BIEG
Sandia Laboratories, Albuquerque, NM 87185
D. K. OTTESEN
Sandia Laboratories, Livermore, CA 94550

Polymer thin films deposited in an rf electrical discharge have been suggested for use as dielectric materials in electrical capacitors (1,2). As a preliminary step toward the study of the electrical and aging properties of thin film capacitors made from plasma polymerized 2-vinylpyridine, we have undertaken an investigation of the chemical structure of these films deposited under a variety of plasma reactor conditions. Unfortunately, plasma polymerized organic films are difficult to analyze by conventional means, due primarily to their insoluble nature and availability as only milligram samples. In particular, conventional dispersive infrared transmission techniques have traditionally used artificially thick films on other than metallic substrates and have generally yielded poorly resolved spectra. We have found Fourier transform infrared spectroscopy (FTIR) to be a useful technique for the characterization of plasma polymerized 2-vinylpyridine thin films (1,000-40,000 Å) deposited on aluminum substrates. This technique has been used to observe variations in the chemical structure of poly(2-vinylpyridine) films as a function of reactor conditions (pressure, power, and carrier gas). Chemical and thermal behavior of these films was further investigated by elemental and thermogravimetric analyses.

Experimental

The equipment used in this study (Figure 1) consisted of a capacitively-coupled plasma reactor similar to the apparatus described by Poulsen (3) for the plasma etching of integrated circuits. This arrangement resulted in uniform depositions over a range of flow rates and improved utilization of monomer. Monomer and carrier gas are introduced beneath the lower (ground) electrode and are forced to sweep radially inward across the 5 in. diameter aluminum electrodes. The gases are pumped out through the tube in the center of the lower electrode. Substrates were mounted on the lower electrode. Electrode spacing was maintained at 2.3 cm. Power is supplied by an International Plasma Model

0-8412-0510-8/79/47-108-127$05.00/0

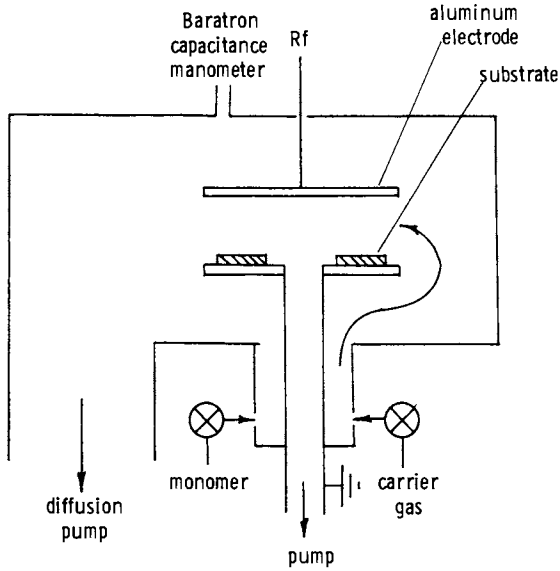

Figure 1. Capacitively coupled plasma reactor

PM 101 rf power generator operating at 13.56 MHz. Chamber pressure was monitored with an MKS Baratron Type 90H-1 capacitance manometer. The reactor was evacuated to less than 10^{-6} Torr with a diffusion pump prior to introduction of monomer. During the actual deposition, a mechanical pump with an in-line liquid nitrogen cold trap was used to maintain monomer and carrier gas flow.

2-Vinylpyridine (2-VP) monomer was used as received from ICN-K&K Laboratories. However, no impurities were detected by gel permeation chromatography or infrared spectroscopy. Monomer was thoroughly degassed by repeated freeze-pump-thawing under vacuum prior to use. Research grade argon (99.99% purity, Matheson Gas Products) was used as the carrier gas. Substrates were prepared by vapor deposition of an opaque layer of aluminum on glass microscope slides. Polymer film thicknesses were determined by measuring the step height between a masked and unmasked portion of the specimen with a Rank, Taylor, and Hobson Talystep 1 traversing stylus. Deposited films were stored in a vacuum dessicator prior to measurement of the infrared spectra in order to minimize the absorption of moisture from the atmosphere.

Infrared spectra were obtained with a Digilab FTS-14 FTIR spectrometer in the reflection-absorption mode (4). A single external reflection from the sample surface was used, with an angle of incidence of 75°. The spectra were taken at a resolution of 6 cm^{-1} while the instrument was purged with dry nitrogen. Elemental analyses were performed on a Perkin-Elmer Model 240 elemental analyzer. Thermal analyses in dry argon were obtained with a DuPont Model 951 thermogravimetric analyzer. Sample weight was approximately 1 mg. with a heating rate of 10°C/min.

Results and Discussion

Plasma conditions under which the various films were prepared are presented in Table I. Except in the case of Sample 6, the reactor was operated near the minimum power below which the glow would extinguish. The Fourier transform infrared transmission spectrum of conventional, linear poly(2-vinylpyridine)(Polysciences #1050) is shown in Figure 2. The broad feature at 3450 cm^{-1} is due to water which was difficult to eliminate from the KBr pellet. The assignments for the major bands in this spectrum (Table II) are relatively straight-forward based on the assignments for polystyrene (5), poly(4-vinylpyridine)(6), and substituted pyridines (7). The reflectance FTIR spectrum for the plasma polymerized film prepared under the conditions specified for Sample 1 in Table I is shown in Figure 3. This spectrum is quite similar to that for the linear polymer. In particular, the plasma polymer spectrum contains the strong ring CH stetch at 3060 cm^{-1}, along with the aromatic CH wagging vibration at 745 cm^{-1} characteristic of the expected 2-substituted pyridine ring. Also, the CH_2 backbone stetching and wagging bands are observed at 2930 cm^{-1}

In Plasma Polymerization; Shen, M., et al.;
ACS Symposium Series; American Chemical Society: Washington, DC, 1979.

Table I

PLASMA POLYMERIZATIONS CONDITIONS

Sample	Power (Watts)	Voltage P to P, Volts	2VP Pressure (Torr)	Ar Pressure (Torr)	Thickness (Angstrom)
1	10	250	0.23	—	28,000
2	10	250	0.23	—	5,500
3	4	150	0.03	0.20	38,000
4	4	150	0.03	0.20	5,700
5	4	180	0.03	—	5,000
6	40	250	0.03	0.20	9,000

Table II

INFRARED FREQUENCIES AND BAND ASSIGNMENTS FOR LINEAR POLY(2-VINYLPYRIDINE) (From Figure 2)

Frequency, cm^{-1}	Band Assignments*
3060	ν_{20b}
3002	ν_{7b}
2930	$\nu_{(CH_2)}$
2860	$\nu_{(CH_2)}$
1590	ν_{8a}
1570	ν_{8b}
1470	ν_{19a}, $\delta_{(CH_2)}$
1430	ν_{19b}
1150	ν_{18b}
1050	ν_{18a}
995	ν_{12}
775	ν_{10a}
745	ν_{10b}

*Wilson (8) Nomenclature.

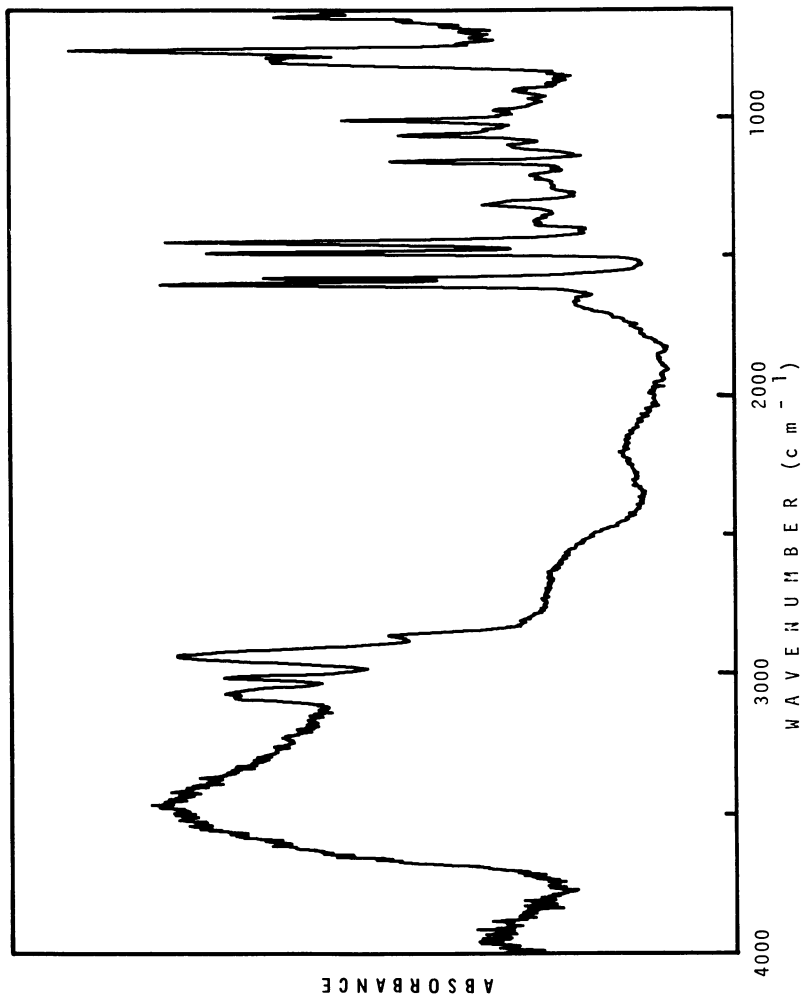

Figure 2. Transmission FTIR spectrum of conventional poly(2-vinylpyridine) in KBr pellet

In Plasma Polymerization; Shen, M., et al.;
ACS Symposium Series; American Chemical Society: Washington, DC, 1979.

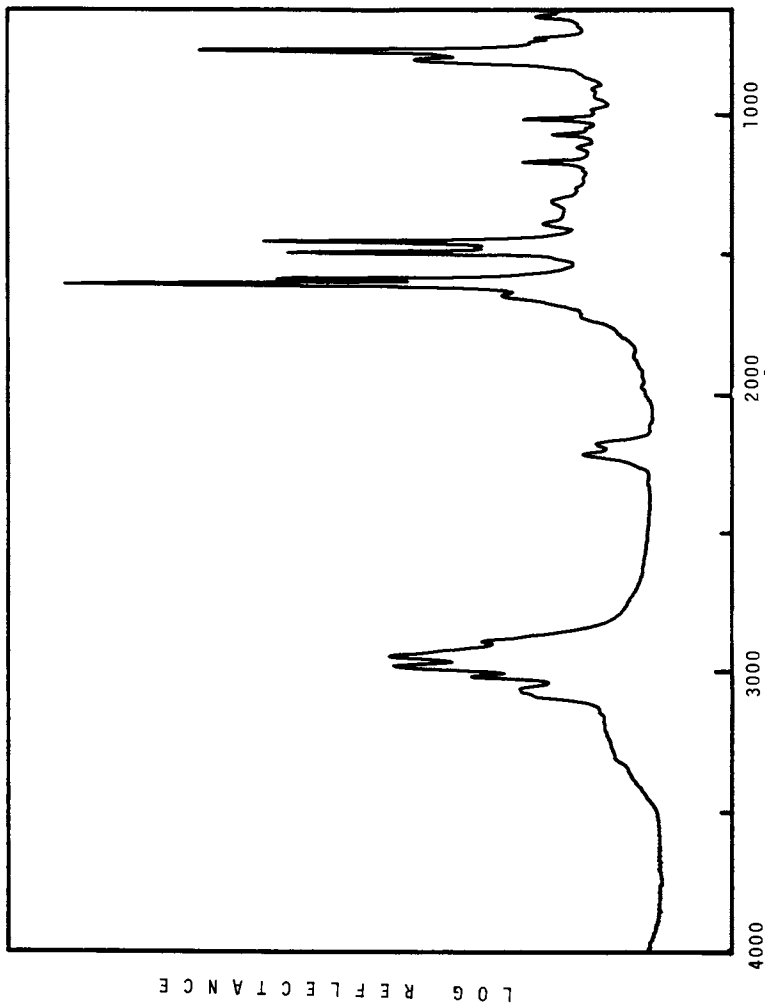

Figure 3. Reflectance FTIR spectrum of Sample 1, Table 1

and 1470 cm^{-1}, respectively. The presence of the intense CC and CN ring stretching bands at 1590 cm^{-1} and 1570 cm^{-1} and the strong ring vibration at 1430 cm^{-1} indicates a substantial retention of aromaticity in the plasma polymer.

A number of important differences are also apparent. Additional relatively strong absorptions are present at 2200 cm^{-1} and 2165 cm^{-1}. Considering the starting material and lack of other absorptions in this region, this band can clearly be assigned to a nitrile group. Other researchers have also found a strong tendency to form nitrile groups during the plasma polymerization of nitrogen-containing monomers (9,10). However, this peak is shifted to an abnormally low energy for either an aliphatic or aromatic nitrile (11). A possible explanation is an enamino-or imino-nitrile type structure (12,13) which have been observed to absorb at these energies. This interpretation is further supported by the appearance of a broad band in the 3200-3400 cm^{-1} region which may be associated with an amino or imino NH stretch. The absorption at 1630 cm^{-1} may be identified as an olefinic (C = C) or imino (C = N) stretching band or an amino deformation band. Cleavage of the pyridine ring to form nitrile groups is not unexpected from ion chemistry studies relevant to the present investigation. Ion sampling of radio-frequency discharges of benzene (14) have shown that significant fragmentation of the benzene ring occurs in low pressure discharges at conditions similar to those considered in this study. Further, fragmentation threshold measurements on pyridine (15) indicate that the aromatic CN bond is weaker to electron impact than the corresponding CC bond in benzene. Thus, cyano or nitrogen-containing fragments in the discharge may be incorporated into the polymer. Also noteworthy in the spectrum of the plasma polymer is the strong new band at 2965 cm^{-1} and the rather weak band at 1370 cm^{-1}. These absorptions may be assigned to methyl CH_3 stretching and deformation vibrations, suggesting a significant amount of branching in the plasma polymer. A very small carbonyl shoulder is present near 1700 cm^{-1} which was observed to increase in intensity with exposure to dry air, indicative of the expected post-oxidation of trapped radicals (16). The FTIR spectrum of a thinner film (Sample 2, Table I) of this same material is shown in Figure 4. This spectrum contains the same bands as those observed for the thicker film. However, the CH stretching bands in the 2900-3100 cm^{-1} region are noticeably more intense relative to the ring and deformation bands in the 600-1600 cm^{-1} portion of the spectrum. This may be a result of variations of the net electric field in the film as a function of frequency caused by the phase shift at the polymer-metal interface (17) rather than actual structural variations in the films. This effect is unique to reflection techniques.

Figures 5 and 6 show the FTIR spectra of films of differing thickness (Sample 3 and 4, Table I) prepared at the same total pressure but at a much lower monomer pressure than Sample 1 and 2.

In Plasma Polymerization; Shen, M., et al.;
ACS Symposium Series; American Chemical Society: Washington, DC, 1979.

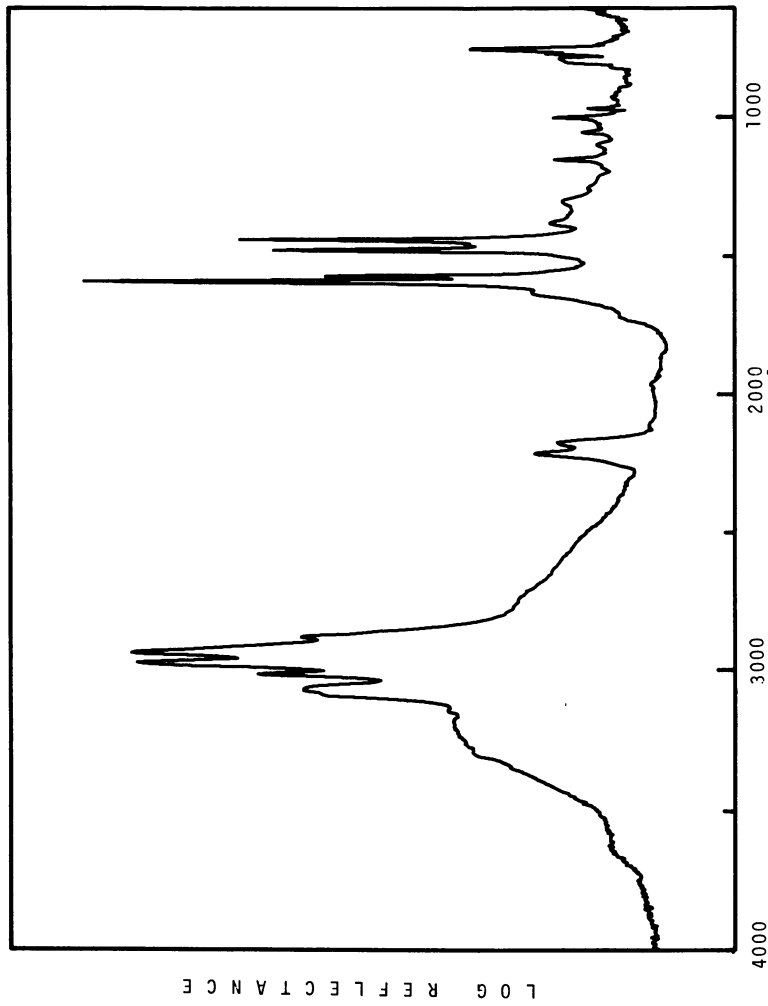

Figure 4. Reflectance FTIR spectrum of Sample 2, Table I

In Plasma Polymerization; Shen, M., et al.;
ACS Symposium Series; American Chemical Society: Washington, DC, 1979.

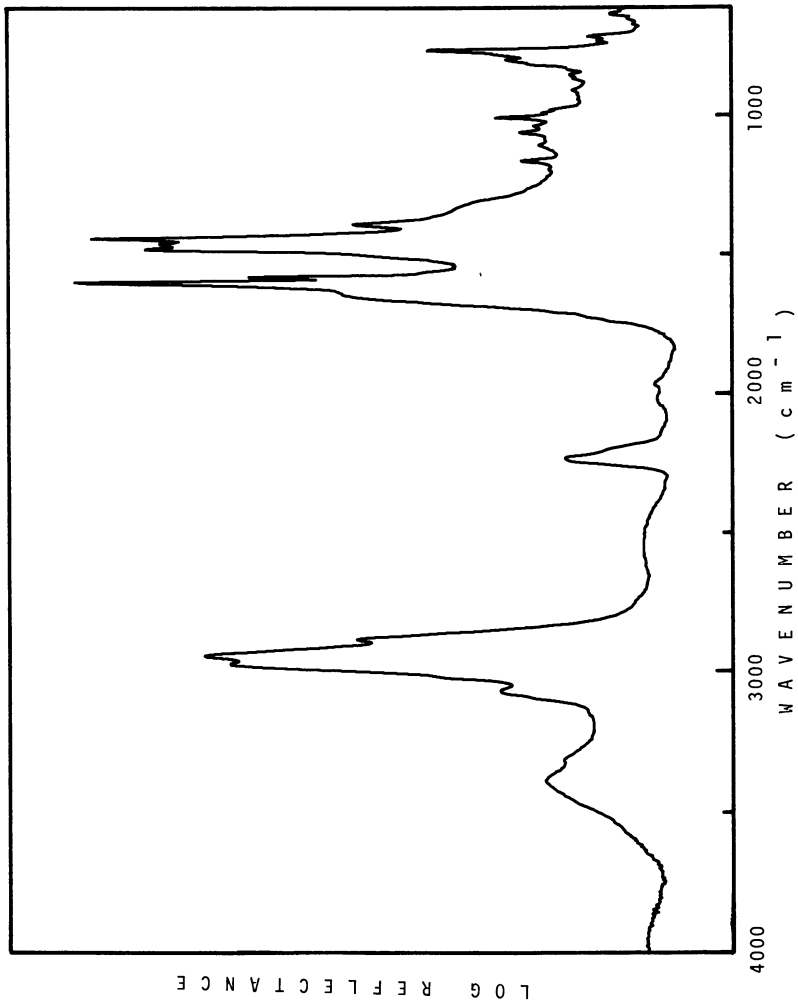

Figure 5. Reflectance FTIR spectrum of Sample 3, Table I

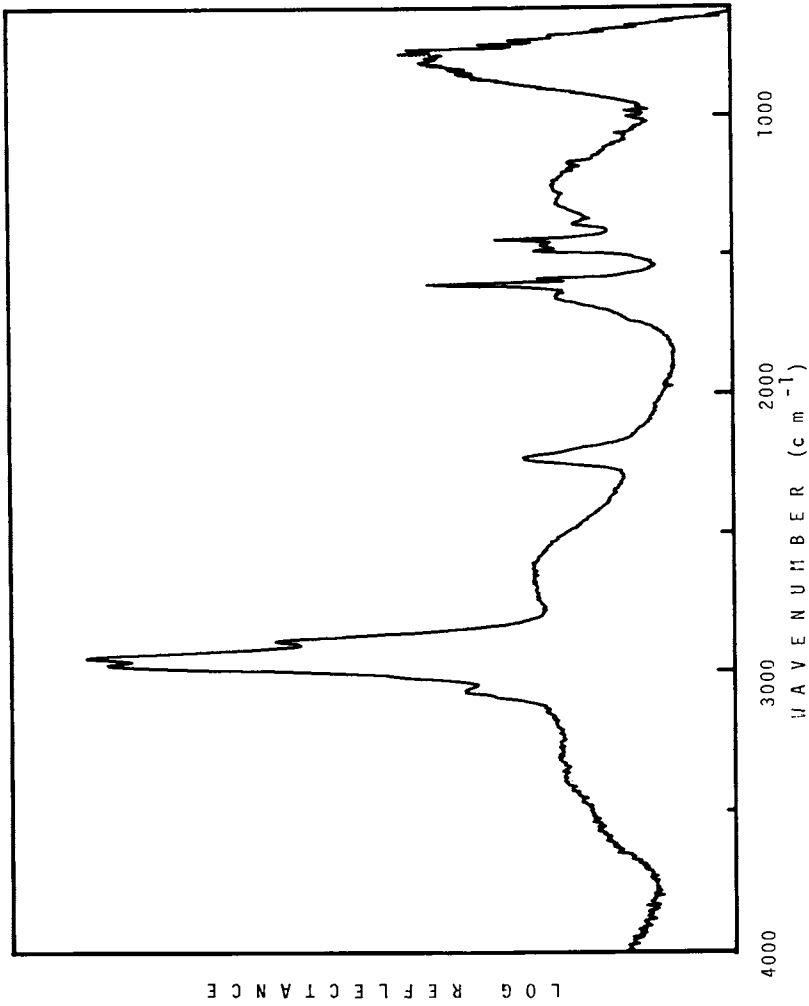

Figure 6. Reflectance FTIR spectrum of Sample 4, Table I

In Plasma Polymerization; Shen, M., et al.;
ACS Symposium Series; American Chemical Society: Washington, DC, 1979.

The balance was argon carrier gas. The broad feature at 600-900 cm^{-1} is an artifact from phase differences in the interferogram due to variations in sample position with respect to the collection optics. These spectra display structural features similar to Samples 1 and 2. However, the nitrile band is no longer split and is shifted by approxiamtey 20 cm^{-1} to higher energy. This observation suggests this group is conjugated, but probably does not exist in an enaminonitrile form. Further, the presence of a new CH_2, CH_3 deformation band at 1450 cm^{-1} indicates that additional branching and crosslinking is present.

An FTIR spectrum of a polymer prepared under similar conditions but without the argon carrier gas (Sample 5, Table I), is shown in Figure 7. In general, the same bands are present as were observed with films prepared with the argon implying that the rare gas has no substantial influence on the resulting structure of these plasma polymers. This conclusion is not surprising in view of the fact that the addition of rare gases has little apparent effect on the ion chemistry of comparable benzene discharges (14). Figure 8 shows the FTIR spectrum of a film prepared at a high rf power level. It is clear from the presence of only a few, broad absorption bands that substantial degradation of the monomer occurred under these conditions. In particular, the ring CH stretch is no longer apparent, indicating nearly complete breakup of the aromatic pyridine ring. Also, the previously well resolved features at 1550-1600 cm^{-1} are manifested as a broad band at 1630 cm^{-1}, assignable primarily to C = C and C = N vibrations. The remaining features are the CH_2 and CH_3 deformation bands at 1450 cm^{-1} and 1370 cm^{-1}. This structure is one of a highly branched, unsaturated aliphatic polymer.

It is interesting to compare the relative degree of aromaticity retained by the polymers of Table I. This may be accomplished roughly by calculating the ratio of the ring CH stretch peak height at 3060 cm^{-1} to the aliphatic CH stretch band at 2930 cm^{-1}. These comparisons are presented in Table III. It is apparent that aromatic degradation in the plasma polymers is most severe at conditions of lower monomer pressure or high power.

Table IV shows the results of the elemental analyses of the plasma polymers, kept in dry air for 20 days prior to analysis. All the plasma polymers have a relatively high concentration of oxygen. In addition, this percentage is highest for the polymers prepared under the more severe conditions, suggesting that the concentration of trapped free radicals is higher for these films. Nitrogen retention is nearly stoichiometric with the linear polymer in all cases. Hydrogen yield is also quite low, as has been observed for plasma polymers formed from other types of aromatic monomers (18). The H/C ratio was also observed to increase in polymers formed at lower pressures or higher powers, apparently due to the increased number of aliphatic groups, particularly chain branches, in these polymers.

In Plasma Polymerization; Shen, M., et al.;
ACS Symposium Series; American Chemical Society: Washington, DC, 1979.

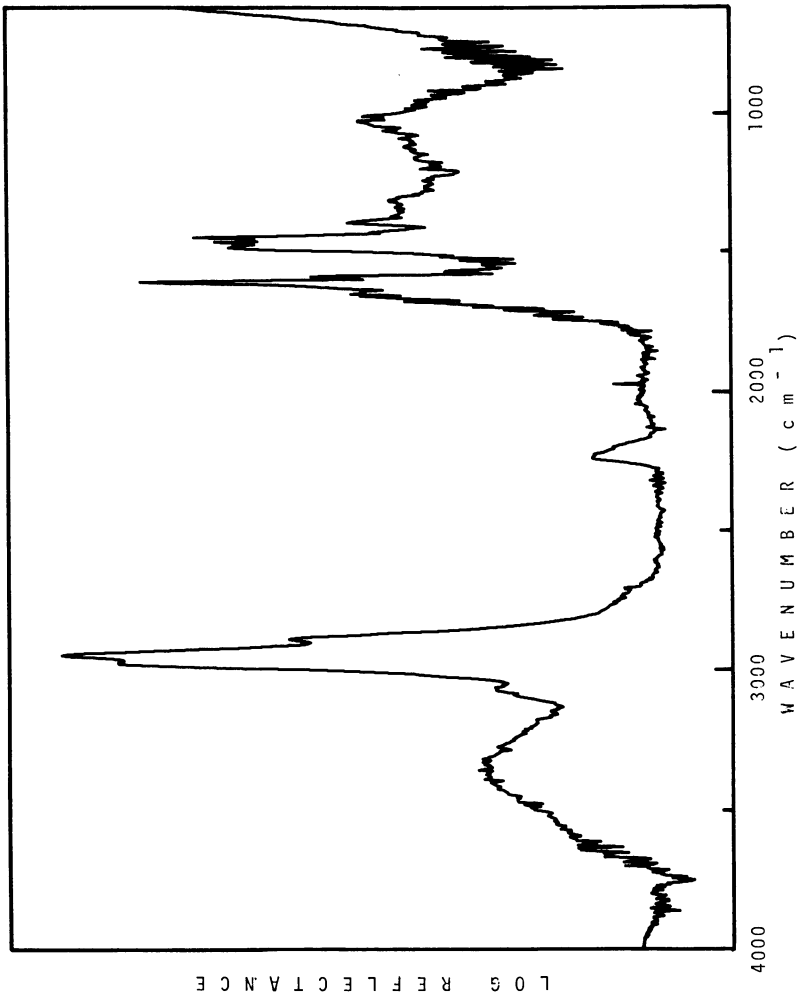

Figure 7. Reflectance FTIR spectrum of Sample 5, Table I

In Plasma Polymerization; Shen, M., et al.;
ACS Symposium Series; American Chemical Society: Washington, DC, 1979.

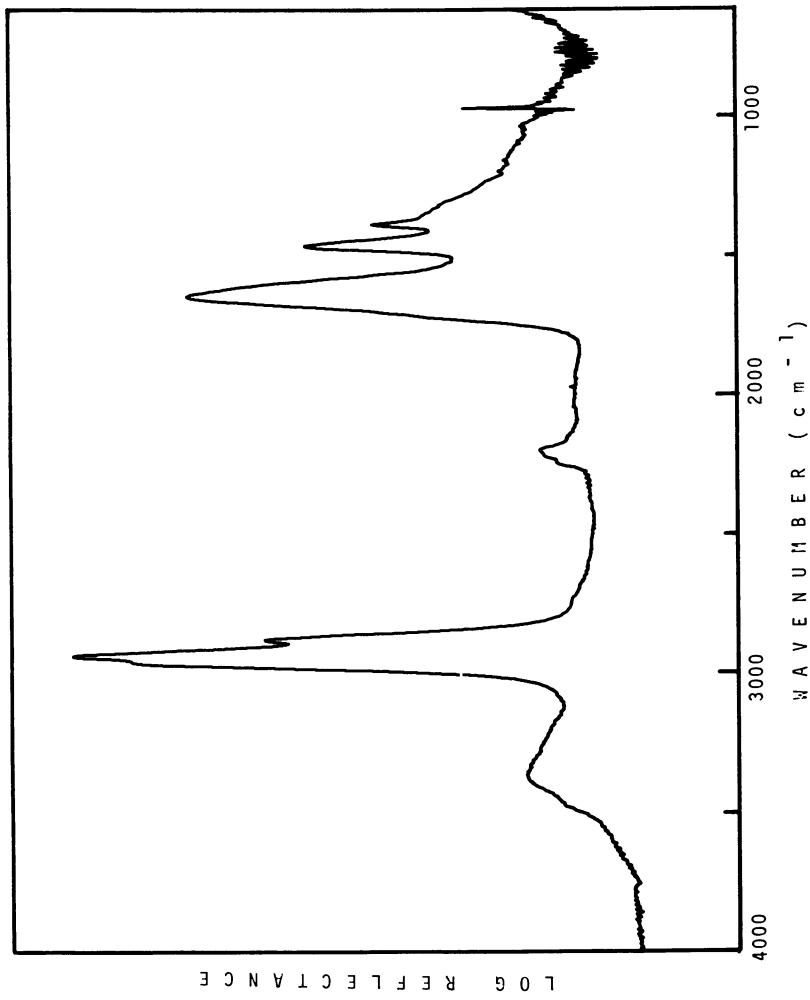

Figure 8. Reflectance FTIR spectrum of Sample 6, Table I

In Plasma Polymerization; Shen, M., et al.;
ACS Symposium Series; American Chemical Society: Washington, DC, 1979.

Table III

AROMATICITY RETENTION OF PLASMA POLYMERS
AS INDICATED BY PEAK HEIGHT RATIOS

Sample	(3060 cm^{-1}/2930 cm^{-1})
Linear	0.58
1	0.41
2	0.45
3	0.26
4	0.20
5	0.15
6	-0-

Table IV

ELEMENTAL ANALYSES OF PLASMA-DEPOSITED
POLY(2-VINYLPYRIDINE)

Sample	% C	% H	% N	% O	Formula
Linear	80.0	6.7	13.3	---	C_7H_7N
1	77.0	6.15	13.0	3.9	$C_7H_{6.71}N_{1.01}O_{0.26}$
3	73.8	6.01	12.2	8.0	$C_7H_{6.84}N_{0.99}O_{0.57}$
5	74.2	6.20	12.0	7.6	$C_7H_{7.02}N_{0.97}O_{0.54}$
6	71.8	6.54	11.9	9.8	$C_7H_{7.66}N_{0.99}O_{0.71}$

In Plasma Polymerization; Shen, M., et al.;
ACS Symposium Series; American Chemical Society: Washington, DC, 1979.

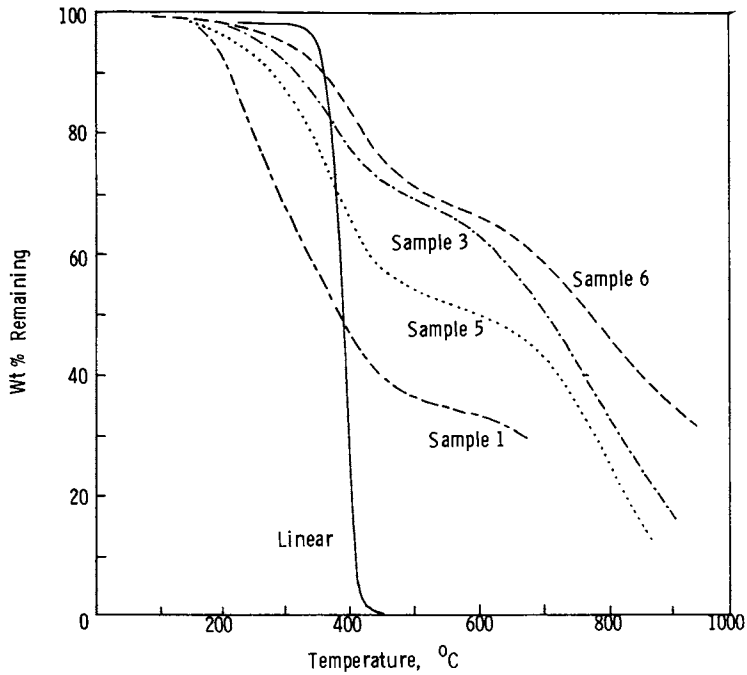

Figure 9. Thermograms of poly(2-vinylpyridines) in argon

In Plasma Polymerization; Shen, M., et al.;
ACS Symposium Series; American Chemical Society: Washington, DC, 1979.

Table V

THERMAL STABILITY OF POLY(2-VINYLPYRIDINES) IN ARGON

Sample	T_p (°C)[1]	50% DT (°C)[2]	E(kcal/mole)[3]
Linear	400	395	58.5
1	325	385	7.6
3	375	710	5.0
5	375	610	6.4
6	405	770	6.2

[1]Temperature of maximum rate of weight loss.

[2]50% decomposition temperature.

[3]Activation energy for 100-450°C decomposition, determined by method of Freeman and Carroll (19).

In Plasma Polymerization; Shen, M., et al.;
ACS Symposium Series; American Chemical Society: Washington, DC, 1979.

Thermal stability of the plasma polymers, as determined by thermogravimetric analyses, is compared in Figure 9. The conventional, linear poly(2-vinylpyridine) begins to unzip to monomer at about 370°C. The plasma-deposited polymers all begin to lose weight at a lower temperature (150-200°C) than conventional poly(2-vinylpyridine), but show a slower rate of weight loss above this temperature, due to their high degree of crosslinking. Table V presents the results of the analysis of the TGA scans. Interestingly, the activation energy for the decomposition of the plasma polymer below 450°C is much lower than that for the linear material. In addition, all plasma polymer scans displayed a relative plateau at 450-650°C, suggesting the occurrance of a relatively stable product in this region. Plasma polymers formed with the argon carrier gas appear to be the most stable, whereas the polymer formed at a high monomer pressure lost 50% of its weight by 385°C, perhaps indicating incomplete polymerization in the latter case.

Conclusions

External reflection Fourier transform infrared spectroscopy has been found useful in the characterization of thin films of poly(2-vinylpyridine) plasma deposited on aluminum substrates. Significant structural differences were noted between polymers formed at a high monomer pressure and those made at lower monomer pressures or higher powers. In particular, increased aromatic degradation accompanied by increased unsaturation and chain branching were apparent at the latter, more severe, conditions. Additional variations were evident in the chemical compositions of the polymers and their thermal behavior. Although all of the plasma polymers showed a nearly stoichiometic retention of nitrogen, those prepared at the more severe conditions had a significantly higher H/C ratio than the conventional polymer. Also, TGA scans of the plasma materials indicated a highly crosslinked product whose initial degradation was controlled by a low activation energy process.

In Plasma Polymerization; Shen, M., et al.;
ACS Symposium Series; American Chemical Society: Washington, DC, 1979.

Literature Cited

1. Gregor, L. V., IBM Journal, March (1968).
2. Mearns, A. M., Thin Solid Films, 3, 201 (1969).
3. Poulsen, R. G., J. Vac. Sci. Technol., 14, 266 (1977).
4. Greenler, G. R., J. Chem. Phys., 50, 1963 (1969).
5. Liang, C. Y. and Krimm, S., J. Poly. Sci., 27, 241 (1958).
6. Panov, V. P., Kazarin, L. A., Dubrovin, V. I., Gusev, V. V. and Kirsh, Y. E., J. Appl. Spect., 21, 1504 (1974).
7. Cook, G. L., and Church, F. M., J. Phys. Chem., 61, 458 (1957).
8. Wilson, E. B., Phys. Rev., 45, 706 (1934).
9. Bell, A. T., Wydeven, T., and Johnson, C. C., J. Appl. Poly. Sci., 19, 1911 (1975).
10. Hollahan, J. R., and Wydeven, T., J. Appl. Poly. Sci., 21, 923 (1977).
11. Kitson, R. E., and Griffith, N. E., Anal. Chem., 24, 334 (1952).
12. Baldwin, S., J. Org. Chem., 26, 3288 (1961).
13. Grassie, N. and McGuchan, R., Eur. Polym. J., 7, 1356 (1971).
14. Smolinsky, G., and Vasile, M. J., Int. J. Mass. Spectrom. Ion Phys., 24, 311 (1977).
15. Rosenstock, H. M., and McCulloh, K. E., Int. J. Mass. Spectrom. Ion Phys., 25, 327 (1977).
16. Tibbitt, J. M., Bell, A. T., and Shen, M., J. Macromol. Sci.-Chem., A10(3), 367 (1976).
17. Allara, D. L., Baca, A., and Pryde, C. A., "Distortions of Band Shapes in External Reflection Infrared Spectra of Thin Polymer Films on Metal Substrates," to be published.
18. Yasuda, H., and Hirotsu, T., J. Poly. Sci. Poly. Chem. Ed., 16, 743 (1978).
19. Freeman, E. S. and Carroll, B., J. Phys. Chem., 62, 394 (1958).

RECEIVED March 29, 1979.

9

ESCA Characterization of Plasma-Polymerized Fluorocarbons

M. R. PENDER, M. SHEN, and A. T. BELL
Department of Chemical Engineering, University of California, Berkeley, CA 94720
M. MILLARD
Western Regional Research Center, U.S. Department of Agriculture, Berkeley, CA 94710

The use of ESCA to determine the structure and composition of plasma-polymerized fluorocarbons has been discussed in several recent publications (1-6). In the present study this technique was used to determine the influence of monomer composition on polymer structure and to establish the effects of film deposition conditions. A point of particular interest was to determine whether polymers resembling those produced by conventional polymerization could be obtained by locating the substrate on which polymer deposition occurs in a region adjacent to the plasma but in minimal contact with it. These experiments were motivated by the work of O'Kane and Rice (4) which showed that the polymer obtained in a region just downstream from the plasma was more linear than polymer deposited within the plasma.

Experimental

Polymer deposition was carried out in a plasma sustained between two parallel plate electrodes supported within an evacuable bell jar. Both electrodes were 20 cm in diameter and were separated by a gap of 7.3 cm. The lower electrode was cooled by circulating water and was grounded. Power for the plasma was provided by a 300 watt rf generator operating at 13.56 MHz. Monomer flow was supplied to the apparatus through an annular cup surrounding the lower electrode. The pressure within the bell jar was monitored by a capacitance manometer.

Polymer deposition in two locations was studied. The first was the surface of the lower electrode. To collect the polymer, aluminum foil was placed over the electrode. Following film deposition a small sample

0-8412-0519-9/79/47-108-147$05.00/0

In Plasma Polymerization; Shen, M., et al.;
ACS Symposium Series; American Chemical Society: Washington, DC, 1979.

of the foil was cut out for ESCA characterization. The second location for polymer deposition was midway between the two electrodes. To minimize direct plasma contact with the substrate, a glass slide covered by aluminum foil was isolated within a Faraday cage made of fine copper mesh. The Faraday cage and the substrate were supported off the lower electrode by small ceramic cylinders.

Tetrafluoroethylene (TFE), hexafluoropropene (HFP) and perfluoro-2-butene (PF2B) were used as monomers. TFE and HFP of greater than 97% purity were obtained from PCR Research Chemicals and used as received. Part of the impurity in TFE was d-limonene (4-isopropenyl-1-methylcyclohexane) a polymerization inhibitor. PF2B was obtained from the Linde Specialty Gases division of Union Carbide Corporation and was used as received.

Structural analysis of the deposited films was carried out by ESCA. Two instruments were used in this work, a Dupont Model 650 and a GCA/McPherson ESCA 36. Spectra of the C(1s), F(1s), and O(1s) regions were recorded for each sample. The C(1s) region was scanned eight times to improve the signal to noise ratio. A larger number of scans could not be used since this led to a progressive degradation of the sample. Only single scans of the F(1s) and O(1s) regions were taken. The F/C and O/C ratios of each polymer sample were determined from the ratios of appropriate peak areas corrected for the elemental sensitivities.

Theoretical

To aid in the assignment of peaks in the C(1s) region of ESCA spectra, theoretical predictions were made of C(1s) binding energy shifts as a function of molecular structure and composition. A charge potential model was used for this purpose (1). The binding energy for a given carbon atom is given by

$$\Delta E_i = k_c q_i + \sum_{j \neq i} q_j / r_{ij} + b \qquad (1)$$

where q_i is the charge on atom i, r_{ij} is the distance between atoms i and j, and k_c and b are empirical parameters. Atomic charges were estimated from CNDO molecular orbital calculations on a variety of small fluorocarbon molecules.

To determine the contants k_c and b, the difference between the experimentally observed values of ΔE_i, reported by Davis (8), and the second term on the right hand side of eqn. 1, evaluated from CNDO calculations,

In Plasma Polymerization; Shen, M., et al.;
ACS Symposium Series; American Chemical Society: Washington, DC, 1979.

was plotted versus q as shown in Fig. 1. A least squares fit of a straight line to the data points gives a value of k_c = 23.6 eV/unit charge and b = -11.1 eV.

The charge-potential model was used to predict the chemical shifts for functional groups in a number of model compounds containing primarily carbon, fluorine, and hydrogen. The molecular structure examined included aliphatics, olefins, aromatics, and several ketones.

Results and Discussion

Identification of Functional Groups. Representative ESCA spectra of the C(1s) and F(1s) regions are shown in Figs. 2 and 3. Qualitatively similar spectra were obtained for films prepared from TFE, HTP, and PF2B. Only one distinct peak is seen in the F(1s) region, corresponding to covalently bonded fluorine. The spectrum of the C(1s) region is more complex, exhibiting a series of overlapping peaks. Deconvolution of this spectrum into five separate peaks was achieved by means of a non-linear least squares fitting program (9). The average binding energy associated with each peak and the standard deviation from the average value are listed in Table I. To compensate for sample charging, the binding energy of the highest energy peak was set to 293.8 eV, the energy characteristic of $-CF_3$ groups (6). This selection was based upon the observation that the position of $-CF_3$ peaks is weakly affected by nearest neighbor groups, in contrast to other fluorine containing groups in the polymer.

Assignment of the give C(1s) peaks to specific functional groups was achieved by comparing the chemical shift in binding energy for each peak with those for peaks appearing in the spectra of known compounds and with shifts calculated for well-defined structures. The solid bars shown in Fig. 4 represent experimentally determined shifts based upon data taken from several sources (8,10). Similar information obtained from the charge-potential model, eqn. 1, are shown by the horizontal lines. The quantity ΔE_k shown along the abscissa of Fig. 4 represents the shift in C(1s) binding energy relative to that for an uncharged carbon atom.

The broad range of shifts associated with a given functional group reflects the fact that the chemical shift for a given carbon atom depends not only on the atoms bonded directly to this carbon atom but also the

In Plasma Polymerization; Shen, M., et al.;
ACS Symposium Series; American Chemical Society: Washington, DC, 1979.

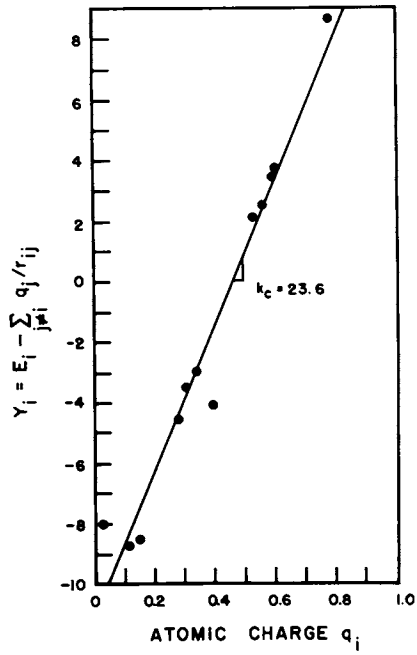

Figure 1. Charge–potential model correlation for determination of k_c *and* b

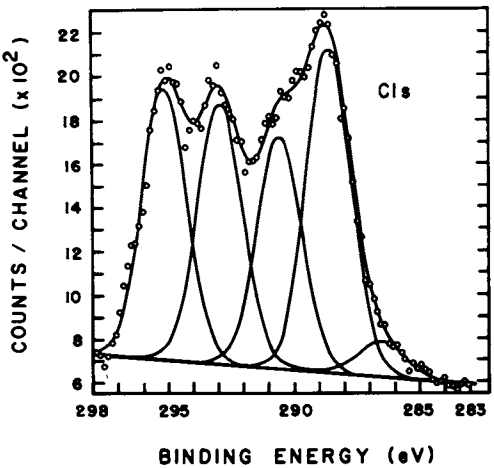

Figure 2. ESCA spectrum of C(1s) region

In Plasma Polymerization; Shen, M., et al.;
ACS Symposium Series; American Chemical Society: Washington, DC, 1979.

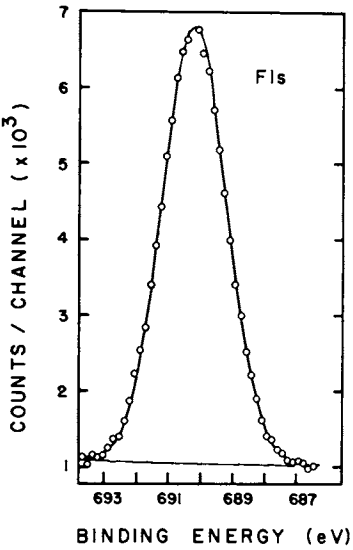

Figure 3. ESCA spectrum of F(1s) region

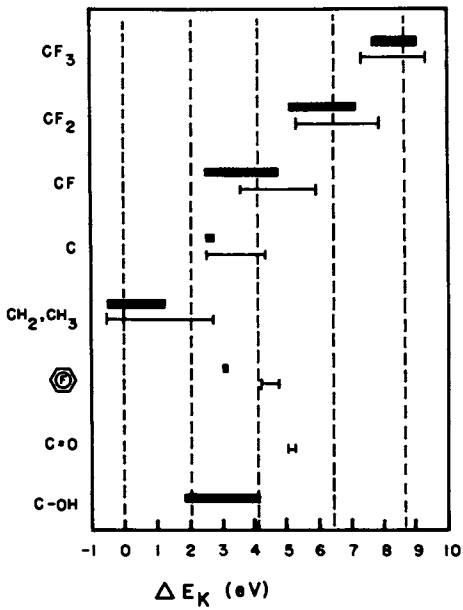

Figure 4. C(1s) binding energy shifts for selected functional groups. (▬) Experimental, (——) calculated.

In Plasma Polymerization; Shen, M., et al.;
ACS Symposium Series; American Chemical Society: Washington, DC, 1979.

Table I. Assignment of C(ls) Binding Energy Shifts

This Study				Nakajima et al. (6)			
Peak	B.E.(eV)	ΔE_K(eV)	Assignment	Peak	B.E.(eV)	ΔE_K(eV)	Assignment
1	285.1	0.0±0.3	CH_2	1	285.0	0.0±0.3	CH_2(I)
2	287.2	2.1±0.2	C/CH_2	2	286.9	1.9±0.1	CH_2(II)
3	289.2	4.1±0.2	CF/C	3	288.2	3.2±0.2	CF(I)
4	291.6	6.5±0.2	CF_2	4	289.5	4.5±0.2	CF(II)
5	293.8	8.7±0.0	CF_3	5	291.8	6.8±0.1	CF_2
				6	293.8	8.8±0.0	CF_3

In Plasma Polymerization; Shen, M., et al.;
ACS Symposium Series; American Chemical Society: Washington, DC, 1979.

atoms bonded to the nearest and next-nearest carbon atom. This point is illustrated in Fig. 5 which shows the chemical shift associated with each carbon atom in a series of linear aliphatic compounds of varying F/C ratio. The chemical shift for a given carbon atom is seen to be a function of the overall fluorine density, the shift for $-CF_3$, $-CF_2-$ and $-CH_2-$ groups increasing with the F/C ratio. It is also seen that the shift for a $-CF_2-$ group increases with distance from $-CH_2-$ groups, while the shift for a $-CH_2-$ group decreases with distance from $-CF_2-$ groups. The influence of fluorine can be felt as many as five carbon atoms distant as shown in the compound $C_5H_{11}-C_4F_9$. Thus, for example, the terminal CH_3 group is shifted 0.3 eV from its value in a pure hydrocarbon.

The dashed vertical lines appearing in Fig. 4 represent the binding energy shifts for the five peaks listed in Table I. Peak 1 clearly falls within the range of shifts associated with $-CH_2-$ and $-CH_3$ groups. Similarly, peaks 4 and 5 can be assigned to $-CF_2-$ and $-CF_3$ groups respectively. The assignment of the remaining two peaks is not as clear cut and requires some discussion.

The binding energy shift for peak 2 lies within the upscale end of the range for $-CH_2-$ and $-CH_3$ groups and the downscale end of the range for $-CH-OH$ groups. Assignment to the latter group can immediately be ruled out since the measured O/C ratio is much smaller than would be necessitated. Identification of peak 2 with $-CH_2-$ groups, occurring within a fluorocarbon structure is more likely. As seen in Fig. 5, the binding energy shifts associated with such groups lie in the vicinity of 2 eV. The only difficulty with assigning peak 2 to CH_2 groups is that it leads to a very large overestimation of the H/C ratio of the polymer. As a result we are forced to conclude that peak 2 is only partially due to $-CH_2-$ groups. The remaining portion of the contribution may well come from quaternary carbon atoms. While the range of binding energy shifts for quaternary carbons shown in Fig. 4 does not overlap the line for peak 2, this is due to the fact that only perfluorinated compounds containing quaternary carbon atoms were considered. If one or more of the groups attached to the quaternary carbon contained hydrogen, the binding energy shift would be shifted to lower values. In view of these considerations we have assigned peak 2 to both quarternary carbon atoms and $-CH_2-$ groups.

Unambiguous assignment of peak 3 is also difficult. As seen from Fig. 3, this peak can be associated with

In Plasma Polymerization; Shen, M., et al.;
ACS Symposium Series; American Chemical Society: Washington, DC, 1979.

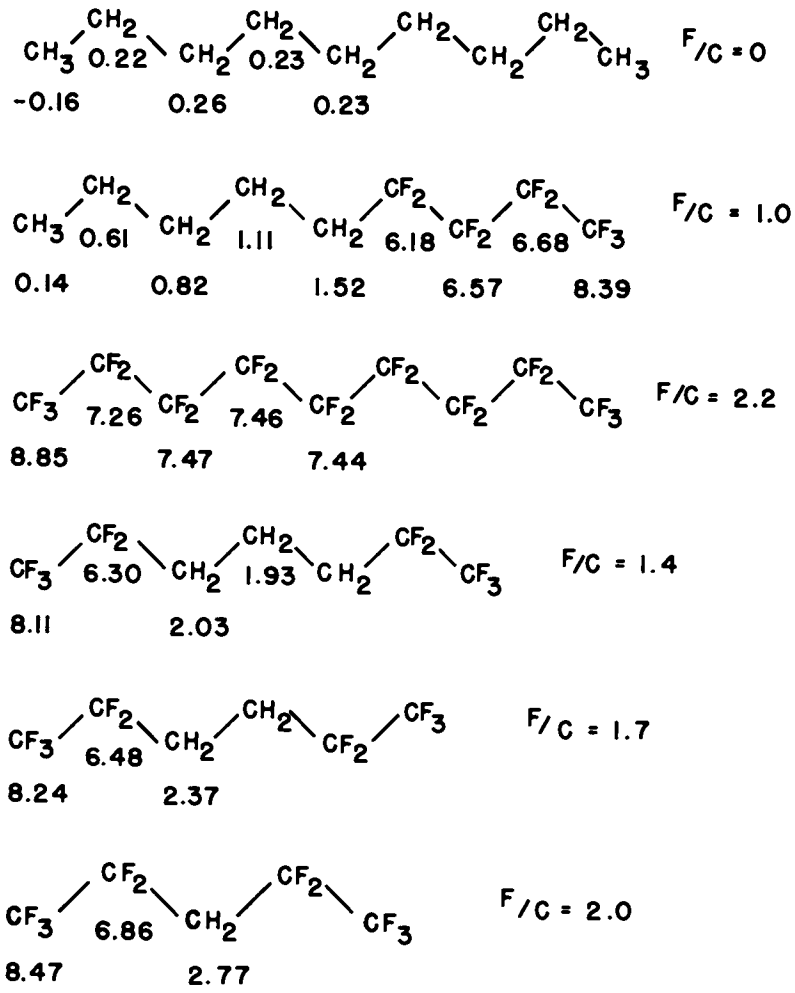

Figure 5. Predicted C(1s) binding energy shifts for fluorine-containing aliphatics

In Plasma Polymerization; Shen, M., et al.;
ACS Symposium Series; American Chemical Society: Washington, DC, 1979.

-ĊF groups or with quaternary carbon atoms. A possible assignment to perfluorinated phenyl groups or -Ċ-OH groups is also possible but less likely. Since we are unable to distinguish between the remaining alternatives, we must conclude that both -ĊF groups and -Ċ- can contribute to peak 3.

The peak assignments proposed here differ somewhat from those given by Nakajima et al. (6). In that study six C(1s) peaks were required to obtain a satisfactory deconvolution of ESCA spectra of films produced from TFE. The positions of these peaks and their assignments are given in Table I. The binding energy shifts and assignments for peaks 1, 5, and 6 of that study agree very closely with those of peaks 1, 4, and 5 of the present study. Peak 2 in both studies has nearly the same binding energy shift but the computational efforts reported here suggest that this peak is not due totally to $-CH_2-$ groups and that a part of the contribution arises from -Ċ- groups. The binding energies of peaks 3 and 4 in the study of Nakajima et al. bracket that of peak 3 in this study. Here again, the results of the present investigation suggest that peaks in this part of the spectrum are due to -Ċ- groups as well as -ĊF groups. The fact that two peaks arise in the work of Nakajima et al. and only one here is not considered very critical and may be a result of the manner in which the curve fitting routine is used.

Influence of Monomer Composition and Deposition Conditions on Film Composition

Table II shows the distribution of functional groups present in films obtained from TFE, HFP, and PF2B under identical plasma conditions. In each case, the deposition occurred on the lower electrode surface. The composition of all three films is strikingly similar. In particular the distribution of $-CF_3$, $-ĊF_2$, and -ĊF/-Ċ- groups in the polymer bears no correlation with the monomer used. This fact and the observation that the F/C ratio of the film is substantially smaller than that of the monomer indicate that a considerable degree of molecular rearrangement has occurred during film deposition. The large concentrations of -ĊF and -Ċ- groups and the low F/C ratio, also indicate a high degree of branching and cross-linking. Elimination of fluorine from the growing polymer produces reactive free radical sites which can become branch and cross-link points.

In Plasma Polymerization; Shen, M., et al.;
ACS Symposium Series; American Chemical Society: Washington, DC, 1979.

Table II. Effect of Monomer on the Distribution of Functional Groups in Plasma-Polymerized Fluorocarbon Films

	Distribution of Functional Groups (%)						Deposition Rate
Monomer	CF_3–	CF_2–	CF/C	C/CH_2	CH_2–	F/C	(mg/cm^2-min)
TFE	18.1	22.8	22.9	30.4	5.8	1.2	2.45×10^{-2}
HFP	21.0	23.2	23.4	27.5	5.0	1.2	3.29×10^{-2}
PF2B	15.3	19.0	21.9	29.3	14.5	1.0	4.32×10^{-2}

Deposition conditions: Power = 40 W; pressure = 0.25 torr;

Flow rate = 30 STP cm^3/min

In Plasma Polymerization; Shen, M., et al.;
ACS Symposium Series; American Chemical Society: Washington, DC, 1979.

The effects of monomer flow rate on film structure and composition are shown in Table III. The films prepared from TFE exhibit an increase in the concentrations of $-CF_3$ and $-CF_2-$ groups as the flow rate of the monomer increases. Concurrently, the concentrations of -CF, -C-, and $-CH_2-$ groups decline. For films prepared from PF2B the concentrations of $-CF_3$, $-CF_2-$, -CF, and -C- groups all increase with monomer flow rate and only the concentration of $-CH_2-$ groups declines. In addition, it is seen that films made from both monomers show an increase in the F/C ratio with increasing flow rate.

The trends observed in Table III suggest that the reduction in monomer residence time in the plasma, which occurs as the flow rate increases, results in a decrease in the amount of molecular rearrangement and fluorine elimination. A greater fraction of monomer is incorporated by direct addition polymerization as evidenced by the particularly large increase in the concentration of $-CF_2-$ in the polymer prepared from TFE and the increases in $-CF_3$ and -CF groups in the polymer prepared from PF2B. Consistent with this interpretation, the F/C ratio increases from 1.0 to 1.3. The observed decrease in CH_2 group concentrations with flow rate suggests that backstreaming of pump oil is the source of hydrocarbon impurities incorporated into the films. As flow rate increases the extent of backstreaming decreases and the partial pressure of hydrocarbons in the plasma decreases.

Table IV illustrates the dependance of polymer composition on pressure and power for films prepared from TFE and HFP. With increasing pressure the concentration of $-CF_3$ groups, which acts as a measure of molecular rearrangement, decreases in films made from TFE but increases in films made from HFP. These trends suggest that as the pressure increases, polymer formed by addition polymerization undergoes a lesser degree of molecular rearrangement. However, when the power is increased from 15 to 40 watts, molecular rearrangement becomes more significant and the trends with increasing pressure become less significant.

The influence of substrate location on the structure and composition of the deposited film is presented in Table V. The polymer deposited within the Faraday cage exhibits higher concentrations of $-CF_3$ groups and a higher F/C ratio than polymer deposited on the electrode surface. It should also be noted that the deposition rate within the Faraday cage is two orders of magnitude slower than on the electrode surface. Despite this fact, and the near total absence

In Plasma Polymerization; Shen, M., et al.;
ACS Symposium Series; American Chemical Society: Washington, DC, 1979.

Table III. Effect of Flow Rate on the Distribution of Functional Groups in Plasma-Polymerized Fluorocarbon Films

Monomer	Flow Rate (STP cm^3/min)	Distribution of Functional Groups (%) CF_3–	CH_2–	CF/C	C/CH_2–	CH_2–	F/C
	10	15.5	23.2	22.2	29.2	9.9	1.0
TFE	30	17.0	25.9	21.6	27.2	8.3	1.1
	60	20.0	31.9	20.0	24.2	3.8	1.3
	10	17.2	15.7	18.2	25.5	23.4	1.0
PF2B	30	21.6	19.4	21.2	27.8	10.1	1.1
	60	23.6	19.5	22.7	28.4	5.8	1.3

Deposition conditions: Power = 15 W; pressure = 0.25 torr

In Plasma Polymerization; Shen, M., et al.;
ACS Symposium Series; American Chemical Society: Washington, DC, 1979.

Table IV. Effects of Pressure and Power on the Concentration of CF_3 Groups in Plasma-Polymerized TFE and HFP Films

Power (W)	Pressure (torr)	Concentration of CF_3 (%) TFE	HFP
	0.10	19.1	18.4
15	0.25	15.5	19.4
	0.50	13.0	24.5
	0.10	21.2	16.0
40	0.25	18.6	15.5
	0.50	17.8	16.8
	0.10	22.7	-
80	0.25	19.3	-
	0.50	19.4	-

In Plasma Polymerization; Shen, M., et al.;
ACS Symposium Series; American Chemical Society: Washington, DC, 1979.

Table V. Effect of Substrate Location on the Distribution of Functional Groups in Plasma-Polymerized Fluorocarbon Films

Substrate Location	Monomer	CF_3	CF_2	CF/C	C/CH_2	CH_2	F/C	Deposition Rate (mg/cm^2-min)
On lower electrode surface	TFE	18.6	23.0	24.3	26.5	7.5	1.1	2.31×10^{-2}
	HFP	15.5	17.6	19.8	27.3	19.9	1.0	2.63×10^{-2}
	PF2B	17.3	20.2	22.0	27.4	13.2	0.9	2.64×10^{-2}
Within Faraday Cage	TFE	23.0	22.6	19.0	26.1	9.3	1.2	3.15×10^{-4}
	HFP	22.7	19.7	18.2	25.8	13.6	1.2	3.78×10^{-4}
	PF2B	25.0	21.0	29.0	26.8	7.4	1.3	3.36×10^{-4}

In Plasma Polymerization; Shen, M., et al.;
ACS Symposium Series; American Chemical Society: Washington, DC, 1979.

of visible plasma within the Faraday cage, the polymer deposited inside the cage is quite similar to that formed outside. Evidently the active species which penetrate the mesh of the cage are capable of inducing significant molecular rearrangement so that the polymer deposited bears little resemblance to the original monomer.

Acknowledgment

This work was supported by the NSF through Grant DMR74-12530A01.

Abstract

Structural characterization of fluorocarbon films produced by plasma polymerization was carried out using ESCA. The monomers examined were tetrafluoroethylene, hexafluoropropene, and perfluoro-2-butene. ESCA spectra revealed that the films produced from all three monomers are structurally similar and that a large degree of molecular rearrangement and fluorine elimination occurs during polymerization. Assignment of peaks in the C(1s) portion of ESCA spectra was aided by computations of binding energy shifts using a charge-potential model. The effects of power, pressure, flow rate, and substrate location within the plasma on film structure were investigated.

References

1. Millard, M. M., Windle, J. J., and Pavlath, A. F., J. Appl. Polym. Sci. (1973), 17, 2501.

2. Anderson, H. R., Fowkes, F. M., and Hielscher, F. J., J. Polym. Sci., Polym. Phys. Ed. 1976, 14, 879.

3. Washo, B. D., J. Macromol. Sci.-Chem. (1976), A10 559.

4. O'Kane, D. F. and Rice, D. W., J. Macromol. Sci.-Chem.-Chem. (1976), A10, 567.

5. Millard, M. M. and Pavlath, A. F., J. Appl. Polym. Sci.-Chem. (1976), A10, 579.

6. Nakajima, K., Bell, A. T., and Shen, M., J. Appl. Polym. Sci. in press.

7. Sieghban, K., Nordling, C., Johansson, G., Hedman, J., Heden, P. F., Hamrin, K., Gelins, U. Bergmark, T., Werme, L. O., Manne, R., and Baer, Y., "ESCA Applied to Free Molecules", North Holland, Amsterdam, 1969.

8. Davis, D. W., Ph.D. Thesis, Department of Chemistry, University of California, Berkeley, California, 1973.

9. Fadley, C. S., Ph.D. Thesis, Department of Chemistry, University of California, Berkeley, California, 1970.

10. Clark, D. T., "The Application of ESCA to Studies of Structure and Bonding in Polymers" in "Structural Studies of Macromolecules by Spectroscopic Methods", ed. by K. J. Ivin, Wiley, New York, 1976.

RECEIVED March 29, 1979.

Plasma Polymerization of Tetrafluoroethylene in a Capacitively Coupled Discharge with Internal Electrodes

N. MOROSOFF and H. YASUDA[1]

Research Triangle Institute, P.O. Box 12194, Research Triangle Park, NC 27709

A capacitively coupled reactor designed to permit continuous coating of a moving substrate with plasma polymer has been described [1]. In this paper the results of a study of the plasma polymerization of tetrafluoroethylene in such a reactor presented. Plasma polymer has been deposited on aluminum electrodes as well as on an aluminum foil substrate placed midway between electrodes. The study particularly explores conditions in which deposition is minimized on the electrode. For this reason the chemical nature of the polymer formed in a low flow rate ($F = 2$ cm^3 (S.T.P.)/min) and low pressure (p_m = 60 millitorr) plasma has been analyzed by the use of ESCA (electron spectroscopy for chemical analysis) and deposition rate determinations. This method combined with the unusual characteristics of TFE plasma polymerization (described below) has yielded information concerning the distribution of power in the inter-electrode gap. The effects of frequency (13.56 MHz, 10 KHz and 60 Hz), power and magnetic field have been elucidated. The properties of the TFE plasma polymer prepared in this apparatus are compared to those of the plasma polymer deposited in an inductively coupled apparatus [2,3].

The present work is not an exhaustive investigation of TFE plasma polymerization as a function of the variables mentioned. Rather its aim is to uncover broad trends that can be used in choosing conditions for plasma polymerization and in planning more intensive experimental work.

A. Unusual Aspects of TFE Plasma Polymerization

ESCA is particularly well suited for the study of plasma polymerization because it yields information about the elemental make-up of the surface to a depth of 50 Å or less and is

[1] Current Address: Department of Chemical Engineering
University of Missouri-Rolla
Rolla, Missouri 65401

0-8412-0510-8/79/47-108-163$05.00/0

not influenced by the substrate properties. However, it yields little information about the functional groups present in the polymer, except for some special cases where a large enough chemical shift is observed. Thus little besides information concerning elemental composition can be obtained from an ESCA invesigation of the plasma polymerization of hydrocarbons. However, fluorine does cause a large enough chemical shift that the position of the C_{1s} peak of a carbon bonded to 3 fluorines (CF_3) can be distinguished from that of one bonded to 2 fluorines (CF_2) and both are clearly separated from the normal C_{1s} peak, i.e., one not bonded to any fluorines [2]. It is clear that the plasma polymerization of tetrafluoroethylene is particularly amenable to study by ESCA.

The plasma polymerization of tetrafluoroethylene (TFE) has been found to be unusual in that the monomer is sensitive to discharge power [3]. Both deposition rate data and ESCA analysis of plasma polymerization in inductively coupled systems demonstrate that fluorine poor polymers are formed when the excited monomer passes through a high power density region of the plasma. Because of the non-negligible atmomic weight of fluorine this fluorine abstraction results in lower deposition rates at very high energy per unit mass of monomer feed.

Deposition rate and ESCA results on blanks placed at various sites in the plasma reactor may therefore be used as a probe of the power density distribution in a given reactor with a glow discharge fed by tetrafluoroethylene.

B. Plasma Polymerization of TFE in Inductively Coupled Systems.

We may compare results presented here with those obtained in two types of inductively coupled reactors [2,3]. One is the reactor we have used for many years [4], in which the portion of the reactor inserted into the r.f. coil is smaller than the main portion of the reactor, in which plasma polymer is collected. Monomer flux is directed into the main portion of the reactor, not through the r.f. coil. Electron bombardment of plasma polymer and substrate is reduced in this way [5]. Active species are formed mainly under the r.f. coil and are transported by diffusion to the entire volume of the reactor. Interaction of these non-polymerizable energy carrying species (e.g. electrons, excited atoms) with the monomer entering the reactor leads to plasma polymerization [5].

The energy supplied per gram of monomer feed may be given as W/FM, where W is the power input, F is the flow rate and M is the molecular weight. Initially, the deposition rate gradually increases with increasing power but begins to decrease because of the above mentioned fluorine abstraction occuring in this system when W/FM exceeds 4.7×10^8 Joules/kg [2,6].

In Plasma Polymerization; Shen, M., et al.;
ACS Symposium Series; American Chemical Society: Washington, DC, 1979.

The plasma polymerization of tetrafluoroethylene has also been studied in a straight tube reactor. Deposition rates and ESCA results were obtained as a function of location upstream from, within, and downstream from the induction coil [3]. It was found that fluorine poor polymer was formed downstream from the coil even at the relatively low power level of 1.9×10^7 Joules/kg. Fluorine poor polymer was formed at all locations at 7.7×10^8 Joules/kg.

C. Plasma Polymerization in Capacitively Coupled Systems

In a capactively coupled system the flow rate into the plasma is not known as precisely as for the systems described above. This is because not all monomer feed must drift into the inter-electrode gap. On the other hand the flow into the gap cannot be obtained from the knowledge of the fraction of reactor volume the inter-electrode gap represents, because the plasma polymerization process acts as a pump.

Moreover the range of power or current that can be used for plasma polymer deposition is limited for capacitively coupled glow discharges at low pressure. This is because at low pressure and high powers, RF plasma tend to expand outside the inter-electrode gap and arcing occurs in AF and AC plasma. The use of a magnetic field to confine the plasma allows the polymerization to be carried out over a wide range of powers.

In contrasting the results obtained for the RF glow discharge with those for the AF and AC glow discharges, it is well to bear in mind the fundamental difference between the two types of glow discharges [7,8]. The AC and AF glow discharges may be considered to be DC glow discharges of alternating polarity. Positive ions hitting the cathode give rise to secondary electrons. These are accelerated through the Aston dark space, cathode glow and Crookes dark space gaining enough energy to ionize neutral species in the negative glow. These ions can then reinitiate the process insuring a self-sustaining glow discharge. Free radicals and other active species are formed in or near the negative glow and react yielding a plasma polymer. Internal conducting electrodes are necessary to sustain such a discharge as buildup of a positive charge on the cathode would repel cations thus shutting off the required source of secondary electrons. In an RF glow discharge, electrons oscillate in the field set up between (and/or around the electrodes) gaining enough energy to form free radicals, ions and other active species by random collisons. Conducting electrodes are therefore not required.

Experimental

The apparatus used in this study is similar to that described in reference 1. It differed in that pumping was

In Plasma Polymerization; Shen, M., et al.;
ACS Symposium Series; American Chemical Society: Washington, DC, 1979.

through 3/4 inch diameter glass tubing and stopcocks and the apparatus had only one reaction chamber. Magnetic enhancement of the glow discharge was achieved as described in reference 1.

The power supplies for RF, AF, and AC have been described elsewhere [9]. In order to collect polymers at the center of the inter-electrode gap, an aluminum foil substrate, 8 cm in width was suspended between electrodes as shown in reference 1. Deposition rates at various locations on the substrate and electrode were obtained by measuring the weight gain of small pieces of aluminum foil (sampling blank) affixed to a given site so that electrical contact was maintained between the site of interest and the sampling blank. This was accomplished by folding the ends of a 0.5 cm x 3 cm piece of aluminum foil around the ends of a 0.5 cm x 2.2 cm piece of glass cover slip and affixing the center of the glass cover slip to the electrode or substrate with double coated scotch tape.

Samples for ESCA analysis were prepared in the same manner and on the same sampling blanks as used for the deposition rate studies. The following spectral lines were obtained from each blank: O_{1s}, F_{1s}, C_{1s} and Al_{2s} by using a DuPont model 650 spectrometer with a MgK_{α} X-ray source, and equipped with a microcomputer data acquisition and processing system. Spectra are corrected for charging. Details of the experimental procedure are described elsewhere [10]. It may be noted that the procedure involves using a fresh sample for each element and is such as to keep hydrocarbon contamination small and constant.

Results and Discussion:

As shown in the previous paper, the use of a magnetic field leads to an annular zone of intense glow, slightly removed from the electrode and with a mean radius of 4 cm. from the electrode center axis. For this reason plasma polymer was collected on aluminum blanks placed on the electrode center axis and at a radius of 4 cm. These blanks were placed on the electrode and on the aluminum substrate suspended between electrodes. For some of the glow discharges where no magnetic field was used, samples of plasma polymer were collected only on the intersection of the electrode center axis with the electrodes and substrate.

ESCA spectra were collected for O_{1s}, F_{1s}, C_{1s} and $A\ell_{2s}$. After correction for the photo-electric cross-sections of these lines, the peak areas indicate the relative number of each element at the surface. As will be shown below, these results cannot be interpreted in terms of the F/C ratio in the plasma polymer because bonding of fluorine to aluminum can also occur. However, a measure of the F/C ratio in the deposited plasma polymer can be obtained from the shape of the C_{1s}

In Plasma Polymerization; Shen, M., et al.;
ACS Symposium Series; American Chemical Society: Washington, DC, 1979.

spectrum. The C_{1s} spectrum obtained for a sample of plasma polymer collected on the electrode center with a power of 10 watts is shown in Figure 1.

It has peaks at 293.5 eV, (CF_3), 291.5 eV, (CF_2) and the peak at 284.6 attributed to hydrocarbon or graphitic carbons. The peaks between 291.6 eV and 284.6 eV, are attributed to carbons bound to one fluorine atom or other electronegative species (e.g., O or N). Spectra obtained for sample collected in very active regions of the plasma with a high power input show much less prominent peaks indicative of carbons bound to fluorine and a very prominent carbon peak at 284.6 eV. An obvious qualitative numerical indicator of these characteristic peak shapes is the ratio of the peak height at 291.5 eV (CF_2) to that at 284.6 eV. The use of this ratio as a means of identifying trends, i.e., the conditions that will yield a fluorine rich polymer as opposed to those that will yield a fluorine poor polymer, is clearly justified. However, it should not be thought of as being directly proportional to CF_2/CH_2 or F/C ratios in the polymer, in part because no effort has been made to correct for the shoulders of neighboring peaks and in part because the peak height at 284.6 eV will include a contribution from contamination in the ESCA instrument. Our experimental procedure is such as to keep the latter small and constant [10].

The values of such peak height ratios obtained for various powers or current levels in the RF, AF and AC plasmas are shown in Figures 2,3 and 4 respectively. It may be noted that the use of straight lines in these graphs is intended only as a visual aid to connect points representing identical locations in the interelectrode gap. No inference concerning the actual value of the ordinate at intervening points on the abscissa is justified.

If we equate a fluorine rich polymer with proximity of the sampling site to a low power density region of the plasma and a fluorine poor plasma polymer with proximity to a high power density region of the plasma, the following observations may be made. The data in Figure 2 indicate that, as expected, plasma polymers generally decrease in fluorine content as the power is raised from 10 to 100 watts. The one exception is plasma polymer collected at the electrode with no magnetic field. In this case the peak-height ratio increases with increasing power at the electrode, although evidence of a highly active plasma is seen at the substrate. The evidence of a low power density at the electrode at a high power input is in line with the model of capacitively coupled RF glow discharge discussed earlier [1]. According to this model, the most active zone of the glow discharge is in the center of the interelectrode gap with a relatively inactive zone immediately adjacent to the electrode. The extent of inactive zone is expected to increase with increasing power. The use of a

In Plasma Polymerization; Shen, M., et al.;
ACS Symposium Series; American Chemical Society: Washington, DC, 1979.

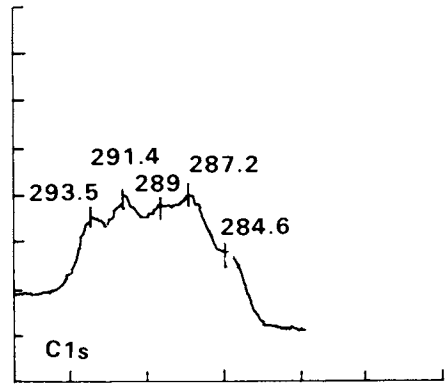

Figure 1. C (1s) spectrum of plasma polymer deposited on the electrode 4 cm from the electrode center with a flow rate of 2 (STP)mL/min, P_M = 60 mtorr, 19 mA AF current and no magnets

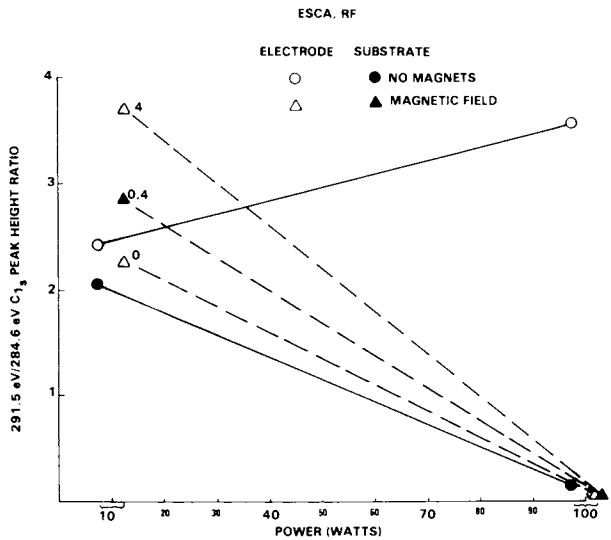

Figure 2. Plot of the 291.5 eV/284.6 eV C (1s) peak height ratios vs. RF power

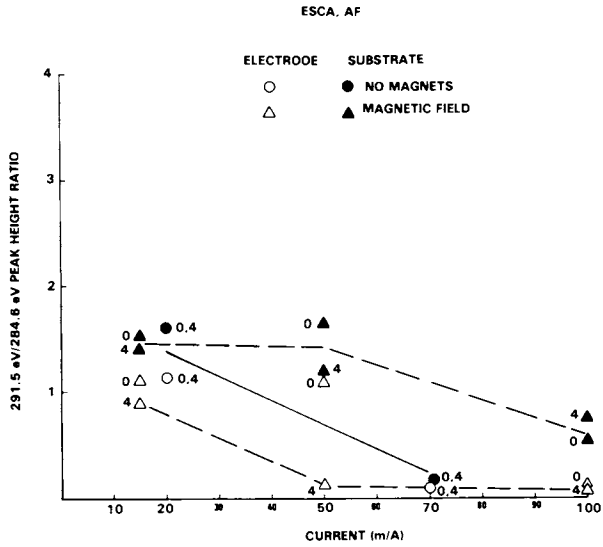

Figure 3. Plot of the 291.5 eV/284.6 eV C (1s) peak height ratios vs. AF current

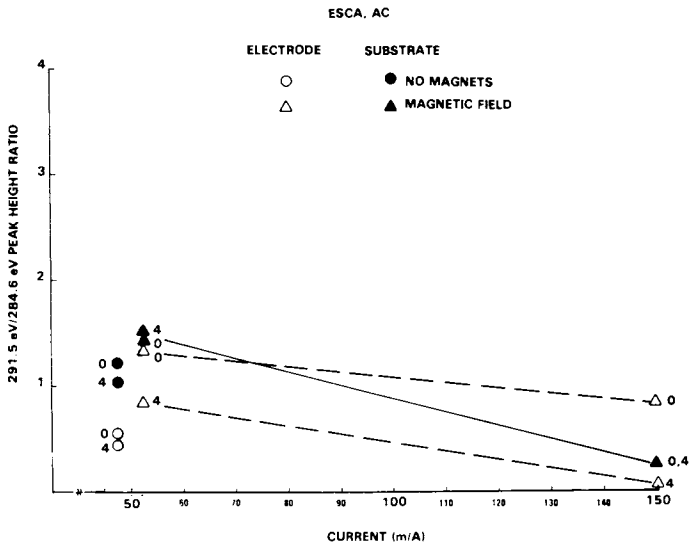

Figure 4. Plot of the 291.5 eV/284.6 eV C (1s) peak height ratios vs. AC current

In Plasma Polymerization; Shen, M., et al.;
ACS Symposium Series; American Chemical Society: Washington, DC, 1979.

magnetic field tends to move the active zone closer to the electrode with the result that a decrease in fluorine content is observed at both electrode and substrate as the power is increased from 10 to 100 watts.

In contrast, the peak height ratios observed for AF and AC, shown in Figures 3 and 4, indicate that the power density is generally greater at the electrode than at the substrate. When a magnetic field is employed a fluorine poor polymer is formed at a radius of 4 cm at a lower current than is required to form a fluorine poor polymer at the center of the electrode. This was expected in light of the concentration of glow at a radius of 4 cm, near the electrode, when magnets are used. Finally it may be noted that for AC little change occurs in the nature of the plasma polymer deposited at the center of the electrode on increasing the current to 150 mA. In fact, the plasma polymer deposited at the center of the electrode deposited in an AC glow discharge at 150 mA is more fluorine rich than that deposited at the substrate. In this case there appears to be more of a contrast in the type of the polymer deposited at locations on the electrode than between that deposited on the electrode and the substrate.

In summary the distribution of power in the RF plasma appears to be the opposite of that in the AF and AF plasma. Power is concentrated near the substrate in the RF plasma, near the electrode for AF and AC. The magnetic field causes a localization of glow on a ring of 4 cm radius for the AF and AC glow discharges, resulting in the most fluorine poor polymer at a radius of 4 cm on the electrode. The opposite is the case for RF at low power, there is no differentiation between the two at high power. Between AF and AC, there appears to be more differentiation between the center of the electrode and the 4 cm radius on the electrode for AC than AF. Finally it may be noted that at low powers more fluorine appears to be present in the RF polymer than in the AF or AC polymer suggesting that the mildest conditions are found in the RF plasma.

The elemental ratios obtained from the ESCA data are presented in Figures 5, 6, 7 for RF, AF and AC respectively. It may be noted that in all cases the F/C ratio remains between 1 and 2 regardless of frequency or power. As the C_{1s} spectra indicate that a fluorine poor polymer is achieved at high powers, it is clear that under high power conditions fluorine is bonded to some other element, aluminum being the only likely candidate. It may be additionally observed that a high proportion of aluminum and oxygen is observed on the surface under conditions of high power density. This latter trend had been previously observed for TFE plasma polymerization in an inductively coupled straight tube reactor [3]. However, the F/C ratio was somewhat more variable for this inductively coupled reactor than for the present capacitively coupled reactor, presumably because of a shorter residence time for

In Plasma Polymerization; Shen, M., et al.;
ACS Symposium Series; American Chemical Society: Washington, DC, 1979.

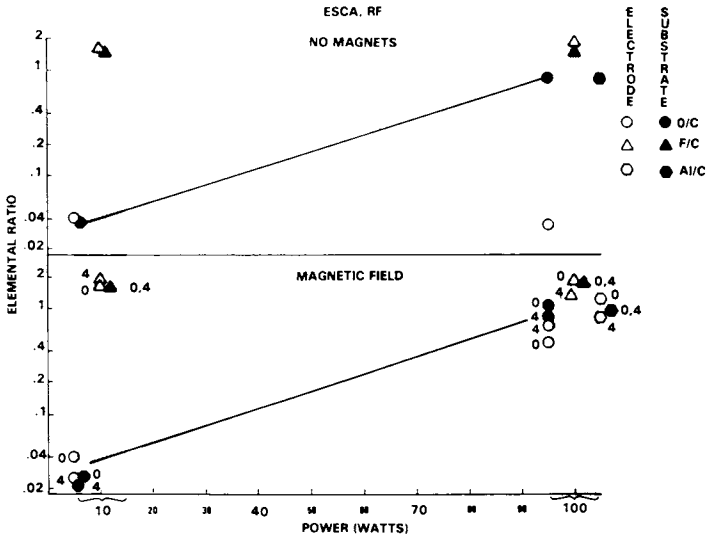

Figure 5. Semilogarithmic plot of the O/C, F/C, and Al/C elemental ratios vs. RF power

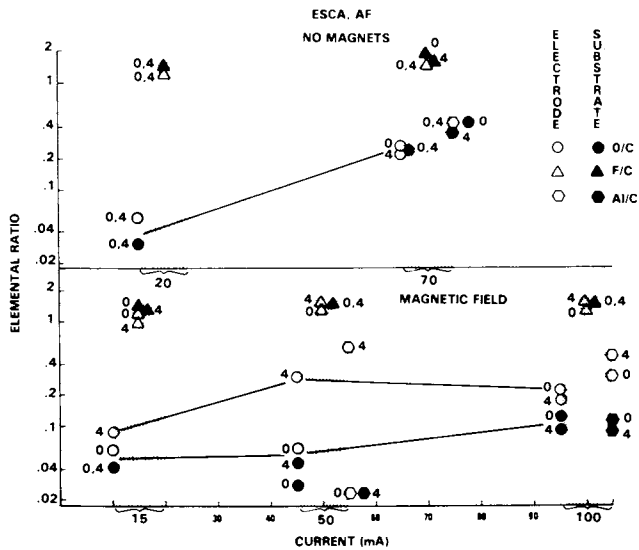

Figure 6. Semilogarithmic plot of the O/C, F/C, and Al/C elemental ratios vs. AF current

gaseous byproducts (fluorine) in the straight tube reactor.

By equating high O/C and Aℓ/C elemental ratios with high power density, one arrives at the same conclusions regarding the distribution of power density in the interelectrode gap as in the discussion of C_{1s} peak height ratios.

In Figure 5 the O/C ratio remains unchanged on increasing power from 10 to 100 watts only for the electrode without magnets. In addition only for this case is no aluminum observed on the plasma polymer surface. This confirms the presence of a low power density environment near the electrode for 100 watts RF power without a magnetic field. As shown below, (See Figs., 11-12), no negative deposition rates are observed for RF. Aluminum appears to be constantly ablated and redeposited in a high power density environment. The oxygen observed on the surface is assumed to be formed after exposure of plasma polymer to the air.

The trends observed for an AF plasma from the evaluation of the C_{1s} peak height ratios are confirmed in the elemental ratios in Figure 6. Generally the electrode O/C and Aℓ/C ratios are higher than the correponding substrate elemental ratios for the same set of conditions. For the case of a magnetic field, high O/C and Aℓ/C ratios are observed at a lower current for an electrode radius of 4 cm than at the electrode center. It may be noted that negative deposition rates are observed at the electrode at high currents (See Figs., 12, 13 and 14).

For AC (Fig. 7), the marked localization of power density in the presence of a magnetic field at the annular zone of radius, 4 cm, is confirmed at a current of 150 mA. Again the elemental ratios for the substrate are intermediate between those of the electrode at radii of 0 and 4 cm. Additionally, high O/C and Aℓ/C ratios are observed at an electrode radius of 4 cm even at a current of only 50 mA.

An additional differentiation between the effects of RF and AF, AC plasma is found in the position of the oxygen peak position as shown in Figures 8-10. For RF, the oxygen binding energy is less than 532 eV at the substrate at 100 watts power, indicating that oxygen is bound to aluminum for this case. The oxygen peak position at the electrode without magnets stands out because it remains unchanged on increasing power from 10 to 100 watts, confirming conclusions drawn above. It may be noted that much less change is seen in oxygen peak position as a function of current for AF and AC (Figs. 9 and 10).

Deposition rate data were obtained at radii of 0, 2, 4 and 6 cm on electrodes and substrate. There are reported in detail and integrated to % conversion of the monomer to plasma polymer elsewhere [9]. The results are shown in Figures 11 and 12. For RF, it is clear that conversion is less at the substrate than at the electrode. However the effect of a

In Plasma Polymerization; Shen, M., et al.;
ACS Symposium Series; American Chemical Society: Washington, DC, 1979.

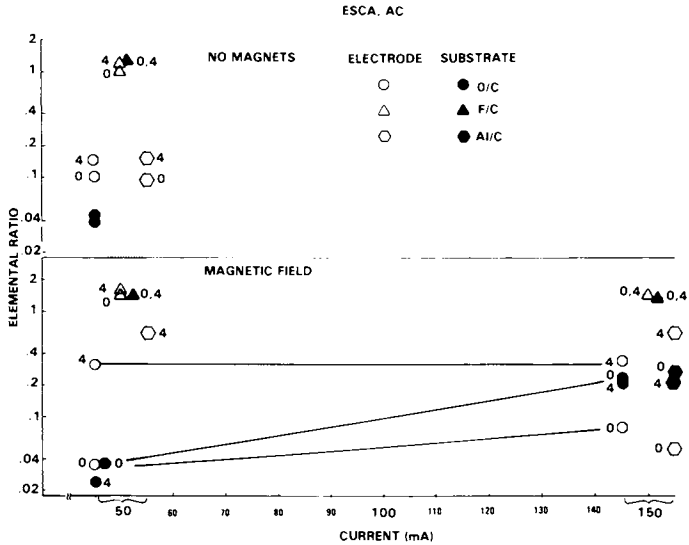

Figure 7. Semilogarithmic plot of the O/C, F/C, and Al/C, elemental ratios vs. AC current

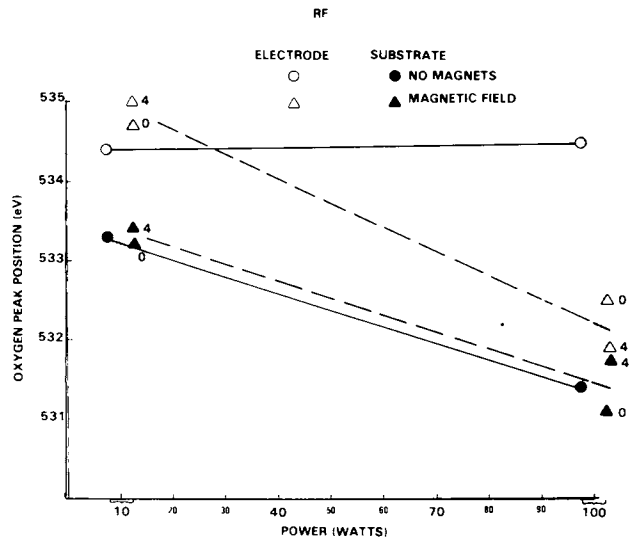

Figure 8. Plot of O (1s) binding energy vs. RF power

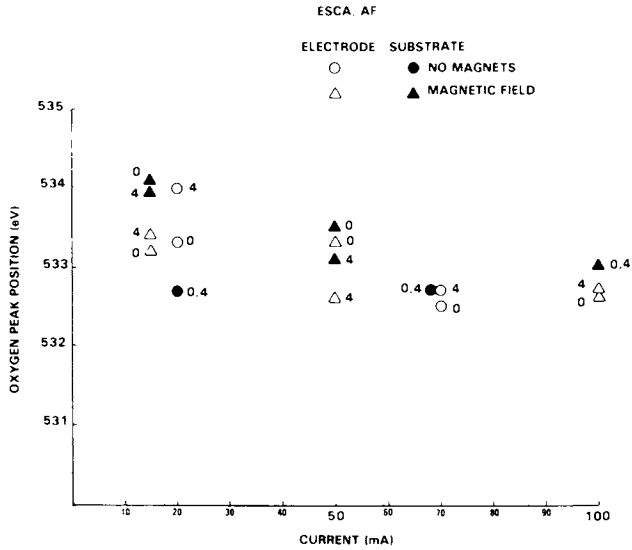

Figure 9. Plot of O (1s) binding energy vs. AF current

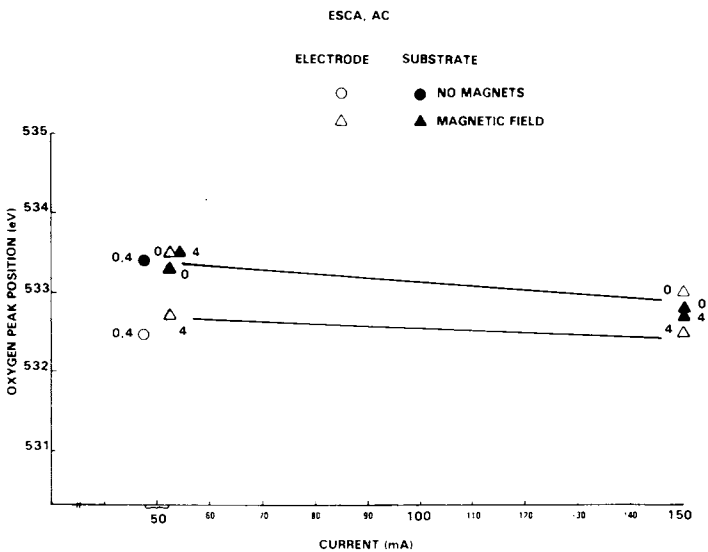

Figure 10. Plot of O (1s) binding energy vs. AC current

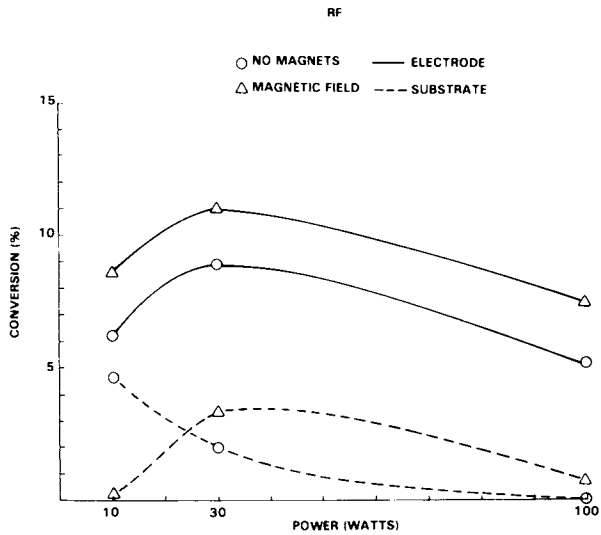

Figure 11. Plot of apparent conversion of monomer feed to plasma polymer at the electrode and substrate vs. RF power

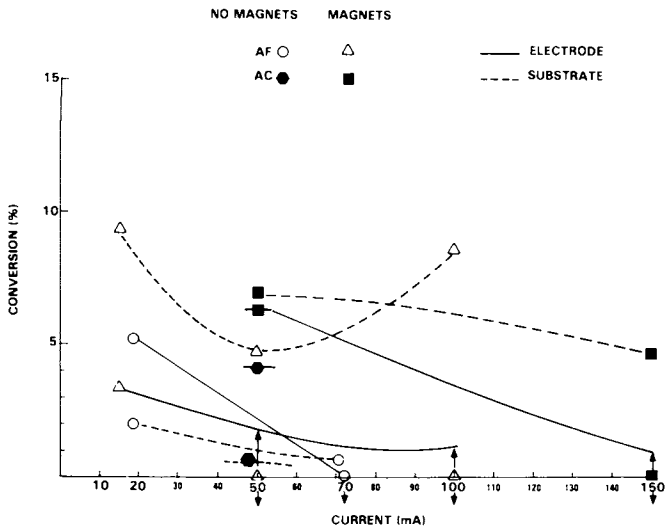

Figure 12. Plot of apparent conversion of monomer feed to plasma polymer at the electrode and substrate vs. AF or AC current. Symbols on the abscissa with arrows pointing down indicate negative deposition rates. Those with arrows pointing up and down indicate both negative and positive deposition rates at the electrode. No conversions were calculated for such cases.

In Plasma Polymerization; Shen, M., et al.;
ACS Symposium Series; American Chemical Society: Washington, DC, 1979.

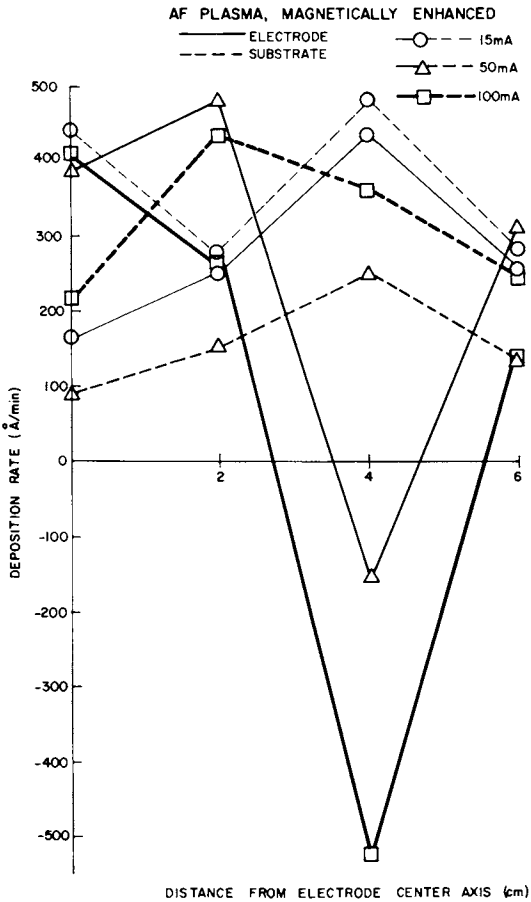

Figure 13. Deposition rate profiles on electrodes and substrate for AF plasma at a flow rate of 2 (STP)mL/min, $P_M = 60$ mtorr with a magnetic field

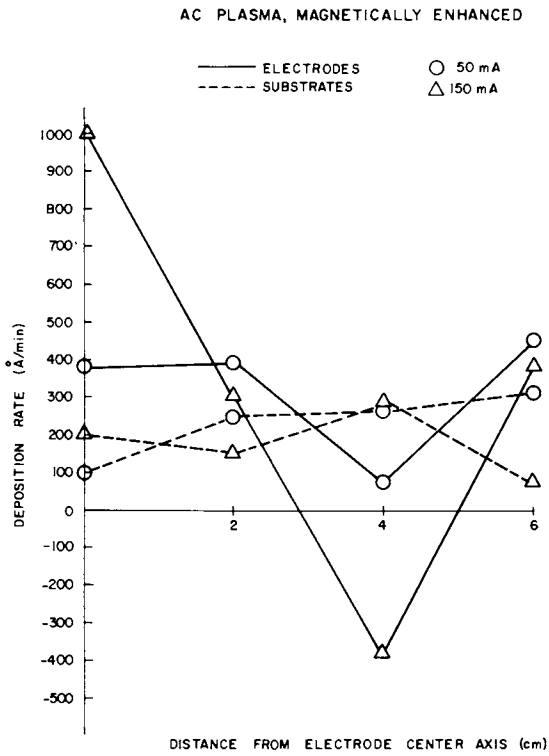

Figure 14. Deposition rate profiles on electrode and substrate for an AC glow discharge at a flow rate of 2 (STP)mL/min, P_M = 60 mtorr with a magnetic field

magnetic field is to moderate the ablation at the substrate to some degree. In Figure 12 the symbols on the absicca axis with arrows pointing downward indicate that no conversions were calculated because of a negative deposition rate. It may be noted that negative deposition rates were only observed on the electrode. Where a magnetic field was used both negative and positive deposition rates were observed at different sites on the electrode. The conversion on the electrode is less than that on the substrate for the AF but not for AC. The ESCA data above indicated greater differentiation between the center and the 4 cm position on the electrode for AC than between the electrode and substrate. For AF the greatest differentiation was between electrode and substrate. These trends are confirmed in Figures 13 and 14, plots of deposition rate versus distance from the electrode center axis for AF and AC, respectively. The very high deposition rate on the electrode at 0 cm may be noted for AC as compared to the corresponding deposition rate for AF.

Conclusions: The following conclusions may be drawn for plasmas at a pressure of about 40 millitorr, and a flow rate of 2 cm^3/min:

1.) Plasma polymers similar to those observed for inductively coupled plasmas are laid down in a capacitively coupled plasma. CF_2, CF_3, CF groups and aliphatic or graphitic carbons are present. An increase in power or current generally leads to a more fluorine poor polymer.

2.) In an RF capacitively coupled plasma increasing the power leads to an increasing power density at the substrate but not at the electrode. A magnetic field tends to move the most active region of the plasma closer to the electrode.

3.) For an AF and AC plasma the most active region is near the electrode. The use of a magnetic field confines the most active region to a zone of 4 cm radius close to the electrode for over set-up. This is seen visually [1] and is reflected in the ESCA and deposition rate data.

4.) At high currents the greatest difference in the deposition rate and character of plasma polymer is between the 4 cm radius and electrode center for AC, between electrode and substrate for AF.

5.) The mildest conditions were obtained with RF at low power input. Etching resulting in negative deposition rates was observed only for AF and AC, at high current levels. Definite bonding of oxygen to aluminum was only obtained with RF at high power.

In Plasma Polymerization; Shen, M., et al.;
ACS Symposium Series; American Chemical Society: Washington, DC, 1979.

Acknowledgment:

This work was supported by the Office of Water Research and Technology of the U. S. Department of the Interior under Contract Nos. 14-30-3301 and 14-34-0001-7537. Measurement of deposition rates and plasma polymer preparation was carried out by Barry Hill whereas the ESCA spectra were obtained by E. S. Brandt under the supervision of C. N. Reilley at the Department of Chemistry of the University of North Carolina at Chapel Hill.

Literature Cited:

1. H. Yasuda and N. Morosoff, "Tandem Plasma Polymerization Apparatus for Continuous Coating of Fibers Films", in paper presented at Plasma Polymerization Symposium, ACS meeting Miami Beach, September 1978.
2. H. Yasuda, T. S. Hsu, E. S. Brandt, C. N. Reilley, J. Polymer Sci., Polymer Chem. Ed., 16, 415 (1978).
3. H. Yasuda, N. Morosoff, E. S. Brandt, C. N. Reilley, J. Appl. Polymer Sci., in press.
4. H. Yasuda and C. E. Lamaze, J. Appl. Polymer Sci., 17, 1519 (1973).
5. H. Yasuda and T. Hirotsu, J. Polymer Sci., Polymer Chem. Ed., 16, 313 (1978).
6. H. Yasuda and T. Hirotsu, J. Polymer Sci., Polymer Chem. Ed., 16, 743 (1978).
7. N. Morosoff, W. Newton, and H. Yasuda, J. Vac. Sci. Tech., in press.
8. L. Maissel, "Application of Sputtering to the Deposition of Films", in L. Maissel and R. Glang, eds. "Handbook of Thin Film Technology," McGraw Hill, N.Y.(1970).
9. N. Morosoff, H. Yasuda, E. S. Brandt and C. N. Reilley, J. Appl. Polymer Sci., in press.
10. H. Yasuda, H. C. Marsh, E. S. Brandt and C. N. Reilley, J. Polymer Sci., Polymer Chem. Ed., 15, 991 (1977).

RECEIVED March 29, 1979.

11

Plasma Deposition of Fluorinated Compounds

ATTILA E. PAVLATH and ALLEN G. PITTMAN

Western Regional Research Center, Science and Education Administration, U.S. Department of Agriculture, Berkeley, CA 94710

The unusual surface properties of poly(tetrafluoroethylene) have initiated many attempts to cover organic and inorganic surfaces with fluorinated coatings possessing similar characteristics (1). For a number of reasons, vapor phase deposition could have practical advantages. However, the polymerization of most of the highly fluorinated compounds, needed for desirable surface properties, is quite difficult and slow in the vapor phase. Polymeric films and non-polymeric coatings can be obtained through vapor phase reactions in an electric glow discharge (2) and therefore this method appears to be an excellent tool for preparing fluorine containing surfaces. In previous studies, we were able to obtain fluorine containing films on glass even from monomers such as octafluorobutene-2 (3). Tetrafluoroethylene alone (4) or ethylene with fluorocarbons (5,6) resulted in polymeric film deposition. Hexafluoroethane, a saturated and relatively inert fluorocarbon, resulted in a fluorinated surface on wool (7). The adhesion of these films to substrate depends mostly on the chemical nature of the substrate. Fluorocarbon deposited on an inorganic surface, such as glass, is generally easily removable with the aid of solvents and/or swelling agents, however, organic surfaces can yield a fluorocarbon-substrate graft. In this paper, we report the formation of fluorinated surfaces from various saturated fluorocarbon in a glow discharge and compare the results with those obtained using unsaturated fluorocarbons.

Experimental

The glow discharge was created through external capacitive coupling. In order to minimize polymer deposition on the reactor wall, the fluorinated compounds were introduced in the glow discharge immediately above the sample. For this purpose a specifically designed reactor was used (3). Even so, a build-up of a fluorinated compounds was observed on the reactor walls with certain unsaturated monomers. The discharge was created in an argon flow. The radiofrequency (rf) generator (13.56 MHz) had a maximum capacity

In Plasma Polymerization; Shen, M., et al.;
ACS Symposium Series; American Chemical Society: Washington, DC, 1979.

of 100 W, but the highest power attainable in the system in the presence of a fluorocarbon was 70 W. The lowest power setting required to maintain a steady glow discharge was 10 W. The exposure time varied from 5 seconds to 5 minutes at 1 Hgmm pressure. Gases were introduced through a micrometer valve to control the flow. Liquid fluorinated compounds were first volatized by bubbling a regulated flow of argon through them at room temperature.

Compounds tested were perfluoroethylene, -propylene and -butene-2, heptafluoroisopropyl allylether,perfluoroethane, a commercial mixture of isomeric C_7F_{16} (b.p. = 60-70 °), hexafluoroacetone, $CF_3(CF_2)_2CH_2OH$ and ethyl perfluorobutyrate. The isomeric perfluoroheptane mixture was manufactured by Pierce Co., others were obtained from regular laboratory chemical outlets. Substrate materials were glass microscope slides, poly(ethylene) and polyester films, undyed wool fabric. All substrates were cleaned by Soxhlet extraction in $C_2F_3Cl_3$, acetone and finally rinsing in distilled water. The same procedure was used,when indicated, after glow discharge treatment. The analysis of the surfaces was made using X-ray photoelectron spectroscopy (XPS) (DuPont 650 Electron Spectrometer) and surface wettablity via the measurement of the advancing liquid contact angle. The XPS analysis involved the determination of the carbon,fluorine and oxygen binding energy spectra. The fluorine and oxygen spectra were simple, though somewhat wider than the average single peak observed for model compounds. The halfwidth was in the range of 2.4-2.6 instead of 2.3-2.4 eV. The carbon 1s spectrum was wide and complex in each case, the binding energy ranged from 296 to 284 eV. The number of major components and their approximate position was determined by a recently developed method using the second derivative of the spectra (8). Using these data the carbon 1s spectra were deconvoluted by a non-linear least square curve fitting program (9). Caution was applied in interpreting the quantitative results of the deconvolution of such complec spectra, since small changes in the characteristics of the instrument, can cause considerable changes in the calculated ratio of the components. Curve fitting was applied in case of surface fluorination of poly(ethylene) to identify shifts of 0.5-1.0 eV (10). While the method could provide deceivingly good fits in the case of numerous and close peaks, critical evaluation could point to certain shortcomings which may invalidate the quantitative data. For this reason, the presence of only five characteristic carbon components was assumed in this analysis : 285.0-285.5,287.0-288.0,289.0-290.0,291.5-292.0 and 293.2-294.0 eV. The first binding energy is for the normal aliphatic carbon, while the last three were assigned to CF, $CF_2$and CF_3 respectively. The second range, between 287.0-288.0 eV, could be a joint peak of C-O, C=O and a quaternary carbon surrounded by four CF_x groups.

Surface wettability was determined by the measurement of advancing contact angles of hydrogen bonding liquids (ethylene glycol, formamide, glycerol and water) and non-hydrogen bonding

In Plasma Polymerization; Shen, M., et al.;
ACS Symposium Series; American Chemical Society: Washington, DC, 1979.

liquids (decane, dodecane, tetradecane and hexadecane) (11).

Results and Discussion

Unsaturated fluorinated compounds readily polymerized when injected in the glow discharge and a film deposition, generally colored brown-yellow, was equally visible on all substrates. Rapid polymer formation occurred with the heptafluoroisopropyl allylether monomer. Other olefins with fluorine atoms on the double bond (perfluoroethylene, -propylene and -butene-2), polymerized more slowly, but still fast enough to obtain substrate coverage at an exposure time as short as 5 seconds. While varying the reaction time from 5 seconds to 5 minutes,it was found that the fluorine to carbon ratio on a poly(ethylene) surface was 1.2:1 to 1.5:1 after a 15 second treatment, and that additional exposure did not significantly change this ratio. Similarly,the advancing contact angles of hydrophobic and hydrophilic liquids did not significantly change after 15 seconds of fluorocarbon-plasma treatment.

XPS-analysis of surface exposed to the perfluorinated monomers showed the presence of all possible CF_x species regardless of monomer structure. Fig. 1 shows the deconvoluted carbon 1s XPS spectrum of a poly(ethylene) surface after exposure of hexafluoropropylene in a glow discharge. A 1:1:1 ratio of the CF_3, CF_2 and CF groups was found suggesting the structure of a normal addition polymer. The evidence for fragmentation was more obvious with the tetrafluoroethylene monomer. Fig. 2 is a carbon 1s XPS spectrum obtained after exposing wool to CF_2=CF_2 in a glow discharge. The same three groups were present although not in a 1:1:1 ratio. Difluoromethylene was, as expected, the major component. We observed that as the power and exposure time were increased, fragmentation increased as did the oxygen concentration. The appearance of oxygen is attributed to the formation of long-life free radicals on the surface, and their reaction with oxygen after their removal from the reactor chamber.

The films deposited in various substrates after plasma treatment in the presence of perfluorinated olefins were subject to partial removal with extraction. Generally, after extraction, the fluorine to carbon ratio, determined through XPS analysis, decreased to 0.2:1 to 0.3:1 regardless of the applied power and residence time used during the formation of the film. In all cases a moderate but consistent amount of oxygen was detected in the fluorocarbon film. The oxygen to carbon ratio 0.12:1 to 0.14:1 before extraction and 0.08:1 to 0.1:1 after extraction.

Saturated fluorocarbons do not polymerize under normal conditions, although their pyrolysis at high temperatures (500-800°) is well-known. However, they can exhibit surprising reactivity in a glow discharge. The rate of polymer deposition decreased with increasing number of fluorine atoms in unsaturated compounds. However the rate of fluorinated film deposition increased with increasing fluorine content in saturated compounds. The presence of C-H inter-

In Plasma Polymerization; Shen, M., et al.;
ACS Symposium Series; American Chemical Society: Washington, DC, 1979.

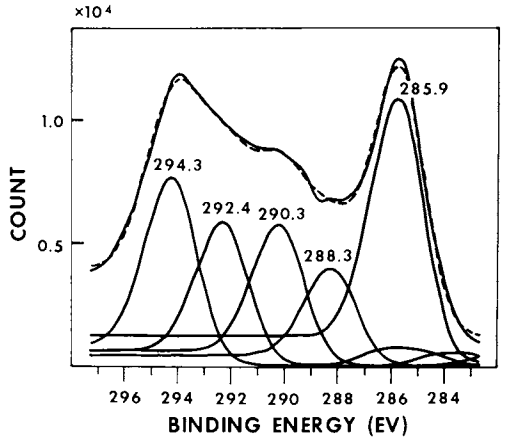

Figure 1. C(1s) XPS spectrum of hexafluoropropylene deposit on polyethylene. Power, 50 W; time, 1 min. Dotted line is the calculated composite.

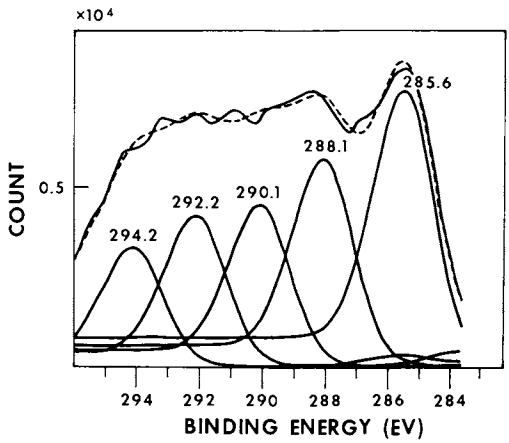

Figure 2. C (1s) XPS spectrum of tetrafluoroethylene deposit on wool. Power, 50 W; time, 1 min. Dotted line is the calculated composite.

In Plasma Polymerization; Shen, M., et al.;
ACS Symposium Series; American Chemical Society: Washington, DC, 1979.

fered with the formation of fluorocarbon radicals necessary for film formation. For example, when the alcohol, $CF_3(CF_2)_2CH_2OH$, was injected into a glow discharge, no fluorocarbon deposition was detectable by XPS-analysis. When the ester, $CF_3(CF_2)_2COOC_2H_5$, was used the deposition of a brown film occurred, but the amount of fluorine was very low even before extraction (F:C = 0.1:1 to o.2:1) Presumably, the ester decomposes to form $C_2H_5\cdot$ radicals or ethylene which is known to polymerize rapidly in glow discharge (12).

The initial concentration of fluorocarbon deposited on the various substrates was less after glow discharge exposure with hexafluoroethane than after exposure with tetrafluoroethylene. For example, the F:C ratio ranged 0.4:1 to 0.55:1 on wool and 0.6:1 to 0.8:1 on poly(ethylene) and polyester surface following exposure to hexafluoroethane, compared to about 1.2-1.5:1 after tetrafluoroethylene treatment. However, successive extractions with $C_2F_3Cl_3$, acetone and water did not remove as much of the fluorocarbon which was deposited using hexafluoroethane, as it did with the fluorocarbon deposited using tetrafluoroethylene in the glow discharge. The F:C ratio, for exaple, of poly(ethylene) treated with hexafluoroethane was 0.4:1 to 0.55:1 (following extraction) compared to the values of 0.2:1 to 0.3:1 following extraction of a tetrafluoroethylene treated surface. Fig. 3 and 4 show the deconvoluted carbon ls XPS spectrum of a poly(ethylene) sample treated in a glow discharge with hexafluoroethane before and after extraction respectively. It can be seen that extraction decreases the CF_3 signal very little compared to the signals of the other carbon-fluorine groups. We assume that CF_3 groups are introduced through direct coupling of CF_3 radicals with the substrate surface and are thus resistant to extraction procedures. Similar to the findings with unsaturated fluorocarbons, increasing the rf power or extending the residence time did not have significant effect on the F:C ratio. An increase in the O:C ratio did occur with increasing power or residence time with both saturated and unsaturated fluorocarbons.

When a commercially available mixture of perfluoroheptane isomers was used instead of perfluoroethane, the amount of fluorine detected by XPS analysis was much higher. The F:C ratio was 0.9:1 to 1:1 for wool and 1.4:1 to 1.5:1 for synthetic polymer substrates before extraction. Fig. 5 and 6 show the deconvoluted carbon ls spectra for both examples. Extraction reduced the fluorine content uniformly by 25-40% The F:C values after extraction are higher than for hexafluoroethane. F agmentation of perfluoroheptane isomers can create a wide variety of perfluoroalkyl radicals which may couple with the surface.

Hexafluoroacetone is not known to polymerize by a free radical mechanism, however, it reacts readily with nucleophilic reactants and can form copolymers via nucleophilic intermediates (13). Many of its derivatives create surfaces with low critical surface tensions (1). It was theorized that in a mild glow discharge reaction, the carbonyl group could be activated and the C_3F_6O group might

In Plasma Polymerization; Shen, M., et al.;
ACS Symposium Series; American Chemical Society: Washington, DC, 1979.

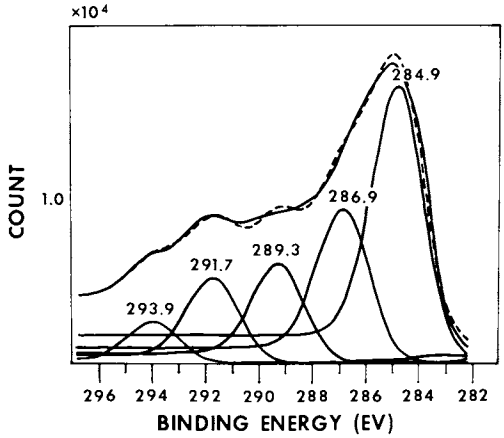

Figure 3. C (1s) XPS spectrum of hexafluoroethane deposit on polyethylene before extraction. Power, 50 W; time, 1 min. Dotted line the calculated composite.

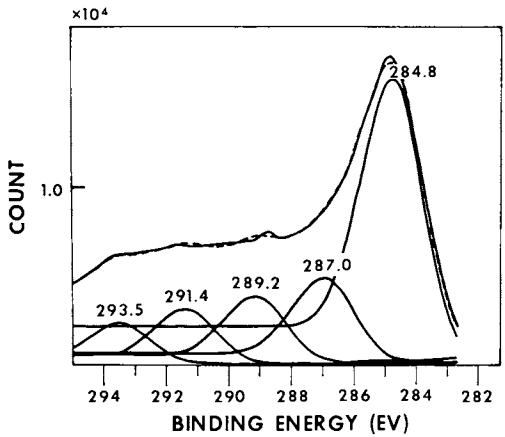

Figure 4. Same as Figure 3, after extraction

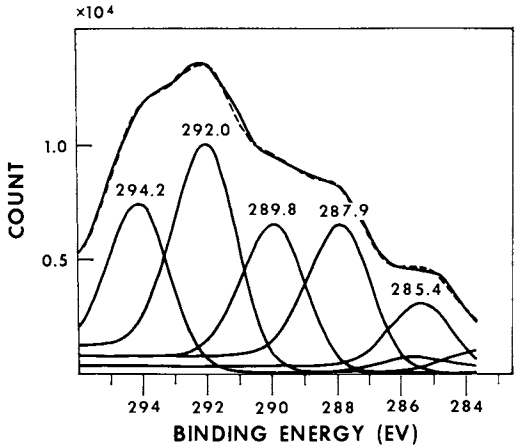

Figure 5. C (1s) XPS spectrum of perfluoroheptane deposit on polyethylene. Power, 50 W; time, 1 min. Dotted line is the calculated composite.

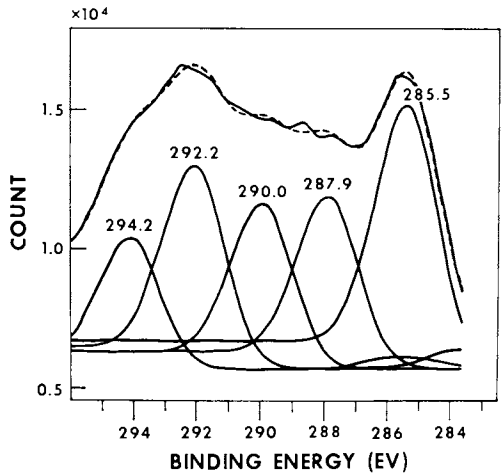

Figure 6. Same as Figure 5, on wool

become attached to the surface without fragmentation. The presence of fluorine was readily detected after a 30 second exposure of all substrates at 25W power. Deconvolution of the carbon 1s XPS spectrum, however, revealed that the fragmentation of hexafluoroacetone in glow discharge is similar to that of hexafluoroethane. Fig. 7 and 8 show the spectrum before and after extraction for the deposition of hexafluoroacetone obtained on polyethylene. Extraction eliminated some of the fluorocarbon deposition, decreasing the F:C ratio from 0.9-1.0:1 to 0.5-0.6:1. Interestingly, the extraction eliminated a larger percentage of the CF_3 group than that of other CF_x groups. This could indicate that some of the hexafluoroacetone might have been deposited on the surface in some non-fragmented but easily removable form.

The degree of surface coverage and wettability of the fluorocarbon depositions were examined by liquid contact angle measurement. When the cosine of these contact angles was plotted against the surface tension of the test liquids, a straight line plot was obtained for the hydrogen bonding and non-hydrogen bonding liquids separately. Due to the high electronegativity of the fluorine atom it has a quenching effect on discharges acting as an electronsink. In order to keep the characteristics of the glow discharge as similar as possible, hexafluoropropylene,hexafluoroacetone and hexafluoroethane were selected for comparative study since they contain the same number of fluorine atoms. It is evident from Fig. 9 that the hydrophobic character of the poly(ethylene) surface increased after exposure to these fluorocarbons in glow discharge, since increasing contact angles, i.e. small or negative cosine values, indicated higher water repellence. However, extraction eliminated this improvement except for the film obtained for hexafluoroethane. This suggests that the grafting was more prevalent with hexafluoroethane than with the other two compounds. In order to evaluate the effect of the fluorine deposition we must take into consideration the fact that a glow discharge alone will also have an effect on the surface wettability. Fig. 11 illustrates that the hydrophylic nature of poly(ethylene) is much higher after glow discharge treatment. Increased hydrophylicity is believed to be the result of free radical formation on the poly(ethylene) surface during glow discharge treatment, followed by oxidation when the surface is exposed to air.

The wettability of plasma deposited coatings can be compared with poly(tetrafluoroethylene) and poly(ethylene). When the cosine of contact angles obtained with non-hydrogen bonding liquids are plotted against their surface tension, extrapolation of the resulting straight line to cos $\emptyset$=1 yields a term called the critical surface tension (CST) which is characteristic of that surface (11). CST is expressed in terms of the surface tension of a liquid which just wets the surface, i.e. has a 0 contact angle. Fig. 12 gives CST plots for the same surfaces shown in Fig. 9 and 10 before and after extraction. It can be seen that all films have lower CST values than poly(tetrafluoroethylene) before extraction, but after

In Plasma Polymerization; Shen, M., et al.;
ACS Symposium Series; American Chemical Society: Washington, DC, 1979.

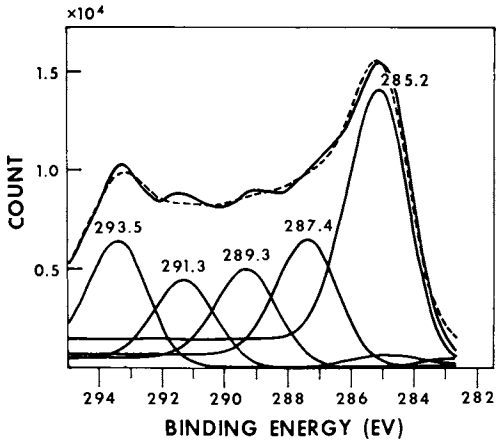

Figure 7. C (1s) XPS spectrum of hexafluoroacetone deposit on polyethylene before extraction. Power, 50 W; time, 1 min. Dotted line is the calculated composite.

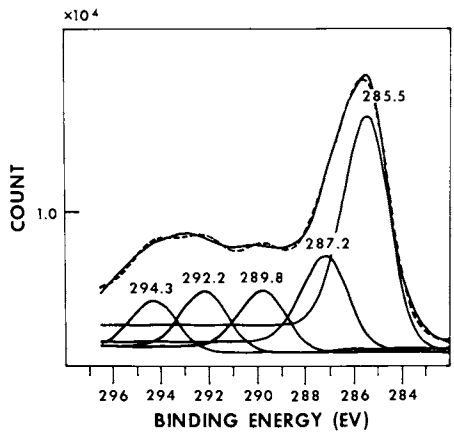

Figure 8. Same as Figure 7, after extraction

In Plasma Polymerization; Shen, M., et al.;
ACS Symposium Series; American Chemical Society: Washington, DC, 1979.

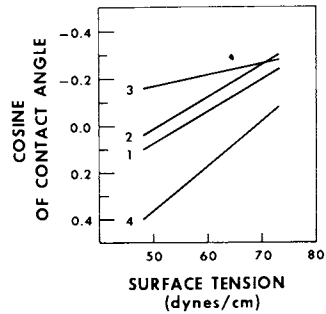

Figure 9. Cosine of contact angles of hydrogen-bonding liquids on fluorocarbon deposits on polyethylene before extraction. Power, 50 W; time, 1 min. (1) Hexafluoropropylene; (2) hexafluoroacetone; (3) hexafluoroethane; (4) glow discharge treated polyethylene without fluorocarbon.

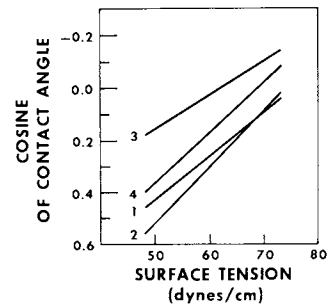

Figure 10. Same as Figure 9, after extraction

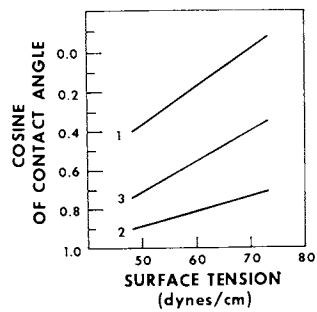

Figure 11. Cosine of contact angles of hydrogen-bonding liquids on glow discharge treated polyethylene. Power, 50 W; time, 1 min. (1) Before discharge; (2) after discharge and before extraction; (3) after discharge and after extraction.

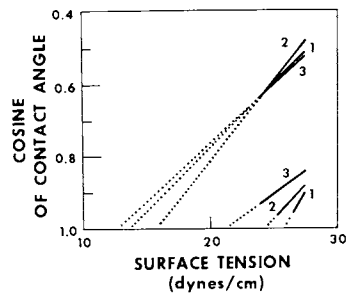

Figure 12. Cosine of contact angles of nonhydrogen-bonding liquids on fluorocarbon deposits on polyethylene both before (upper curves) and after (lower curves) extraction. Power, 50 W; time, 1 min. (1) Hexafluoropropylene; (2) hexafluoroacetone; (3) hexafluoroethane. The dotted lines are the extrapolations to zero contact angle.

In Plasma Polymerization; Shen, M., et al.;
ACS Symposium Series; American Chemical Society: Washington, DC, 1979.

extraction the CST values are between that of the poly(tetrafluoroethylene and poly(ethylene). It is also evident that the deposit obtained after glow discharge treatment with hexafluoroethane gives a lower CST (hence more oleophobic) value after extraction than either hexafluoropropylene or hexafluoroacetone. This,too, suggests a more permanently bonded (or grafted) coating.

Conclusions

Fluorine containing surfaces can be obtained by the introduction of fluorocarbons into a glow discharge in the presence of organic and inorganic substrates. The composition of these films indicates that fragmentation, rearrangment and oxidation occur during glow discharge deposition. Evidence exists that a higher degree of surface grafting results from saturated fluorocarbons than from perfluoroolefins. The presence of hydrogen in a saturated fluorine compound may inhibit the formation of a fluorinated surface. Perfluorinated saturated compounds yield a fluorine containing film which provides increased oleophobicity on a level similar to that of many fluorocarbon polymers.

Abstract

Both saturated and unsaturated fluorocarbons yielded fluorine containing films on organic and inorganic surfaces when exposed to a radiofrequency glow discharge. The analysis of the surfaces by X-ray photoelectron spectroscopy indicated a higher fluorine content using unsaturated compounds than with saturated ones. The relation, however, was reversed after extracting the surface with $C_2F_3Cl_3$and acetone. This lead to the conclusion that, while unsaturated fluorocarbons will readily polymerize in a glow discharge, the main result is deposition of polymeric materials and not their grafting. On the other hand, radicals from saturated fluorine compounds react mostly with the surface, creating a more permanently attached fluorinated layer. The conclusions drawn from XPS analysis were reinforced by the examination of surface wettability.

Disclaimer

Reference to a company or product name does not imply approval or recommendation of the product by the U.S. Department of Agriculture to the exclusion of others that may be suitable.

Literature Cited

1. Pittman,A.G., Surface Properties of Fluorocarbon Polymers, Chapter 13, in "High Polymers, XXV. Fluoropolymers", ed. by Wall,. Wiley-Interscience (1972)
2. Millard,M.M.,Polymer Deposition in Glow Discharge,Chapter V, in "Application of Plasma Chemistry",ed. by Bell,A.T.,Hollahan,J.,

In Plasma Polymerization; Shen, M., et al.;
ACS Symposium Series; American Chemical Society: Washington, DC, 1979.

Wiley,New York (1974)
3. Millard,M.M., Windle,J.J., Pavlath,A.E., J.Appl.Polym.Sci. (1973) 17. 2502
4. O'Kane,D.F., Rice,D.W., J. Macromolecular Science, Chem. (1976) A10. 567
5. Kobayashi,H., Shen,M., Bell,A.T., J. Macromolecular Science, Chem. (1974) A8. 1345
6. Rice,D.W., O'Kane,D.F., J. Electrochem. Soc., (1976) 123. 1308
7. Millard,M.M., Pavlath,A.E., J. Macromolecular Science, Chem. (1976) A10. 579
8. Pavlath,A.E., Millard,M.M., To be published
9. Fadley,C.S, Ph.D. Thesis, University of California Radiation Laboratory, Berkeley, (1970) 19353
10. Clarke,D.T., Feast,W.J., J. Macromolecular Science Rev. Macromol. Chem. (1975) C12(2), 191
11. Zisman,W.A., "Advances in Chemistry", Series 43, ACS, Chapter 1, (1964)
12. Kobayashi,H., Shen,M., Bell,A.T., J. Macromolecular Science, Chem. (1974) A10. 373
13. Madison,M.L., Polymer Preprints (1966) 7(2) 1099.

RECEIVED March 29, 1979.

12

Metal Containing Fluoropolymer Films Produced by Simultaneous Plasma Etching and Polymerization

A. DILKS[1] and ERIC KAY

IBM Research Laboratory, San Jose, CA 95193

The incorporation of metals into polymer films produced by plasma techniques is an attractive prospect since it can be envisaged that careful choice of the metal and organic phases, and close control of the overall composition of the product would greatly extend the scope of these plasma polymerized materials in, for example, electrical, magnetic and optical applications. In a previous paper (1) we have outlined a convenient method for the preparation of such materials derived from fluorinated 'monomers' by simultaneous chemical plasma etching and polymerization in the same system.

In the present paper we describe a detailed systematic investigation of these materials for an extended range of cathode materials, including silicon, germanium, molybdenum, tungsten and copper. The injected monomer is perfluoropropane and the polymers are analyzed by means of X-ray photoelectron spectroscopy (XPS or ESCA), while the low molecular weight neutral products in the plasma effluent are monitored by means of mass spectrometric techniques.

The synthesis of the metal containing polymer films involves a capacitively coupled diode reactor configuration in which one electrode is grounded, (the anode). Radiofrequency power, of 13.56 MHz is applied to the other electrode, which at this frequency attains an overall negative potential, due to the greater mobility of the electrons than the ions in the plasma, and is therefore termed the cathode. The positive ions therefore arrive at the cathode with increased kinetic energy and material is removed from its surface by competitive physical sputtering, in which momentum transfer to the surface is involved, as well as chemical plasma etching, through the formation of volatile species, which

[1] Current Address: University of Durham, Chemistry Dept., South Road, Durham City, England.

0-8412-0510-8/79/47-108-195$06.00/0

subsequently desorb and enter the gas phase. In the present investigation silicon, germanium, molybdenum and tungsten have been employed as examples of materials which may form volatile fluorides, in a fluorocarbon plasma environment, encompassing both non-metals and metals. Chemical plasma etching will be expected to dominate for these materials. Copper, on the other hand, forms involatile fluorides and therefore material can only be removed from this cathode, in a plasma environment, by a physical sputtering mechanism.

Previous work in these laboratories (2) has shown that the relative rates of etching and polymerization for a given fluorocarbon in which a discharge is sustained depends strongly on its effective fluorine/carbon stoichiometric ratio, as well as the residence time which is directly related to the flow rate and pressure. Thus, while CF_4 is an efficient etching gas C_2F_4 shows little etching but a high degree of polymerization. The choice of C_3F_8 for this investigation has therefore proved to give convenient rates of both etching and polymerization (1). The effective removal of fluorine from the system by the etching process, to form stable volatile fluorides, tends to lower the overall fluorine/carbon ratio in the plasma and thus enhance polymerization (2), and indeed it has been shown from *in situ* mass spectrometry that the rate of polymer deposition is either directly or indirectly related to the concentration of unsaturated species in the plasma (3). The primary points to which this work has been addressed are as follows:

(i) What are the restrictions on the cathode material which may be incorporated into the polymer?
(ii) What is the structure of the polymer matrices containing the metals and how is the metal bonded in the matrix?
(iii) How do the low molecular weight species, in the plasma effluent, relate to the polymer structure, and is it possible to say anything about the precursors to polymerization and the likely mechanisms involved in the formation of the polymer films?

In an extensive series of publications, X-ray photoelectron spectroscopy (XPS or ESCA) has been demonstrated to be an extremely powerful tool for the investigation of structure, bonding and reactivity in polymeric systems (4,5,6). Its small sample requirement, non destructive nature and ability to study solid samples in their working environment with a minimum of preparation, have made it particularly amenable to the study of crosslinked materials whose insolubility make them difficult to study by any other technique (7). Indeed a perusal of the literature readily affirms that in the field of plasma polymerization ESCA has played an important role in recent

In Plasma Polymerization; Shen, M., et al.;
ACS Symposium Series; American Chemical Society: Washington, DC, 1979.

years, and for plasma polymerized fluorocarbon based systems in particular, ESCA has often provided the only detailed information available concerning their structure and bonding (7,8,9,10,11). Fluorine containing systems are well suited to examination by ESCA since fluorine, being the most electronegative element in the periodic table, induces the largest chemical shifts in the C_{1s} levels (4), and a large volume of background data is available in the literature for these materials (4,5,6).

The application of mass spectrometric techniques is now well established as one of the most useful and convenient techniques for the interrogation of the gas phase chemistry occuring in a plasma (2,3,12,13). The published work to date has included monitoring of both neutral species and positive ions and it has become increasingly apparent that the information derived from these methods aids considerably the understanding of the processes involved in the plasma (2,3,12,13). It will become clear from the present investigation that the combination of ESCA analysis of the polymers and mass spectrometric analysis of the low molecular weight neutral products in the plasma effluent provides a sound basis for the discussion of the likely reaction mechanisms leading to polymer formation, in the systems described here, and indeed the wider ranging potential of this powerful combination will become evident.

Experimental

A schematic of the reactor and pumping configuration is shown in Figure 1. The total volume of the plasma reactor is ~25 litres, the main chamber being a cylinder ~30 cms diameter and ~30 cms deep, containing the cathode and anode mounted 6 cms apart at the center. In this arrangement the plasma is largely confined to a volume of ~1 litre which minimizes any extraneous effects due to interactions with the walls of the reactor. The top plate of the chamber, containing the cathode mounting, is sealed by a 'Viton' gasket, and is removable to allow access to the interior.

The cathode consists of a 10 cm diameter disc which is electrically isolated from the chamber by means of ceramic insulators, vacuum sealed by 'Viton' O-rings, and is surrounded by a grounded shield so as to confine the contact of the plasma to the front surface of the cathode assembly. The active surface of the cathode is removable to allow the measurement of etch rates by its weight loss and also to allow the cathode materials to be interchanged.

The anode is constructed from aluminum and is 15 cms in diameter. It is electrically grounded to the reactor chamber and both the anode and cathode assemblies are water cooled. Three mountings for the substrate holders are inset into the

In Plasma Polymerization; Shen, M., et al.;
ACS Symposium Series; American Chemical Society: Washington, DC, 1979.

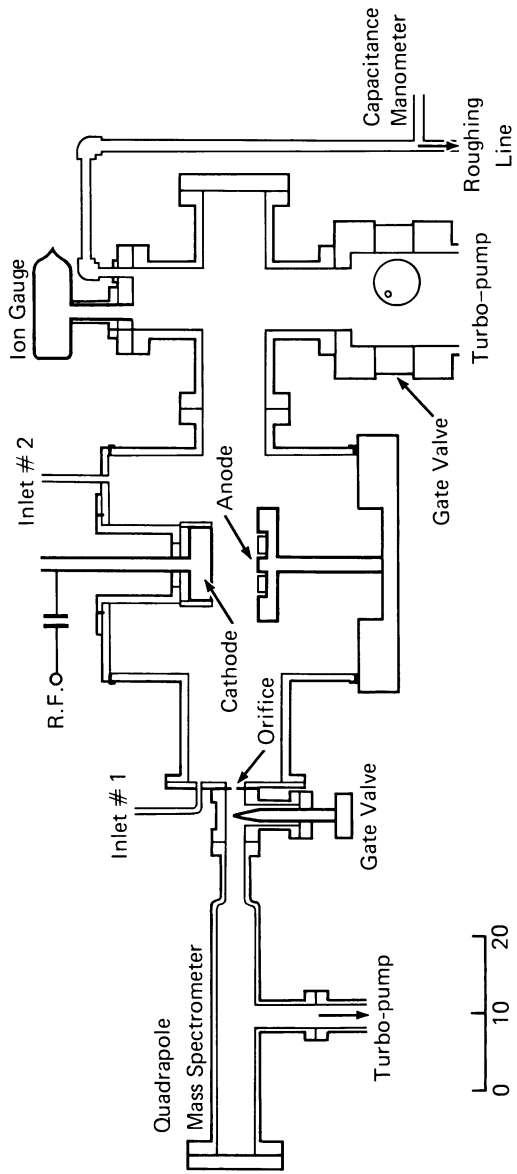

Figure 1. Schematic of the plasma reactor configuration

anode plane centered at the corners of an equilateral triangle of side ~15 mm. The substrate mountings are electrically isolated from the anode whilst good thermal contact is maintained, by the use of beryllium oxide insulators. The substrates may therefore be electrically biased with respect to the plasma potential, if so desired, as well as temperature controlled. However, in the present investigation only films for which the substrate is electrically isolated from the anode are discussed. The substrate will therefore attain a potential somewhere between the plasma potential (typically +20 volts) and ground. In all cases the substrates were maintained at a constant temperature of ~16°C which was monitored by iron-constantan thermocouples inserted into the substrate holders.

The substrate holders are machined from nickel and bolted directly onto their mountings. Two types of substrates were used; namely 0.010 inch gold foil, bolted directly to the holder, or 0.020 inch × 0.5 inch diameter sapphire discs, mounted by means of gallium solder to ensure good thermal contact. Deposition rates were determined by the weight gain of the sapphire substrates. The substrates could be covered by a removable inverted pan maintained at ground potential such that in the covered condition no reaction occured at the anode. This facility allowed the plasma to be established and stabilized before exposure of the substrates.

The reactor is pumped via a 4 inch pumping tube by a Leybold-Haraeus turbomolecular pump, which has a pumping speed of ~200 litre sec^{-1}, backed by a 350 litre min^{-1} two stage rotary pump. The pumping system may be isolated from the reactor by means of a gate valve, which also serves as a throttle to maintain a constant pressure in the system during film preparation. The pressure, normally in the range 0.005 to 0.050 torr, is monitored by means of a Datametrics Baracel electronic capacitance manometer. The base pressure of the system, measured by an ionization gauge, is ~10^{-6} torr.

Gases are metered into the system by means of a flow rate controller mechanism which is able to maintain constant flow rates in the range 0-15 cm^3 min^{-1} measured at STP.

The quadrupole mass spectrometer is a UTI type 100C mounted opposite the reactor chamber pumping tube. It is separated from the reactor by a gate valve and a 0.003 inch diameter × 0.010 inch long orifice, and is positioned ~30 cms from the center of the plasma region, which is sufficiently far to prevent polymer build up on the orifice. The mass spectrometer is differentially pumped via a 1 inch pumping tube, by an Airco Temescal tubomolecular pump, backed by a 350 litre min^{-1} two stage rotary pump. The mass spectrometer has a base pressure of ~10^{-9} torr and with the gate valve open can be maintained typically four to five orders of magnitude lower in pressure than the plasma. The spectrum of the effluent gases can be

In Plasma Polymerization; Shen, M., et al.;
ACS Symposium Series; American Chemical Society: Washington, DC, 1979.

conveniently recorded over the range 2-300 a.m.u. in 10 mins. The ion energy and focusing voltage were 14.5eV and -20 volts respectively, whilst the average electron energy in the ionizer region, is variable from ~15-100eV. These voltages are only approximately related to the actual ionizing energy due to the complex geometry of the ionizer. The nature of the electrode potentials in the mass spectrometer is such that only neutral species are allowed to enter, although it is unlikely that ions would be present at this distance from the plasma.

The radiofrequency power is provided by a Heathkit model DX-60B r.f. generator, run at a frequency of 13.56 MHz, via a National Radio Company Inc. model NCL-2000 power amplifier and a Bendix Corporation model 263 power meter. This system can deliver 0-300 watts of radiofrequency power maintained at a constant level by a power level control unit. The output of the r.f. power unit is impedance matched to the cathode of the reactor via an LC matching network.

The perfluoropropane used in this investigation was obtained from PCR Research Chemicals, Inc. and used without further purification. The cathode materials were obtained from Haseldon Company and were typically 99.999% purity.

ESCA spectra of the films deposited onto the gold foil substrates were recorded on a Hewlett-Packard 5950B spectrometer employing monochromatic Al $K\alpha_{1,2}$ exciting radiation. In this system the angle between the X-ray source and analyzer entrance slits is fixed, as is the angle of the sample with respect to the analyzer, (electron take off angle), since dispersion compensation is employed in the electron optics. Under the conditions employed in this investigation the full width at half maximum (FWHM) of the Au $4f_{7/2}$ core level of a clean gold sample at a binding energy of 84.0eV, used for calibration purposes, was 0.85eV. The effects of sample charging phenomena were alleviated by preparing the samples sufficiently thin (i.e., <10,000Å) such that the incident X-rays could penetrate the polymer film, to the gold substrate maintained in electrical contact with the spectrometer, and thus create sufficient charge carriers in the sample to effectively neutralize the sample surface (14). Energy referencing was achieved by monitoring the signal at 285.0eV binding energy arising from the C_{1s} levels of the extraneous hydrocarbon contamination which built up on the sample to detectable levels after it had remained in the spectrometer overnight (4). The typical time taken to accumulate the spectrum for a given sample, (typically six core levels), was ~1 hour, during which time no degradation or contamination was evident.

The samples were also studied by Transmission Electron Microscopy and ESR spectroscopy.

In Plasma Polymerization; Shen, M., et al.;
ACS Symposium Series; American Chemical Society: Washington, DC, 1979.

The procedure for film deposition was the same in all cases. For each preparation three substrates were mounted in the anode plane, (which had been previously carefully cleaned), and numbered as follows: (i) 0.5 inch sapphire disc, (ii) gold foil in electrical contact with the anode and (iii) gold foil electrically isolated from the anode, all of which had been cleaned, degreased and weighed. The cover pan was then moved over the substrates. The weighed cathode surface, of the material required, was mounted, the system assembled and pumped overnight, typically reaching a pressure of $\sim 2 \times 10^{-6}$ torr. A background mass spectrum was recorded (gate valve open) and then the perfluoropropane gas was allowed in at the desired flow rate, and the pressure adjusted by throttling the main turbomolecular pump. The variation of flow rate and pressure within the timescale of a preparation was less than 2%. The radiofrequency power was then applied at its preset level and the impedance matched by the LC network to give a standing wave ratio of 1.0 (zero reflected power). The substrate cover pan was removed as the timer was started. Since the cathode is undoubtedly etched to a small extent before the timer is started (~10 secs), the total time of deposition was made large (3000 secs) to render this source of error negligible, as well as to minimize effects due to the oxide layer on the cathode. Mass spectra of the neutral products in the effluent of the plasma were recorded after ~100 secs and then at intervals throughout the deposition, and in all cases it was found that the spectrum was not time dependent, (at least after the initial ~100 secs). The radiofrequency power was turned off after 3000 secs and the system pumped for 2-3 mins at $< 10^{-5}$ torr before removing the active part of the cathode and the substrates for weighing. Analysis of the samples by ESCA was carried out after air exposure.

Results and Discussion

1. Polymer Formed in a Molybdenum-Perfluoropropane System

In a previous paper (1), we have presented in a preliminary form, data pertaining to the system employing molybdenum as the cathode material and perfluoropropane as the injected 'monomer' gas. This paper therefore forms a logical extension to that initial study.

Typical F_{1s}, O_{1s}, C_{1s} and Mo_{3d} core level spectra of the polymer formed in this system, (designated Mo-C_3F_8), are displayed along the second row in Figure 2. The monomer flow rate, f=5 cm^3 min^{-1} (at STP), the pressure in the reactor, p=0.015 torr, and the power loading, w=100 watts.

The C_{1s} spectrum clearly exhibits several distinct types of carbon environment. Comparison with previously well characterized fluoropolymers allows the individual components

to be assigned to particular structural features (4,6). Thus, the peak centered at ~293.9eV on the binding energy scale is attributable to carbon attached to three fluorine atoms in $\underline{C}F_3$ whilst those at ~291.7eV and ~289.6eV are due to $\underline{C}F_2$ and $\underline{C}F$ structural features respectively. The signal centered at ~287.3eV can be assigned to carbon atoms not directly attached to fluorine but having fluorine substituents in a beta position (4,6), whilst the peak at ~285.0eV arises from either carbon atoms in a highly crosslinked environment, having no alpha or beta fluorine substituents (5) or from a small amount of contamination of the sample arising from extraneous hydrocarbon species present in the plasma reactor. The full width at half maximum (FWHM) of the components of the C_{1s} spectrum increases in going from $\underline{C}F_3$ to carbon not directly attached to fluorine, which can be related to the increasing number of possible beta fluorine substitution patterns, each of which will result in a slightly different binding energy for a particular structural feature (4). Since there are a large number of chemically different environments for each structural type, a more detailed analysis than this convolution of five broad components would not be tenable.

Although the chemical shifts induced in the C_{1s} levels by fluorine are large, due to the high electronegativity of fluorine, the corresponding shifts in the F_{1s} levels are very much smaller (4) and span a range of only ~1eV, with fluorine in more highly fluorinated systems being at higher binding energy. The intense signal at 689.2eV in the F_{1s} spectrum having an increased FWHM can therefore be assigned to a convolution of all the various carbon-fluorine environments. In addition to this peak, however, there is a smaller signal to lower binding energy, (~685.7eV), which may be assigned to fluorine attached directly to molybdenum, having a somewhat greater ionic character.

The Mo_{3d} core level signal is a spin orbit split doublet with a peak separation of ~3.2eV. The binding energies and large FWHM are consistent with the metal being in a mixture of the +5 and +6 oxidation states, from a comparison with data reported in the literature (16). The relative intensity of the signal due to fluorine attached to molybdenum is much too small to account for this high oxidation state and as it will be seen more clearly from the next section the metal is present mainly in the form of its oxides which are produced on exposure of the sample to the atmosphere.

The lowest binding energy component in the O_{1s} spectrum (at ~532.0eV) is consistently ~1.3eV higher than that found in bulk molybdenum oxides (16), and there also appears to be a second component of lower intensity at a higher binding energy.

Comparisons of the Mo_{3p}/Mo_{3d} core level signal intensity ratio with standard homogenous samples containing molybdenum

In Plasma Polymerization; Shen, M., et al.;
ACS Symposium Series; American Chemical Society: Washington, DC, 1979.

gives a close agreement. Since the photoelectrons emitted from these levels, by Al $K\alpha_{1,2}$ radiation, have widely different mean free paths through the polymer, inhomogeneities in the sample within the ESCA sampling depth (~50Å) would manifest themselves as a change in this ratio. This correspondence of the $Mo3_p/Mo3_d$ ratio with standard samples therefore demonstrates that the outermost ~50Å of the material is homogeneous (6). Furthermore, comparison of the empirical formula determined from the ESCA signal intensities (corrected for total relative sensitivity derived from standard samples) with information relating to the bulk composition derived from X-ray fluorescense analysis also gives excellent agreement (1), demonstrating that, as far as the molybdenum content is concerned, the composition of the polymer, within the ESCA sampling depth, is the same as that of the bulk material. In this respect it is also important to refer to previous work on similar systems (8,17) which showed that the carbon-fluorine structure of the outermost surface regions of these plasma polymerized fluoropolymers is entirely representative of the bulk.

Transmission electron microscopy studies of the polymer films formed in the Mo-C_3F_8 system confirmed that the molybdenum entities were homogeneously dispersed throughout the film.

Experiments to determine the effects, on the film structure and composition, of varying the plasma parameters, within moderate limits, were also carried out for the Mo-C_3F_8 system. The range of the parameters studied was: flow rate=1.7-8.3 $cm^3\ min^{-1}$ (at STP), pressure=0.005-0.050 torr and power=20-100 watts. It is not appropriate, in the context of this investigation, to discuss the absolute variations of, for example, the etch and deposition rates, since this type of analysis is highly system dependent. However the most important general features, which will apply to any system, can be summarized as follows: (i) while the amount of metal incorporated into the films varies within narrow limits, (18-26% by weight of molybdenum), in this range of operating parameters, it is directly related to the ratio of the etch rate divided by the deposition rate, (ii) the structure of the metal containing entities is essentially unchanged in this range, (iii) while the polymer structure varies very little as a function of the plasma parameters there is a distinct tendancy for those formed at higher power loadings to be more highly crosslinked, as evidenced by a greater amount of CF and carbon not directly attached to fluorine in the ESCA spectrum, as well as a decrease in the overall fluorine/carbon stoichiometry of the film.

In Plasma Polymerization; Shen, M., et al.;
ACS Symposium Series; American Chemical Society: Washington, DC, 1979.

2. Film Formation as a Function of Cathode Material

The core level spectra of the polymers synthesized in three separate experiments using germanium, molybdenum and copper cathodes respectively and gold substrates (maintained at ~16°C) electrically isolated from the anode, are displayed in Figure 2. (The designations Ge-C_3F_8, Mo-C_3F_8 and Cu-C_3F_8 refer to the cathode material and the 'monomer' gas injected into the plasma chamber, rather than information concerning the polymer product.)

The plasma parameters of f=5 cm^3 min^{-1} (at STP), p=0.015 torr and w=100 watts are the same in all cases. The ESCA data immediately affirm that both molybdenum and copper are incorporated into the polymer films although as previously noted the method of cathode erosion must be different in the two cases, (chemical plasma etching versus physical sputtering). Consideration of the relative signal intensities, corrected for the total relative sensitivities of the core levels, derived from standard homogeneous samples, allows estimates of the empirical formulae to be written for these materials as follows: $[C_3F_{4.0}O_{0.6}Mo_{0.3}]_n$ and $[C_3F_{3.9}O_{0.3}Cu_{0.3}]_n$ representing ~19% molybdenum and ~14% copper by weight respectively. In contrast, Figure 2 confirms that germanium is not incorporated into the polymer when employing a germanium cathode and the estimated empirical formula in this case is $[C_3F_{3.6}]_n$. A similar situation is also found when employing a silicon cathode and both the empirical formula and deposition rate of the polymer produced in the silicon system are very similar to those for the Ge-C_3F_8 system. The ESCA spectra of the polymers produced when using either germanium or silicon cathodes show only a very small broad oxygen signal, which is due to carbonyl features formed by reaction of free radical sites, trapped in the polymer structure, with atmospheric oxygen. The low intensity of this oxygen signal is consistent with previous estimates of the concentration of carbonyl features in similar films (15), and indeed ESR measurements on both the metal containing films, and films containing none of the cathode material, described here, revealed broad, intense singlet structures which decayed over a period of hours.

In situ mass spectrometric analysis of the plasmas involving either molybdenum or germanium cathodes, for example, have demonstrated that the major inorganic products of the plasma etching are indeed MoF_6 and GeF_4 respectively (18), and from a consideration of cathode weight loss it is found that under the conditions employed here the amount of material removed from the germanium cathode, in terms of the number of atoms, is a factor of ~2.6 greater than the corresponding figure for molybdenum. It is clear, therefore, there must be a significant quantity of GeF_4 in the gas phase, thus we might

In Plasma Polymerization; Shen, M., et al.;
ACS Symposium Series; American Chemical Society: Washington, DC, 1979.

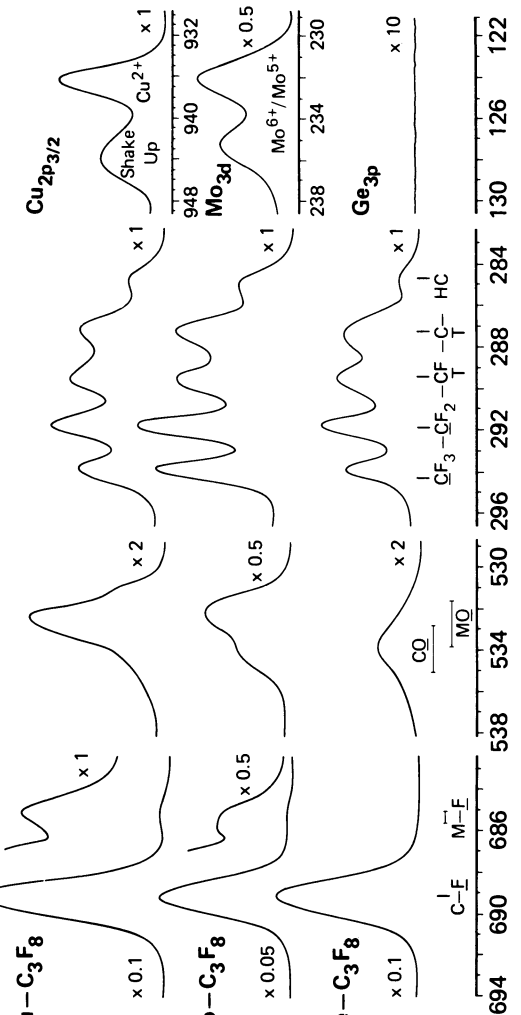

Figure 2. ESCA spectra of the polymers formed in three experiments involving Ge, Mo, and Cu cathodes, respectively

speculate why germanium is not incorporated into the polymer, and similar arguments will also apply to silicon. Two alternative explanations suggest themselves. They are: (1) If simple trapping of the inorganic fluorides in the polymer matrix is the dominant process, then the relatively smaller size of GeF_4 might allow it to diffuse out of the polymer. (2) If the incorporation of metal proceeds via an intermediate adduct formation between the inorganic molecule and some species at the forming polymer surface, the greater ability of molybdenum than germanium to participate in this type of coordination chemistry would also discriminate against the incorporation of germanium. The use of a germanium cathode provides an excellent method to prepare polymer films which contain none of the cathode material for comparison purposes, under similar plasma conditions to those used in preparing the metal containing films.

With tungsten as the cathode material the situation is analogous to that found when employing molybdenum although slightly less tungsten is incorporated into the polymer, ~15% by weight. The discussions for molybdenum therefore also apply in qualitative terms for tungsten.

The discussion of the polymer containing copper is also qualitatively the same as that previously presented for molybdenum. However, although surface fluorination of the copper cathode will undoubtedly be a significant process forming involatile CuF_2, the competitive physical sputtering process will almost certainly reduce the metal back to its zero oxidation state, (due to the relatively weak Cu-F bond strength), ejecting it into the plasma as copper atoms (19). However inspection of the Cu $2p_{3/2}$ region of the ESCA spectrum (Figure 2), of the resultant copper containing polymer film, reveals the presence of copper in its divalent oxidation state, as evidenced by the high binding energy of the direct photoionization peak, as well as the intense low energy shake-up satellite (20). For both molybdenum and copper there is evidence of a small amount of fluorine attached to the metal, but insufficient to account for the high oxidation state of the metal. The large increase however in oxygen content in going from the polymer containing none of the cathode material to the metal containing films, along with the lower binding energies of the centroids of the O_{1s} signals in the metal containing films, confirms that the metals are largely attached to oxygen atoms. The oxygen originates from the exposure of the samples to the atmosphere.

For molybdenum the metal is most likely present in the films predominantly as MoF_6 (with perhaps some MoF_5) before removing the samples from the reactor. The hydrolysis of these species however is a well known phenomenon (21) and thus reactions converting molybdenum-fluorine bonds to molybdenum-oxygen bonds can be expected to occur on exposure

In Plasma Polymerization; Shen, M., et al.;
ACS Symposium Series; American Chemical Society: Washington, DC, 1979.

to air. Further evidence to support this derives from the fact that when freshly prepared films are stored, in air, in glass containers, the glass shows signs of being etched by HF which would be evolved during a hydrolysis process. The films do however become stable after ~1 day in the atmosphere. For copper on the other hand the fluoride has a much greater stability in air and therefore the formation of cupric oxide is probably due to the reaction of zero valent copper, originally present in the film, with oxygen, permeating the polymer matrix, after exposure to air. The higher binding energy component in the asymmetric O_{1s} spectra of both samples is then at least partially attributable to the coordination of water to the inorganic molecules, although the final size of the coordination complex might be expected to be limited by the size (22) of the interstices in the polymer structure.

The possibility of observing organo-metallic bonding which may be present in the metal containing films is likely to be destroyed by exposure of the samples to the air.

The chemical plasma etching process, which involves the formation of stable volatile fluorides (13,18) will lower the effective fluorine/carbon ratio in the plasma, thus increasing the possibility of the formation of unsaturated species, which is known to ultimately enhance polymerization (3). The polymer deposition rates for the molybdenum and germanium systems therefore are greater than that for the copper system since the physical sputtering mechanism for non-volatile copper fluoride does not result in effective removal of fluorine from the plasma, as CuF_2 is expected to be dissociated during the sputtering process. For example, under the conditions pertaining to Figure 2 the deposition rate for the Mo-C_3F_8 system is ~2.6 times greater than that in the Cu-C_3F_8 system when corrected for the empirical formula weights of the films produced. A similar comparison of the Mo-C_3F_8 and Ge-C_3F_8 systems shows the polymer deposition rate to be ~20% greater for the system having a germanium cathode, which is consistent with the fact that germanium is etched much faster than molybdenum.

The close similarity of the C_{1s} spectra for these three examples (Figure 2) suggests that in all cases, irrespective of the mechanism of removal of material from the cathode or the nature of the cathode material, the polymer matrix formed at the film forming electrode is essentially the same. Furthermore, the overall band profile of the C_{1s} spectra and fluorine/carbon stoichiometries are strikingly similar to those which have previously been reported in the literature for the polymer produced in the plasma polymerization of tetrafluoroethylene (8).

It is of interest at this point to add as a footnote to this work that we have found that for films formed under enhanced ion bombardment conditions (i.e., substrate biased

In Plasma Polymerization; Shen, M., et al.;
ACS Symposium Series; American Chemical Society: Washington, DC, 1979.

negative with respect to the plasma) using a copper cathode, the organic phase can become completely graphitized, producing electrically conducting films, consisting essentially of a mixture of copper and graphite.

3. Mass Spectrometric Analysis of the Plasma Effluent

a) Calibration of the Mass Spectrometer

As a prerequisite to the interpretation of the results obtained from a mass spectrometic analysis of the plasma Table 1 summarizes the calibration data obtained for several fluorocarbons which we might expect to be present in the plasma effluent. The calibration data was accumulated, in the absence of a discharge for each gas, at a fixed pressure of 0.015 torr in the plasma reactor, corresponding to $\sim 10^{-6}$ torr in the differentially pumped mass spectrometer. The intensities of the signals are given relative to each other in arbitrary units and the figures in parentheses are the appearance potentials of the ions where these are available (23).

Since the electron impact ionizer of the mass spectrometer is operated here with an electron energy of ~15eV ions with an appearance potential ≥15eV are not observed. Thus fragmentations involving C-C bonds are favored over those involving C-F bonds and the largest signals are observed for ions derived from simple ionization of unsaturated species, for which the appearance potentials are comparatively low. For CF_4 therefore no spectrum is observed and for C_2F_6 only a small CF_3^+ signal is present. For C_3F_8 and n-C_4F_{10} more structure appears in the spectrum and each shows a characteristic fragmentation pattern. The unsaturated species, C_2F_4 and C_3F_6, which have been studied, show intense parent peaks and very little fragmentation. Extrapolation of the general trends in Table 1 for the systems which have been explicitly studied to those which have not, along with data available in the literature derived from similar investigations (12), allows one to decide which species may be observed and what their major fragments will be. For example all species with unsaturation will be easily observable since their appearance potentials are much lower than ~15eV (23). These will include C_4F_8, C_2F_2 and C_3F_4 (i.e., olefins, acetylenes, diolefins). The cyclic structures will manifest themselves as small signals at 100 and 131 a.m.u. for hexafluorocyclopropane and at 100, 131 and 181 a.m.u. for octafluorocyclobutane (12). The total sensitivity factor of the spectrometer itself decreases quite rapidly with increasing mass number.

In Plasma Polymerization; Shen, M., et al.;
ACS Symposium Series; American Chemical Society: Washington, DC, 1979.

b) Plasma Effluent Mass Spectra

Figure 3 shows the plasma effluent mass spectra obtained with the spectrometer operated under the same conditions as those pertaining to Table 1, for systems employing Ge, Mo and Cu cathode materials ($f=30$ cm^3 min^{-1}, $p=0.015$ torr, $w=100$ watts) and for pure C_3F_8 in the absence of a discharge. The measured deposition rates of the films produced in these systems are Cu:5.1×10^{-10}, Mo:1.3×10^{-9} and Ge:1.6×10^{-9} g-formula weights sec^{-1} cm^{-2}. The signals at 69, 119 and 169 are present in all of the spectra in virtually the same intensity ratio and can therefore be assigned to the unreacted C_3F_8 modulated to a minor extent by the fragmentation patterns of C_2F_6, C_3F_8 and maybe some C_4F_{10} produced in the plasma. Consequently, a small part of the signals at 100 and 150 a.m.u. are also attributable to these saturated species (Table 1). However, the most striking feature in going from the spectrum corresponding to the discharge off to any one of the spectra of the plasma effluent species is the large increase in unsanurated (taken here to include cyclic) structures at the overall expense of the saturated molecules. The relative intensities of these unsaturated species in the spectra in going from one cathode material to another is then a direct manifestation of the ability of the cathode material to interact with the plasma, to produce precursors to polymerization, and indeed, the intensity of the signals relating to unsaturated species is directly related to the polymer deposition rate. The new species may readily be assigned from a consideration of Table 1 and are as follows, where the most intense mass spectrometer fragmentation product is given with minor products in parentheses:

i) C_2F_4 $-C_2F_4^+$

ii) cyclo-C_3F_6 $-C_2F_4^+$ $(C_3F_5^+)$

iii) C_3F_6 $-C_3F_6^+$ $(C_2F_4^+)$

iv) cyclo-C_4F_8 $-C_3F_5^+$ $(C_2F_4^+, C_4F_7^+)$

v) C_4F_8 $-C_4F_8^+$ $(C_2F_4^+, C_3F_6^+)$

The major polymerizable products of the plasma can, therefore, be summarized as $(CF_2)_n$ which, as will be seen later, can be derived either directly from the injected 'monomer' by electron impact or from reactions involving tetrafluoroethylene and difluorocarbene formed as a consequence of the etching process, the latter mechanism being the more favorable. It is interesting to note that these observations

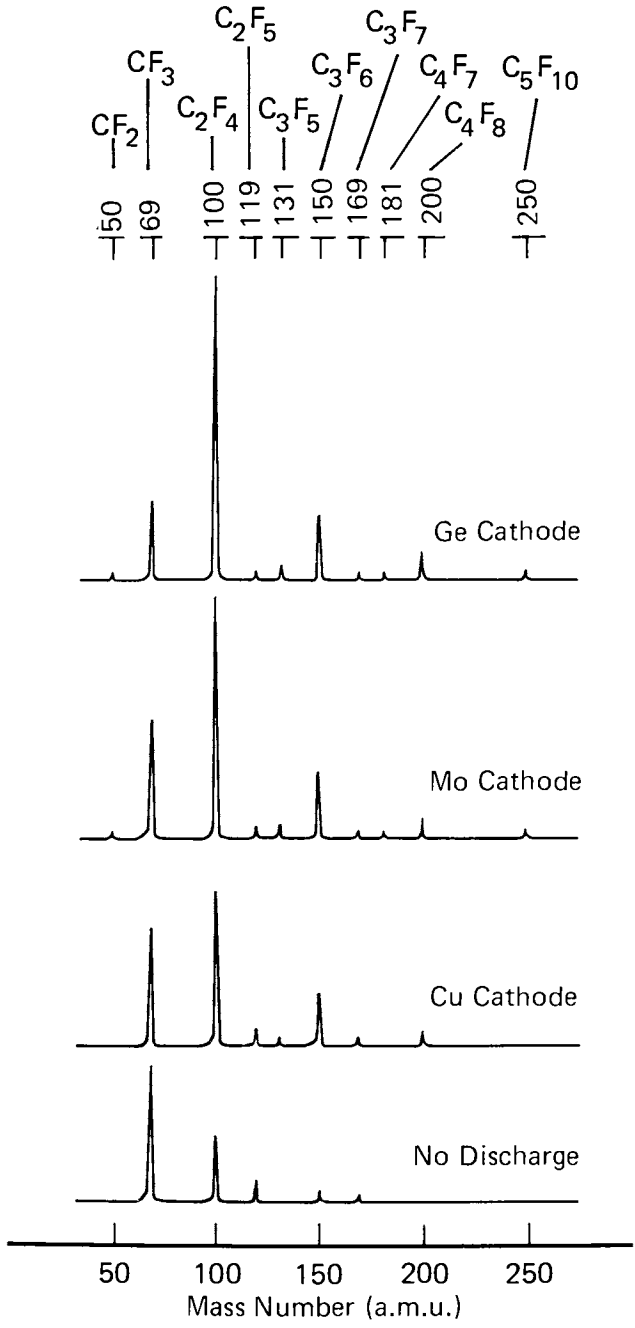

Figure 3. Mass spectra of the plasma effluent neutral species obtained with an electron impact ionization energy of ~ 15 eV

In Plasma Polymerization; Shen, M., et al.;
ACS Symposium Series; American Chemical Society: Washington, DC, 1979.

TABLE I

Calibration Data for the Mass Spectrometer. Signal Intensity (Appearance Potential)

Molecule	Ion (Mass) $C_2F_2^+$ 62	CF_3^+ 69	$C_2F_4^+$ 100	$C_3F_4^+$ 112	$C_2F_5^+$ 119	$C_3F_5^+$ 131	$C_3F_6^+$ 150	$C_3F_7^+$ 169	$C_4F_8^+$ 200	$C_4F_9^+$ 219
CF_4	0	0(15.5)								
C_2F_6	0	8(13.6)	0(20.7)		0(15.5)					
C_3F_8	0	51(13.2)	25(13.5)	0	7(13.3)	0	4	1(15.4)		
n-C_4F_{10}	0	32(13.2)	11	0	17(13.1)	0(15.7)	17	4(13.3)	0	0(15.4)
C_2F_4	0	0(13.7)	400(10.1)							
C_3F_6	0	0(15.0)	5(12.5)	0	0	0(14.8)	120(11.1)			
2-C_4F_8									(11.3)	
C_2F_2	(11.4)									
C_3F_4				(<15)						
△F		(15.4)	(11.9)			(14.1)				
□F		(15.7)	(12.3)			(12.3)				

from our work involving perfluoropropane injected into the plasma are qualitatively the same as those previously reported for in situ mass spectrometric analysis of plasmas excited in tetrafluoroethylene (3,12). The relatively long distance between the plasma and the mass spectrometer, in the present investigation, accounts for the fact that almost all of the difluorocarbene itself has reacted before reaching the point of analysis. Therefore, Figure 3 reveals only a small peak at 50 a.m.u. (CF_2^+) in the most favorable cases.

It should be noted that the conclusion, drawn here, that $(CF_2)_n$ species are the most important in the plasma polymerization of these perfluorinated 'monomers' is in contrast to that reported for hydrocarbon and fluorohydrocarbon systems where acetylenic species are thought to dominate (9,24).

Figure 4 shows the plasma effluent mass spectrum, on a logarithmic scale, of a Mo-C_3F_8 discharge (f=5 cm^3 min^{-1}, p=0.015 torr, w=100 watts) obtained employing a much higher electron impact energy (~70eV) in the spectrometer. With this high ionization energy the overall sensitivity of the instrument is considerably increased, although a larger degree of fragmentation of the analyzed species is evident. The presence of high molecular weight oligomers, however, is readily apparent, extending up to and presumably beyond the 300 a.m.u. mass limit of the spectrometer. At higher pressures carbon chains as long as C_{12} are observable. It is interesting to note that a tetrafluoroethylene discharge at the same pressure but much reduced power (~20 watts) produces an essentially identical spectrum in all respects above 170 a.m.u. This again emphasizes the similarity as far as products are concerned, between the C_2F_4 discharge and those employed here, involving C_3F_8 in an etching environment.

Mechanistic Aspects of Polymerization

Since we have already elaborated the likely mechanisms by which the inorganic material is incorporated into the polymer film, in an earlier section, the discussion here will be restricted to the plasma polymerization mechanism which is responsible for the formation of the organic phase. In the light of the data presented in this paper, it is clearly evident that the primary route to polymerization is via the formation of species with the general formula $(CF_2)_n$, for all of the systems discussed. The strong dependence of deposition rate, and the concentration of these unsaturated species in the gas phase, on the cathode material, confirms that the major origin of these primary precursors is derived from the etching process, although direct formation of these species by electron impact processes may also play a minor role. The mechanisms involved in the formation of these primary precursors are not well understood at this point in time and

In Plasma Polymerization; Shen, M., et al.;
ACS Symposium Series; American Chemical Society: Washington, DC, 1979.

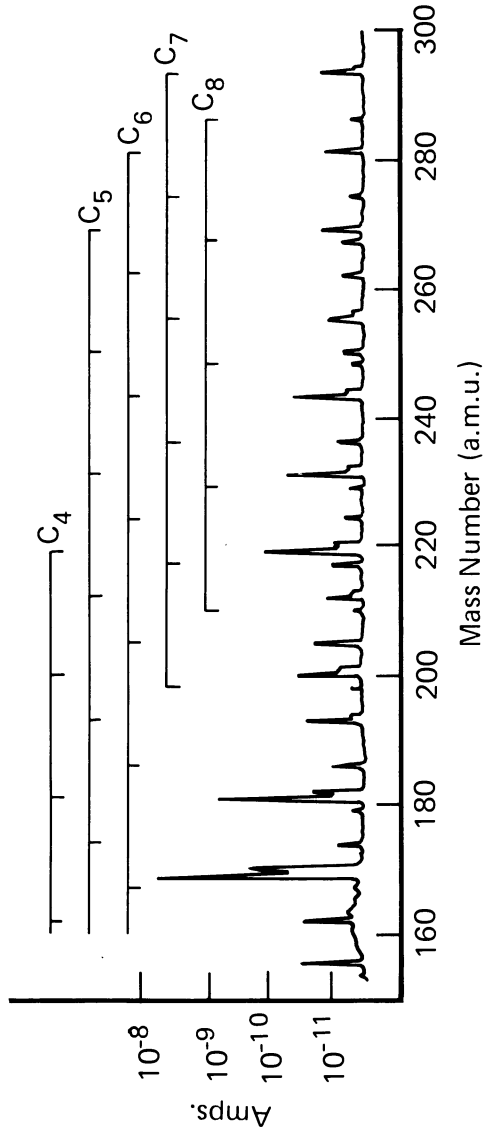

Figure 4. Mass spectrum of the plasma effluent neutral species of a Mo–C_3F_8 system obtained with an electron impact ionization energy of ~ 70 eV

it would, therefore, be inappropriate to attempt to speculate on them here. The fact that they do occur however is amply demonstrated by the plasma effluent mass spectrometric studies (Figure 3).

It has been stated (12) that in contrast to hydrocarbon based plasmas, fluorocarbon plasmas produce a high yield of gaseous products as well as polymer. This has been confirmed in this work by the observation of both low molecular weight species and higher molecular weight oligomers. Clearly any reaction scheme invoked must allow for homogeneous (gas phase) reactions as well as polymer production at a surface.

The low molecular weight primary precursors to polymerization of general formula $(CF_2)_n$ can be accounted for by the following well known reactions of $:CF_2$ and C_2F_4 (12,25,26).

i) $CF_2{=}CF_2 \overset{e^-}{\rightleftharpoons} 2{:}CF_2$

ii) $:CF_2 + CF_2{=}CF_2 \rightleftharpoons \triangle F^* \xrightarrow{M} \triangle F$

iii) $\triangle F^* \longrightarrow CF_3CF{=}CF_2$

iv) $CF_2{=}CF_2^* + CF_2{=}CF_2 \longrightarrow \boxed{F}^* \xrightarrow{M} \boxed{F}$

v) $\boxed{F}^* \longrightarrow (CF_3)_2C{=}CF_2$

vi) $\boxed{F}^* \longrightarrow CF_3CF{=}CF_2 + :CF_2$

Further gas phase oligomerization may well occur by addition of $:CF_2$ to C_3F_6, C_4F_8, etc., or by radical (or ionic) chain reactions of these species. Polymerization is likely to occur in a fashion analogous to conventional polymerization processes via homogenous or heterogeneous chain reactions of the primary precursors, $(CF_2)_n$, which include cyclic alkanes as well as mono-olefins. However, the relatively large concentration of available initiators and chain terminators in the plasma as well as the low pressure of the system will ensure that the chain lengths of these initial polymer products are relatively short. Since the overall fluorine/carbon stoichiometry of the final polymer products has been found to be somewhat less than 2, this polymerization process, involving $(CF_2)_n$, is almost certainly accompanied by a concomitant process involving the interaction of photons, ions and metastables with the forming polymer, to eliminate fluorine atoms (27). This latter process results in the formation of crosslinks, unsaturation and free radicals in the polymer structure. The unsaturated structures and free radical sites may further react with incoming lower molecular weight free radicals ($CF_3^{\cdot}$, $C_2F_5^{\cdot}$, oligomers, etc.) or may remain in the final polymer product.

In Plasma Polymerization; Shen, M., et al.;
ACS Symposium Series; American Chemical Society: Washington, DC, 1979.

Although this reaction scheme is largely speculative it is entirely consistent with all our findings with respect to both the mass spectrometric analysis of the plasma effluent and ESCA analysis of the polymer films, as well as the available data in the literature (3,12,25,26,27). The ESCA spectra of several plasma polymerized fluorocarbons have appeared in the literature, including those derived from, (in decreasing order of F/C stoichiometric ratio of the 'monomer'), tetrafluoromethane (28), hexafluoroethane (10), tetrafluoroethylene (8,10), perfluorocyclohexane, perfluorocyclohexene, perfluorocyclohexa 1,3 and 1,4 dienes and perfluorobenzene (7). It is generally the case that while the polymers derived from fluorocarbons of $F/C<2$ have structures containing greater amounts of CF structural features (7), those derived from fluorocarbons of $F/C\geq2$ exhibit spectra which are closely related to each other (8,10,28), and are, indeed, very similar to the spectra displayed in Figure 2 for the polymers discussed in this paper. Since difluorocarbene has been previously inferred to play a central role in the plasma chemistry of tetrafluoroethylene (12,29), it seems likely that the involvement of $(CF_2)_n$ species is also prominent in the plasma polymerization of the other fluorocarbons of $F/C\geq2$. In a subsequent paper (30) we shall demonstrate that this is indeed the case, in an investigation of metal containing polymers produced in plasmas excited in the series of perfluoroalkanes; C_nF_{2n+2} $(n=1,2,3,4)$.

Acknowledgments

Thanks are due to IBM Corporation for granting a one-year research fellowship to one of the authors (A.D.) and to A. P. Poenisch for his technical skills in the construction of the reactor system employed in this work.

ABSTRACT: The synthesis of metal containing fluorocarbon films by simultaneous chemical plasma etching and/or physical sputtering together with polymerization in the same system is described. A comparison is drawn between germanium, molybdenum and copper as the cathode material using perfluoropropane as the plasma medium. The polymer films are characterized by X-ray photoelectron spectroscopy, and it is found that while germanium is not incorporated into the polymer, molybdenum and copper are, (~20% and ~14% by weight respectively) although the mechanisms of transference of these metals from the cathode surface to the polymer must be different. Although the polymer deposition rate is strongly dependent on the cathode material, the structure of the polymer is the same in all cases, and is also the same as that derived from plasma polymerization of tetrafluoroethylene as well as a number of other perfluorinated 'monomers'. This is rationalized by a consideration of the mass spectrometric analysis of the major low molecular weight products in the plasma effluent which are observed to be multiples of [CF_2], thus providing strong evidence that the primary precursors to polymerization, in the systems discussed, as well as fluorocarbons in general with an effective fluorine/carbon ratio not less than two, are difluorocarbene and tetrafluoroethylene.

In Plasma Polymerization; Shen, M., et al.;
ACS Symposium Series; American Chemical Society: Washington, DC, 1979.

Literature Cited

1. Eric Kay, A. Dilks and U. Hetzler, J. Macromol. Sci.-Chem., submitted (1978).

2. J. W. Coburn and Eric Kay, IBM J. Res. Develop., submitted (1978).

3. Eric Kay, J. W. Coburn and G. Kruppa, Le Vide, 183, 89 (1976).

4. D. T. Clark in, "Advances in Polymer Friction and Wear," Vol. 5A, Ed. L. H. Lee, Plenum Press, New York (1975).

5. D. T. Clark in, "Advances in Polymer Science," Springer-Verlag, Berlin (1977).

6. A. Dilks in, "Electron Spectroscopy. Theory, Techniques and Applications," Vol. 4, Ed. C. R. Brundle and A. D. Baker, Academic Press, in preparation (1978).

7. D. T. Clark, A. Dilks and D. Shuttleworth in, "Polymer Surfaces," Ed. D. T. Clark and W. J. Feast, J. Wiley and Sons, London, in press (1978).

8. D. W. Rice and D. F. O'Kane, J. Electrochem. Soc., 123, 1308 (1976).

9. D. T. Clark and D. Shuttleworth, J. Polym. Sci., Polym. Chem. Edn., in press (1978).

10. H. Yasuda, J. Macromol. Sci.-Chem., A10, 383 (1976).

11. M. M. Millard and A. E. Pavlath, J. Macromol. Sci.-Chem., A10, 579 (1976).

12. M. J. Vasile and G. Smolinsky, J. Phys. Chem., 81, 2605 (1977).

13. J. W. Coburn and Eric Kay in, "Proc. 7th Int. Vac. Cong. 3rd Int. Conf. Solid. Surf." Vol. 2, Ed. R. Dobrozemsky, et al., Vienna (1977).

14. D. T. Clark, A. Dilks, H. R. Thomas and D. Shuttleworth, J. Polym. Sci., Polym. Chem. Edn., in press (1978).

15. U. Hetzler and Eric Kay, J. Appl. Phys., in press (1978).

16. K. S. Kim, W. E. Baitinger, J. W. Amy and N. Winograd, J. Elect. Spec., 5, 351 (1974).

In Plasma Polymerization; Shen, M., et al.;
ACS Symposium Series; American Chemical Society: Washington, DC, 1979.

17. D. T. Clark and D. Shuttleworth, J. Polym. Sci., Polym. Chem. Edn., 16, 1093 (1978).

18. J. W. Coburn, unpublished results.

19. J. W. Coburn, E. Taglauer and Eric Kay, Jap. J. App. Phys., Suppl., 2, 501 (1974).

20. P. E. Larson, J. Elect. Spec., 4, 213 (1974).

21. N. S. Nikolaev, S. V. Vlasov, Y. A. Buslaev and A. A. Opalovskii, Izv. Sibirzk. Otd. Akad. Nauk. SSSR, 47 (1960).

22. A. Diaz, A. Dilks, K. K. Kanazawa and Eric Kay, in preparation (1978).

23. H. M. Rosenstock, K. Draxl, B. W. Steiner and J. T. Herron, "Energetics of Gaseous Ions," ACS and AIP publication, New York (1977).

24. H. Kobayashi, A. T. Bell and M. Shen, Macromols., 7, 277 (1974).

25. S. V. R. Mastrangelo, J. Amer. Chem. Soc., 84, 1122 (1962).

26. J. R. Dacey and J. G. F. Littler, Can. J. Chem., 47, 3871 (1969).

27. D. T. Clark and A. Dilks, J. Polym. Sci., Polym. Chem. Edn., 16, 911 (1978), and references therein.

28. V. Minkiewicz, T. C. Chen and W. Lee, IBM J. Res. Develop., submitted (1978).

29. H. Kobayashi, M. Shen and A. T. Bell, J. Macromol. Sci.-Chem., A8, 1345 (1974).

30. A. Dilks, Eric Kay and D. Seybold, in preparation (1978).

RECEIVED March 29, 1979.

13

Plasma-Polymerized Organosilicon Thin Films—Structure and Properties

M. KRYSZEWSKI, A. M. WROBEL, and J. TYCZKOWSKI

Centre of Molecular and Macromolecular Studies, Polish Academy of Sciences, 90-362 Lódz, Poland

Numerous recent developments in advanced technology have drawn attention to thin films produced by low temperature plasma polymerization. One of the outstanding advantages of plasma polymerization for preparation of thin polymer films is the wide variety of organic compounds that may be polymerized by this technique eg. monomers which do not polymerize using conventional methods. Among the numerous monomers which have been used in plasma polymerization the organosilicons were found to form films of unique properties. The plasma polymerized organosilicon films show: a) high thermal stability (1,2), b) high dielectric constant (3), c) outstanding optical properties which may be utilized in conventional and integrated optics (4), d) they may be applied as protective coatings for many materials and as dielectrics in microelectronics. The mechanism of formation of those films and their structure are very complex due to many elementary reactions taking place in a glow discharge. These films are insoluble in common solvents due to the high degree of crosslinking; thus to characterize their structure complex methods must be used.

Preparation of thin films by plasma polymerization of organosilicons and especially of organosilazanes and

0-8412-0510-8/79/47-108-219$05.00/0

some aspects of the mechanism of these reactions were discussed in our previous papers (5-7). The aim of this paper was to study the structure and crosslinking mechanism of polymers obtained by low temperature plasma polymerization of hexamethylcyclotrisilazane (HMCTSN) and of hexamethylcyclotrisiloxane (HMXTSO) as well as some problems related to the changes of their structure due to thermal treatment.

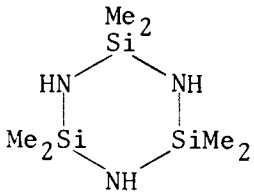

HMCTSN

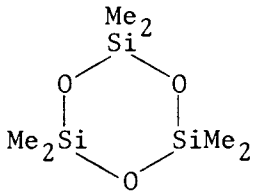

HMCTSO

The present paper reports also some results of d.c. conductivity studies of films obtained from some monomers and especially from HMCTSN. The investigations seem to be a step in the attempts to reach a correlation between the structure of these thin films and their electrical properties.

Complex reactions occuring during glow discharge polymerization lead to the formation of materials which should not be simply called polymers obtained from given monomers; it would be more appropriate to use the expression: plasma-polymerized hexamethylcyclotrisilazane etc. for other monomers but for the sake of simplicity the terms polysilazanes and polysiloxanes will be used in this paper.

EXPERIMENTAL

Hexamethylcyclotrisilazane and hexamethylcyclotrisiloxane were purified by rectification in vacuum following which their purity was tested by gas chromatography. Plasma polymerizations were carried out in an electrode system described previously (5). Thin film were deposited in a 20 kHz glow discharge on the surface of stainless steel electrodes or on gold or silicon electrodes in the case of thin layers intended for further studies of electrical properties. All polymerizations were carried out at constant discharge parameters: current density $j = 1\ mA/cm^2$, discharge duration $t = 30$ sec, monomer vapour pressure $p = 0.3$ Torr.

In Plasma Polymerization; Shen, M., et al.;
ACS Symposium Series; American Chemical Society: Washington, DC, 1979.

For further analytical investigations 0.2 mg polymer samples were removed from electrodes and pyrolysed in a Jeol pyrolyser unit, Model 727. Pyrolyses were carried out in a helium atmosphere at a temperature of 400° C for 30 sec. The volatile pyrolysis products were fed directly to the injection part of a Jeol gas chromatograph, Model JGC 1100, equipped with a flame ionization detector; the apparatus incorporated a 2.5 m x 2 mm stainless steel separation column filled with OV 101 10 % supported on Varaport 80/100 mesh. The volatile pyrolysis products, isolated by gas chromatography, were analysed using a LKB mass spectrometer,Model 2091, equipped with a PDP11 computer. Mass spectrometric analyses were carried out with an electron beam energy of 70 eV.

Studies of the electrical properties of thin polymer films were carried out in a standard electrometric system. The films under investigation were prepared under the same conditions as those used for their structure studies. They were prepared on the surfaces of different vacuum deposited metal electrodes or on the surface of Si-single crystals. The appropriate upper electrode was vacuum deposited on the surface of a thin polymer layer. Film thickness was determined by double beam interference method.

RESULTS AND DISCUSSION

Structure of Polymer Films. Previous studies of plasma-polymerized organosilicon films have shown that their chemical structure is very complex (6-13). In order to obtain more detailed information about the chemical structure of these films, they were examined using combined analytical techniques of pyrolysis-gas chromatography-mass spectrometry (PGCMS).

Gas chromatograms of volatile pyrolysis products formed from plasma-polymerized HMCTSN and HMCTSO are shown in Figs. 1 and 2, respectively. They were identified by mass spectrometry and with the aid of certain standard compounds. For the sake of brevity it is not possible to discuss the mass spectra here. The structures of pyrolysis products corresponding to the respective chromatographic peaks are presented in Table I for both polymers. It should be noted that the peaks marked by X (Figs. 1 and 2) correspond to unseparated mixture of light hydrocarbons. As can be seen from Table I, the pyrolysis products in the case of both polymers consist of low molecular cyclic organosilicon compounds.

In Plasma Polymerization; Shen, M., et al.;
ACS Symposium Series; American Chemical Society: Washington, DC, 1979.

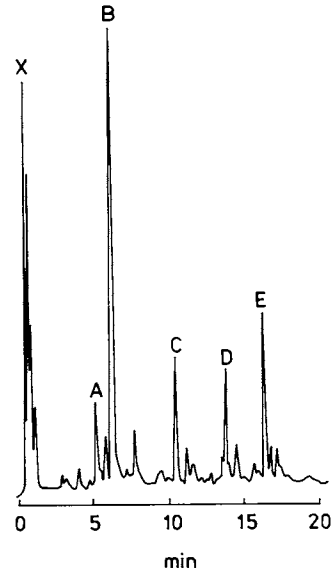

Figure 1. Gas chromatogram of the volatile cyclic products of pyrolysis at 400°C of plasma-polymerized hexamethylcyclotrisilazane

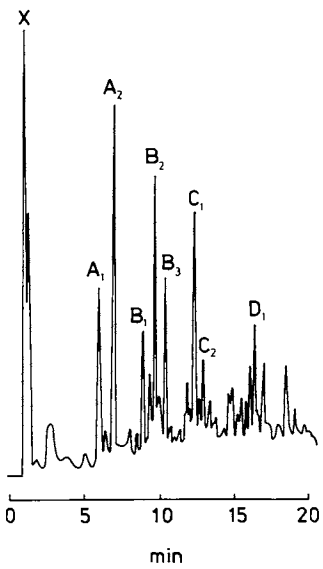

Figure 2. Gas chromatogram of the volatile cyclic products of pyrolysis at 400°C of plasma-polymerized hexamethylcyclotrisiloxane

In Plasma Polymerization; Shen, M., et al.;
ACS Symposium Series; American Chemical Society: Washington, DC, 1979.

TABLE I. Composition of the volatile products of pyrolysis at 400°C of plasma polymerized cyclic organosilicones.

Polymer	Pyrolysis products
Plasma polymerized hexamethylcyclotri-silazane	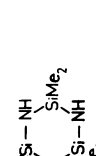 A 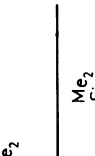 B 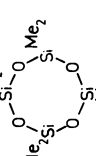 C 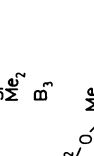 E
Plasma polymerized hexamethylcyclotri-siloxane	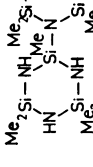 A_1 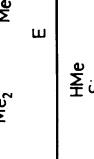 A_2 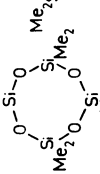 B_1 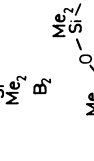 B_2 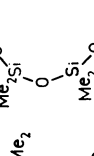 B_3 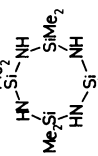 C_1 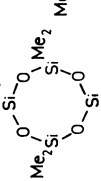 C_2 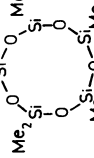 D_1

Our earlier studies (7) have shown that plasma polymer formed from HMCTSN, under similar conditions as in the present work contained few percent of a soluble fraction having almost identical composition as its pyrolysis products. It may be concluded that the compounds listed in Table I are formed by plasma conversion of monomer molecules in the gas phase, and that these are then incorporated into polymer film during its growth. These oligomeric compounds are liberated from the polymer during pyrolysis. In order to confirm this conclusion, similar PGCMS examinations have been carried out following ectraction of the polymers in boiling carbon tetrachloride. It was found that these products disappear in the case of extracted polymers.

Among the pyrolysis products of plasma-polymerized HMCTSN we found monomer (B), its oxy-derivative (A), octamethylcyclotetrasilazane (C) and bicyclic dimer (E) (Fig. 1 and Table I). It was difficult to identify the structure of compound D, but on the basis of mass spectrometric data we speculate that it is an unstable product formed by ammonia elimination from the dimer molecule.

The presence of octamethylcyclotetrasilazane and bicyclic dimer in the pyrolysis products strongly suggests that at least two competitive reactions take place during plasma polymerization of HMCTSN namely, ring enlargement and dimerization. However, dimerization seems to be predominant and it is considered to be the first step of reaction leading to polymer formation. A scheme for bicyclic dimer formation from HMCTSN under plasma conditions has been proposed in our previous paper (7). According to this scheme, formation of new Si-N bonds with tertiary nitrogen between trisilazane rings leads to crosslinking of the polymer, and involves the production of hydrocarbons such as methane and ethane. Indeed, gas chromatographic analysis of the gaseous residue after plasma polymerization has shown that it consists mainly of three hydrocarbons : methane, ethane and ethylene in the 5:33:4 ratio.

The presence of multimembered cyclic organosiloxanes in the pyrolysis products of plasma-polymerized HMCTSO (Fig. 2 and Table I) indicates that siloxane ring-opening reactions play a fundamental role in this polymerization process. In this case, 12 membered cyclic dimer (D_1) may be formed only through bimolecular reaction, proceeding with a cleavage of Si-O bonds in the monomer molecules. Regarding the presence of SiH groups in the compounds A_1,B_1,B_2 and C_1, one may conclude that under plasma conditions abstraction of methyl groups from silicon, and hydrogen from carbon,

In Plasma Polymerization; Shen, M., et al.;
ACS Symposium Series; American Chemical Society: Washington, DC, 1979.

takes place. These results agree with infrared spectrum of the polymer which displays a distinct absorption band due to SiH group at 2130 cm^{-1}. The abstraction of methyl groups from silicon atoms appears to be a basic process in plasma polymerization of organosilicon compounds. The absence of products of higher molecular weight than those corresponding to bicyclic silazane and cyclic siloxane dimers, suggests that their formation is less probable. This is in agreement with the results of other authors (14) who found structures no higher than dimeric during plasma polymerization of styrene.

Our earlier structural studies (15) have shown that in the case of plasma-polymerized HMCTSN and HMCTSO other crosslinking reactions may take place. Ultraviolet radiation emitted by the plasma may cause a homolytic cleavage of Si-C and C-H bonds in $SiCH_3$ groups, followed by crosslinking in the polymer via formation of methylene and ethylene linkages between silicon atoms.

On the basis of these results one can conclude that plasma polymerization of HMCTSN proceeds via cleavage of Si-C and N-H bonds and formation of new Si-N bonds. Polasma polymerization of HMCTSO occurs by ring-opening reactions and new Si-O bonds are formed via complex reactions. The cleavage of $SiCH_3$ groups is of importance and crosslinking in both polymers may take place through formation of methylene and ethylene bridges between Si-atoms.

One could write a number of reactions which may lead to the formation of structures or groups observed in the polymer films. This has been done by some authors (13). The quantitative correlation between the concentration of particular groups, as detected by the analytical methods, and the reaction scheme requires a knowledge of the rate constants of particular reactions which in the actual state of plasma polymerization, due to the complex mechanisms, are byond a real experimental access and therefore will not be given here.

Thermal Properties. The high thermal stability of plasma-polymerized HMCTSN films (2,16) and their relatively low content of organic structure (6), suggested that they may be transformed by an appropriate pyrolytic process into new materials of almost completely inorganic structure and of considerably higher thermal stability. Our detailed studies (17) have shown that pyrolysis leads to significant changes in the chemical structure of these films. This process gradually eliminates the carbon and hydrogen containing groups from the polymer film while an inorganic material of Si_xN_y type is formed. Following such thermal modification

In Plasma Polymerization; Shen, M., et al.;
ACS Symposium Series; American Chemical Society: Washington, DC, 1979.

plasma-polymerized HMCTSN films were found to be colourless, glassy materials with extremely strong adhesion to the metal substrate (16). They displayed excellent resistance to corrosive agents.

It is interesting to note that pyrolysis of films formed by plasma polymerization of HMCTSO involved significant deterioration in film adhesion to the metal substrate.

Electrical Properties. The electrical properties of thin polymer films obtained by glow discharge from a variety of monomers have been discussed in a number of papers (18,19,20). In recent years more and more attention has been paid to the electrical properties of plasma-polymerized organosilicon films (3,21,22,23, 24), the expectation being that they can find application in electronics, e.g. as a passivation coatings of semiconductor surfaces (3). It has also been shown that heat-treatment of organosilicon polymers gives riese to basic changes in their structure which, in view of the current search for a correlation between the electrical properties of thin dielectric polymer films and their structure, creates understandable interest.

The first step to the understanding of the electrical properties of any polymer is to determine what kind of carriers are responsible for charge transport. In the case of typical polymers obtained by conventional methods the contribution of the ions as basic charge carriers can, in most cases, be neglected. In the case of polymers obtained by the glow-discharge process the presence of ion structures is much more likely. An analysis of the capacitance - voltage (C-V) characteristics of polysiloxane in the silicon-polymer-metal system has shown that in addition to an electron component of electrical conductivity there is also an ion component (23). When a stationary external field of $+2 \times 10^8$ V/m was applied to a metal electrode in the Si-polysiloxane-Au system, the successively recorded C-V characteristics kept shifting, and did not attain a stationary value until after a few hours. This effect was attributed to accumulation at the Si-polysiloxane contact of positive ions which drift away from the sample under the influence of the stationary field. The time required for equilibrium to be reached is taken to be the time which the ions located at the greatest distance from the Si-polymer contact take to reach it, i.e. the ions which initially were at the Au-polymer contact. On this basis ion mobility was estimated to be 10^{-16} cm^2/Vs. The hysteresis cycles observed on the C-V characteristics, on the other hand, were attributed to the electrons aggregating at the silicon-polysi-

In Plasma Polymerization; Shen, M., et al.;
ACS Symposium Series; American Chemical Society: Washington, DC, 1979.

loxane contact. Electrons exhibit a much higher mobility than positive ions. Electron mobility was estimated from C-V characteristics obtained from the samples studied after they had been polarized in high electric field. A pulse voltage of variable amplitude was applied to the film, the value of the voltage being selected in such a way as to obtain the maximum and minimum capacitance values on the curves characterizing the C-V hysteresis of the system under study for the smallest voltage of the pulse applied. This corresponds to a transfer of the electrons accumulated at one contact to the other. The mobility values estimated in this way are 3×10^{-10} cm^2/Vs.

By analyzing the C-V characteristics one can estimate the density of the charge stored at the Si-polysiloxane contact (3); for a "virgin" contact the charge density was estimated to be $10^{11} - 5 \times 10^{11}$ cm^{-2}. As the external applied field kept acting on it the above value increased quite considerably. Minimization of that parameter could play a decisive role if polysiloxane were applied to passivation of silicon surfaces. It has been found that heat-treatment of the contact under nitrogen up to about 450° C, i.e. still below the pyrolysis temperature, brings about a stabilization of the charge density value at 10^{11} cm^{-2} and external field affects in only to a very small extent. Also, the shifting of the C-V curve during polarization with stationary external field decreases distinctly which suggests that the density of ion structures decreases as a result of heat treatment.

Ionic conductivity affects the electron conductivity. Aggregating at the negative electrode the positive ions lower the contact barrier and thus increase electron injection. Observing the polarization curve of a polysiloxane sample in a metal-polymer-metal system over a period of time one can see the appearance of a minimum from which point the current begins to rise until it reaches a statnionary value (21,22). A similar curve can be observed in the case of thin polysilazane films (25). The effect can be accounted for by overlapping of ionic polarization currents and increasing injection from the electrode. Polarization of the sample under a pressure of 2000 bar leads to the formation of a polarization curve of a similar character, but its minimum is shifted towards longer times, and the current values are initially about 3 times smaller than those obtained under a pressure of 1 bar, regardless of the magnitude of the applied field (21). It is only after a prolonged period of time that the current flowing across the sample under pressure becomes larger than

In Plasma Polymerization; Shen, M., et al.;
ACS Symposium Series; American Chemical Society: Washington, DC, 1979.

the current recorded under atomspheric pressure, which is to be expected for systems where electron conductivity dominates. The above effects are attributed to decreased ion mobility due to steric phenomena. Thus, because of the pressure the initially dominant ionic conductivity decreases and the time it takes for the barrier to be modified in such a way that electron conductivity becomes the dominant one increases.

After a suitably long polarization, when stationary currents are attained, ionic conductivity virtually ceases to exist, and the current observed is taken to be of an entirely electronic nature. It has to be remembered, however, that there remain in the sample ions aggregated at the negative contact which may modify the barrier.

Determination of the sign of the carriers responsible for the electronic conductivity in thin polymer films constitutes a separate problem. The classical methods of differentiating between holes and electrons in inorganic semiconductors, such as measurement of the Hall effect, or measurement of the thermoelectric force, are inapplicable to thin polymer films, but some conclusions can nevertheless be reached by studying the electrical properties. As has already been said, an analysis of C-V curve for the silicon-polysiloxane-metal system has shown that the charge carriers in polysiloxane are electrons.On the other hand, photoconductivity measurements in plasma-polymerized styrene conducted by Morita and Shen (26) in new Au-polystyrene-Au samples that had not been exposed to air have been interpreted on the assumption of the hole character of conductivity. This was taken to be due to the high concentration of free radicals in the polystyrene film, which exhibit high electron affinity and thus act as acceptor centres. ESR spectra for new thin polysiloxane films obtained by plasma polymerization of octamethyltrisiloxane also point to a high concentration of free radicals (of the order of 2×10^{16} spin/g) (27). Thus, in accordance with the ideas of Morita and Shen hole conductivity can also be expected in polysiloxanes.

When samples of plasma polymers are exposed to air the concentration of free radicals decreases. In the case of polysiloxane there is initially a rapid drop of free radical concentration to reach a steady level of 4×10^{15} spin/g after ca. 30 hours (27). The quenching of radical states in polystyrene manifests itself in increased photosensitivity threshold from 1.6 eV for a fresh sample to 2.1 eV for a sample exposed to air for 1 nour (26). Also in this case is the hole conductivity postulated, where holes are generated as a

In Plasma Polymerization; Shen, M., et al.;
ACS Symposium Series; American Chemical Society: Washington, DC, 1979.

result of optical activation of the electrons to trapping states of the kind that arise due to radical oxidation. However, similar studies carried out for thin polystyrene films in a Au-Ps-Al system show that the conductivity is dominated by electrons supplied to the sample as a result of photoinjection from the Al electrode.

Apart from the determination of the sign of the electronic carriers responsible for the conductivity in thin plasma polymer films, of great importance is also the establishment of the conductivity mechanism and its relation to the molecular and supermolecular structure of the polymer films. Current flow across a thin polymer film consists of: a) - generation process during which charge carriers appear in the polymer film and b) - carrier transport in the sample. The transport processes are related exclusively to the volume of the polymer film under study, while the generation phenomena take place either in the sample as a result of dissociation of donor or acceptor centres (Poole-Frenkel process), or at the contact, where carriers are injected from the electrode across the contact barrier (Schottky or Fowler-Northeim processes). In spite of the fact that the basic mechanisms of the above processes differ considerably (28) they are not always easy to distinguish, and analysis of the current-voltage (j-V) and current-temperature (j-T) characteristics, frequently employed as a criterion for differentiating between those mechanisms, is certainly not sufficient.

Attempts have recently been made to determine the dominat electric conductivity mechanism using the results of measurements of the current flow across asymmetric systems, such as $metal_1$-polymer-$metal_2$ (Me_1-P-Me_2) and metal-polymer-semiconductor (M-P-S); such studies involved plasma-polymerized styrene (29), siloxane (21) and silazane (24). The possibility of tunneling through the polymer film was excluded since its thickness considerably exceeded the 100 Å, i.e. the maximum thickness at which tunnelling has ever been observed (30) and the j-T characteristics obtained were of a typically activating character.

The possibility of space charge limited transport was verified by measuring the dependence of the conducting current on film thickness. That this mechanism does make a contribution could, in accordance with the SCLC theory (31), follow from the second branch of the lnj-lnV characteristics where $n \geqslant 2$ (Fig. 3). However, in no case do the results obtained confirm the $j \sim d^{-n}$ dependence required by the SCLC theory, where d is film thickness, and n - a parameter depending on trap distri-

In Plasma Polymerization; Shen, M., et al.;
ACS Symposium Series; American Chemical Society: Washington, DC, 1979.

bution, $n \geq 3$. In the case of polysiloxane the above dependence cannot be precisely established becauese of excessively large scatter of the measuring points. On the other hand, the results obtained for both polystyrene and polysilazane satisfy the Poole-Frenkel and Schottky equations quite well ($\ln j \sim d^{-1/2}$) (28). Our recent results of high-field conductivity (up to 4×10^8 V/m) performed on plasma-polymerized hexamethyldisilazane showed a third branch on the $\ln j$-$\ln V$ plot, for which $n >> 2$ (Fig. 3). It is useless, however, to look in this case for the thickness dependence of the conducting current in order to eliminate SCLS. It was shown, by means of numerical computation, that for such high fields even Schottky or Poole-Frenkel currents plotted in $\ln j$-d^{-n} coordinates yield a dependence, which can be approximated by a straight line with $n > 3$, which in turn is expected for space charge limited currents (25). However the second and the third branches of $\ln j$-$\ln V$ plot for this polymer merge into one straight line when replotted in $\ln j$-$V^{1/2}$ coordinates, thus suggesting that also the third branch may be due to the same process, i.e. Schottky or Poole-Frenkel. It can thus be assumed that one of these two mechanisms does play a decisive role in the electric conductivity of the films under discussion. However, it is not easy to distinguish between the two mechanisms, especially in the case of polymer systems. The simplest test, usually applied to crystal semiconductors, is the comparison of experimental coefficients β determined form the slope of the linear part of the j-V characteristic drawn in the $\ln j$ - $V^{1/2}$ system with theoretical values of that coefficient (the values of the coefficient are collected in Table II; the theoretical values were calculated for dielectric constant $\varepsilon = 3.5$).

Table II. The values of coefficients β obtained from experiments and calculated according to Schottky and Poole-Frenkel mechanisms.

Plasma-Polymerized:	β_{exp}	$\beta_{Schottky}$	$\beta_{Poole-Frenkel}$
	x 10^5 eV(m/V)$^{1/2}$		
Styrene (29) Hexamethyldisiloxane(21) Hexamethyldisilazane(25) Hexamethylcyclotrisilazane(24)	2.4 1.8 2.3±0.4 1.7±0.3	2.03	4.06

In Plasma Polymerization; Shen, M., et al.;
ACS Symposium Series; American Chemical Society: Washington, DC, 1979.

It follows (Table II) that the experimental values are in good agreement with the theoretical assumptions of the Schottky mechanism. However, this cannot be treated as a definite solution, if only because of the fact that in some cases $\beta_S = \beta_{P-F}$ (32,33), and in simple models values of the coefficient differ by a factor of 2 only, which is insufficient for unequivocal differentiation between the two mechanisms.

In view of the above, conductivity measurements were conducted in asymmetric systems: Au-polymer-Si for polystyrene and polysilazane, and Au-polymer-In for polysiloxane. The difference in barrier height between Au-polymer and Si-polymer estimated on the basis of measurements of the Au-Si barrier is ca. 0.5 eV (34) which, in the case of the conductivity limited by the electrodes, should produce a difference in the intensity of the currents of opposite polarizations equal to about 8 orders of magnitude. The difference in work function of Au and In, on the other hand, is ca. 1 eV so, on the assumption of the Schottky mechanism of conductivity, the difference in the intensity of opposite polarizations should amount to 17 orders of magnitude (35). As can be seen in Fig. 4 in the case of an asymmetric polysilazane sample there is a difference in the intensity of the currents; although this difference does take the expected course, it is several times smaller than expected, and is thus virtually negligible. A similar result was obtained for the polystyrene sample, while in the case of the asymmetric system based on polysiloxane there was no difference in the intensity of the opposite-biassed fields over the entire range of fields used - up to 3×10^8 V/m. It can thus be assumed that the conductivity in the films under study is dominated by the Poole-Frenkel volume generation independent of the contact effects. Such were also the conclusions of the workers who studied the conductivity in polystyrene (29) and polysiloxane (21).

A more searching analysis of the Poole-Frenkel mechanism performed for polysiloxane on the basis of the Hill model (36) showed that charge carrier emission should proceed from the isolated Coulomb centre and should take place in the hemisphere related to that centre. The depth of the centres, determined form the activation dependence of the temperature, was E_A = = 0.76 eV.

It has been shown recently that the presence of Poole-Frenkel centers in the sample should lead to the appearance in TSC spectra of peaks for which the temperature T_m corresponding to their maxima are electrical field strenght-dependent according to the following

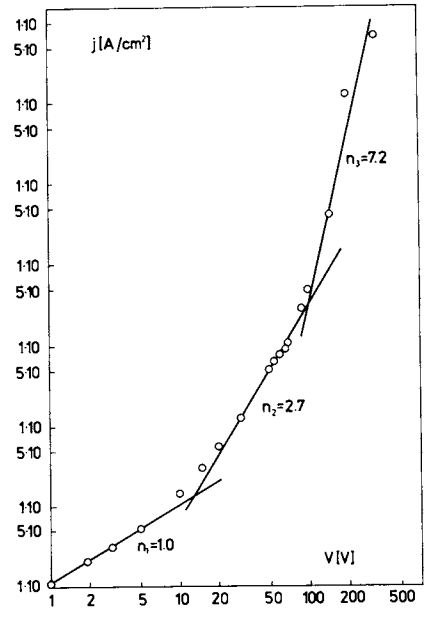

Figure 3. Current–voltage characteristics for plasma-polymerized hexamethyldisilazane (film thickness 0.87 μm)

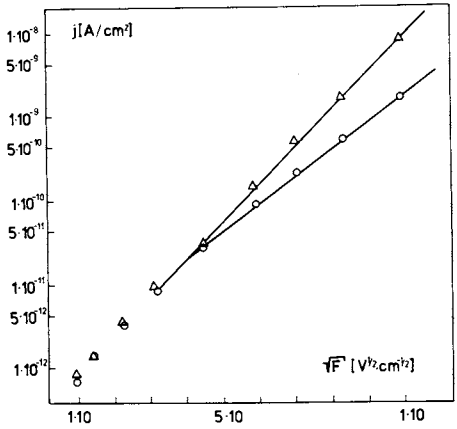

Figure 4. Schottky plot for asymmetric system Au–poly(hexamethylcyclotrisilazane)–Si; (△) Au electrode positive, (○) Au electrode negative.

In Plasma Polymerization; Shen, M., et al.;
ACS Symposium Series; American Chemical Society: Washington, DC, 1979.

relation T_m - $F^{1/2}$ (37). The experimentaly obtained TSC spectra in polysilazane measured in the field range of 10^6 - 10^8 V/m did not show field dependent maxima. These results enabled us to exclude the presence of Poole-Frenkel centers in the investigated films giving a strong argument against the opperation of the Poole-Frenkel mechanism of conductivity in polysilazanes. This leads to a reconsideration of the significance of the Schottky mechanism. The results of current density studies in samples supplied with asymmetric electrodes mentioned above did not confirm its importance unequivocally, but assuming the existence of surface states one has to take it into account. In fact, Mizutani at al. (38) have shown that the barrier hights at the metal-polymer contacts as estimeted by photoinjection for two differen metals may differ only by 0.07 eV, while theoretical predictions are 1.1 eV. This disappearance of the barrier hights difference is related to the surface states. Similar effects may be expected in the case of polysilazane films. Measurements of thermal activation energies in the system Au-polysilazane-Si for opposite biased fields have shown a small but distinct difference: for polarization of +50 V E_A = 0.980 ± ± 0.005 eV and for polarization of -50 V E_A = 1.01 ± ± 0.01 eV. These differences are similar to those reported in (38). These results seem to show that for polysilazanes - in the range of the investigated film thicknesses and field strengths - injection from electrodes dominates when considering the role of surface states.

It would be interesting to obtain actual systems with asymmetric contact barriers on polymer. It seems that heat treatment or plasma modification by chemically active gases may lead to such systems from plasma polymers. One could expect for such systems an increase of the activation energy difference for two opposite polarizations of the film.

ABSTRACT

The chemical structure of thin films formed by plasma polymerization of hexamethylcyclotrisilazane (HMCTSN) and hexamethylcyclotrisiloxane (HMCTSO) was studied. The investigations were carried out using combined techniques of pyrolysis - gas chromatography - mass spectrometry. The results showed that the pyrolysis products of highly crosslinked plasma polymers contained low-molecular weight compounds trapped in the

In Plasma Polymerization; Shen, M., et al.;
ACS Symposium Series; American Chemical Society: Washington, DC, 1979.

polymer film during its growth. The distinct difference between the structure of the pyrolysis products of both polymers showed silazane and siloxane monomers to undergo polymerization according to two different mechanisms. It was found that heat treatment of plasma-polymerized HMCTSN films leads to the formation of thermally stable materials of almost inorganic structure. D.C. conductivity and thermally stimulated currents examinations showed that Schottky effects were of importance for the elucidation of the electrical conductivity mechanism of plasma polymer films.

In Plasma Polymerization; Shen, M., et al.;
ACS Symposium Series; American Chemical Society: Washington, DC, 1979.

LITERATURE CITED

1. Tuzov L.S., Kolotyrkin V.M. and Tunitskij N.N., Vysokomol.Soed., (1970) A12,849.
Tkatschuk B.W., KolotyrkinV.M. and Smetankina N.P., Vysokomol.Soed., (1970) A12, 1458.
2. Wróbel A.M. and Kryszewski M., Bull.Acad.Pol.Ser. Sci.Chim. (1974) 22, 471.
3. Maisonneuve M., Segui Y. and Bui A., Thin Solid Films, (1976) 33, 35.
4. Tien P.K., Riva-Senseverion S., Martin R.J. and Smolinsky G., Appl.Phys.Lett., (1974) 24, 547.
5. Wróbel A.M., Kryszewski M. and Gazicki M., Polymer, (1976) 17, 673.
6. Wróbel A.M., Kryszewski M. and Gazicki M., Polymer, (1976) 17, 678.
7. Gazicki M., Wróbel A.M. and Kryszewski M., J.Appl.Polym.Sci., (1977) 21, 2013.
8. Tkatschuk B.W., Bushin U.V., KolotyrkinV.M. and Smetanskina N.P., Vysokomol.Soed., (1967) A9, 2018.
9. Tkatschuk B.W., Koloryrkin V.M. and Kirey G.G., Vysokomol.Soed. (1968) A10, 585.
10. Vasile M.J. and Smolinsky G.J., J.Electrochem.Soc., (1972) 119, 451.
11. Denes F., Ungutenasu C. and Hajduc J., J.Europ. Polym.,(1970) 6, 1155.
12. Tkatschuk B.W. and Kolotyrkin V.M, "Formation of Thin Polymer Films from Gase Phase" Izd.Khimia, Moscow 1977.
13. Möller W. and Schmidt M., Beitr.Plasmaphys., (1977) 17, (2), 121.
14. Tiller H.J., Berg D., Herzberg D. and Dumke K., J.Macromol.Sci.Chem. (1977) A11, 547.
15. Wróbel A.M., Gazicki M. and Kryszewski M., IUPAC - Macromolecular Symposium, Taskent 1978.
16. Wróbel A.M. and Kryszewski M., IUPAC-International Round Table for Plasma Polymerization and Surface Treatment, Limoges 1977.
17. Wróbel A.M. and Kryszewski M., Polymer Preprints, (1978) 19, 521.
18. Bradley A. and Hammes P., J.Electrochem.Soc. (1963) 110, 15.
19. Mearns A.M., Thin Solid Films, (1969) 3, 201.
20. Pechonik H. and Seebacher G., Thin Solid Films, (1974) 38, 343.
21. Desbarax N., These de Doctorat, Universite Paul Sabatier, Toulouse, France 1975.

In Plasma Polymerization; Shen, M., et al.;
ACS Symposium Series; American Chemical Society: Washington, DC, 1979.

22. Desbarax N., Lacoste R., et Segui Y., Colloque "Phenomenes de vieillissement dans les dielectriques solides et methodes d'essais", Toulouse 1975.
23. Maisonneuve M., Segui Y. and Bui A., Thin Solid Films (1977) 44, 209.
24. Tyczkowski J., Zieliński M. and Kryszewski M. Thin Solid Films, in press.
25. Tyczkowski J., unpublished data.
26. Morita S. and Shen M., J.Polym.Sci.,(1977) 15, 981.
27. Tkatschuk B.W., Ganiuk L.J., Laurs E.P., Khim.Vys. Energ. (1977) 11, 350.
28. Simmons J.G., J.Phys.D.,(1971) 4, 613.
29. Carchano H. and Valentin M., Thin Solid Films, (1975) 30, 335.
30. Chybicki M., Phys.Stat.Sol., (1977) a39, 271.
31. Kryszewski M. and Szymański M., Macromol.Rev., (1970) 4, 245.
32. Simmons J.G., Phys.Rev., (1967) 155, 657.
33. Hall R.B., Thin Solid Films, (1971) 8, 263.
34. Deal B.E., Snow E.H. and Mead C.A., J.Phys.Chem. Solids, (1966) 27, 1873.
35. Wintle H.J., J.Non-Cristalline Solids, (1974) 15 471.
36. Hill R.M.,Phil. Mag. (1971) 23, 59.
37. Zieliński M. and Samoć M., J.Phys.D. (1977) 10, L. 105.
38. Mizutani T., Takai, Osawa T. and Ieda M., J.Phys.D.,(1976) 9, 2253.

RECEIVED March 29, 1979.

Thermal Modification of Plasma-Polymerized Organosilazane Thin Films

A. M. WROBEL and M. KRYSZEWSKI

Polish Academy of Sciences, Centre of Molecular Studies, Boczna 5, 90-362 Lódz, Poland

Consideration of the structure of organosilicon compounds focussed our attention on the possibility of producing plasma polymer films with particulary interesting thermal properties from organosilazanes. The high thermal stability of these films [1,2] and their relatively low content of organic structure [3], suggested that they may be transformed by an appropriate pyrolytic process into new materials of almost completely inorganic structure and thus, of superior thermal stability. The present paper reports results of thermally produced modifications in the structure and properties of polymer films formed by plasma polymerization of hexamethylcyclotrisilazane (I).

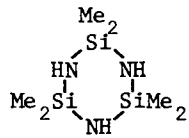

I

Experimental

Hexamethylcyclotrisilazane (HMCTS) monomer, product of PCR Research Chemicals Inc., was purified by rectification in vacuum.

Plasma polymerizations were carried out in an apparatus described previously [4]. This apparatus incorporates a vacuum bell jar containing two parallel circular electrodes spaced 3 cm apart, each having a surface area of 40 cm^2. Polymer films were deposited in a 20 kHz glow discharge on 0.1 mm thick stainless steel tape placed on the lower electrode. Polymer depositions were performed under the following constant conditions: current density, $j = 1\ mA/cm^2$; monomer vapour pressure, $p = 0.3$ Torr; and discharge duration, $t = 20$ s.

Polymer films were modified by vacuum pyrolysis at 10^{-5} Torr and at temperatures of 600 and 800°C.

Infrared spectra of polymer films were obtained on a Perkin-

0-8412-0510-8/79/47-108-237$05.00/0

Elmer, Model 457, spectrophotometer using the attenuated total reflection (ATR) technique.

Results and Discussion

Effect of Pyrolysis on the Chemical Structure of Polymer Films. In order to study the effect of thermal modification on chemical structure of plasma-polymerized hexamethylcyclotrisilazane (PP-HMCTS), an infrared analysis of the polymer film was carried out after different durations of pyrolysis. IR spectra of polymer films pyrolysed at 600 and 800°C are shown in Figs 1a and b, respectively. The spectrum of untreated polymer film (Fig. 1a A) shows strong absorption bands at 1160 and 890 cm^{-1} which originate from Si-NH-Si bonds, and correspond to δ(NH) and ν_{as}(SiNSi) vibrations, respectively [5]. The presence of methyl groups attached to silicon is demonstrated by a strong, sharp absorption band at 1250 cm^{-1}, due to $\delta_s(CH_3)$ vibrations, and by absorption at 780 cm^{-1} corresponding to ν(SiC) and $\rho(CH_3)$ vibrations. The unmodified polymer spectrum (Fig. 1a A) also exhibits new bands at 2120 and 1020 cm^{-1}, absent in the monomer spectrum. The former band (at 2120 cm^{-1}) corresponds to ν(SiH) vibrations. These groups are formed by the fragmentation of the monomer molecules leading to the abstraction of methyls from silicom atoms [3]. The second band (at 1020 cm^{-1}) is typical of methylene groups between two silicon atoms, and is assigned to $\omega(CH_2)$ vibrations [5]. The presence of these groups in the polymer indicates crosslinking through the formation of methylene and ethylene linkages between silicon atoms.

The spectra in Fig. 1a clearly show that pyrolysis leads to significant changes in the structure of PP-HMCTS. For example, the absorptions at 2120 (SiH), 1250 ($SiCH_3$), and 1160 cm^{-1} (NH) decay markedly with increasing pyrolysis time. At higher temperature (Fig. 1b) these changes proceed considerably faster and lead to a polymer film of almost inorganic structure. A strong, broad absorption band at 1000 - 800 cm^{-1} (Fig. 1b E) is very similar to that observed in the spectrum of silicon nitride [6,7,8]. Hence, one may conclude that thermally modified film is enriched in silicon-nitrogen inorganic linkages.

Analogous heat treatment was carried out also on films deposited from a mixture of monomer and ammonia; equal partial pressures of 0.3 Torr were utilized and the same discharge parameters as described previously applied here also. Our earlier studies [2] had shown that addition of ammonia to HMCTS vapour improves the thermal stability of resulting polymer films, and their adhesion to metal substrates. It was found also that pyrolysis of these films induces similar changes in the IR spectra as those in Fig. 1. However, these pyrolysed films were found to have a more intense and broader absorption band within the 1000 - 800 cm^{-1} range (Fig. 2). The intensification of absorption in this region was felt to be due to a more saturated structure of the pyrolysis product, caused by Si-N bonds, according to the previously reported [2] higher concentration of Si-NH-Si linkages in this latter type of polymer films.

In Plasma Polymerization; Shen, M., et al.;
ACS Symposium Series; American Chemical Society: Washington, DC, 1979.

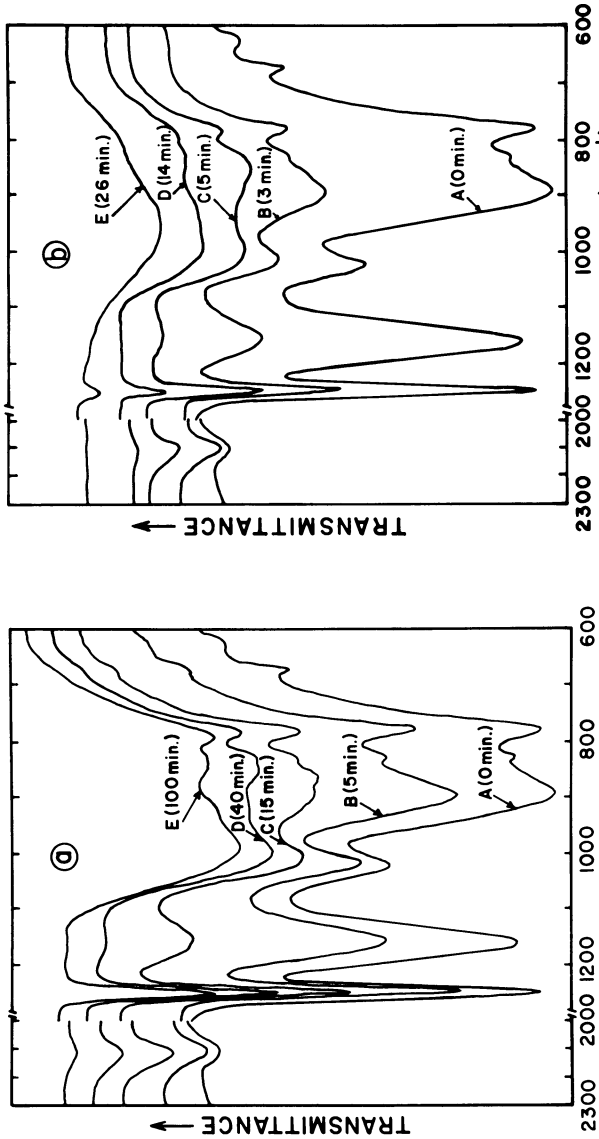

Figure 1. Infrared ATR spectra of PP–HMCTS film after different durations of pyrolysis in vacuum at: (a) 600°C and (b) 800°C.

Kinetics of Thermal Decomposition. In order to examine the kinetics of thermal decomposition reactions, relative changes in IR absorption intensity at 2120, 1250 and 1160 cm^{-1} (Fig. 1), corresponding to SiH, $SiCH_3$ and NH groups, respectively, were studied as a function of pyrolysis time. Absorption data were evaluated as the ratio of areas under the peaks, A/A_o; A_o being the initial peak area, and A the area after a given time of pyrolysis. The ratio A/A_o for SiH, $SiCH_3$ and NH groups is shown as a function of pyrolysis time at 600 and 800°C in Figs 3a and b, respectively. The relative concentration of these groups is seen to decrease with increasing pyrolysis time. However, a large increase in the concentration of SiH groups at the early stages of pyrolysis is also noted. This is presumably due to rapid recombination of atomic hydrogen, evolving from NH groups, with silicon radicals formed through the scission of Si-C bonds. The decay of NH groups proceeds very rapidly as a result of hydrogen abstraction; new Si-N bonds with tertiary nitrogen are subsequently formed according to the following simplified scheme:

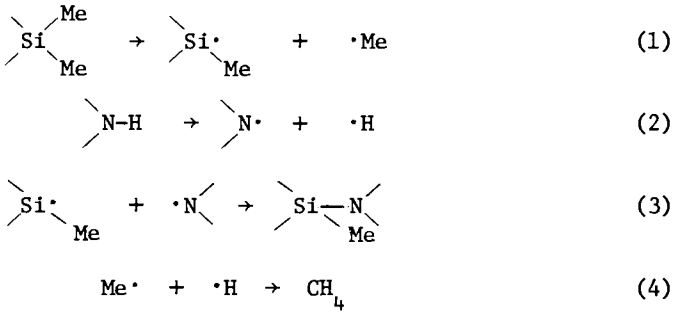

(1)

(2)

(3)

$$Me\cdot + \cdot H \rightarrow CH_4 \qquad (4)$$

From reaction (4) we might expect to find methane in the gaseous residue following pyrolysis. Gas-chromatographic analysis of the gaseous pyrolysate has indeed shown methane to be the main component [3]. This process gradually eliminates the organic structure from the polymer film, and the remaining solid acquires an even increasing inorganic character.

To establish the order of thermal decomposition reactions, the kinetic data were verified using the first order reaction equation:

$$-\frac{dC}{dt} = kC \qquad (5)$$

where concentration may be expressed as $C = A/A_o$; following integration, equation (5) becomes

$$-\ell n \frac{A}{A_o} = kt \qquad (6)$$

Plots of $\ell n(A/A_o)$ as a function of pyrolysis time (t) for the decomposition of SiH, $SiCH_3$ and NH groups are linear at both temperatures (Figs 4a and b), indicating that the reactions are indeed first order. For the case of $SiCH_3$ (Fig. 4a), thermal scission of Si-C bonds appears to take place in two stages. This may be due to the presence of some $Si(CH_3)_2$ groups in the polymer, remnants

In Plasma Polymerization; Shen, M., et al.;
ACS Symposium Series; American Chemical Society: Washington, DC, 1979.

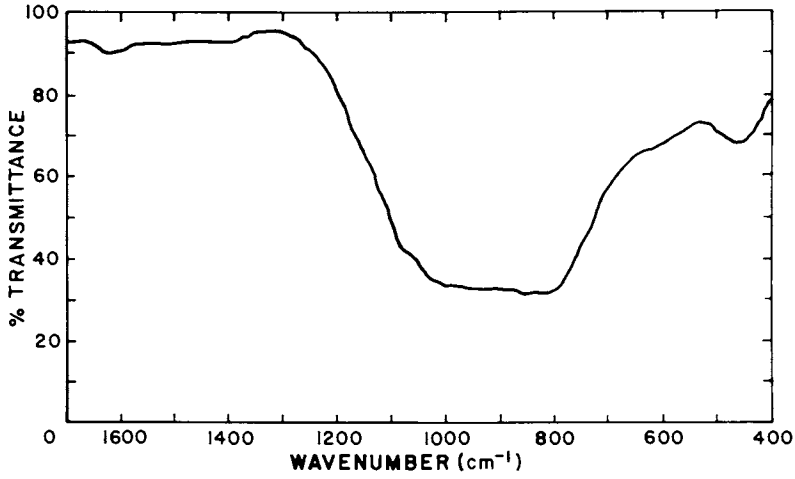

Figure 2. Infrared ATR spectrum of PP–HMCTS film deposited in the presence of ammonia after 45-min pyrolysis in vacuum at 800°C

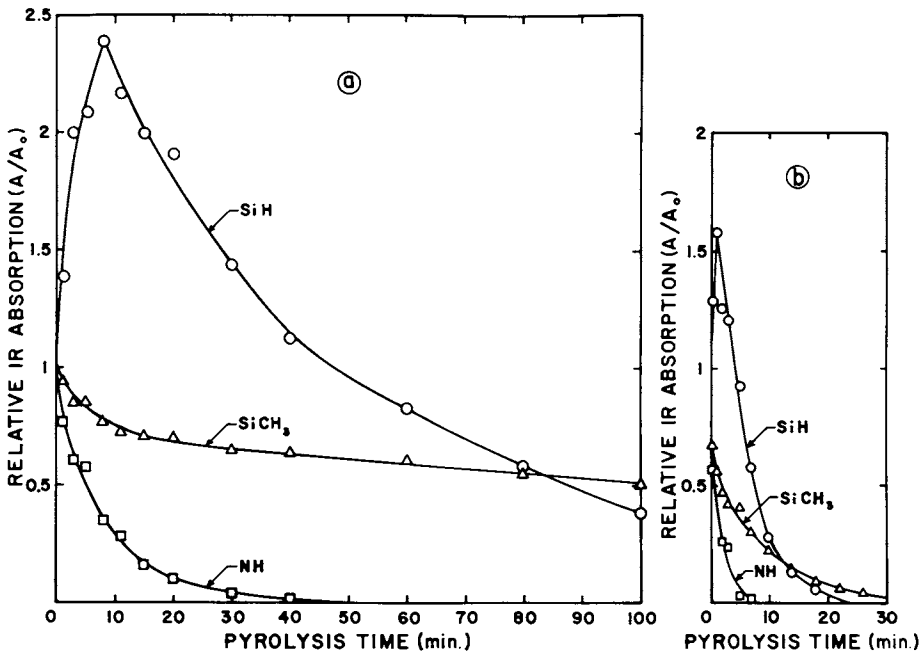

Figure 3. Relative intensity of IR absorption, A/A_o, as a function of pyrolysis time at: (a) 600°C and (b) 800°C.

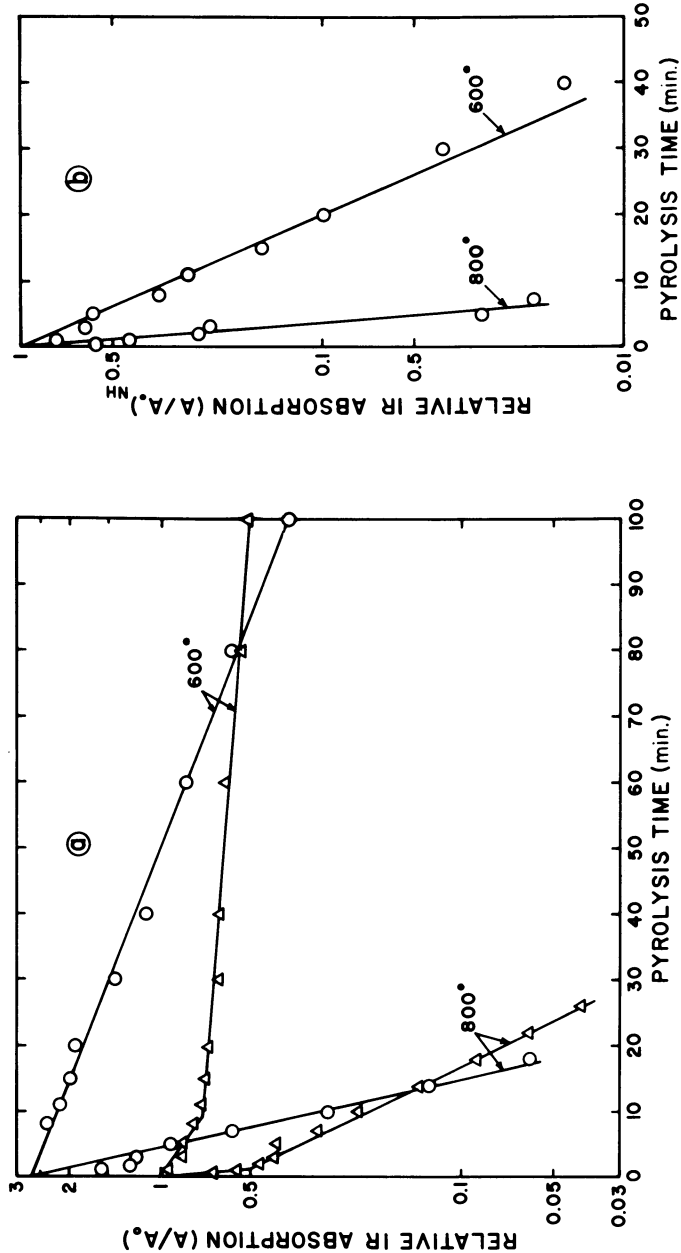

Figure 4. Plots of ln (A/A_o) as a function of pyrolysis time at different temperatures for: (a) SiH, $SiCH_3$ and (b) NH groups. (○) SiH, (△) $SiCH_3$.

of the original structure of the monomer. The first reaction stage, which proceeds at a significantly higher rate than the second, is presumably due to abstraction of one methyl from $Si(CH_3)_2$. We note that the pyrolysis time at the break points of the $SiCH_3$ curves in Fig. 4a agrees well with that determined from the maxima of the SiH curves in Figs 3a and b. These results strongly suggest that the sharp rise in the SiH curve noted in Figs 3a and b is due to the higher concentration of the silicon radicals produced through Si-C bonds scission during the first stage of this reaction.

In view of the experimentally observed linear relationship between $\ell n(A/A_o)$ and t, an Arrhenius equation has been used to determine the apparent activation inergies for the particular decomposition reactions. We find 15 kcal/mole for N-H, 23 kcal/mole for Si-H and 31 kcal/mole for Si-C bonds scissions. These values are very approximate, since they were evaluated assuming a linear relationship $\ell n\ k = f(1/T)$ for the temperatures under study. As pyrolyses were carried out at only two experimental temperatures, the validity of this assumption could not be verified.

The activation energy values suggest that scission of N-H bonds seems to be a predominant reaction during the pyrolysis process. This reaction, according to the scheme (1-3), leads to the formation of a highly corsslinked inorganic structure in the polymer film.

The kinetics of thermal decomposition were also examined for polymer film deposited from the mixture of monomer and ammonia under the plasma conditions, as described earlier. The relative intensity of IR absorption, A/A_o, was evaluated for SiH, $SiCH_3$ and NH groups as a function of pyrolysis time at 600°C. As shown in Fig. 5, the shape of the resulting curves is similar to that noted for polymer film deposited without ammonia (Fig. 3a). However, the initial increase in concentration of SiH groups is considerably smaller and a maximum peak in the SiH curve is less sharp than in the earlier case (Fig. 3a). Moreover, the $SiCH_3$ curve reveals a more rapid decay of methyl-silicon groups during the initial stage of pyrolysis.

The order of thermal decomposition reactions was established as previously by plotting $\ell n(A/A_o)$ vs t. The resulting linear plots, shown in Figs 6a and b, indicate that decomposition of SiH, $SiCH_3$ and NH groups in polymer film deposited from the mixture of monomer and ammonia also proceeds by a first order reaction mechanism. In Fig. 6, the kinetics for the two types of films (i.e. polymerized with and without ammonia) are compared. The identical slopes of the SiH curves shown in Fig. 6a indicate that the same reaction rate constants apply for scission of Si-H bonds in both polymers. The shape of the $SiCH_3$ curves is very similar and distinct overlaping of these curves is observed for the later stages of the reaction (Fig. 6a). This shows that scission of Si-C bonds during the second stage of the reaction proceeds at nearly the same rate for both polymers; only in initial pyrolysis times is

In Plasma Polymerization; Shen, M., et al.;
ACS Symposium Series; American Chemical Society: Washington, DC, 1979.

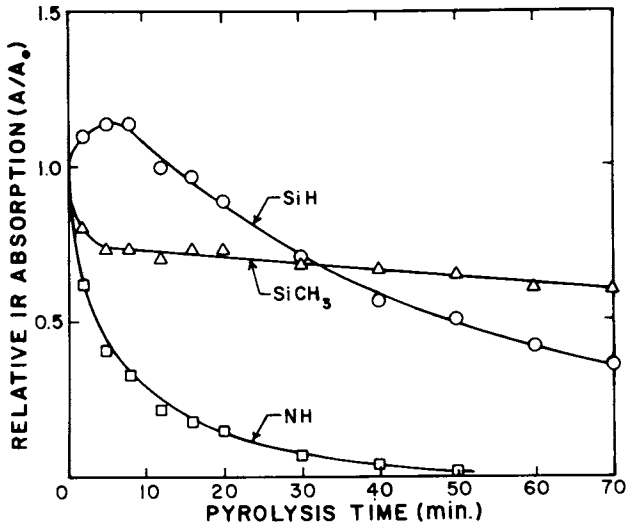

Figure 5. Relative intensity of IR absorption, A/A_o, as a function of pyrolysis time at 600°C for PP–HMCTS film deposited in the presence of ammonia

In Plasma Polymerization; Shen, M., et al.;
ACS Symposium Series; American Chemical Society: Washington, DC, 1979.

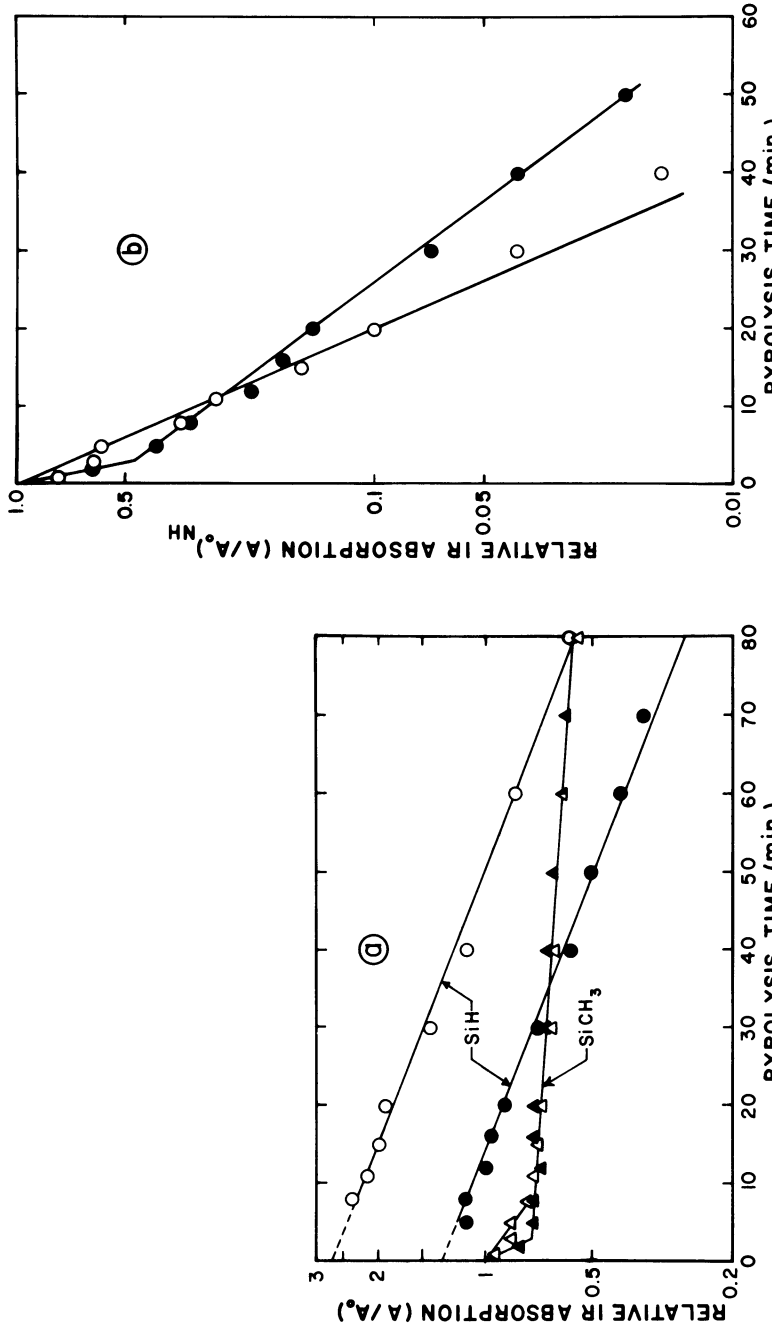

Figure 6. Plots of ln (A/A_o) as a function of pyrolysis time at 600°C for: (a) SiH_3, $SiCH_3$ and (b) NH groups; open symbols: polymer film deposited without ammonia; full symbols: polymer film deposited in the presence of ammonia.

there a difference. Here a sharper break in the $SiCH_3$ curve is observed for polymer film deposited with ammonia; this occurs due to more rapid decay of $SiCH_3$ groups, as seen from the curve shown in Fig. 5. A distinct break noted in the NH curve for polymer deposited with ammonia (Fig. 6b) shows that decomposition of NH groups also takes place by a two-stage reaction.

These results are in a good agreement with our previous studies [2], which showed that ammonia under glow discharge conditions is a reactive comonomer and that the polymerization of HMCTS in the presence of this gas produces higher crosslinking of the polymer film through methyl abstraction from silicon atoms and the formation of Si-NH-Si linkages. Hence, crosslinking significantly reduces the concentration of $Si(CH_3)_2$ groups remaining in the polymer film. This could explain the more rapid decay of $SiCH_3$ groups in polymer deposited in the presence of ammonia, as observed during the initial pyrolysis stage (Figs 5 and 6a) when an abstraction of single methyls from $Si(CH_3)_2$ groups takes place. According to our earlier considerations, the smaller rise noted in the SiH curve (Fig. 5), is due presumably to the lower concentration of silicon radicals produced through scission of Si-C bonds during the first stage of this reaction. Furthermore, due to the greater concentration of Si-NH-Si bonds in the polymer film, crosslinking via formation of new Si-N bonds with tertiary nitrogen, according to scheme (1-3), seems to take place more readily during pyrolysis than the generation of SiH groups.

In general, our data attest to the complexity of thermal decomposition reactions in the polymer film. A good example of this is the apparent two-stage decomposition of NH groups in the polymer deposited in the presence of ammonia (Fig. 6b). Additional experimentation will be required to fully account for the mechanisms involved in this process.

Properties of thermally modified films. Thermally modified films produced in this work were found to be colourless, glassy materials with extremely strong adhesion to the metal substrate. Passivation tests have shown that the coated metals displayed excellent resistance to corrosive chemicals. Exposure of films to concentrated acids, such as $HC\ell$, HNO_3, H_2SO_4 and H_3PO_4 for several hours had no visible effect upon their surface.

In order to examine the effect of oxygen on the properties and chemical structure of thermally modified films in vacuum, these were heated in oxygen under atmospheric pressure at a temperature of 600°C. It was found that even after such treatment films still exhibited strong adhesion to the metal substrate, and good resistance to attack by corrosive agents. Infrared analyses of the previously modified films following different durations of heating in oxygen have shown significant structural changes. The spectra in Fig. 7 reveal a new absorption band at $1100 \div 1000\ cm^{-1}$, which is characteristic of Si-O-Si bonds, and corresponds to ν_{as} (Si-O-Si) vibrations [5]; a similar absorption band is observed in the spectra of silicon oxide films [7].

In Plasma Polymerization; Shen, M., et al.;
ACS Symposium Series; American Chemical Society: Washington, DC, 1979.

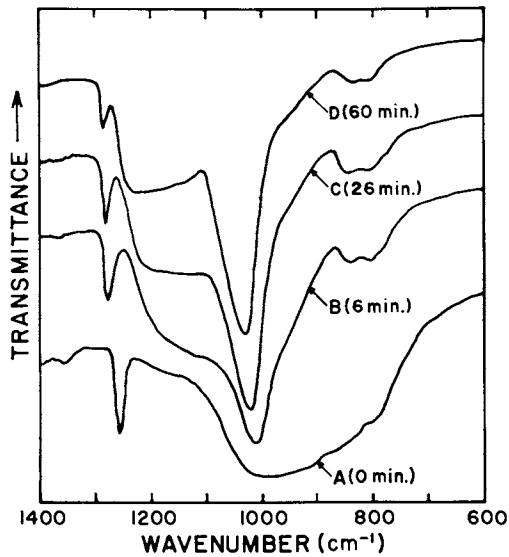

Figure 7. Infrared ATR spectra of PP–HMCTS film. (A) previously pyrolysed in vacuum; (B, C, and D) following various durations of heating in oxygen atmosphere at 600°C.

Moreover, as seen from Fig. 7, the intensity of the absorption in this region increases markedly with treatment time (Fig. 7C and D). These results suggest that PP-HMCTS films previously pyrolysed in vacuum may be transformed, by controlled oxidative heat treatment, into new materials with a high content of silicon oxynitride inorganic structure.

It is interesting to note that plasma polymer films obtained from other organosilazanes, such as hexamethyldisilazane and cyclic compounds with four and eight-membered methyl silazane rings, were found to form films of similar properties when pyrolysed in vacuum. In contrast with present results, however, heat treatments carried out on polymer films deposited from organosiloxanes, such as hexamethyldisiloxane, hexamethylcyclotrisiloxane and octamethylcyclotetrasiloxane, resulted in significant deterioration in film adhesion to the metal substrate. In the case of siloxane polymer films a strong peeling effect may be observed after only 1 min. of pyrolysis in vacuum at 600°C.

From these observations it may be concluded that organosilazanes are particularly useful for the production of films with excellent thermal properties; the Si-N structural unit in these compounds appears to play a most significant role.

Our results show that PP-HMCTS films, following thermal modification, may be suitable as passivation coatings for metals. Their other properties as electrical, optical and mechanical are presently under study in our laboratory.

Conclusions

Based on the results reported in this paper, the following conclusions may be drawn.

1. Thermal modification of PP-HMCTS films gradually reduces the organic structure from the polymer which evolves towards a material of essentially inorganic character.
2. Formation of Si-N inorganic linkages through the scission of N-H and Si-C bonds seems to be a predominant process during thermal decomposition of PP-HMCTS.
3. Thermal decomposition of Si-H, Si-C and N-H bonds in PP-HMCTS proceeds by a first order reaction mechanism.
4. Thermally modified PP-HMCTS films due to their high thermal stability, strong adhesion to the metal substrate and high resistance to corrosive agents, appear very promising as a passivation coatings for metals.

Acknowledgments

The authors wish to thank Professors M.R. Wertheimer and H.P. Schreiber (Ecole Polytechnique of Montreal) for valuable suggestions and critical reading of the manuscript.

Abstract

Plasma-polymerized hexamethylcyclotrisilizane thin films were pyrolysed in vacuum at 600 and 800°C. Infrared analysis of the polymer films carried out after different durations of pyrolysis revealed significant changes in their structure. A distinct decay of SiH, $SiCH_3$ and NH groups in the polymer with increasing pyrolysis time was observed. The appearance and growth of an absorption band at 1000 - 800 cm^{-1}, suggested the formation of silicon-nitrogen inorganic linkages in the polymer film. Study of thermal decomposition processes showed that scission of Si-H, Si-C and N-H bonds proceeds according to a first order reaction mechanism. The apparent activation energies evaluated for the respective decomposition reactions suggest that scission of N-H bonds dominates during pyrolysis. Thermally modified films were found to be colourless, glassy material with extremely strong adhesion to metal substrates; they displayed excellent resistance to corrosive chemicals.

References

1. A.M. Wróbel and M. Kryszewski, Bull. Acad. Pol. Ser. Sci. Chem. (1974) 22, 471.
2. A.M. Wróbel and M. Kryszewski, IUPAC Symposium, "International Round Table for Plasma Polymerization and Surface Treatment", Limoges, June 1977.
3. A.M. Wróbel, M. Kryszewski and M. Gazicki, Polymer, (1976) 17, 678.
4. A.M. Wróbel, M. Kryszewski and M. Gazicki, Polymer, (1976) 17, 673.
5. A.L. Smith, Spectrochimica Acta, (1960) 16, 87.
6. G. Turban and Y. Catherine, Thin Solid Films, (1976) 35, 179.
7. W.A. Pliskin, J. Vac. Sci. Technol., (1977) 14, 1064.
8. W. Kern and S. Rosler, J. Vac. Sci. Technol., (1977) 14, 1082.

RECEIVED March 29, 1979.

15

Plasma-Initiated Polymerization and Copolymerization of Liquid Vinyl Monomers

YOSHIHITO OSADA[1], ALEXIS T. BELL, and MITCHEL SHEN

Department of Chemical Engineering, University of California, Berkeley, CA 94720

Generally, polymers produced via ionized plasma are highly branched, highly crosslinked networks whose chemical structure and compositions are not simply related to those of the starting monomers. This process is known as plasma polymerization, and has received considerable attention. In recent communications (1,2), from this laboratory we have reported on a polymerization process whereby the plasma is used to initiate conventional polymerization of liquid methyl methacrylate, followed by post-polymerization without the plasma. The resulting polymer is an uncrosslinked conventional poly(methyl methacrylate) with a very high molecular weight. This process may be called plasma initiated polymerization. In this work, we shall report on the results of plasma-initiated polymerizations and copolymerizations of a number of vinyl monomers in either bulk liquid state or in solution in an effort to shed some light on the mechanism of this phenomenon.

Experimental

Monomers were purchased from Polysciences, Inc. The liquid monomers (methyl methacrylate, ethyl methacrylate, n-butyl methacrylate, methyl acrylate, n-butyl acrylate, methacrylic acid, acrylic acid, styrene and α-methylstyrene) were purified by vacuum distillation under nitrogen, poured into thin-walled ampules, degassed at 10^{-3} - 10^{-4} torr and subsequently frozen in liquid nitrogen. The partially filled ampules were then inserted between a pair of parallel plate electrodes connected to an International Plasma Corporation Model 3001 Radiofrequency Generator, which operates at 13.56 MHz and delivers up to 150 watts of power. In most of these experiments discussed in this work, the power input was limited to 40 - 80 watts. The ampules were allowed to warm up until droplets of liquids appeared. A glow discharge was then in-

[1] Current address: Department of Chemistry, Ibaraki, University, Mito 310 Japan

0-8412-0510-8/79/47-108-253$05.00/0

itiated in the gas space above the monomer in the ampule for various periods of time (see Table). During discharge the temperature of the gaseous phase in the ampules increased slightly. Following the plasma initiation the ampules were left standing at constant temperature for prescribed lengths of post-polymerization periods, after which the seal was broken and the contents precipitated and analyzed.

Solid monomers acrylamide and methacrylamide were recrystallized twice from methanol. Bulk monomers were polymerized in the manner described above, but in the solid state (no melting). Aqueous solutions of these monomers were handled as the liquid monomers.

The molecular weight of one of the polymers, poly(methacrylic acid) was determined by intrinsic viscosity measurements at 25°C. Methanol was used as the solvent. The following equation was used in calculating the molecular weight (3):

$$[\eta] = 2.42 \times 10^{-3} M^{0.5}$$

Copolymer compositions were determined by a high resolution nuclear magnetic resonance spectrometer (180 HMz). Copolymers of methyl methacrylate and styrene were dissolved in deuterated chloroform for the analysis. Deuterated pyridine was the solvent for the methyl methacrylate - methacrylic acid copolymers. Elemental analysis was also used in copolymer composition analysis to complement the NMR data.

Results and Discussion

1. Monomers Polymerizable by Plasma Initiation. Polymerization data for all of the vinyl monomers utilized in this study are summarized in Table 1. As shown previously, methyl methacrylate is readily polymerizable (1,2). Methacrylic acid (MAA) and acrylic acid (AA) are polymerized immediately upon exposure to the plasma. Because the resulting polymers are insoluble in their monomers, the products are precipitated out and conversion is low despite prolonged post-polymerization. However, if water is now added as solvent, polymerization becomes homogeneous and high conversions can be readily achieved with post-polymerization. For example, after a 15 second plasma initiation period more than 80% yield was obtained for a 75% aqueous solution of MAA. The molecular weight, determined by intrinsic viscosity measurements, was found to be 4.5×10^6 gm/mole.

When solid monomers of acrylamide (AM) and methacrylamide (MAM) were subjected to plasma initiation, only trace amounts of insoluble polymers were obtained. Now if aqueous solutions of AM and MAM were used in the plasma initiated polymerization high conversions were again achievable upon post-polymerization. Polyacrylamide was found to be completely soluble, whereas polymethacrylamide forms a gel. It is of interest to note that no polymer is formed with post-polymerization alone without plasma initiation

In Plasma Polymerization; Shen, M., et al.;
ACS Symposium Series; American Chemical Society: Washington, DC, 1979.

Table 1. Plasma Initiated Polymerization Data of Vinyl Monomers

Monomer	Polym. Medium	Plasma Duration (Sec)	Post-Polym. Condition	Yield (%)	Notes
Methyl Methacrylate	Bulk Liq.	60	100 hr., 25°C	40	
Methacrylic Acid	Bulk Liq.	30	168 hr., 5°C	3	
	75% Aq.Soln.	15	90 hr., 5°C	80	
Acrylic Acid	Bulk Liq.	30	168 hr., 5°C	3	
	75% Aq.Soln.	15	90 hr., 5°C	50	
Methacrylamide	Bulk Solid	120	45 hr., 20°C	Trace	Insol. film.
	30% Aq. Soln.	12	45 hr., 20°C	80	Swollen gel.
Acrylamide	Bulk Solid	40	45 hr., 20°C	Trace	Insol. film.
	50% Aq.Soln.	15	45 hr., 20°C	60	Partial film.
Ethyl Methacrylate	Bulk Liq.	60	168 hr., 5°C	1	
n-Butyl Methacrylate	Bulk Liq.	30	168 hr., 5°C	1-2	
Methyl Acrylate	Bulk Liq.	180	200 hr., 20°C	0	
	Bulk Liq.	900	168 hr., 5°C	0	
n-Butyl Acrylate	Bulk Liq.	20	168 hr., 5°C	0	
Styrene	Bulk Liq.	60	168 hr., 5°C	0	Yellowish color; Insol. film.
	94% CCl_4 Soln.	60	66 hr.,-15°C	0	Dark brown color; Considerable Insol. film.
	50% CCl_4 Soln.	15	66 hr.,-15°C	0	
α-methylstyrene	Bulk Liq.	30	168 hr., 5°C	0	Yellowish color; Insol. film.

In Plasma Polymerization; Shen, M., et al.;
ACS Symposium Series; American Chemical Society: Washington, DC, 1979.

(dark reaction).

We have recently shown that solid state polymerizations can also be carried out via plasma initiation (4). In that work, 1, 3,5-trioxane and 1,3,5,7-tetraoxane were used as monomer crystals. Highly crystalline polyoxymethylene were obtained using either monomer. However, if the monomers were dissolved in an appropriate solvent, such as cyclohexane, then no polymer was formed with plasma initiation. These observations are the reverse of those for AM and MAM, where plasma initiated polymerizations in solution appear to proceed satisfactorily during homogeneous post-polymerization periods, but not in the bulk crystalline state. The unresolved question is then if water molecules may have dissociated in the plasma in highly active radical species, perhaps OH• or H•, to promote efficient initiation.

We note in Table 1 that although methyl methacrylate polymerizes readily upon plasma initiation, ethyl methacrylate (EMA) and n-butyl methacrylate (BMP) gave only low yields (1-2) of polymer regardless of the length of post-polymerization period. Apparently a small amount of polymer was formed during the plasma initiation period (up to 60 seconds), and no further polymerization took place when plasma was turned off. Parallel experiments of dark polymerization (no plasma initiation) under the same conditions also resulted in no polymer formation.

2. Monomers Not Polymerizable by Plasma Initiation. When styrene and α-methylstyrene were subjected to plasma treatment, the monomers became yellowish and only trace amounts of insoluble films were formed. The discoloration was intensified and extensive formation of dark films were observed if carbon tetrachloride was added as the solvent. No post-polymerization was detectable for these monomers. Generally styrene and α-methylstyrene readily undergo thermal polymerization. However, no thermal polymerization was possible for these monomers after having been subjected to plasma treatment for one minute or less. It has been demonstrated from the emission spectra of glow discharge plasma of benzene (6) and its derivatives (7) that most of the reaction intermediates are phenyl or benzyl radicals which subsequently form a variety of compounds such as acetylene, methylacetylene, allene, fulvene, biphenyl, poly(p-phenylenes) and so forth. It is possible that styrene and α-methylstyrene also behave similarly, so that species from the monomer plasma are poor initiators for polymerization.

In contrast to methacrylic esters, methyl acrylate (MA) and n-butyl acrylate (BA) did not polymerize at all upon plasma treatment. The observation holds true even when the initiation period was increased to 15 minutes (see Table 1), despite the fact that the propagation constants from photopolymerization studies (5), indicate that its value is higher for MA (k_p = 720 ℓ/mole-sec) than for MMA (k_p = 143 ℓ/mole-sec) at 30°C.

In Plasma Polymerization; Shen, M., et al.;
ACS Symposium Series; American Chemical Society: Washington, DC, 1979.

3. Copolymerizations of Methyl Methacrylate. Copolymerizations of methyl methacrylate with styrene (STY) were carried out by subjecting the monomer mixtures to plasma for 20-30 seconds, followed by post-polymerization at 5°C for 120 hours. Parallel dark polymerizations (no plasma initiation) experiments were also conducted under similar conditions. The results are given in Table 2. The presence of styrene monomer appears to exert a strong inhibiting effect on the reactions, as seen in the precipitous decreases in yield with increasing styrene concentration. When styrene exceeded 40% in the monomer mixture discoloration and insoluble film formation were again observed as in the case of styrene homopolymerization. To analyze the chemical composition of the copolymers, insolubles were filtered off and the dissolved polymers were precipitated in methanol. Copolymer composition data are shown in Figure 1. The results from NMR and elemental analyses are seen to be in satisfactory agreement. Those for copolymers obtained from dark reactions (not shown) were found to be similar. These data are compared with the curve calculated from the copolymer composition equation, using r (MMA) = 0.46 and r (STY) = 0.52 reported for free radical copolymerizations (8). The typical sigmoidal curve is followed by our plasma initiated copolymerization data, indicating the free radical nature of these reactions. The NMR spectra (Figure 2) show a splitting at 3.5 ppm, which is attributed to the screening effect of the neighboring phenyl groups. The implication is that each monomer unit in the copolymer is distributed randomly which is typical of STY/MMA copolymers obtained via free radical mechanism.

Copolymerization data for methyl methacrylate and methacrylic acid are shown in Table 3. In this system, post-polymerization proceeded more rapidly and with better yields than the MMA/STY system. Monomer mixtures with high molar ratios of MAA became cloudy with increasing conversion because of the poor solubility of the copolymer in the monomer. Dark reaction proceeded slowly, and it was necessary to heat the reacting mixture to 80°C for a few hours to start the polymerization. Mole fractions of MMA units in the copolymer were determined by NMR spectra (Figure 3). The methoxy peak at 4.5 ppm was used to monitor the MMA concentration. However, with decreasing MMA content the peak becomes too broad to permit accurate analysis. Nevertheless, the estimated copolymer composition data appear to be in rough agreement with those obtained from free radical copolymerizations (5). It is of interest to note that the methoxy peak did show splitting with increasing MAA content as a result of the screening effect of the neighboring carboxylic groups. This observation is indicative of random sequence distribution in the copolymer, which is characteristic of radical initiated copolymerization of MMA and MAA.

Abstract

A series of vinyl monomers were polymerized via plasma in-

In Plasma Polymerization; Shen, M., et al.;
ACS Symposium Series; American Chemical Society: Washington, DC, 1979.

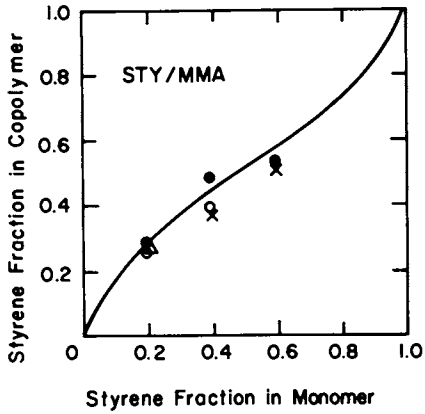

Figure 1. Monomer–copolymer composition relationship for the plasma-initiated copolymerization of methyl methacrylate with styrene. Plasma-initiated polymerization: (●) NMR, (×) elemental analysis. Thermal polymerization: (○) NMR, (△) elemental analysis, (—) theoretical curve. $r_{MMA} = 0.46$; $r_{sty} = 0.52$.

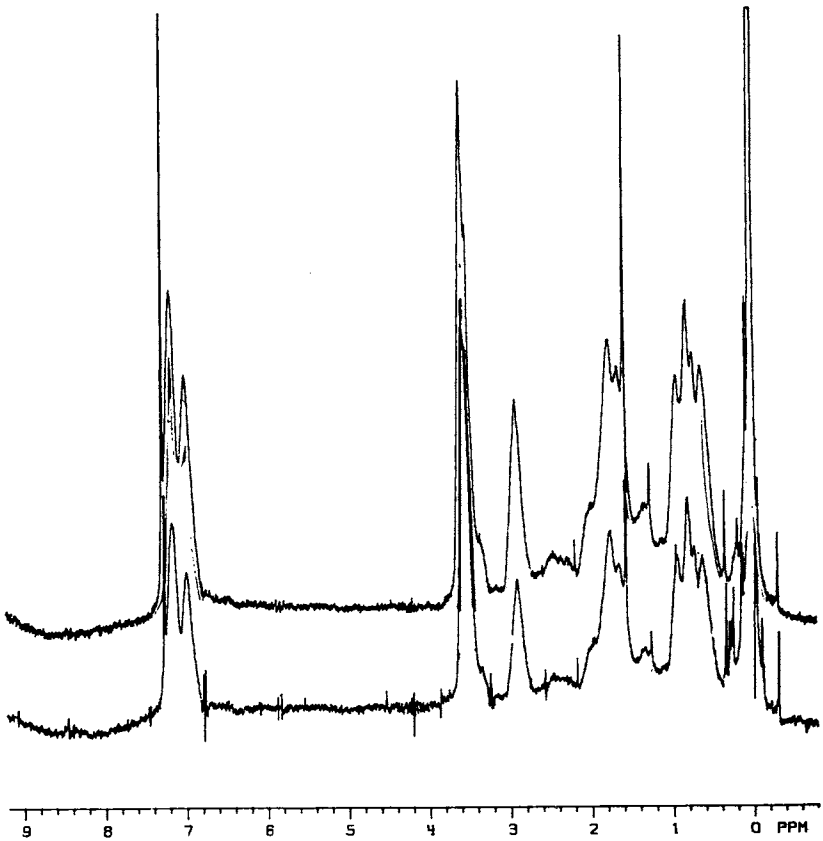

Figure 2. NMR spectra of poly(methyl methacrylate–co–styrene) obtained by (1) plasma-initiated polymerization and (2) thermal polymerization. In 0.2% $CDCl_3$; (A) monomer feed: MMA 0.6, sty 0.4; (B) monomer feed: MMA 0.8, sty 0.2.

In Plasma Polymerization; Shen, M., et al.;
ACS Symposium Series; American Chemical Society: Washington, DC, 1979.

Table 2. Plasma-Initiated Copolymerization of Methyl Methacrylate and Styrene*

Monomer Molar Ratio (MMA/STY)	% Conversion Plasma Initiated	Dark**
10/0	16.7	1.8
8/2	0.4	0.3
6/4	0.5	0.2
4/6	0.2	0.3
2/8	trace	0.15
0/10	none	0.14

* Polymerization Conditions: Power 50W; plasma duration 20-30 sec; post-polymerization at 5°C for 120 hr.

** Dark polymerization was carried out in the same condition but without plasma-exposure.

Table 3. Plasma-Initiated Copolymerization MMA with MAA

Monomer Molar Ratio (MMA/MAA)	% Conversion Plasma*	Dark**
76/24	1.7	4.9
55/45	2.2	3.2
35/65	4.6	1.25
17/83	4.5	2.2

* Polymerization Conditions: Power 50W; plasma duration 30-60 sec; post-polymerization at 5°C for 48 hr.

** Dark polymerization was carried out at 80°C for 2-3 hr. without plasma-exposure.

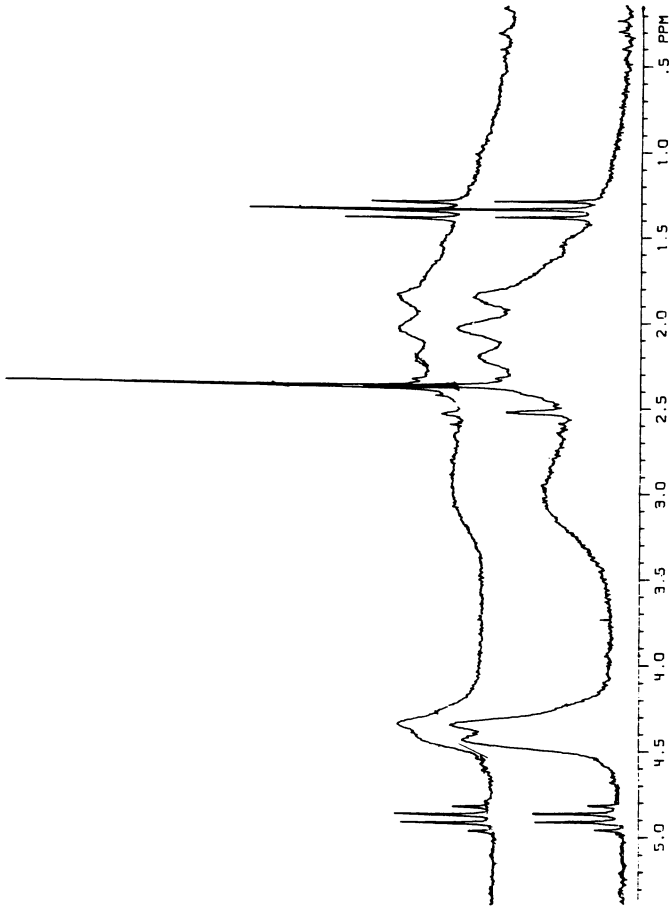

Figure 3. NMR spectra of poly(methyl methacrylate–co–methacrylic acid) obtained by (1) plasma-initiated polymerization and (2) thermal polymerization in 0.2% deuterated pyridine. Monomer feed: MMA 0.55, MMA 0.45.

In Plasma Polymerization; Shen, M., et al.;
ACS Symposium Series; American Chemical Society: Washington, DC, 1979.

itiation. Monomers were frozen in ampules, evacuated and sealed. The ampule was then inserted between parallel plate electrodes, and plasma was generated in the vapor phase above the frozen monomer. Post-polymerization was carried out in the liquid state. Methyl methacrylate has been found to yield ultrahigh molecular weight polymers to high conversion. Methacrylic acid, acrylic acid, acrylamide and methacrylamide in aqueous solutions were also polymerized with high yields. However, styrene, α-methylstyrene and higher acrylic esters were not polymerizable via plasma initiation. Copolymerizations of methyl methacrylate with styrene and with methacrylic acid were also carried out. The copolymer composition diagrams are characteristic of those polymerized by free radical mechanism.

Literature Cited

1. Osada, Y., Bell, A. T., Shen, M., Polymer Letters, (1978), 16, 309.
2. Osada , Y., Johnson, D. R., Bell, A. T., Shen, M., this issue.
3. Wiederhorn, N. M., Brown, A. R., J. Polymer Sci., (1952), 8, 651.
4. Osada, Y., Bell, A. T., Shen, M., Polymer Letters, in press.
5. Brandrup, J., Immergut, E. H., eds. "Polymer Handbook" Interscience, New York, 1966.
6. Stille, J. K., Sung, R. L., Vander Kooi, J., J. Org. Chem., (1965), 30, 3116.
7. Bindley, T. F., Walker, S., Trans. Far. Soc., (1962), 58, 217; ibid, 58, 849 (1962).
8. Lewis, F. M., Walling, C., Commings, W., Briggs, E. R., Mayo, F. R., J. Amer. Chem. Soc., (1948), 70, 1527.
9. Ito, K., Iwase, S., Iwakura, K., Yamashita, Y., J. Macromol. Sci., (1967), A1, 891.

RECEIVED March 29, 1979.

Characterization of Crystalline Poly(trioxane) and Poly(tetraoxane) Obtained through Plasma-Initiated Polymerization

AKIRA ODAJIMA
Department of Applied Physics, Hokkaido University, Sapporo, Japan
YOSHIAKI NAKASE
Japan Atomic Energy Research Institute, Takasaki, Japan
YOSHIHITO OSADA[1], ALEXIS T. BELL, and MITCHEL SHEN
Department of Chemical Engineering, University of California, Berkeley, CA, 94720

Crystals of trioxane (TOX) and tetraoxane (TEOX) have been polymerized in the solid state by high energy irradiation followed by post-polymerization. α-ray (1), γ-ray (2,3) as well as x-ray (4) were utilized in initiating the polymerization. Recently, it has been demonstrated that crystalline polyoxymethylene (POM) can also be obtained through plasma initiated polymerization in the solid state (5). Preliminary characterization studies indicate that structures of polytrioxane (PTOX) and polytetraoxane (PTEOX) polymerized by both techniques are similar. In this work, further fine structural investigations were carried out using small angle x-ray scattering (SAXS), wide angle x-ray scattering (WAXS) and differential scanning calorimetry (DSC).

Experimental

Single crystals of TOX and TEOX of the approximate dimensions of 1 mm × 10 mm were prepared by sublimation under reduced pressure. Radiation-initiated polymerizations of these crystals were carried out by γ-ray pre-irradiation (1 MR) at room temperature in air. They were subsequently post-polymerized at 55°C for TOX, and at 62, 81 and 105°C for TEOX (6). Plasma initiated polymerizations were conducted by sealing the crystals in a glass ampule after degassing at 10^{-3} - 10^{-4} torr. A glow discharge was initiated in the gaseous space in the ampule by inserting the ampule between parallel electrodes. Excitation was provided by an International Plasma Corporation Model 3001 Radiofrequency Generator. A power of 40 watts at 13.56 MHz was used. Post-polymerizations were permitted to proceed at 45°C FOR TOX AND 110°C FOR TEOX. Details of the polymerization conditions for both techniques were summarized in Table 1.

X-ray measurements were carried out on a Rigaku Denki RU-100PL Rotating Anode X-ray Unit. Nickel-filtered copper

[1] Current address: Department of Chemistry, Ibaraki University, Mito, Japan.

0-8412-0510-8/79/47-108-263$05.00/0

Table I. Solid State Polymerizations of Trioxane and Tetraoxane by γ-Ray or Plasma Initiation

Sample	Post-Polymerization Temperature (°C)	Post-Polymerization Duration (hrs)	Yield (wt %)	M.P. (°C)
RADIATION INITIATION				
PTOX-80	55	20	80	187
PTEOX-12	62	25	12	173
PTEOX-25	81	25	25	181
PTEOX-40	105	6	40	179
PTEOX-80	105	6	80	174
PLASMA INITIATION				
PTOX-20-1P	45	18	20	189
PTOX-20-2P	45	46	20	185
PTOX-40P	45	66	40	186
PTEOX-4P	110	24	4	183
PTEOX-5P	110	24	5	---
PTEOX-83P	110	3	83	182

In Plasma Polymerization; Shen, M., et al.;
ACS Symposium Series; American Chemical Society: Washington, DC, 1979.

radiation was generated at 40 kV and 80 mA. WAXS profiles of the (009) and (0018) reflections were measured by a step scanning method with a fixed time of 80 or 400 sec in a symmetrical transmission arrangement. For the line broadening analysis of PTOX, instrument broadening was corrected by using a TOX single crystal of comparable dimensions as a reference sample. The x-ray rotation diagram of PTOX was obtained photographically with the fiber axis as the rotation axis. To obtain the volume fraction of subcrystals in the polymer, integral intensities were measured by a microdensitometer for two (100) reflections, i.e., one produced only by twin orientation and the other on the equator with contributions from both orientations.

Thermal analyses of the polymer samples were conducted on a Perkin-Elmer DSC-1B Differential Scanning Calorimeter. Approximately 1 mg of sample was used in each determination. The heating rate employed was 16°C/min. The instrument was calibrated using indium as a standard.

Scanning electron micrographs were taken on an ISI Mini-SEM. Samples for observation were coated with an evaporated 60% gold and 40% platinum alloy to a thickness of approximately 200Å.

Results and Discussion

The scanning electron micrograph of plasma samples of PTOX is shown in Figure 1. The crystals are seen to consist of rod-like fibrils well aligned with respect to each other. The appearance of these crystals is similar to that of the monomer as well as radiation samples of PTOX (7). The PTEOX crystal (Figure 2), on the other hand, consists of coarse fibers with rather irregular sizes and shapes and no preferential orientation. There is also considerable branching in PTEOX, whereas in PTOX no branching is evident.

Recent studies in the fine structures of radiation polymerized PTOX show that they are disordered crystals in which main-crystallites and sub-crystallites are arranged in series (7). The fine structures of PTEOX are even more disordered and complex than those of PTOX, and are believed to possess an oriented lamellar morphology. However, when the post-polymerization is carried out at temperatures above 90°C, the sub-crystallites disappear. WAXS studies indicate that the (009) and (0018) reflections of PTEOX have an asymmetrical profile, suggesting the existence of two different lattice spacings along the fiber axis. Odajima, et al. (8) suggested that there may be two kinds of crystallites present, namely those with the extended fibrillar and the folded lamellar morphologies.

SAXS pattern of radiation-polymerized PTOX in Figure 3A shows only a sharp equatorial scattering, but no meridional scattering. Those for PTOX obtained by plasma initiated polymerization (samples PTOX-20-1P and PTOX-40P shown in Figures 3B and 3C) are similar. In the case of PTEOX, those polymerized through radiation initiation but post-polymerized below 80°C (sample PTEOX-12)

In Plasma Polymerization; Shen, M., et al.;
ACS Symposium Series; American Chemical Society: Washington, DC, 1979.

Figure 1. Scanning electron micrograph of polytrioxane (Sample PTOX-40P) obtained by plasma-initiated polymerization

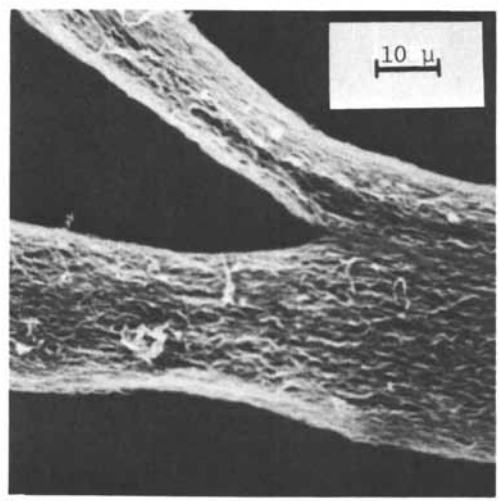

Figure 2. Scanning electron micrograph of polytetraoxane (Sample PTEOX-4P) obtained by plasma-initiated polymerization

In Plasma Polymerization; Shen, M., et al.;
ACS Symposium Series; American Chemical Society: Washington, DC, 1979.

also show no meridional scattering in their SAXS patterns. However, for those polymerized above 80°C (sample PTEOX-40) both equatorial and meridional scattering are present (Figure 4A). (This photograph was taken by using a point focussing camera with a mirror-and-monochrometer optical system, hence the sharper equatorial scattering.) The spot-like scatterings beyond the meridional scatterings are indicative of a long spacing of about 100 Å associated with stackings of the folded chain lamella oriented parallel to the fiber axis (9). The equatorial scattering is attributed to the existence of needle-like voids between PTEOX fibers oriented in the direction of the fiber axis. The SAXS pattern for PTEOX-5P is similar (Figure 4B), although the spot-like scattering is very faint. We note that the PTEOX-5P pattern is more similar to the annealed sample of radiation polymerized PTEOX (10). It is not clear why the SAXS data for PTEOX-83P exhibit only weak meridional scattering, even though the post-polymerization was carried out at the same temperature (110°C).

Figures 5A and 5B show the WAXS patterns for PTOX obtained through radiation initiation (sample PTOX-80) and plasma initiation (sample PTOX-40P). Both show the highly oriented fiber diagrams. The (100) reflections clearly indicate the twin spots in addition to spots on the equator. The amorphous halo is very weak in both samples. For PTEOX, Figure 6A shows that the radiation polymerized sample (PTEOX-80) also possesses highly oriented fiber diagrams. It appears to have no twin spots, but samples PTEOX-12 and 25 do. In the case of plasma samples, the (100) twin spots are present in PTEOX-5P, though very faint (Figure 6B). Sample PTEOX-83P, on the other hand, shows a ring-like WAXS pattern (Figure 6C). The reason for the absence of discrete scattering may possibly be attributed to the isotropic structure of lamella stacking. The amorphous halos in all of the PTEOX samples may be due to the amorphous regions between the lamellae of folded chain crystals.

Sub-crystal fractions in PTOX from both radiation and plasma initiated polymerizations were determined from the (100) reflections and summarized in Table 2. Their values are somewhat, but not substantially, lower for the plasma samples than for the radiation samples. However, since the amount of subcrystal fraction depends on both the temperature and the yield, meaningful comparisons between these two types of samples are difficult on the basis of these rather limited data.

In their recent publication, Odajima and his coworkers (11) have shown that the rather broad and asymmetric (009) and (0018) WAXS profiles of PTEOX polymerized above 80°C by radiation initiation may be resolved into two curves. One can be attributed to the extended chain crystals (the only kind present in sample PTEOX-12), and the other is the lamellar type crystals with thicknesses of about 100 Å. Figure 7 shows that the line shape of the (009) profile of the plasma sample PTEOX-5P is rather sharp and similar to that of the radiation sample PTEOX-25. The half width $(\Delta 2\theta)_{\frac{1}{2}} = 1.72^{\circ}$ or $0.012\ \text{Å}^{-1}$) of the (0018) profile is narrower than those of PTEOX-25 (2.50° or $0.017\ \text{Å}^{-1}$) and PTEOX-80 (2.25° or

In Plasma Polymerization; Shen, M., et al.;
ACS Symposium Series; American Chemical Society: Washington, DC, 1979.

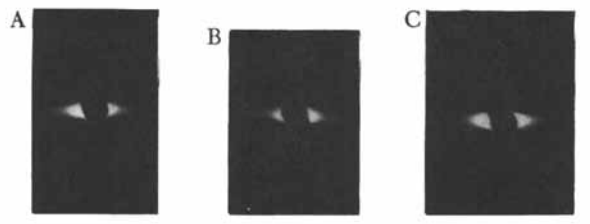

Figure 3. Small-angle x-ray scattering patterns of polytrioxane. (A) Sample PTOX-80 by radiation initiation; (B) Sample PTOX-20-1P by plasma initiation; and (C) Sample PTOX-40P by plasma initiation.

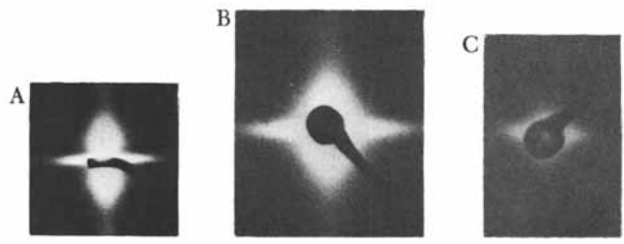

Figure 4. Small-angle x-ray scattering patterns of polytetraoxane. (A) Sample PTEOX-40 by radiation initiation; (B) Sample PTEOX-5P by plasma initiation; and (C) Sample PTEOX-83P by plasma initiation.

In Plasma Polymerization; Shen, M., et al.;
ACS Symposium Series; American Chemical Society: Washington, DC, 1979.

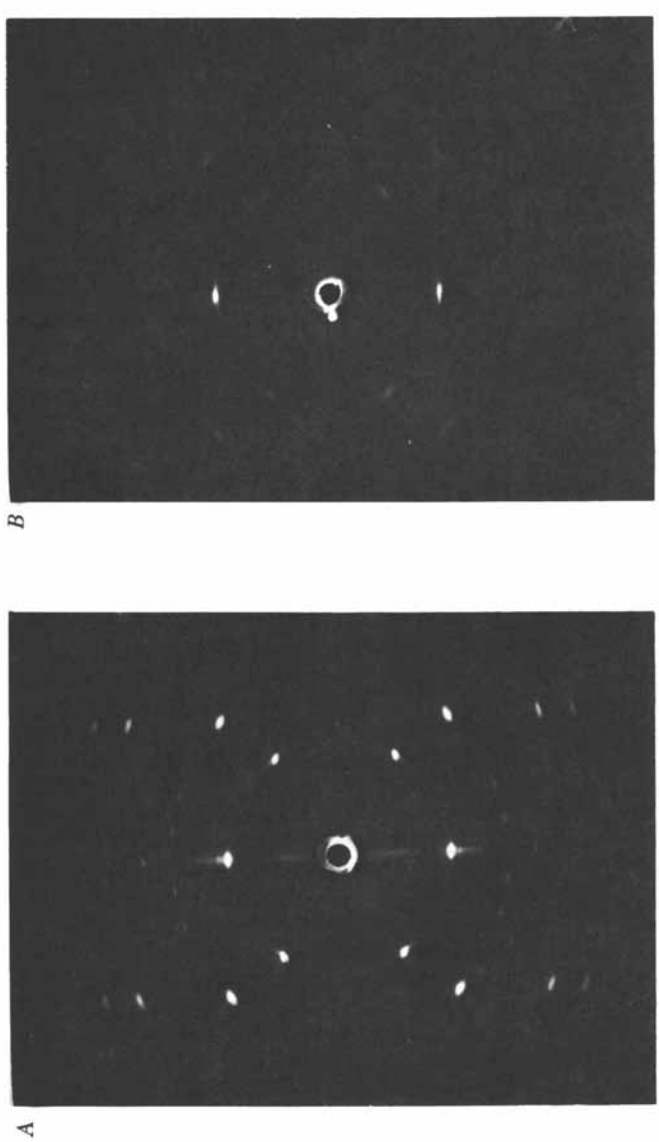

Figure 5. Wide angle x-ray scattering patterns of polytrioxane. (A) Sample PTOX-80 by radiation initiation; and (B) Sample PTOX-40P by plasma initiation.

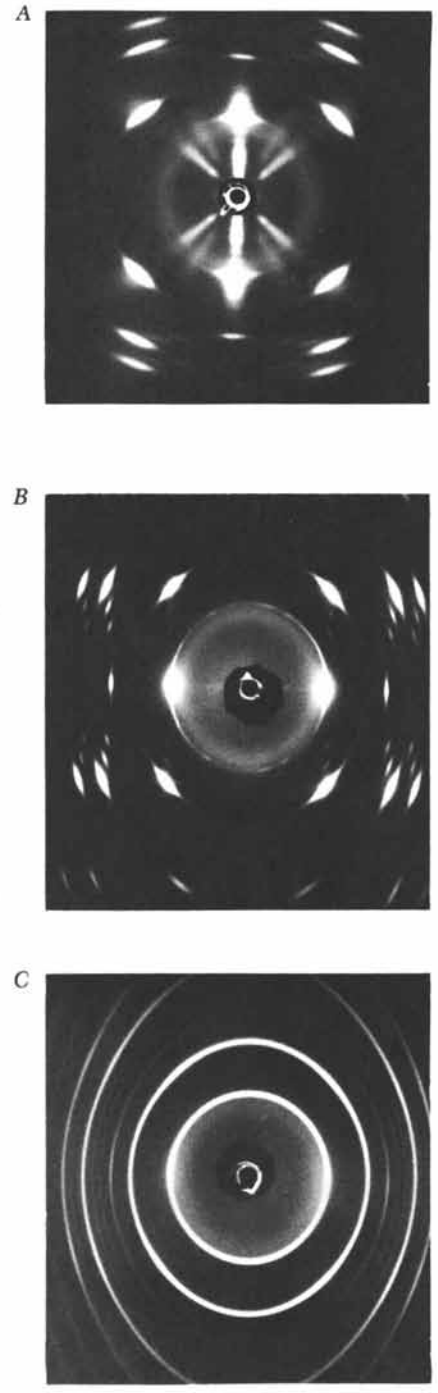

Figure 6. Wide-angle x-ray scattering patterns of polytetraoxane. (A) Sample PTEOX-80 by radiation initiation; (B) Sample PTEOX-5P by plasma initiation; and (C) Sample PTEOX-83P by plasma initiation.

In Plasma Polymerization; Shen, M., et al.;
ACS Symposium Series; American Chemical Society: Washington, DC, 1979.

Table II. Subcrystal Fractions in Polytetoxane

Sample	Yield (wt %)	Post Polymerization Temperature (°C)	Sub-crystal Fraction (Vol %)
RADIATION INITIATION			
PTOX-80	80	55	36 - 39
PTOX-2	2	50	∿45
PTOX-19	19	50	∿40
PTOX-50	50	50	∿30
PLASMA INITIATION			
PTOX-20-1P	20	45	∿40
PTOX-40P	40	45	27 - 31

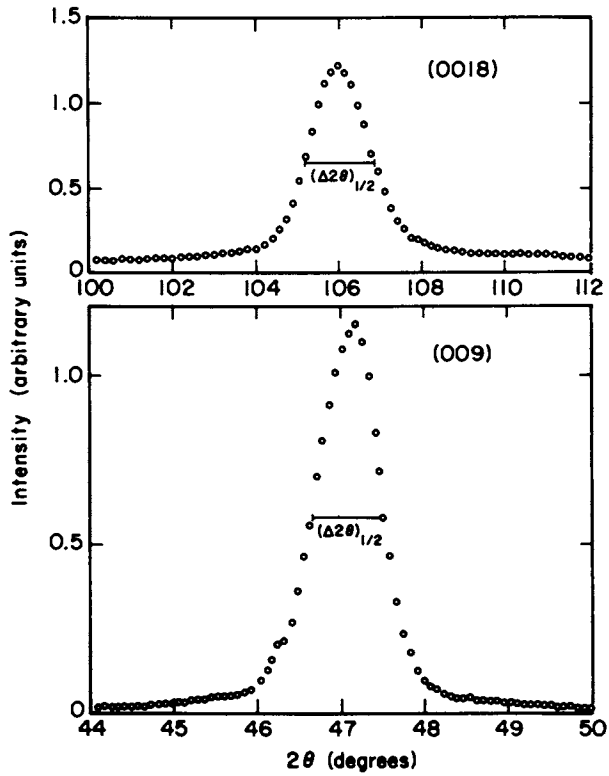

Figure 7. X-ray diffraction profiles of the (009) and (0018) reflections of PTEOX obtained by plasma initiation (s = 2 sin Θ/Λ)

0.015Å^{-1}). On the basis of these findings, one might conclude that PTEOX-5P contains less folded chain crystals and its c-spacings in the extended chain crystals are longer than those in the radiation samples. This conclusion, however, must be qualified by the possibility that the higher post-polymerization temperature used in the plasma initiation method may have annealed out some of the longitudinal compression during the post-polymerization period.

On the basis of the paracrystalline theory, the Cauchy-plot method can be employed in line-broadening analysis (12). In this method, the integral breadth of the first order reflection is approximated by

$$\Delta S_1 = 1/\bar{D}_w + \bar{c}(\pi g S_1)^2$$

where $\bar{D}w$ is the weight average crystallite size along the c-axis, $\bar{c}$ is the averaged c-spacing, g is the paracrystalline distortion parameter and $S_1 = 2 \sin \theta/\lambda$. From the slope and intersection of a S_1 vs. S_1^2 plot, values of g and $\bar{D}w$ can be readily obtained. For the plasma sample PTOX-40P, $\bar{D}_w$ = 650 Å and G = 1.25%. By contrast, the comparable radiation samples have values of 550 Å and 0.7%, respectively. The longitudinal dimensions for both samples are considerably shorter than the extended length of the microfibril, which is of the order of 10^4 Å. The most likely interpretation for this observation is that the type of defects suggested by the kink model (7) must exist in the chain direction.

DSC thermograms for plasma samples of PTOX and PTEOX are shown in Figure 8. The endothermic profiles of PTOX exhibit no superheating phenomenon, resembling those of the radiation samples post-polymerized below 50°C at high yield or above 50°C at low yield. It has been observed that a double endothermic peak appears in the heating curve of radiation polymerized PTOX at 55°C with a yield of over 20% (13). Superheating in these polymers was attributed to a new type of POM texture produced at the later stage of solid state polymerization.

Also shown in Figure 8 are the thermograms for PTEOX-4P and PTEOX-83P. They are very similar despite the differences in yield and morphologies. Neither sample shows superheating effect, although both have relatively long tail sections in the low temperature range. For the sake of comparison, we show in Figure 9 the endothermic profiles of radiation polymerized PTEOX. The profile of PTEOX-12 is extremely sharp, with a relatively low peak temperature (170°C). Samples PTEOX-25 and PTEOX-80, on the other hand, have much broader heating curves, indicating the presence of superposition of two endothermic curves resolved by the dotted lines. It is believed that these profiles consist of two crystalline forms, namely the lower melting folded chain crystallites and the higher melting extended chain crystallites (6, 9, 14). It is of interest to note that only one melting peak is present in the plasma samples, even though they were post-polymerized at elevated temperatures.

In conclusion, we can state that PTOX obtained through either

In Plasma Polymerization; Shen, M., et al.;
ACS Symposium Series; American Chemical Society: Washington, DC, 1979.

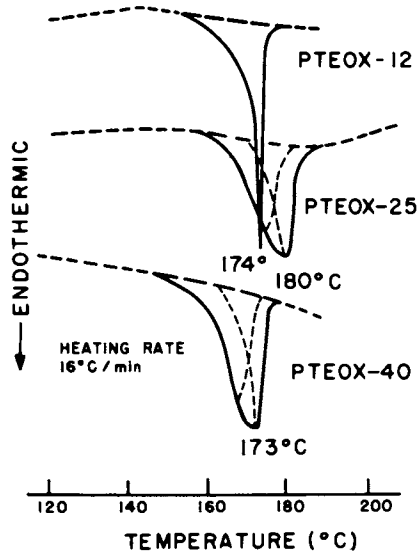

Figure 8. Differential scanning calorimetry thermograms of polytrioxane and polytetraoxane obtained by plasma-initiated polymerization in the solid state

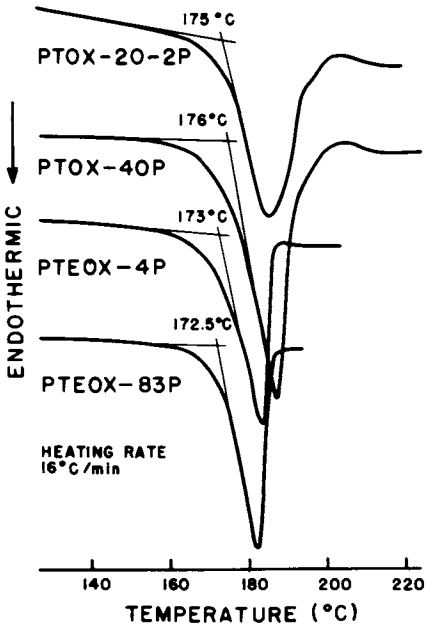

Figure 9. Differential scanning calorimetry thermograms of polytetraoxanes obtained by γ-ray-initiated polymerizations in the solid state. Dotted curves indicate the decomposed endothermic profiles caused by the extended chain crystals and folded chain crystals.

In Plasma Polymerization; Shen, M., et al.;
ACS Symposium Series; American Chemical Society: Washington, DC, 1979.

plasma or γ-ray initiated polymerizations have rather similar fine structures. However, there are some differences in the radiation samples and plasma samples of PTEOX. These differences can not yet be definitively established, since the fine structures are known to depend intimately on the polymerization conditions (temperature, yield, etc.) which are not exactly the same in the two polymerization techniques.

Abstract

Crystals of trioxane and tetraoxane can be polymerized in the solid state by plasma initiation followed by post-polymerization. Scanning electron micrographs indicate that PTOX consists of well aligned fibrils, while PTEOX have irregular coarse fibers with considerable branching. Small and wide angle x-ray scattering patterns indicate that PTOX crystals obtained through plasma initiation resemble those by γ-ray initiation. However, plasma samples of PTEOX appear to consist of one rather than two crystalline forms, as shown by both x-ray and differential scanning calorimetric data.

Literature Cited

1. Coleson, J. P., Reneker, D. H., J. Appl. Phys., (1970), 41, 4296.
2. Okamura, S., Hayashi, K., Nishi, M., J. Polymer Sci., (1962), B60, 526.
3. Lando, J., Morosoff, N., Morowitz, H., Post, B., J. Polymer Sci., (1962), B60, 124.
4. Voigt-Martin, I., Makromol. Chem., (1974), 175, 2669.
5. Osada, Y., Shen, M., Bell, A. T., Polymer Letters, in press.
6. Nakase, Y., Kuriyama, I., Odajima, A., Polymer J., (1976), 8, 35.
7. Wegner, G., Fischer, E. W., Munoz-Escalona, A., Makromol. Chem., (1975), Suppl. 1, 521.
8. Odajima, A., Ishibashi, T., Nakase, Y., Kuriyama, E., Rep. Prog. Polymer Phys. Japan, (1976), 19, 161.
9. Kato, T., Nakase, Y., Yoda, O., Kuriyama, E., Odajima, A., Polymer J., (1976), 8, 331.
10. Nakase, Y., Kato, T., Yoda, O., Kuriyama, I., Odajima, A., Polymer J., (1977), 9, 605.
11. Odajima, A., Ishibashi, T., Nakase, Y., Kuriyama, I., to be published.
12. Hoseman, R., Bagchi, S. N., "Direct Analysis of Diffraction of Matter," North Holland Publ. Co., Amsterdam, 1962.
13. Nakase, Y., Juriyama, I., Nishijima, H., Odajima, A., J. Mat'l Sci., (1977), 12, 1443.
14. Nakase, Y., Kuriyama, I., Polymer J., (1973), 4, 517.

Received March 29, 1979.

Tandem Plasma-Polymerization Apparatus for Continuous Coating of Fibers and Films

H. YASUDA[1] and N. MOROSOFF

Research Triangle Institute, P.O. Box 12194, Research Triangle Park, NC 27709

The study of polymers deposited from glow discharges in inductively coupled systems and on the electrodes of capacitively coupled systems has yielded interesting fundamental information and membranes and surfaces with useful properties. However, such plasma polymerization processes cannot be readily scaled up for efficient production of a desirable end product. A more promising approach is the coating of a substrate passing between the internal electrodes of a capacitively coupled system. It is the aim of this approach to limit the glow discharge to the interelectrode volume, thus avoiding deposition of polymer on the walls of the apparatus and to maximize the deposition rate of the polymer on the moving substrate. The use of a moving substrate is obviously compatible with the continuous coating of lengths of sheets or fibers. It also averages out variations in deposition rates and plasma polymer properties that may occur along the direction of substrate travel.

In this paper a tandem capacitively coupled glow discharge apparatus is described. It consists of two capacitively coupled reaction chambers placed in series so that the substrate may be subjected to two consecutive treatments before being wound up on a cylinder at the top of the apparatus.

The design of the reactor, the effect of plasma polymerization parameters on deposition rate at the electrode and on a substrate passing midway between and initial applications of the reactor are described below.

[1] Current Address: Department of Chemical Engineering
University of Missouri-Rolla
Rolla, Missouri 65401

0-8412-0510-8/79/47-108-277$05.00/0

I. Plasma Polymerization Parameters.

A. Frequency. The apparatus can be operated over a wide range of frequencies from AC to the radio frequency range because of the use of internal electrodes. We have employed frequencies of 60 Hz (AC), 10 kHz (AF) and 13.56 MHz (RF).

The first two of these are fundamentally different from the RF plasma. The AC and AF glow discharges may be considered DC glow discharges of alternating polarity [1]. A DC glow discharge is observed to have several lighter and darker zones. The most important zone for our purposes is the zone between the electrode and the negative glow. In this zone, consisting of the Aston dark space, cathode glow and Crooke's dark space, a major portion of the potential drop between the electrodes is found. The thickness of this zone is approximately the mean distance travelled by an electron from the cathode before it makes an ionizing collision [1]. The thickness is therefore inversely proportional to pressure and decreases with increasing potential drop between the electrodes. The negative glow which occurs after the Crooke's dark space is a zone of high concentration of positive ions formed by collision with energetic electrons emerging from the Crooke's dark space. These positive ions then are accelerated towards the electrode through the large potential drop existing between the negative glow and the cathode where they generate the secondary electrons which insure a self-sustained glow discharge.

The above description of a D.C. glow discharge is found in a variety of sources [1-4] and is applicable to simple di- and mono-atomic gases. The emphasis in these descriptions is on ions and electrons, in part because of the nature of the gases, in part because charged species are essential for a self sustaining glow discharge. In the case of polymerizable species, however, it is important to realize that bond dissociation as well as ionization is likely to occur in the negative glow and Crooke's dark space. It is probable that a high concentration of free radicals as well as of electrons and ions is contained within the negative glow. The presence of a high concentration of reactive species of all types in the zones adjacent to the cathode would favor deposition of plasma polymer at the cathode if the pressure in the plasma were such that the negative glow hugged the cathode. Preferential deposition of plasma polymer on the cathode in a DC glow discharge has been reported [5]. On the other hand the distance between the negative glow and cathode will increase as pressure in the glow discharge decreases. This would favor an increased substrate (midway between electrodes) to electrode deposition rate ratio with decreasing pressure, as has been experimentally observed [6].

In a RF plasma secondary electrons from the electrode do not contribute to the plasma as the positive ions cannot follow

In Plasma Polymerization; Shen, M., et al.;
ACS Symposium Series; American Chemical Society: Washington, DC, 1979.

the periodic changes in field polarity. The mechanism by which electrons pick up sufficient energy to cause bond dissociation or ionization involves random collisions of electrons with gas atoms, the electron picking up an increment of energy with each collision [1]. It is well known that a free electron in a vacuum under the action of an alternating field oscillates with its velocity 90° out of phase with the field, and thus takes no power, on the average, from the applied field. The electron can gain energy from the field only by suffering collisions with the gas atoms, and it does so by having its ordered oscillatory motion changed to random motion on collision. The electron gains random energy on each collision until it is able to make an inelastic collision with a gas atom [2]. It follows that a volume in which electrons are not able to participate in a sufficient number of collisions to reach ionizing energy will be a volume of low reactivity. Such a volume element is found at and near the electrodes where electrons are drawn from the plasma during the positive half of the RF cycle. Both electrodes therefore develop a negative bias with respect to the glow discharge, with the result that cations drift towards the electrodes. The size of the relatively inactive zone next to the electrode is proportional to the electric field and to the electron mobility. It therefore increases with increasing power and decreasing pressure. In fact at high power and low pressure an RF glow discharge is observed to spread outside the inter-electrode volume so that a glow is observed surrounding the set of electrodes while the inter-electrode volume itself remains relatively dark.

B. Flow Rate and Pressure. As shown above the pressure will affect the location and extent of active zones in the plasma. The pressure in a plasma is controlled by pumping rate of plasma reaction products, feed rate of monomer and the number of gaseous reaction product molecules generated per monomer molecule, i.e., γ. For a flow system (no plasma) the relationship between flow rate and pressure (pumping rate constant) is $F = a\,p^b$, where F and p are flow rate and pressure, respectively. Flow rates have been obtained from the slope of plot of pressure vs time (using a pressure transducer) when pumping is suddenly stopped. The relationship $F = a\,p^b$ is invariably satisfied with values of a and b varying from monomer to monomer. It is not possible to relate pressure in the capacitively coupled plasma to γ and F, as was done for an inductively coupled system, because part of the monomer flow will bypass the plasma in the present reactor.

The effect of pressure on glow differs with frequency. For AF and AC glow hugs the electrode at high pressure but extends further into the interelectrode volume at lower pressures. For RF, athe glow fills the interelectrode gap at high pressures

In Plasma Polymerization; Shen, M., et al.;
ACS Symposium Series; American Chemical Society: Washington, DC, 1979.

but begins to leave that gap and surround the electrodes at low pressures and high power.

The effect of increasing pressure on deposition rate is to increase the proportion of deposition on the electrode as opposed to that deposited on a substrate in the middle of the inter-electrode gap. This is particularly evident for AF and AC.

The effect of increasing flow rate in inductively coupled systems is to increase deposition rate as long as power is such as to maintain full glow in the reactor [7]. Other investigators have used a capacitively coupled system with RF and noted that at low flow rates, deposition rate is proportional to flow rate [8]. There is therefore reason to believe that deposition rate will be proportional to flow rate in the capacitively coupled system if the applied power is high enough.

C. Effect of a Magnetic Field. A magnetic field can be used to modify the distribution of the power density in the glow. In our apparatus, magnetic enhancement of the glow discharge was achieved as follows: An iron ring (9.5 cm in diameter) is concentrically attached to, but insulated from, the back of each aluminum electrode. A small disc (4.5 cm in diameter) is similarly attached to the back of the electrode. Four permanent horseshoe magnets are placed with north poles on the iron ring and south poles on the small iron disc. This arrangement is shown in Figure 1. The north-south vectors of the magnets are oriented at 90° intervals. In this way a donut shaped magnetic field is set up projecting into the inter-electrode gap, cylindrically symmetric about an axis passing through the electrode centers. The magnetic field vectors pass out of the electrode near its outer edge into the inter-electrode gap, curve in towards the electrode center axis and turn back towards the electrode re-entering it near its center. A donut shaped field is thus defined with the donut "hole" on the electrode center axis. Such a magnetic field tends to prevent escape of electrons (moving between electrodes) outside of the inter-electrode gap. It also forces electrons to take a convoluted path in oscillating between electrodes. This increases the probability of electron-molecule collisions as compared to the case where no magnetic field is present and electrons may move in a straight line from one electrode to the other.

In such a magnetic field an annular zone of glow is observed close to the electrode for AC and AF as shown in Figure 2. At pressure below 100 millitorr, it is possible to operate the glow discharge over a wider range of current, without arcing, than without magnets. For RF, the zone of intense glow resulting from the magnetic field is much more diffuse than for AF and AC, as shown in Figure 3. However, intense glow is concentrated closer to the electrodes than without magnets (for which an even glow throughout the interelectrode gap is observed) and it

In Plasma Polymerization; Shen, M., et al.;
ACS Symposium Series; American Chemical Society: Washington, DC, 1979.

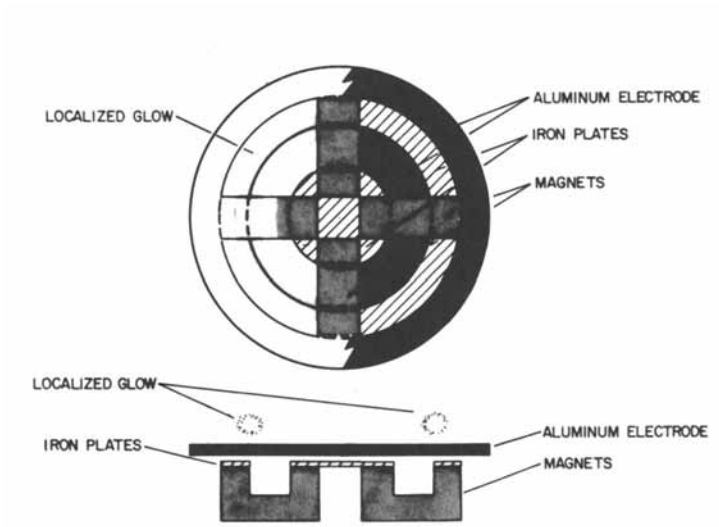

Figure 1. Schematic of the arrangement of magnets behind an electrode. The annular zone of intense glow shown is obtained in an AF or AC glow discharge as described in the text and illustrated in Figure 2.

In Plasma Polymerization; Shen, M., et al.;
ACS Symposium Series; American Chemical Society: Washington, DC, 1979.

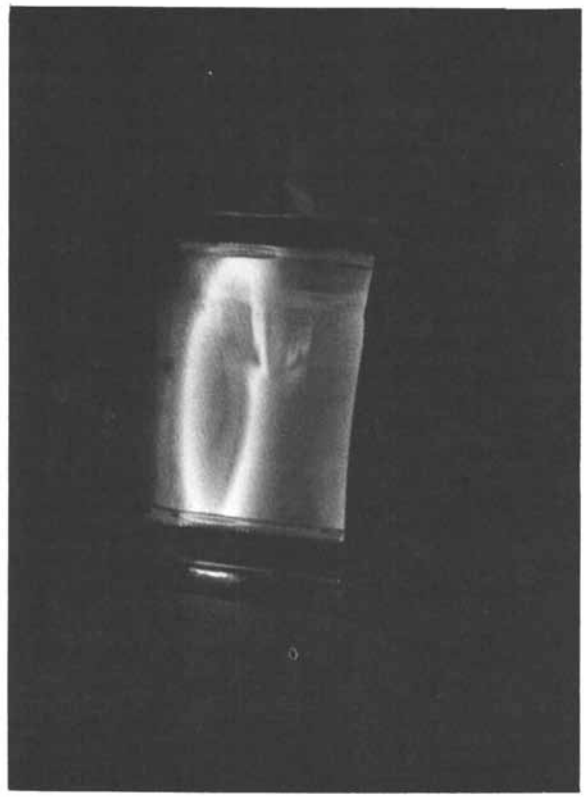

Figure 2. Photograph of an audio frequency glow discharge in the magnetic field. The pressure is 50 mtorr, current is 50 mA., N_2 gas is employed.

In Plasma Polymerization; Shen, M., et al.;
ACS Symposium Series; American Chemical Society: Washington, DC, 1979.

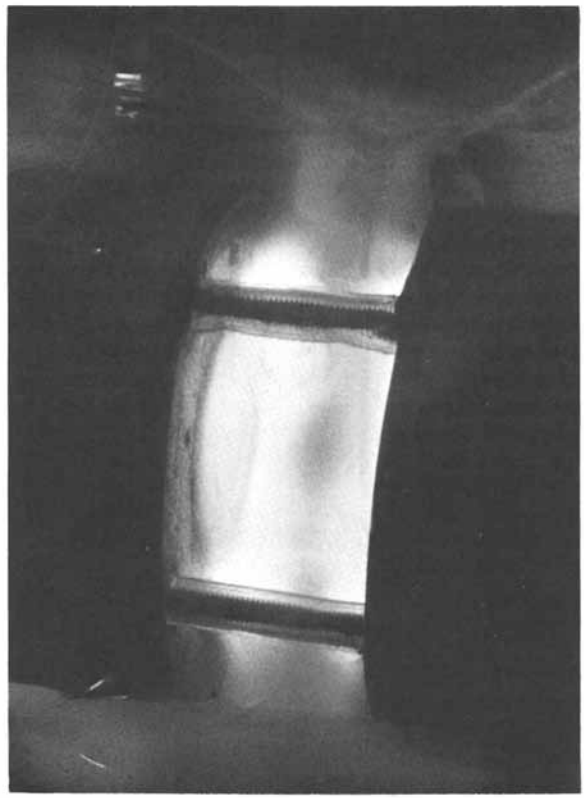

Figure 3. Photograph of a radio frequency glow discharge in the magnetic field. The pressure is 50 mtorr, power is 30 W, N_2 gas is employed.

In Plasma Polymerization; Shen, M., et al.;
ACS Symposium Series; American Chemical Society: Washington, DC, 1979.

is possible to operate the glow discharge over a wider range of power levels (at a pressure below 100 millitorr) without the glow discharge spreading outside the interelectrode gap.

II. Description of Apparatus:

The apparatus is schematically illustrated in Figure 4. It consists of two glass crosses, each containing circular aluminum electrodes, 14 cm in diameter. The interelectrode distance can be varied but we have found 5 cm to be convenient for most experiments. The two glass crosses are separated by a highly evacuated buffer chamber. Fibers (or films) may be pulled from one chamber to another through small holes (or slits) in Teflon plugs installed in the bulkheads between the glass crosses and the buffer chamber. The three chambers are evacuated via 1 1/2" wide (O.D.) metal tubing, electropneumatic valves, and glass traps connected to a Balzer's PST-650E high vacuum pumping station. The apparatus is completed by six spools at the bottom to feed in six hollow fibers which are drawn between the electrodes to a take up roll located in a glass T at the top of the apparatus. By achieving high fiber take-up rates gradually and using light aluminum spools at the bottom of the apparatus, fiber breakage is prevented. Each plasma polymerization chamber is connected to a manifold of metering valves to feed in monomer(s) and to a pressure transducer (MKS Baratron) to monitor pressure both before and after initiation of the glow discharge.

The apparatus has the following advantages:

1. Plasma polymerization can be effected using a variety of frequencies. Presently frequencies of 60 Hz (AC), 10 kHz (AF) and 13.56 MHz (RF) are employed.

2. The deposition rate of plasma polymer is flow rate dependant. For a commercially feasible plasma coating operation plasma polymer should be deposited at a high rate so that the substrate may be pulled through the plasma at a rapid rate of speed. This requirement therefore implies that requirements of high flow rate and operation at low pressures can only be satisfied by using a high capacity pump and wide (1 1/2" I.D.) tubing and valves to the pump. The apparatus is capable of maintaining a pressure of 20 millitorr at a flow rate of better than 10 cm^3 (S.T.P.)/minute.

3.) The combination of two plasma polymerization chambers divided by an evacuated buffer chamber allows two different gases to be introduced into each chamber with and/or without initiation of a plasma. The pressures in each chamber are independent of that in the other and there is no cross-contamination of gas thanks to the buffer chamber. Possible combinations of substrate treatments are:

a. Preabsorbtion of monomer in a controlled manner followed by plasma polymerization.

In Plasma Polymerization; Shen, M., et al.;
ACS Symposium Series; American Chemical Society: Washington, DC, 1979.

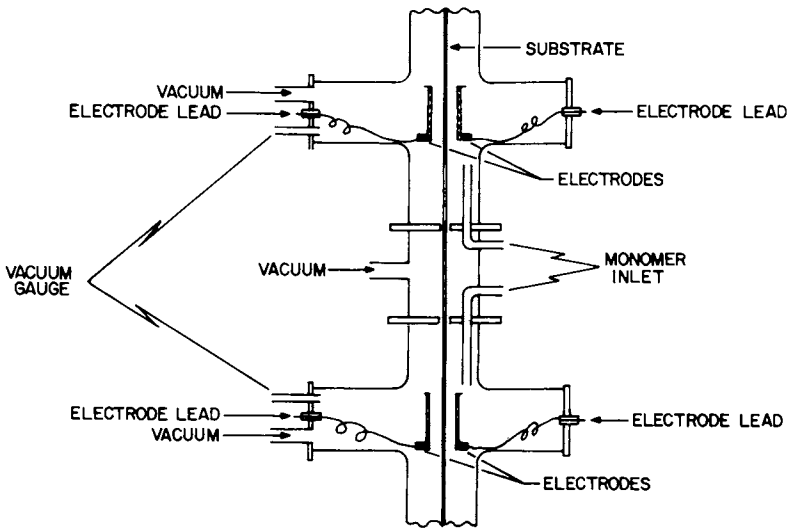

Figure 4. Schematic of the tandem glow discharge apparatus.

b. Plasma polymer coating using different monomers in each stage.
c. Plasma treatment in one stage plus plasma polymer coating in another.
d. Plasma coating or treatment in one stage followed by exposure to vinyl monomers for additional free radical initiated plasma polymerization.

Studies of the plasma polymerization of tetrafluoroethylene in such a capacitively coupled system are described in another paper presented at this symposium [9]. The apparatus has been used to coat polysulfone hollow fibers with pyridine and acetylene + nitrogen plasma polymer to form a composite reverse osmosis desalination membrane. Salt rejections of 90-93% have been achieved at fluxes of 1.5-2.0 g.f.d with a fiber take up rate of 50-100 cm/min.

Acknowledgement: The authors gratefully acknowledge the contributions of W. Newton and B. Hill who helped design, build and operate the apparatus. This work was supported by the Office of Water Research and Technology of the U. S. Department of the Interior under Contract Nos. 14-30-3301 and 14-34-0001-7537.

Literature Cited:

1. L. Maissel, "Application of Sputtering to the Deposition of Films, in L. Maissel and R. Glang eds. "Handbook of Thin Film Technology," McGraw Hill, N. Y. (1970).
2. S. C. Brown, "Introduction to Electrical Discharges in Gases", J. Wiley and Sons, New York (1966).
3. A. von Engel, "Ionized Gases," 2nd ed., Oxford (1965).
4. J. D. Cobine, "Gaseous Conductors", 1st ed., McGraw Hill, New York (1941).
5. H. U. Poll, M. Arzt and K. H. Wickleder, Eur. Polym. J., 12.
6. N. Morosoff, W. Newton, H. Yasuda, J. Vac. Sci. Technol., in press.
7. H. Yasuda, T. Hirotsu, J. Appl. Polym. Sci, 21, 3139 (1977).
8. H. Kobayashi, A. T. Bell, M. Shen, Macromol., 7, 277 (1974).
9. N. Morosoff and H. Yasuda, this symposium.

Received March 29, 1979.

Mechanical Properties of Polymer Composites Using Plasma-Modified Mica Filler

H. P. SCHREIBER

Department of Chemical Engineering, Ecole Polytechnique, P.O. Box 6079, Montreal H3C 3A7, Québec, Canada

M. R. WERTHEIMER and A. U. SRIDHARAN

Department of Engineering Physics, Ecole Polytechnique, P.O. Box 6079, Montreal H3C, 3A7, Québec, Canada

The use of polymer-based composites has been increasing rapidly in recent years. Mica has been an important mineral filler in the evolution of composites, its use being favored particularly in mechanical and in electrical insulation applications because of its well-proven insulating properties, its relative abundance, low cost and environmental safety.

In any preparation of polymer-filler composites, there is concern about the quality of adhesion at the filler/matrix interface, and consequently over the interaction between filler and molten polymer at the compounding stage. Various technologies have been proposed to enhance adhesion; in our laboratories, we have developed surface treatment (encapsulation) techniques in which mica is exposed to a "cold" microwave plasma (i.e. $T_{electron}/T_{gas} >> 1$) in a "Large Volume Microwave Plasma Generator"(LMP) prior to being contacted with the polymer matrix. This method of surface modification is brief, non-polluting, and involves only low-cost materials. Cold plasmas in organic vapours are known to produce thin, solid polymer films (2-4) which are generally highly cross-linked, adhere strongly to the substrate and can be made free of imperfections such as "pinholes". In earlier work we have shown that mica surfaces can be rendered either more hydrophilic or hydrophobic through LMP treatments (5) and that certain mechanical properties of mica filled polyethylene (PE) and polystyrene (PS) can be enhanced when the filler was pre-treated in ethylene (E) and styrene (S) plasmas, respectively (6). The electrical properties of such composites were also shown to respond favorably to plasma-modification of the filler surface (7, 8).

The present paper extends initial work (6) on the modification of mechanical properties in mica-filled PE and PS, and in particular explores the possibility of upgrading the properties of PE/PS blends. These two polymers are incompatible and are known to form 2-phase systems both in the molten and solid states (9). In order to modify favorably the interaction balance at PE/PS contacts, mica was subjected to LMP treatments using E and S monomers in sequence. In principle, the generation of plasma-polymerized ethylene (PPE) and styrene (PPS) on the mica surface might

0-8412-0510-8/79/47-108-287$05.00/0

create wetting/adhesion sites for each of the matrix polymers with benefits to the mechanical responses of the composite systems. An initial view of this principle is presented in this work.

EXPERIMENTAL

A low-density, extrusion grade polyethylene, melt flow index (10) = 1.2 (supplier Canadian Industries, Ltd), and a general purpose polystyrene resin (supplier Dow Chemical Co.) were the base polymers for this study. Blends of these polymers in 1:1 weight ratios (PE/PS) were prepared by roll-milling the materials at 200°C for 10 min, with the addition of 0.1% (wt.) of a commercial thermal stabilizer (Santonox - TM, Monsanto Co.) Roll-milled stocks were reduced to fibril consistency by mechanical grinding. A high aspect ratio phlogopite mica with low water content supplied by Marietta Resources International Ltd. under the trade name of "Suzorite", was used as the filler in this research. Dry-screened fractions (-40/70 mesh) were used in surface modification experiments. In this procedure approx. 5 gm samples were placed in the quartz tube of the plasma generator (1, 5) and the charged tube was evacuated to about 10^{-3} torr. A flow of either E or S monomer gas was then established and controlled with a needle valve and flow meter to produce (dynamic) constant pressures in the experimental range 0.5 - 5 torr. Plasma discharges were produced with about 1.0 KW of 2.45 GHz microwave power. Except where otherwise indicated, plasma treatments were of 90 sec. duration. In a number of instances, mica samples were exposed to sequential treatments in E followed by S-monomer (E/S); the reverse, S/E sequence, was also studied. In these sequential treatments, uniform conditions of 2 torr monomer gas pressure were maintained. Mica samples were re-evacuated to ~ 10^{-3} torr following the first plasma exposure, and only then was the second monomer introduced into the apparatus. The quartz tube reactor containing the mica was continuously rotated during all plasma-treatments, to ensure uniform exposure of surfaces. Following treatment, mica samples were aged in the LMP apparatus for 24 hr. under dry nitrogen, and were then dispersed in molten (190°C) PE, PS and PE/PS, in a Brabender Plasticorder, to give stocks with filler contents of 10 - 30% (W/W). These stocks were then compression molded at 190°C. Specimens cut from the molded plates were used for determination of elastic modulus (ε) and of ultimate tensile strength (U.T.S.) in stress-strain measurements, with the Instron Tester operating at jaw-separation speeds of 0.5 in/min and 5 in/min., respectively. Impact resistance data were obtained using the Tinius-Olsen pendulum apparatus. A number of mica samples was examined by thermo-gravimetric analysis, using the Mettler Thermoanalyser and a heating rate of 5°C/min. Control stocks of filled polymers included some in which micas were heated under nitrogen (300°C, 30 min) but were not exposed to plasmas.

RESULTS AND DISCUSSION

A) Elastic Modulus: The elastic moduli of control and test

In Plasma Polymerization; Shen, M., et al.;
ACS Symposium Series; American Chemical Society: Washington, DC, 1979.

composites containing plasma-modified micas are represented as functions of filler weight per-cent in Figures 1, 2 and 3. Figure 1 shows results for PE-based systems, Figure 2 those for PS, and Fig. 3, the ε values for PE/PS composites. In all cases, the ε datum is a mean of at least 5 separate determinations, with a reproducibility of about ± 10%.

The data for PE(Fig. 1) may be compared with the findings of Woodhams and co-workers (11). In contrast with these authors, no reinforcement due to untreated mica can be discerned - indeed, there is a decrease of some 60% in ε at 30% mica loading. Similarly, untreated mica produces no "benefits" in terms of modulus enhancement in PS and PE/PS stocks (Figs. 2, 3). We conclude that wetting and adhesion at mica/polymer interfaces is poor, leading to significant decreases in the elastic modulus. A very different situation exist in composites with plasma-modified micas. As seen in Fig. 1, micas produced by E, S/E and E/S plasmas reinforce the PE matrix, the sequentially S/E treated fillers more than tripling the elastic modulus relative to PE, and increasing this by an order of magnitude relative to the (20%) composite using untreated mica. On the other hand, S-treated mica is marginally less "compatible" with the polymer than is the untreated filler.

The persistence of the above pattern in Figures 2 and 3 is self-evident. E-modified micas produce a decrease in ε of PS composites, while S-treatment and sequentially-treated micas enhance the elastic modulus. The overall reinforcement of ~ 40% relative to virgin PS is not as pronounced as in the case of PE, though at 20% mica, the relative increase in ε is still a substantial one (e.g. ~ 250% for E/S vs. unmodified, filled stocks). The results for PE/PS blends are analogous to those for PS.

The data in Figs. 1 and 2 clearly indicate the need to match the monomer used in plasma-treatment with the matrix polymer. Allowing for certain structural differences between PPE or PPS and their conventional counterparts (4), it is nevertheless suggested that much stronger bonding occurs at the polymer/filler interface, when the filler contains contact sites which are essentially polyethylene-like, or polystyrene-like. In view of the incompatibility of PE and PS (9) the deterioration in ε when the monomer used in plasma-polymerization and matrix polymer are mismatched, may be rationalized. The superior performance in all cases (Fig. 1, 2, 3) of sequentially-treated micas is particularly noteworthy. Plasma exposure times in these micas have been doubled hence a more effective encapsulation of the filler surface by plasma-polymer is indicated. The frequency of matrix polymer/mica contacts (inherently unfavorable) is thereby reduced, with beneficial consequences. Assuming that polymer sites formed in the final step of sequential plasma treatments are more readily accessible, the advantages of S/E sequences in Fig. 1 and of E/S in Fig. 2 appear logical. The evident advantage of S/E over E/S sequences in the PS/PE blends (Fig. 3) may be due to the fact that styrene is a more readily plasma-polymerized monomer (2). Conceivably, under present conditions, PPS layers may tend to obscure PPE sites in E/S sequences, while in S/E sequences both types of polymer are more readily

In Plasma Polymerization; Shen, M., et al.;
ACS Symposium Series; American Chemical Society: Washington, DC, 1979.

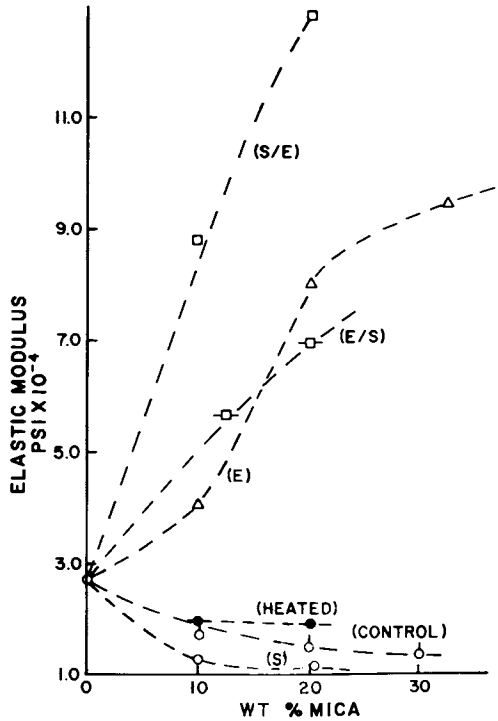

Figure 1. Elastic modulus of PE stocks—effect of mica and various surface treatments

In Plasma Polymerization; Shen, M., et al.;
ACS Symposium Series; American Chemical Society: Washington, DC, 1979.

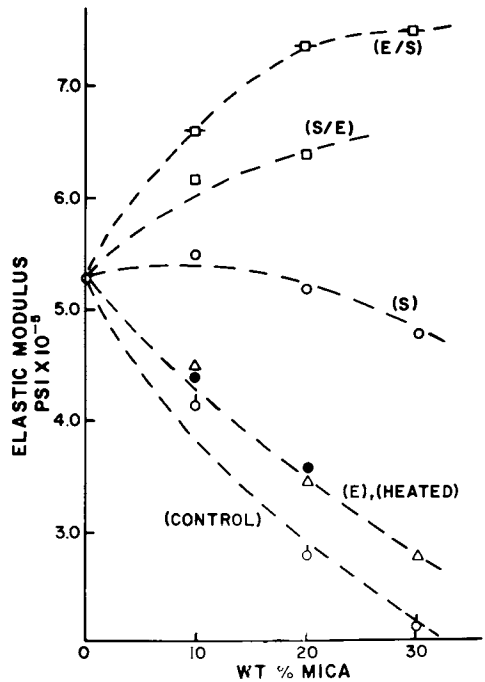

Figure 2. Elastic modulus of PS stocks—effect of mica and various surface treatments

available on the mica surface for bonding with the matrix polymers. The latter treatments thus appear to produce the more effective "bridging" agents, and appreciably modify the inherent incompatibility problem in this polymer pair.

Finally, control experiments using heated micas were performed in order to separate plasma and simple heating effects. As shown in Fig. 1, 2 and 3, modifications in elastic modulus are plasma - and not heat-generated.

B) Tensile and Impact Performance: Table I presents a summary of tensile impact and ultimate tensile data for the three sets of composites. For ease of comparison both sets of data are normalized to the reference tensile impact or ultimate tensile performance of the unfilled polymer matrix.

The tabulation makes clear the embrittling effect of mica on the inherently ductile PE; on the other hand, the tensile impact resistance of filled PS stocks is slightly increased, hence mica acts as a toughener for this polymer. Both sets of performance data in PS/PE blends are deteriorated by the addition of the filler. The general trend, already established by the ε values is repeated in Table I: Marked property improvement is associated with a match of monomer environment used in plasma-treatments of mica and the intended polymer matrix. Mismatches again tend to produce results which are inferior to those obtained with untreated micas. The most interesting results again are those for stocks using sequentially-treated micas. The "bifunctional" filler surfaces are the near equivalents of matched - monomer fillers when used with single polymer matrixes. The effective coupling tendency shown by these bifunctional fillers are particularly evident in the PE/PS blend. Here, tensile strength is raised by 30 - 50% over that of unfilled controls, and by well over 100% relative to compounds with comparable quantities of untreated micas. Even more appreciable inprovements are observed in the tensile impact performance. These results demonstrate the technical feasibility of producing complex, multi-functional surface properties by the LMP route, and consequently suggest the possibility of significantly upgrading and stabilizing the properties of inherently incompatible polymer combinations. These concepts warrant more detailed study in the future.

It was not within the scope of this work to perform detailed analyses of the chemical modifications imparted to plasma-treated mica surfaces. Thermogravimetric analyses were performed, however, and these provide indirect confirmation for the presence of plasma-produced polymers on the filler surface. Weight loss observations in heating various mica specimens to 300°C are given in Table II. Thermogravimetry was also performed on micas as received, without further preparation of the filler. Plasma-treated micas, however, were stored for periods of about 1 week at 70% r.h. and ambient temperature prior to analysis. Of the plasma-modified fillers, only E-treated micas display appreciable weight-loss, though even here this is greatly reduced in comparison with untreated mica. Attributing the bulk of weight losses to the evolution of physisorbed and chemisorbed water (12), the data in Table II attest to

In Plasma Polymerization; Shen, M., et al.;
ACS Symposium Series; American Chemical Society: Washington, DC, 1979.

TABLE I

TENSILE IMPACT AND ULTIMATE TENSILE PERFORMANCE
OF PLASMA - TREATED MICA STOCKS

Filler:		Tensile Impact (ft-lb/in)			U.T.(p.s.i. x 10^{-3})		
		PE	PS	PE/PS	PE	PS	PE/PS
%	Treatment						
-	-	18.6	0.20	0.96	1.92	5.84	1.84
	normalization →	1.00	1.00	1.00	1.00	1.00	1.00
10	-	0.097	1.18	0.65	0.55	0.20	0.79
20	-	0.055	1.13	0.47	0.47	0.15	0.58
30	-	0.047	1.07	0.39	0.31	0.09	-
10	heat	0.16	1.17	0.63	0.61	0.23	0.80
20	heat	0.11	1.20	0.50	0.54	0.20	0.60
10	S	0.044	2.90	0.73	0.33	0.48	1.26
20	S	0.030	2.66	0.59	0.22	0.36	1.19
30	S	-	2.21	-	-	-	-
10	E	0.206	0.65	0.56	1.72	0.11	0.93
20	E	0.217	0.47	0.51	1.59	0.07	0.88
30	E	0.188	0.45	0.40	1.51	-	-
10	S/E	0.180	1.85	1.86	1.25	0.95	1.16
20	S/E	0.167	1.53	1.45	1.18	0.90	1.11
30	S/E	0.188	2.15	2.17	-	-	-
10	E/S	0.172	2.88	1.88	1.41	1.16	1.43
20	E/S	0.163	2.39	2.06	1.18	1.20	1.37
30	E/S	0.115	2.90	1.88	-	-	-

In Plasma Polymerization; Shen, M., et al.;
ACS Symposium Series; American Chemical Society: Washington, DC, 1979.

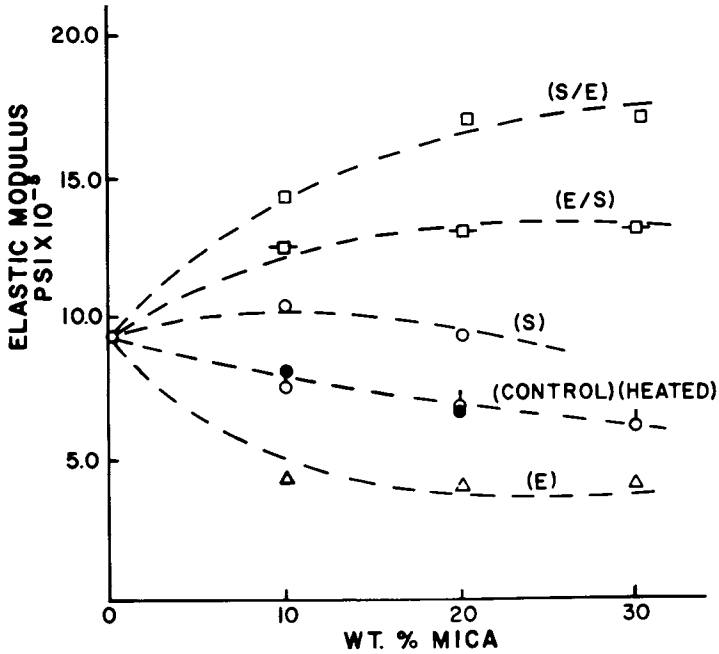

Figure 3. Elastic modulus of PE/PS stocks—effect of mica and various surface treatments

TABLE II

THERMOGRAVIMETRIC ANALYSES ON VARIOUSLY TREATED MICAS: WEIGHT LOSS TO 300°C

Sample	ΔW(%) at 50°C	at 100°C	at 200°C	at 300°C
Control mica	0.07	0.11	0.33	0.36
E-Plasma[(a)]	nil	0.02	0.06	0.11
S-Plasma[(a)]	nil	nil	0.02	0.04
E/S Plasma[(a)]	nil	nil	< 0.01	0.06
S/E Plasma[(a)]	nil	nil	nil	< 0.02

(a) All plasma sequences at 2 torr pressure, 90 sec. duration.

In Plasma Polymerization; Shen, M., et al.;
ACS Symposium Series; American Chemical Society: Washington, DC, 1979.

the presence of essentially impenetrable hydrophobic layers at the filler surface, following plasma treatment. The less impressive performance following ethylene-treatment may be due to incomplete surface coverage; we assume that the arbitrarily chosen plasma-treatment conditions were insufficient to produce such a layer with the less readily polymerized monomer.

C) Plasma-treatment variables: In all of the above comparisons, the various mica samples had been exposed to plasmas under arbitrarily selected, constant conditions of monomer pressure, plasma duration and applied power. It is very probable (2, 4) that these variables and possibly others, such as reactor geometry and post-treatment history, may influence strongly the magnitude of surface modification effects attained by the present route. For this reason the performance modifications of polymer composites will also depend on the exact selection of treatment variables. A detailed study of the problem is called for to permit the design of surface modification procedures capable of meeting desired degrees of performance modification.

As a first step in this direction, we studied the effect of S monomer pressure and of treatment duration on the properties of 10% mica-filled PS stocks.

Monomer pressure was varied in the range 1 - 4 torr, in all cases for 90 sec plasma duration. On the other hand, the standard 2 torr pressure was maintained in a series of treatment durations in the range 60 - 360 sec. The effect of varying S monomer pressure is displayed in Fig. 4; that of varying duration in Fig. 5. Impact strength and elastic modulus are the performance criteria used in each sequence.

It is evident that monomer pressure and plasma duration strongly affect the modifying influence of mica filler in the PS stock. An optimum monomer pressure in the 2-3 torr range is indicated, the tensile impact being particularly sensitive to this variable (Fig. 4). Treatment time is even more significant (Fig. 5), both modulus and impact resistance responding strongly to its variations. An optimum treatment time in the range 100 - 150 sec. appears to be associated with elastic modulus response. We assume that tensile impact of mica filled PS improves with plasma duration up to about 240 sec., and remains near an "optimum plateau" if longer treatment times are used for surface modifications of the mica.

Considering the probable large number of important treatment variables and the likelihood of interdependence among them, the subject becomes one of considerable complexity and importance. Detailed studies are underway to clarify the situation.

CONCLUSIONS

It is concluded that surface modification of mica, produced by exposing the material to microwave plasmas, can create large positive or negative effects in the mechanical properties of filled polymers and polymer blends. Property enhancement is associated with the production of surface layers on the filler which

In Plasma Polymerization; Shen, M., et al.;
ACS Symposium Series; American Chemical Society: Washington, DC, 1979.

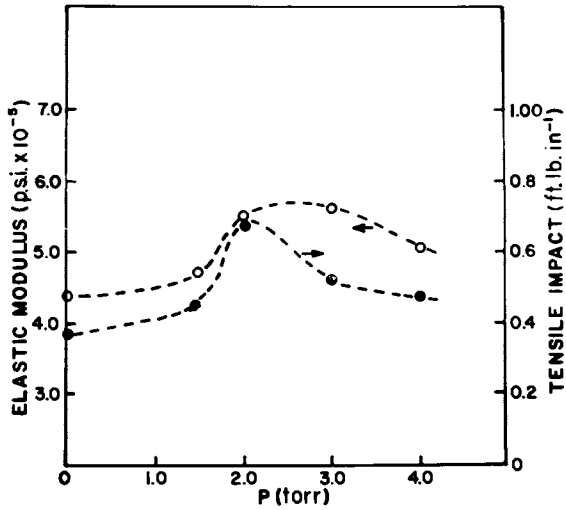

Figure 4. Influence of S monomer pressure on effect of mica (10%) as modifier of PS mechanical properties

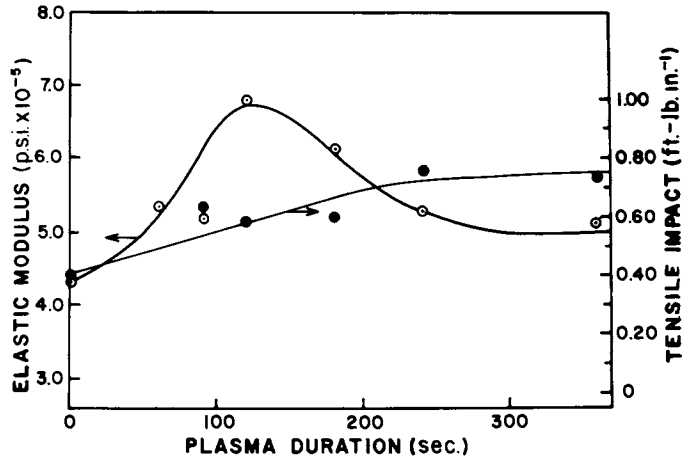

Figure 5. Influence of S-monomer plasma duration on effect of mica (10%) as modifier of mechanical properties in PS

In Plasma Polymerization; Shen, M., et al.;
ACS Symposium Series; American Chemical Society: Washington, DC, 1979.

are chemically similar to the matrix polymer. It is assumed that strong adhesion at polymer/filler contacts is promoted by such plasma-treatments and accounts for the observed property enhancement. It has been shown that several dissimilar surface structures can be produced on micas by sequential plasma treatments with appropriate monomers, allowing the filler to serve as a bridging (stabilising) agent for incompatible polymer pairs. Comprehensive studies of the variables in plasma polymerization will be required to optimize documented effects in the behavior of composites and polyblends.

ACKNOWLEDGMENT

Financial support for this research was received from the National Research Council of Canada, and from the Quebec Ministry of Education. We thank Prof. R.G. Bosisio for the loan of equipment.

ABSTRACT

A "Large Volume Microwave Plasma Generator" (LMP) has been used for surface treatment of phlogopite mica flakes in plasmas of styrene, ethylene and in sequences of these organic vapors. Plasma-modified mica flakes were used as fillers, at 10 - 30 wt.% levels, in polyethylene (PE), polystyrene (PS) and in 1:1 mixtures of these polymers. Tensile and impact properties of the composites show that ethylene and styrene-plasma treatments enhance the properties of PE and PS, respectively, but weaken the composite when the treatment monomer and matrix polymer are mismatched. Micas exposed to the two monomer vapors in sequence are particularly effective in enhancing the mechanical properties of inherently incompatible PE/PS blends, seemingly acting as coupling or compatibilizing agents for this polymer pair. The results are consistent with the formation of plasma-polymerized layers which either act as "bridges" between the polymer matrix and the mica filler, or else (in the case of mismatch due to incompatible polymers) prevent effective bonding. Initial studies have been carried out on the variation in plasma effectiveness due to changes in monomer pressure and treatment time.

LITERATURE CITED

1): R.G. BOSISIO, M.R. WERTHEIMER and C.F. WEISSFLOCH, J.Phys. E., Sc. Instr. 6, 628 (1973).

2): J.R. HOLLAHAN and A.T. BELL: "Techniques and Applications of Plasma Chemistry", Wiley-Interscience Publishers, New York,N.Y. (1974).

3): M.R. HAVENS, M.E. BIOLSKI and K.G. MAYHAN, J. Vac. Sci. and Technol. 13, 575 (1976).

4): "Plasma Chemistry of Polymers" M.Shen, Ed. Marcel Dekker, Inc. New York, N.Y. (1976).

5): A. BIALSKI, R. St.J. MANLEY, M.R. Wertheimer and H.P.

SCHREIBER, J. Macromol. Sci., Chem. A10, 609 (1976).
6) H.P. SCHREIBER, Y. TEWARI, and M.R. WERTHEIMER, J. APpl. Poly. Sci. 20, 2663, (1976).
7) M.R. WERTHEIMER, L. PAQUIN and H.P. SCHREIBER, J. Appl. Poly., Sci. 20, 2675 (1976).
8) L. PAQUIN, A.U. SRIDHARAN, M.R. WERTHEIMER and H.P. SCHREIBER. In Press: Proc. 2nd Int'l Conference on Composite Materials, (ICCM II) Toronto, Canada, April 1978.
9) C.D. HAN and T.C. YU, Polym. Eng. Sci. 12, 81 (1972).
10) A.S.T.M. D-1238-62& Amer. Soc. for Test. Mat. Philadelphia (1962).
11) J. LUSIS, R.T. WOODHAMS and M. XANTHOS, Polym. Eng.Sci. 13, 139 (1973).
12) M.S. METZIK, V.D. PEREVERTAEV, V.A. LIOPO, G.T. TIMOSCHENKO and A.V. KISELEV, J. Coll. Interface Sci. 43, 4223 (1974).

RECEIVED March 29, 1979.

Plasma Etching of Poly[*N,N'*-(*p,p'*-Oxydiphenylene) Pyromellitimide] Film and Photo/Thermal Degradation of Etched and Unetched Film

T. WYDEVEN, C. C. JOHNSON, M. A. GOLUB, M. S. HSU, and N. R. LERNER
Ames Research Center, NASA, Moffett Field, CA 94035

Recently, interest has been shown in a solar sail to propel spacecraft through the solar system, using the pressure of sunlight on the sail as the driving force (1,2). A thin reflective metal-coated plastic film was required for the sail which would be stable for long periods of time to the severe temperature and radiation conditions encountered in space. One of the films considered for the solar sail was the polyimide film prepared from pyromellitic dianhydride and bis-(4-aminophenyl) ether (3,4):

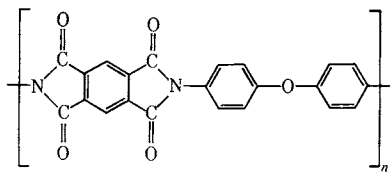

The desired thickness of the film for the solar sail application was ∿2.5 μm, but the thinnest commercially available film of this type was Du Pont's Kapton (5) with a thickness of ∿7.5 μm. Hence, a need existed to thin the latter film and to assess the photo- and thermal stability of the resulting, thinned film. This paper describes the use of a radiofrequency (RF) oxygen plasma for etching (thinning) of poly[N,N'-(p,p'-oxydiphenylene) pyromellitimide] (POP) film, and presents data on the photo/thermal degradation of etched and unetched film in vacuum. Although plasma etching has been applied to many polymers (6,7), it has scarcely been used on polyimides.

Experimental

Plasma Etching. The glow discharge reactor used in oxygen plasma etching of POP film was described previously (8). The reactor pressure was monitored with a capacitance manometer (MKS

Instruments, Inc.), and the temperature measured with a thermocouple attached to the bottom of an aluminum plate used to support the film during thinning. Kapton (5) film (nominal thickness 7.5 μm) was cut into rectangular sheets (12.3 cm × 17.8 cm) which were placed on the plate held midway between the reactor electrodes (5 cm apart). The reactor conditions for etching were as follows:

O_2 pressure (discharge off):	73 Pa (0.55 Torr)
O_2 flow rate:	5×10^{-8} m^3/s
RF (13.56 MHz) power (forward):	90 W
RF power (reflected)	0 W

The plate supporting the film was at ambient temperature at the start of thinning and ∿150-225°C at the end.

Gas Analysis. The gases produced in the etching process were trapped in two liquid nitrogen cold traps in series and identified using a mass spectrometer (Hewlett-Packard Model #5982A). The gases in the first trap consisted of CO_2 and H_2O. The second trap was partially filled with activated 5A molecular sieve adsorbent to trap the products volatile at liquid nitrogen temperature (N_2, O_2, CO, H_2 and some CO_2). The contents of the traps were analyzed separately; the amounts of the gases were determined from pressure measurements in a known volume, while H_2O was determined gravimetrically.

Spectroscopy. Transmission and ATR IR spectra were obtained with a Perkin-Elmer Model 180 or 621 spectrometer. Absorption spectra were obtained on a Cary 14 spectrophotometer, while ESR spectra were obtained with a Varian V-4502 spectrometer in the manner described elsewhere (9). X-ray photoelectron spectra of the etched and unetched films were provided by Surface Science Laboratories, Palo Alto, Calif., using a Hewlett-Packard Model 5950 ESCA spectrometer. Some films were also examined with an International Scientific Instruments Model MSM-2 "Mini-Sem" scanning electron microscope.

Thickness of the plasma-etched films was determined using Beer's Law and measuring the absorbance of the 1770-cm^{-1} cyclic imide band, assuming an average absorbance of 0.844 for the nominal 7.5-μm (unetched) film.

Photo/thermal Degradation. Samples of etched (∿2.5 μm) and unetched (∿7.5 μm) POP film were placed in quartz tubes which were continuously evacuated while being heated at temperatures >450°C in a constant temperature block, controlled to ±2°C. Other film samples contained in quartz tubes evacuated to $<10^{-5}$ Torr were exposed to a Hanovia 450-watt mercury lamp with the etched side facing the lamp. At 14 cm from the lamp, the intensity of the uv radiation incident on the films was equivalent to ∿5.9 times that of the Sun in the 2000-3500-Å range at 1 astronomical unit, i.e., just outside the atmosphere. At that distance from the lamp, the temperature of

In Plasma Polymerization; Shen, M., et al.;
ACS Symposium Series; American Chemical Society: Washington, DC, 1979.

the film was <120°C, not high enough to have an effect in the absence of uv radiation or produce a thermal component in the photochemical effects. The films before and after various times of heating or irradiation were examined by absorption spectroscopy, as well as by IR and/or ESR spectroscopy. The photo/thermal effects were followed by changes in absorbance, $\Delta A = A_t - A_o$, where A is the absorbance at 600 nm and the subscripts o and t refer to a given film before and after heating or irradiation. The gases produced in several photo/thermal degradation runs were collected and analyzed by mass spectrometry.

Results

Appearance and Thickness of Plasma-Etched Films. The etched films were light yellow due to thinning, in contrast to the dark yellow color of the unetched film, and showed no damage, either visually or by scanning electron micrographs (5000X). The thinned films were pliable with no evidence of increase in brittleness or formation of brittle regions. The micrographs revealed that the surface of the thinned films was somewhat more textured or grainy than the original films.

Rate of Oxygen Plasma Etching. The rate of thinning of the POP film was calculated from the average thickness, before and after thinning, and from the time for thinning. The rate was thus found to be 0.92 nm/s (average of 18 samples), with a standard deviation of 0.04 nm/s.

Infrared Spectra. Since the transmission IR spectra of the etched and unetched films were identical, as were also the ATR spectra, and were essentially the same as that for a 2.5-μm POP film presented elsewhere (3,4), there was no need to show them here.

Gas Analysis. The gaseous products formed in plasma etching of POP film are summarized in Table I. The amount of carbon

TABLE I
GASEOUS PRODUCTS FROM PLASMA ETCHING OF POP FILM[a]

Gas	Yield, mmol/g	Elemental composition accounted for, mmol/g[b]		
		C	H	N
CO	8.21 ± 3.6	8.21		
CO_2	37.2 ± 4.3	37.2		
H_2O	13.9 ± 0.8		27.8	
H_2	1.4 ± 0.7		2.8	
N_2	3.5 ± 1.2			7.0

[a] $(C_{22}H_{10}N_2O_5)_n$: C, 57.6; H, 26.0; N, 5.2 mmol/g. (Calcd.)
C, 56.9; H, 29.2; N, 5.3 mmol/g. (Anal.)

[b] Total products: C, 45.4 ± 7.9; H, 30.6 ± 3.0; N, 7.0 ± 2.4 mmol/g.

In Plasma Polymerization; Shen, M., et al.;
ACS Symposium Series; American Chemical Society: Washington, DC, 1979.

accounted for in the products is less than expected, while the amounts of hydrogen and nitrogen are greater than expected. The discrepancies might be due to incomplete conversion of CO to CO_2 which could have the effect of some CO being counted as N_2; this would give rise to a lower carbon and a higher nitrogen than expected. Also, some water absorbed in the film could cause the carbon to be lower and the hydrogen higher than expected.

Photo/thermal Degradation. Although transmission or ATR IR spectra gave no indication of a photo- or thermally-induced alteration in the POP microstructure, the uv-irradiated or heated films showed a definite darkening or blackening. As may be seen from Table II, the rates for photoinduced blackening in etched and

TABLE II
PHOTOINDUCED BLACKENING IN POP FILM

Time of irradiation, hr	ΔA (at 600 nm)	
	Unetched	Etched
88	0.028	0.024
114	0.035	0.035
138	0.040	0.038
166	0.041	0.040
319	0.089	0.082
446	0.106	0.102
560	0.120	0.118

unetched POP films are virtually the same. The increase in ΔA in either case is not quite linear with time of irradiation, the kinetic plot (not shown) being slightly concave downward. Since the absorption spectra of the unetched (7.5 μm) and etched (2.5 μm) films, prior to irradiation, were opaque below 410 and 350 nm, respectively, any photoinduced effects in these films (due to uv light at $\lambda < 350$ nm) must be confined to the surface or 'skin.' This explains why the photoinduced blackening occurred with the same rates in both etched and unetched films, despite their different thicknesses.

Data for the thermally induced blackening in plasma-etched POP film (∿3.8 μm thickness) are shown in Figure 1. Although these data cover the range 459-500°C, the thermal blackening was observed as low as 300°C. Comparable zero-order kinetic plots were obtained for the unetched film (∿7.5 μm). The slopes of the kinetic plots for both etched and unetched films were used to construct the Arrhenius plots given in Figure 2, from which a common activation energy of 61 ± 5 kcal/mole was derived for thermal blackening in the two sets of films. That the Arrhenius plot for unetched films lies at higher values of the ordinate than that for etched films is a reflection of the difference in thickness; since thermal

In Plasma Polymerization; Shen, M., et al.;
ACS Symposium Series; American Chemical Society: Washington, DC, 1979.

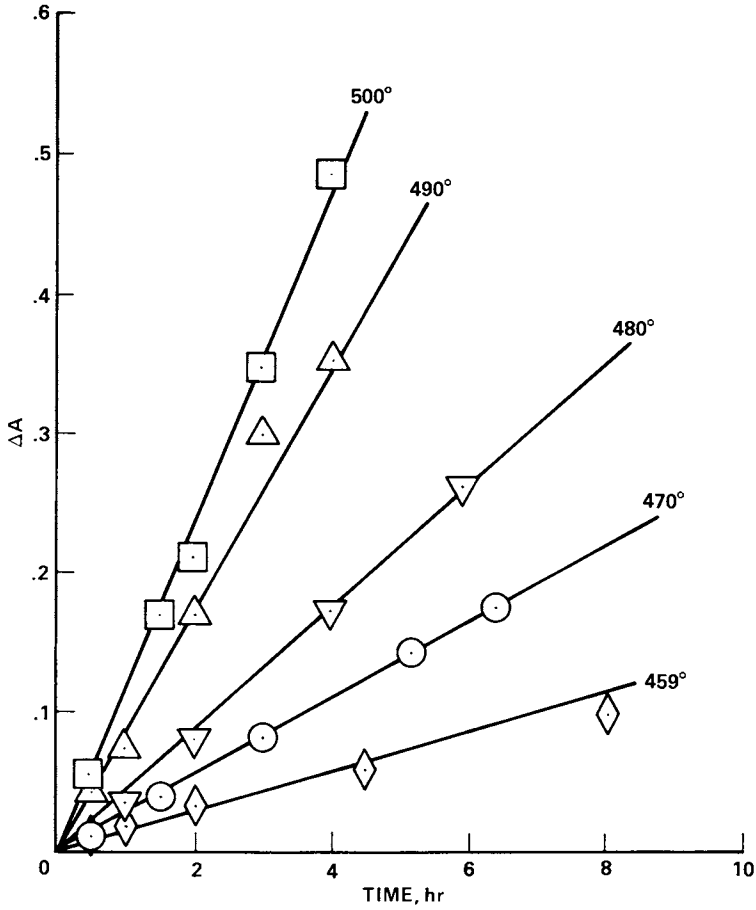

Figure 1. Kinetic plots for thermally induced blackening (increase in absorbance at 600 nm) in 3.8-μm POP film

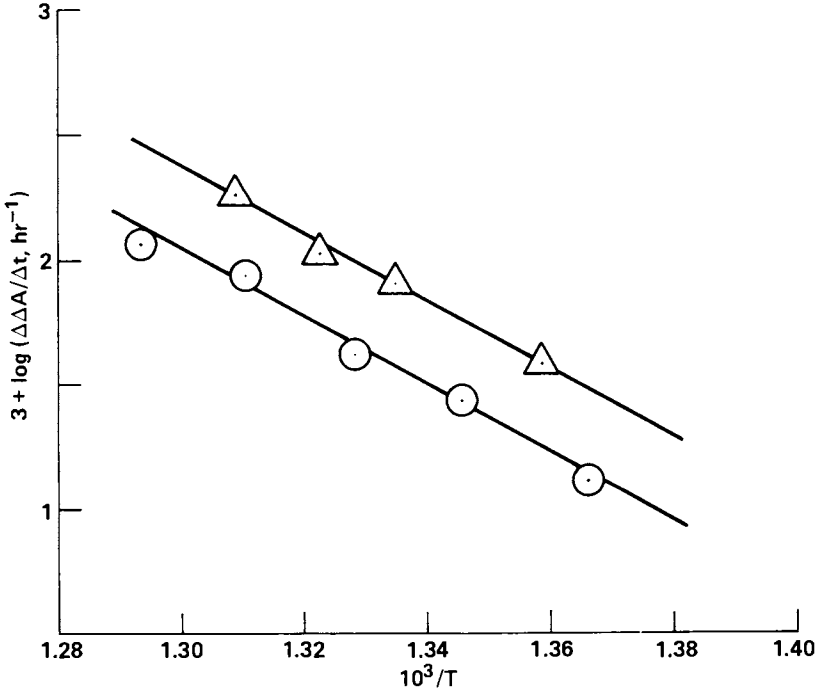

Figure 2. Arrhenius plots for thermally induced blackening in etched (~ 3.8 μm, ○) and unetched (~ 7.5 μm, △) POP films

In Plasma Polymerization; Shen, M., et al.;
ACS Symposium Series; American Chemical Society: Washington, DC, 1979.

blackening, unlike photoblackening, occurs throughout the film and not just at the surface, the observed change in ΔA, for a given time of heating, would be greater the thicker the film. Thus, for the films in question, $\log[(\Delta\Delta A)_{unetched}/(\Delta\Delta A)_{etched}] \cong \log(7.5/3.8)$ or ~ 0.30, which is close to the constant separation of about 0.33 between the Arrhenius plots.

ESR Results. ESR spectra were observed in both etched and unetched samples of POP film. Within experimental error, these samples had the same concentration of unpaired spins ($\sim 2 \times 10^{16}$ spins/g). When samples were heated below 200°C for $\sim$1 hr, the ESR signal decreased to a limiting intensity of one-third its initial value. The rate of decay of the spins or free radicals was proportional to the square of the spin intensity, as might be expected for bimolecular removal of free radicals.

When samples of unetched film were heated under vacuum above 250°C, additional unpaired spins were produced. Figure 3 shows kinetic plots for the thermally induced increase in spin concentration at four different temperatures. The ordinate is the relative ESR signal intensity, N_t/N_o, where the subscripts refer to the film before (o) and after heating for time t. After an initial rapid increase in signal intensity, the rate levels off to a constant value at each temperature. The slopes of the straight-line portions of the kinetic plots were used to obtain the Arrhenius plot shown in Figure 4, from which an activation energy of 68 ± 16 kcal/mole was calculated for the thermal production of unpaired spins.

Exposure of POP film to uv radiation under vacuum for $\sim$200–600 hr caused the ESR signal intensity to increase about 2–4 times its initial value. Because of time limitations, no effort was made to go beyond this qualitative observation of photoinduced production of unpaired spins.

ESCA Results. In contrast to the ATR spectra, ESCA spectra (of the topmost layer, <100-Å deep) of several etched and unetched POP films revealed some alteration in surface composition and structure as a result of thinning. As indicated in Figure 5, there are definite changes in relative intensities of the C_{1s} and O_{1s} peaks but not the N_{1s} peak, negligible shifts in peak positions (or binding energies), and very minor increases in line widths. ESCA data for surface compositional changes due to etching are given in Table III along with data for the effect of heat on the etched and unetched films. Assignments for the various ESCA peaks were based on the known composition and structure of POP and on literature values for core binding energies of the pertinent elements in similar functional groups (10,11,12,13).

As may be seen from Table III, etching of POP results in an increase in surface concentration of carbon atoms attached to oxygen atoms, at the expense of carbons not attached to oxygen, as well as increase in carbonyl oxygen. This suggests that the dominant chemical reaction at the surface, due to plasma etching, is

In Plasma Polymerization; Shen, M., et al.;
ACS Symposium Series; American Chemical Society: Washington, DC, 1979.

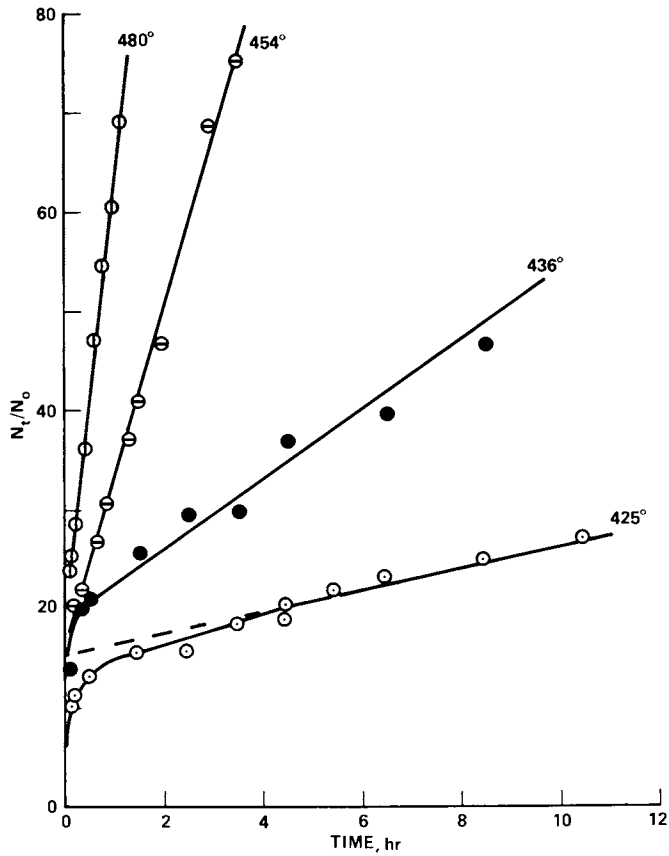

Figure 3. Kinetic plots for thermally induced growth of ESR signal in POP film

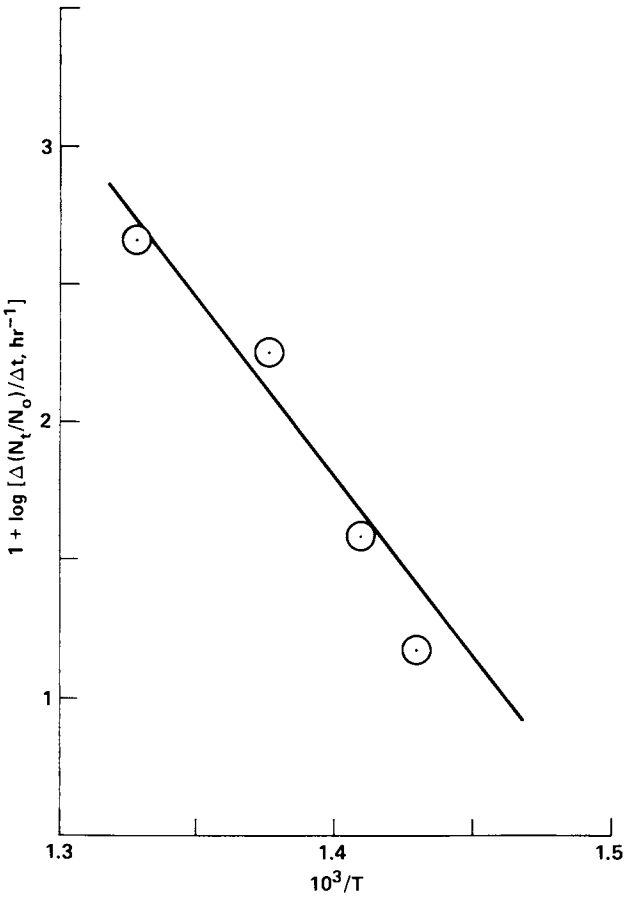

Figure 4. Arrhenius plot for thermally induced growth of unpaired spins in POP film

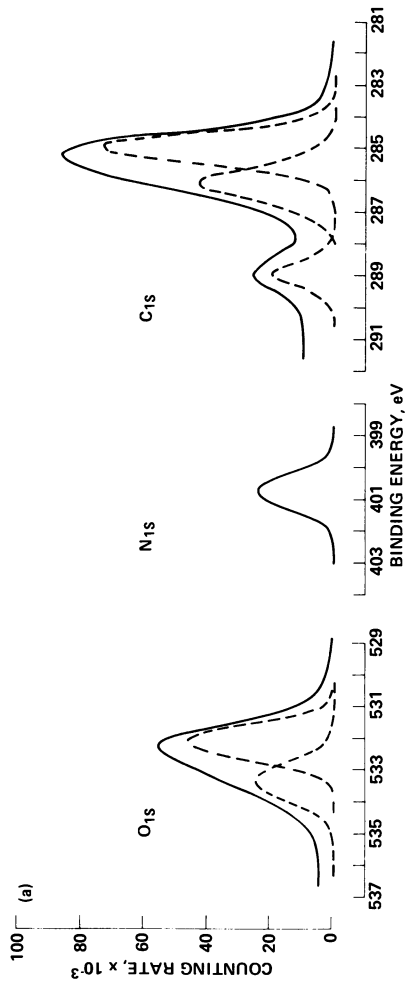

Figure 5. ESCA spectar of POP film: (a) unetched; (b) oxygen plasma-etched. Solid lines are measured peaks; dashed lines represent deconvoluted peaks.

TABLE III
SURFACE COMPOSITION OF PLASMA-ETCHED AND UNETCHED POP FILMS BEFORE AND AFTER HEAT TREATMENT

Element and peaks, eV		Atom percent, unetched*		Atom percent, plasma-etched		Assignments
		Before	After heating	Before	After heating	
C_{1s}	285.0	43.5	44.8	27.4	50.8	$=\underset{\sim}{C}-CO-$; $-\underset{\sim}{C}H=$
	286.1	23.9	24.8	28.4	25.3	$-\underset{\sim}{C}-O-\underset{\sim}{C}-$; $\underset{\sim}{C}-N-CO-$; $(\underset{\sim}{C}-OH)$
	288.9	8.6	8.0	13.7	5.4	$-\underset{\sim}{C}O-$
		76.0	77.6	69.5	81.5	
O_{1s}	532.1	12.2	12.3	17.4	9.5	$\underset{\sim}{O}=C$
	533.4	5.4	3.6	6.6	3.8	$-\underset{\sim}{C}-\underset{\sim}{O}-\underset{\sim}{C}-$; $(\underset{\sim}{C}-\underset{\sim}{O}H)$
		17.6	15.9	24.0	13.3	
N_{1s}	(399-400)	---	2.2	---	0.9	$(-\underset{\sim}{N}H_2)$
	400.7	6.4	4.3	6.6	4.3	$-CO-\underset{\sim}{N}-CO-$
		6.4	6.5	6.6	5.2	

*Atom percent of unetched film by elemental analysis: C, 75.3; O, 17.7; N, 7.0.

oxidation of benzene ring carbon atoms to carbonyls, accompanied by possible formation of hydroxyl groups.

Only minor changes in surface composition occurred in an unetched film when heated in vacuum at 476°C for 7 hr (Table III). The small decrease in oxygen concentration might have been due to desorption of moisture while the new nitrogen functionality might have resulted from cleavage and hydrogenation of the $-\underset{\sim}{N}-CO-$ linkages. On the other hand, major changes were observed in surface composition of the plasma-etched POP film when similarly heated. The latter changes, comprising increased carbon concentration, decreased oxygen concentration and redistribution of the different C_{1s} peaks, were probably due to a thermally induced

In Plasma Polymerization; Shen, M., et al.;
ACS Symposium Series; American Chemical Society: Washington, DC, 1979.

decarbonylation of the etched surface which was richer in carbonyls than the unetched film.

Discussion

Mechanism of Plasma Etching. Apart from the ESCA data, the results presented in this paper support the view that oxygen plasma etching causes no significant chemical alteration in POP film. This view is in line with that of Hansen and co-workers (7) concerning the effect of atomic oxygen (produced by an RF discharge) on a number of polymers, including a polyimide. As we noted, the transmission and ATR IR spectra of the films, before and after thinning, were identical; also, the etched and unetched films had the same rates of photoinduced blackening and the same activation energy for thermal blackening, while their ESR spectra were alike and had the same concentration of unpaired spins. The analysis of gaseous products formed in the etching process, while not yielding an exact accounting of the elemental composition of the polymer removed in the thinning process, suggests that etching involves the complete decomposition of the POP film at the retreating surface, without the build-up of a significant residue or debris layer on the etched film. On the other hand, data from ESCA analysis, which penetrates <100 Å into the film while ATR penetrates 8-10,000 Å, indicate that the topmost layer or 'skin' of the etched film has a higher oxygen content than does the underlying polymer. However, once the etching has begun, the new and retreating 'skin' appears to have an essentially unchanging oxidized structure throughout the thinning. This implies that ESCA detects at the topmost layer a partially oxidized and degraded polyimide which is a more or less steady intermediate in the chemistry leading to polymer decomposition and removal. Yet the photo/thermal degradation data argue that such an oxidized layer is not chemically significant, and in any case the bulk polymer is unaffected by the thinning.

Photo/thermal Degradation. Apparently, the only prior paper concerned with effects of uv radiation on POP film in vacuum was that of Anagnostou (14). It was reported in that paper that a Du Pont H-film (≡ Kapton) showed no IR changes and only slight changes in the visible absorption spectrum after extensive irradiation. The present work thus agrees with that of Anagnostou regarding IR spectra, but differs from that work in showing a strong photoinduced blackening effect. This effect occurred at the same rates in the plasma-etched and unetched films, implying that it is intrinsic to the aromatic polyimide structure and not due to some impurity layer on the surface of the unetched POP. That the photoblackening is probably the result of some chemical breakdown and not just some molecular rearrangement is indicated by the formation of some CO_2 and CO ($\sim$2.0:1.0) as photolysis products. The amounts of these gases, however, were too small to have an effect on the IR spectra of the irradiated POP film.

In Plasma Polymerization; Shen, M., et al.;
ACS Symposium Series; American Chemical Society: Washington, DC, 1979.

A number of papers have dealt with the thermal degradation of POP, and these have been surveyed by Sroog (4). Here we may note that isothermal weight loss in an inert atmosphere becomes important at temperatures >400°C, although thermogravimetric analysis (with temperature programming at 3°C/min) indicates that POP is stable up to 500°C in the same environment. The activation energy for thermal degradation of POP under vacuum or inert atmosphere has been reported to be ∿73-77 kcal/mole from pyrolysis studies (15,16). Gay and Berr (17) found CO and CO_2 to be the major products in the pyrolysis of POP in an inert atmosphere and reported an activation energy of 69 kcal/mole for CO evolution over the entire range of 400-600°C, and activation energies of 47.9 and 69 kcal/mole for CO_2 evolution at the low temperature and high temperature ends, respectively. The activation energies reported in the present study for thermally induced blackening and production of unpaired spins in POP heated in vacuum, namely, 61 ± 5 and 68 ± 16 kcal/mole, respectively, thus agree quite well with relevant data in the literature. The blackening, obtained by uv irradiation as well as by heating, is associated with formation of unpaired spins, presumably due to free radicals resulting from processes involved in the photo- and thermally induced evolution of CO_2 and CO. In this connection, we obtained in a thermal degradation experiment at 390°C a CO_2/CO ratio of ∿10:1 which compares with a value of ∿2.6:1 extrapolated from the data of Gay and Berr (13) for that particular temperature. The latter workers proposed that an equilibrium exists between n-imide and isoimide structures:

and that these structures pyrolyze to yield CO and CO_2, respectively. The high activation energies noted above are compatible with C-C or C-N rupture required to form these gaseous products.

Since the thermal blackening has the same activation energy for the etched and unetched POP films (∿61 kcal/mole), with rates which are proportional to film thickness, the surface composition of the films cannot be a factor in that process. ESCA analysis showed the etched films to undergo major changes, and the unetched films only minor changes, in surface composition when these films were heated in vacuum. Those changes (increases in carbon concentration, decreases in oxygen concentration and partial replacement of one nitrogen functionality by another) were, of course, in the topmost layer (<100-Å thick), but they evidently had no effect on the thermal blackening. On the other hand, these changes in carbon and oxygen concentrations indicated by ESCA are qualitatively what one would expect for thermal evolution of CO_2, i.e., the loss of 2 oxygen atoms per carbon atom has the net result of decreasing the

In Plasma Polymerization; Shen, M., et al.;
ACS Symposium Series; American Chemical Society: Washington, DC, 1979.

overall atom percent of oxygen in the film while increasing that of carbon. Further work is needed to understand better the surface nature of the etched POP films and the significance of their ESCA spectra.

To summarize, POP film can be uniformly thinned by oxygen plasma etching without significant microstructural change. Only the topmost layer of the film is chemically altered by the etching and shows evidence for partial oxidation. Both the etched and unetched films exhibit blackening (and increased concentration of unpaired spins) on exposure to uv radiation or heat in vacuum, the photoblackening being a surface effect and the thermal blackening a bulk effect. The activation energies for the thermally induced blackening and production of unpaired spins (∿61 and 68 kcal/mole) in etched or unetched film are compatible with literature data for the vacuum pyrolysis of POP or Kapton.

Acknowledgment

The experimental assistance of Mr. Mark L. Rosenberg in the photo/thermal degradation work is gratefully acknowledged.

Abstract

A study was made of the oxygen plasma etching (thinning) of the title film (Kapton) and of the effects of ultraviolet radiation and heat on the etched and unetched films in vacuum. Infrared and photo/thermal degradation indicated no significant microstructural changes in the bulk or surface of the title film as a result of oxygen plasma etching, although ESCA data suggested that the topmost layer of the etched film was partially oxidized. The etched and unetched films exhibited photo- and thermally induced darkening (blackening) but no changes in transmission infrared or ATR spectra. The photoblackening, confined to the surface, had the same rate in both sets of films while the thermal blackening, being dependent on thickness, was faster in the thicker unetched films. The thermal blackening had the same activation energy of ∿61 ± 5 kcal/mole for etched and unetched films in the range 459-500°C. Ultraviolet irradiation or heating of the title film in vacuum produced increased concentrations of unpaired spins. The activation energy for the thermally induced enhancement of ESR signal was ∿68 ± 16 kcal/mole. The blackening and growth in ESR signal are attributed to free radicals formed in reactions associated with the photo- and thermally induced evolution of CO_2 and CO from the title film.

Literature Cited

1. Wright, J., and Warmke, J., "Solar Sail Mission Application," Paper 76-808, AIAA/AAS Astrodynamics Conference, August 1976.

2. Friedman, L., Carroll, W., Goldstein, R., Jacobson, R., Kievit, J., Landel, R., Layman, W., Marsh, E., Ploszaj, R., Rowe, W., Ruff, W., Stevens, J., Stimpson, L., Trubert, M., Varsi, G., Wright, J., and MacNeal, R., AIAA 16th Aerospace Sciences Meeting, January 1978.

3. Sroog, C. E., Endrey, A., Abramo, S. V., Berr, C. E., Edwards, W. M., and Olivier, K. L., J. Polymer Sci., Part A, (1965), 3, 1373.

4. Sroog, C. E., J. Polymer Sci., Macromolecular Rev., (1976), 11, 161.

5. "Kapton" Polyimide Film. Physical-Thermal Properties, Bulletin H-2; "Kapton" Polyimide Film — Type H. Summary of Properties, Bulletin H-1D. E. I. Du Pont de Nemours & Co., Los Angeles, CA 90022.

6. Mijovic, J. S., and Koutsky, J. A., Polym. Plast. Technol. Eng., (1977), 9, 139.

7. Hansen, R. H., Pascale, J. V., de Benedictis, T., and Rentzepis, P. M., J. Polymer Sci., Part A, (1965), 3, 2205.

8. Wydeven, T., and Kubacki, R., Appl. Opt., (1976), 15, 132.

9. Lerner, N. R., J. Polymer Sci., Polym. Chem. Ed., (1974), 12, 2477.

10. Clark, D. T., in "Structural Studies of Macromolecules by Spectroscopic Methods," K. J. Ivin, Ed., Wiley, New York, 1976.

11. Gehus, U., et al., Physica Scripto, (1970), 2, 70.

12. Yasuda, H., Marsch, H. C., Brandt, E. S., and Reilley, C. N., J. Polym. Sci., Polym. Chem. Ed., (1977), 15, 991.

13. Siegbahn, K., et al., "ESCA Applied to Free Molecules," American Elsevier Publishing Co., New York, 1969.

14. Anagnostou, E., "Effect of Ultraviolet Irradiation on Selected Plastic Films in Vacuum," (1965), NASA TM X-1124.

15. Bruck, S. D., Polymer, (1964), 5, 435; (1965), 6, 49.

16. Clark, R. P., Thermochim. Acta, (1973), 6, 473.

17. Gay, F. P., and Berr, C. E., J. Polymer Sci., Part A-1, (1968), 6, 1935.

RECEIVED March 29, 1979.

Plasma Polymerization Coating of DT-Filled Glass Shells for Laser Fusion Targets

WAYNE L. JOHNSON, STEPHAN A. LETTS, CHARLES W. HATCHER, and LYMAN E. LORENSEN
University of California, Lawrence Livermore Laboratory, Livermore, CA 94550

CHARLES D. HENDRICKS
University of California, Lawrence Livermore Laboratory, Livermore, CA 94550, and University of Illinois, Urbana, IL 61801

As a part of our national program to fulfill our growing energy needs, considerable effort is being made to achieve controlled fusion by using laser beams to heat and compress deuterium/tritium-containing (DT) targets. One of the requirements for the development of laser fusion as a viable energy source is the ability to produce spherical targets for the laser-driven implosion. One practical target design consists of a multilayer composite shell. A thin inner glass shell contains the pressurized DT gas. An outer plastic coating absorbs the laser energy and ablatively compresses the glass shell and the DT fuel. The outer plastic coating material must satisfy a number of special requirements. It must have a density near that of the glass shell and be of low atomic number. It should be smooth and uniform in thickness to prevent Rayleigh-Taylor instabilities from disrupting the spherical symmetry of the fuel during compression.

Many technologies exist for the deposition of thin films (1,2). Usually such coatings are applied by evaporative deposition, chemical vapor deposition, or sputtering. However, exposure of DT-filled glass microspheres to most of these processes would cause excessive heating of the glass shell allowing the DT gas to escape.

The plasma polymerization process appeared to have considerable promise for coating glass microspheres. Plasma polymerized coatings have been found by previous investigators (3,4) to be homogenous and pinhole free. A wide range of monomers, including saturated as well as unsaturated hydrocarbons (5), fluorocarbons (6,7), and silanes (8), have been plasma polymerized. This provides the flexibility for the process to be adapted to future coating requirements. In addition, the plasma polymerization process would not be expected to heat the glass microspheres above 100-200 °C which would insure preservation of the DT fill.

0-8412-0510-8/79/47-108-315$05.00/0

In view of these potential advantages, the process of plasma polymerization was adapted to coat microsphere targets. A special device for exposing the microspheres to obtain a uniform coating was devised. A major problem which was solved was the elimination of rough surfaces characteristic of these coatings.

Experimental

Vibrating Pan Microsphere Holder. The uniform coating of glass microspheres with diameters in the 100-μm range offers a unique challenge to plasma polymerization technology. To ensure that each sphere received a uniform coating during exposure in the active plasma field, a piezoelectrically-driven vibrating pan was developed. This was constructed by fastening a thin stainless steel plate, which had been hydroformed into the shape of a saucer, to a piezoelectric crystal. The crystal was driven with an audio signal which was both frequency and amplitude modulated.

Paralled-Plate Coater. Parallel-plate discharge devices have been extensively described in literature (9). The parallel-plate device used in this investigation (Figure 1) had a 5-cm diameter perforated aluminum upper electrode held inside an inverted glass funnel. The electrode was held 3 cm above the vibrating pan which served as the lower electrode. This unit was placed in a large glass jar which served as the vacuum chamber. The upper electrode was driven at either 10 kHz or 13.56 MHz. The monomer was admitted to the plasma region through the inverted funnel to diffuse the monomer gas uniformly through the plasma region.

Helical Resonator. Inductively-coupled discharge sources have been reported by other authors (9,10,11). The helical resonator (Figure 2) is a particular type of tuned resonant cavity which inductively couples energy to the plasma, eliminating electrodes and the problems associated with them. The helical resonator is unusual in its ability to produce low-pressure discharges in gases because the magnetic field lines somewhat inhibit the flow of charged species to the walls. The plasma is confined within an interchangeable quartz reaction tube through which the monomer gas flows. Changing the reactor tube size provides a means for altering the electron temperature which affects plasma composition. An RF shield which varies the length of the discharge region controls the amount of time the flowing monomer is subjected to the plasma environment.

Microwave Discharge. A third system for producing a plasma consists of a resonant 2.45-GHz microwave cavity surrounding a 10-mm-diameter quartz tube (Figure 3). Apparatus of this type

In Plasma Polymerization; Shen, M., et al.;
ACS Symposium Series; American Chemical Society: Washington, DC, 1979.

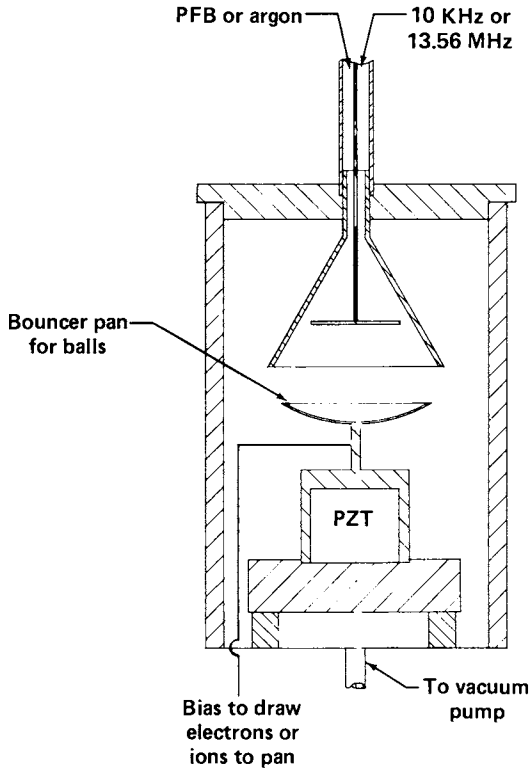

Figure 1. Schematic of the parallel-plate plasma coater showing the location of the vibrating pan used to agitate the glass microspheres.

In Plasma Polymerization; Shen, M., et al.;
ACS Symposium Series; American Chemical Society: Washington, DC, 1979.

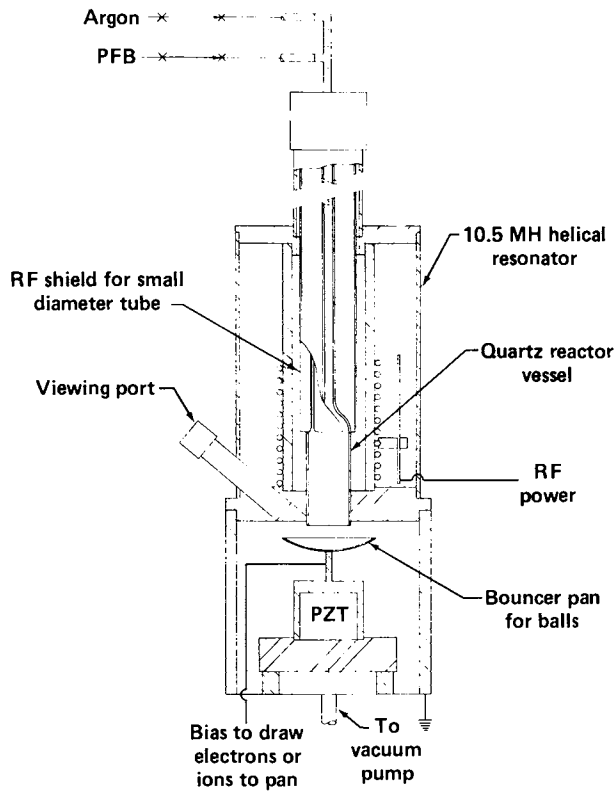

Figure 2. The helical resonator plasma coater

In Plasma Polymerization; Shen, M., et al.;
ACS Symposium Series; American Chemical Society: Washington, DC, 1979.

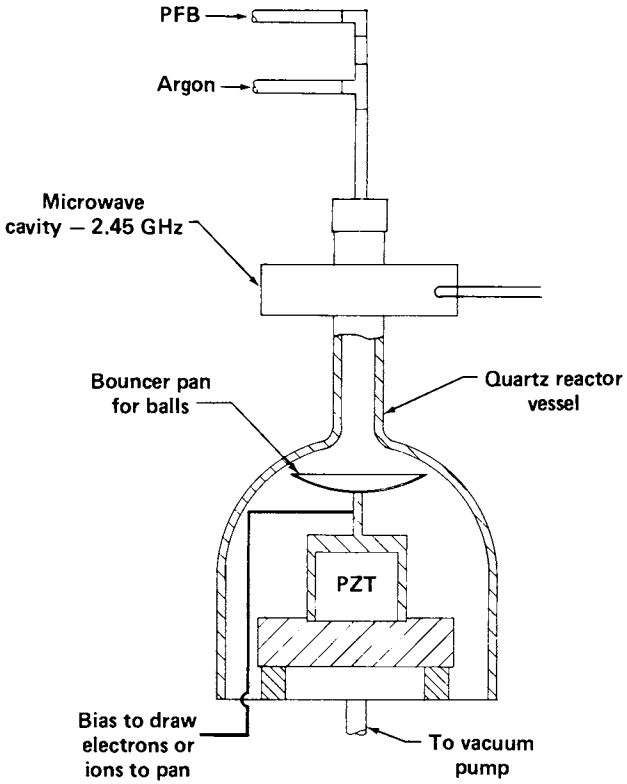

Figure 3. The microwave discharge coater

has been used both for inorganic synthesis (13) and in plasma polymerization (14).

The monomer in the tube is activated by an electrodeless microwave discharge and then flows down the tube to the vibrating pan. The exposure of the monomer to the plasma in this type of reactor can be very brief and intense, and it is controlled by varying its pressure and flow rate through the quartz tube.

Process Control Monitors. Deposition kinetics were investigated by accurately measuring RF power, monomer pressure, and monomer flow. The actual RF power dissipated in the gas discharge was determined by taking the difference between the net power delivered to the gas discharge and the net power delivered to the system under vacuum. Pressure was measured to a precision of 1 millitorr with a capacitance manometer. Gas flow was reproduced to a precision of 0.1 SCCM with a Hastings Mass Flow Meter.

Results and Discussion

The hollow glass microspheres exposed to the plasma while held in the vibrating pan system described earlier were found by interferometry (15) (white light) to be uniformly coated by all discharge systems. However, the critical problem was achieving a high degree of surface smoothness. Most previous investigators have neglected surface smoothness. Those who have looked at plasma polymerized coatings have reported rough surfaces (11,16,17) which were attributed to gas-phase polymerization. To finally achieve the smooth surfaces required, we used several techniques including discharge pulsing, ion bombardment, and periodic addition of chain transfer agents in addition to varying the usual parameters of pressure, gas flow, and power.

Parallel Plate. The parallel plate discharge apparatus used in the initial coating experiments gave rise to several problems. First, the electrodes became coated; arcing on the electrodes could then dislodge polymer particles which could stick to nearby glass shells. Secondly, the power per unit volume is almost a constant in a parallel plate discharge regardless of power input; increased power mostly results in increased plasma volume. This restriction limits the coating rate on shells to 1/2 μm/hr at a pressure of 70 millitorr, the optimum condition for coating smoothness.

The coatings which were obtained by use of our parallel-plate coater had the desired thickness (20 μm), chemical composition ($CF_{1.3}$), and density (1.85 g/cm^3); however, the surface smoothness did not meet specifications for our application. The process conditions (power, pressure, and flow rate) were then adjusted to optimize the coating smoothness. Figure 4 shows the best surface finish produced by adjustment of the process

In Plasma Polymerization; Shen, M., et al.;
ACS Symposium Series; American Chemical Society: Washington, DC, 1979.

conditions. The surface roughness consisted of both large (20 μm) and small (0.5 μm) defects agglomerated into a highly irregular surface. Therefore, even after considerable fine tuning of the process conditions, surfaces were still far from the quality desired.

Helical Resonator Coating. Some of the disadvantages of the parallel-plate apparatus were overcome by developing a helical resonator plasma source. The helical resonator proved to be a system for which process variables could be accurately measured and reproduced. The intense, uniform discharge of the helical resonator was confined within a fixed-geometry chamber. Thus, reproducing chamber pressure, gas flow rate, and the power dissipated in the discharge consistently provided the same discharge conditions. The improved control on the helical resonator allowed the coating rate on shells to be increased to 2 μm/hr at optimum surface finish conditions. However, these surfaces still were too rough to be used for laser fusion targets.

Microwave Discharge Coating. Coatings deposited by use of the microwave discharge ranged from the typical brown-colored film (produced by the parallel plate and helical resonator systems) to a porous, white coating. Production of the white fibrous coating was critically dependent on pressure, flow rate, and power adjustments. Figure 5 is an electron micrograph of a coating produced in the microwave cavity. This unique white, fibrous coating is characterized by its submicron cell size, low density (0.1-0.2 g/cm^3, one-tenth of bulk density) and extreme uniformity. The fiber coating was produced from both perfluoro-2-butene and tetrafluoroethylene.

The coating variation offered by the microwave system may be a result of the short residence time of the gas in the discharge. Investigations with the microwave discharge have only recently been started; however, the unusual character of the product makes this system very promising for production of new materials.

Surface Finish Improvements. In order to solve the surface roughness problems, mechanisms for their growth were hypothesized: 1) Existing irregularities may nucleate growth resembling cones which cause the regular defect pattern on the surface. 2) Polymer particles grown in the gas phase during processing may settle onto the coated substrate. These particles then act as irregularities which also produce cone growth. The suspect causes of the defects suggested the following possible methods for improving the surface: turning the discharge off periodically, pulsing a chain transfer gas such as chloroform or hexafluoroethane into the vacuum system, and ion bombardment.

In Plasma Polymerization; Shen, M., et al.;
ACS Symposium Series; American Chemical Society: Washington, DC, 1979.

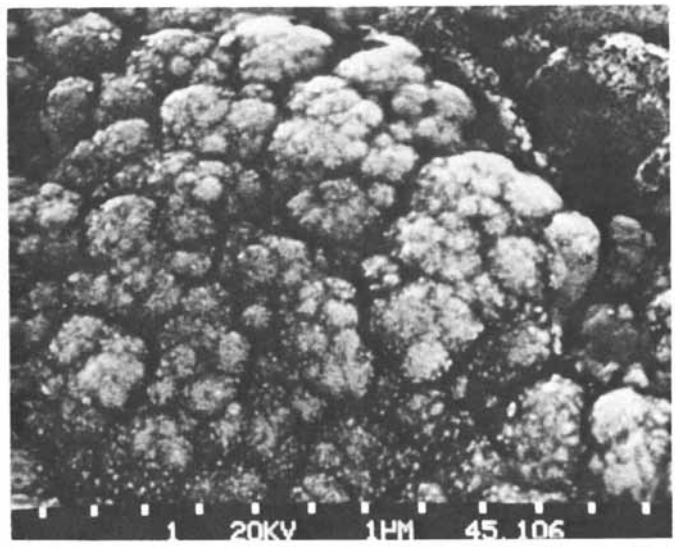

Figure 4. A SEM micrograph of the surface of a glass microsphere coated with 20 μm of fluorocarbon

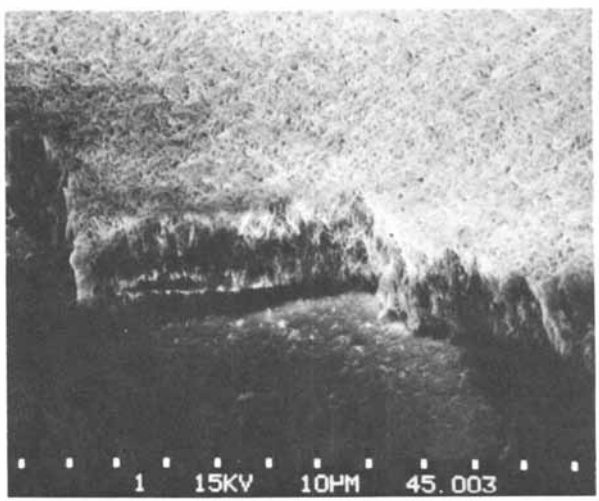

Figure 5. A SEM micrograph of a fractured film deposited in the microwave discharge coater

In Plasma Polymerization; Shen, M., et al.;
ACS Symposium Series; American Chemical Society: Washington, DC, 1979.

Pulsed Discharge. To prevent the growth of spherical particles (4,16) in the gas-phase discharge region, the discharge was terminated for approximately 1 second in every 10 seconds. This allowed these particles to be swept out of the discharge region by removing the electrostatic fields suspending them. Although some improvement could be noted in the coating surface, a satisfactory product was not obtained.

Chain-Transfer Agent Pulsing. The effect of pulsing chloroform into the vacuum system for 5 seconds every 5 minutes is shown in Figure 6. The pressure pulse increased the pressure 100 millitorr in 5 seconds and then exponentially decayed with a half life of 20 seconds. Although still containing defects, the resulting surface is much smoother than could be achieved by fine-tuning process variables alone. Analysis of the film by x-ray fluorescence showed chlorine was present in the film. Chemical analysis gave a chemical formula of $CF_{0.7}Cl_{0.4}$. Although pulsing chloroform provided surface smoothing, the presence of chlorine was not desired.

Fluorocarbon chain transfer agents were substituted to use the chain-transfer concept and not contaminate the film with unwanted elements. The two gases used were tetrafluoromethane and hexafluoroethane. In a glow discharge a dominant decomposition pattern for tetrafluoromethane is for it to lose a fluorine atom and become a trifluoromethyl radical (18), an effective radical chain terminator. A better choice is hexafluoroethane which, in a glow discharge, breaks at the weak C-C bond to form two trifluoromethyl radicals (7). The effect of pulsing hexafluoroethane into the vacuum system is shown in Figure 7. The surface has an ambient roughness of less than 0.5 μm and the pure fluorocarbon composition of the material was maintained.

Ion Bombardment. A third method which improved the surface finish was ion bombardment of the coating surface during the deposition process. This was accomplished by negatively pulse biasing the vibrating pan to approximately 400 volts for 50 microseconds every 2 milliseconds. This produced a 5-10 milliamp current of ions. The effect of the ion flux is to both increase the coating rate and improve surface finish.

The surface finish produced by the combination of ion bombardment and discharge pulsing has a roughness barely observable by scanning electron microscopy. Over the entire surface of the ball the roughness is no greater than 200 Å. Figure 8 shows the high quality of these surfaces.

The Nature and Growth Mechanism of Film Imperfections

The ability to produce ultrasmooth coatings has provided a unique opportunity for observing other surface growth anomalies.

In Plasma Polymerization; Shen, M., et al.;
ACS Symposium Series; American Chemical Society: Washington, DC, 1979.

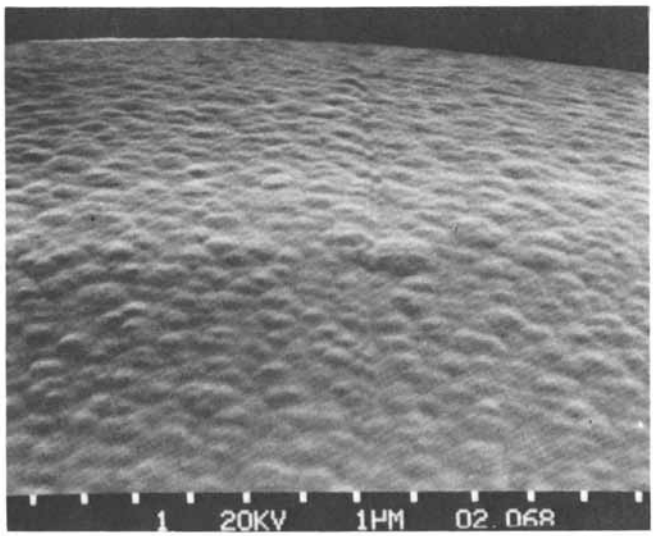

Figure 6. A SEM micrograph of the surface of a glass microsphere coated to a thickness of 20 μm using chloroform pulsing

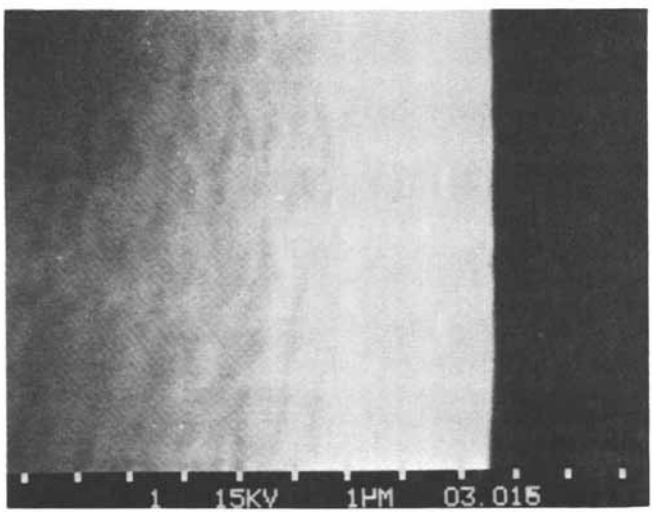

Figure 7. A SEM micrograph of the surface of a glass microsphere coated to a thickness of 20 μm using hexafluorothane pulsing

In Plasma Polymerization; Shen, M., et al.;
ACS Symposium Series; American Chemical Society: Washington, DC, 1979.

In the course of coating, it was often found that otherwise extremely smooth coatings had two to five surface defects. Observation by SEM revealed that they were dome shaped. A study of the glass microsphere substrates showed that many of them, despite rigorous cleaning, also had two to five surface imperfections on the glass substrates. The implication was that any surface imperfection existing on the glass caused a defect in the coating. To check this hypothesis, two experiments were conducted. First, deposited films were fractured to look at a cross section of a defect (Figure 9). In the cross section, a dome shaped defect on the surface of a coating has a conical base with the point on the glass surface. An irregularity originally on the glass or introduced into the coating system during the early stages of coating may have served as the nucleus for the growth of the defect.

In a second experiment, a deliberate imperfection (a scratch) was introduced on a flat glass slide. A portion of the scratch was masked and the slide was then coated. The interface between the coated and masked scratched areas is shown in Figure 10. Where a sharp discontinuity occurs in the scratch, a conical structure is found in the film with a cylindrical top surface. This is the one-dimensional defect analog to the point defects found on glass shells. A line defect generates a cylindrical sector defect (see Figure 11), whereas a point defect generates a cone. Therefore, to achieve blemish-free coatings on glass microspheres or on flat glass slides, the original surface must be defect free.

Deposition Rate Characterization

Understanding the deposition kinetics is important to reproducibly achieve smooth, controlled-thickness coatings. Deposition rate and process-variable sensitivities are determined by accurately measuring RF power, monomer pressure, and monomer flows. Figure 12 illustrates the deposition rate versus power dissipated in the discharge for various flow rates at a pressure of 40 millitorrs. Increasing either flow rate or power produces a deposition rate increase. The plateau reached by the coating rate at high power input indicates deposition has reached a supply-limited condition, a behavior which has been observed by several other investigators (11,18,19). Production of smooth coatings requires operating at low flow (0.5 SCCM), a pressure of 70 millitorr, and low power (20 watts). This reduces gas phase polymerization and the resultant production of polymer particles which roughen the surface. The polymer film produced under these conditions is rigid (which prevents microspheres from adhering to each other) and it grows at a uniform rate allowing the deposition of extremely smooth coatings.

In Plasma Polymerization; Shen, M., et al.;
ACS Symposium Series; American Chemical Society: Washington, DC, 1979.

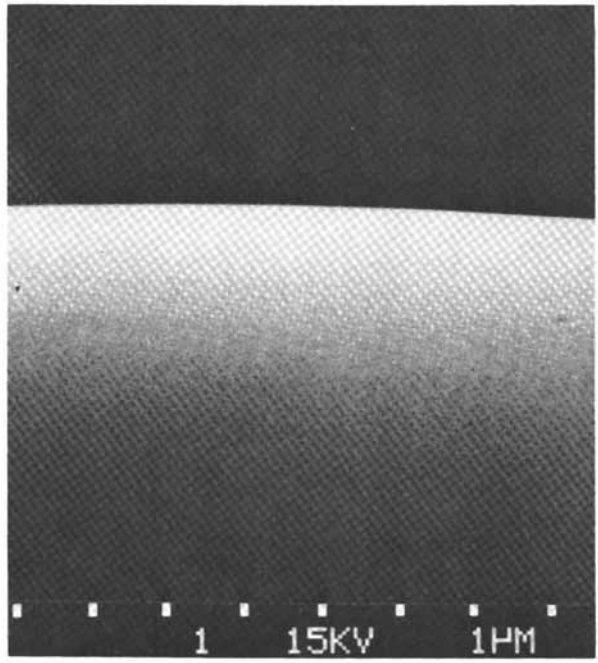

Figure 8. A SEM micrograph of a target-quality microsphere coated with 22 μm fluorocarbon polymer

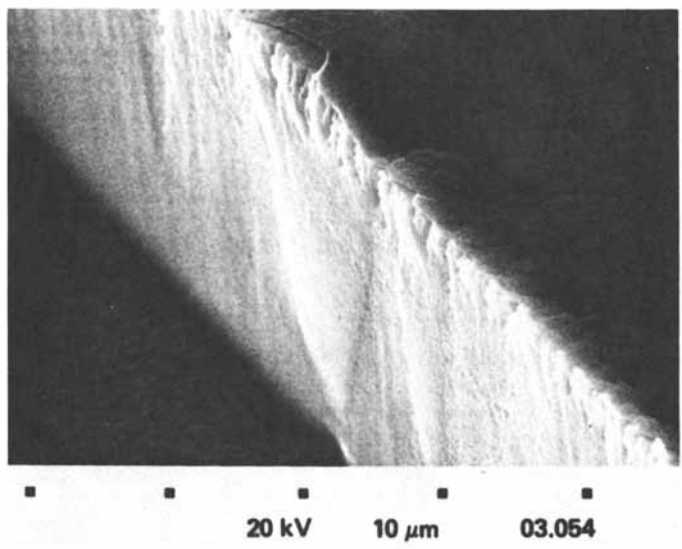

Figure 9. A cross section of a cone growing from a surface imperfection

In Plasma Polymerization; Shen, M., et al.;
ACS Symposium Series; American Chemical Society: Washington, DC, 1979.

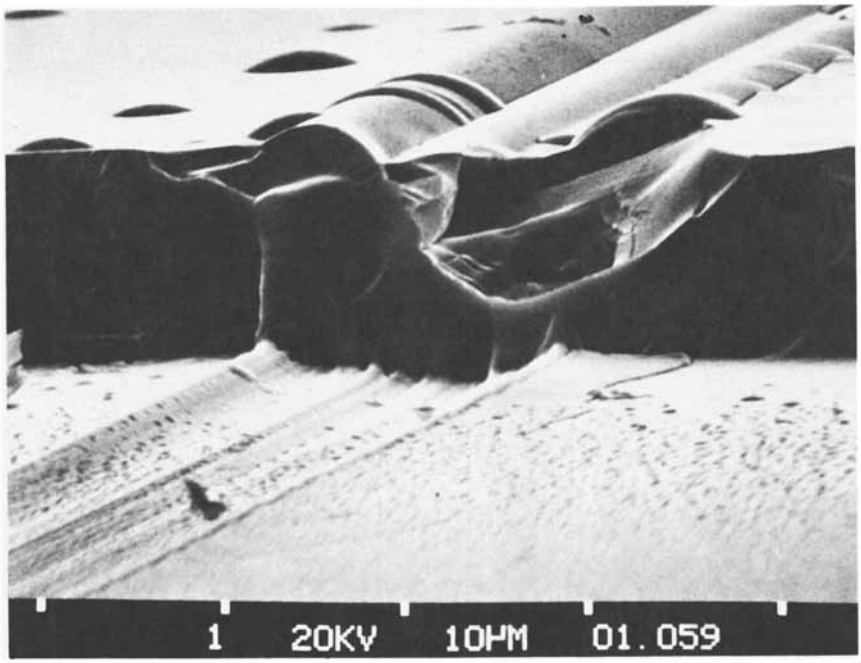

Figure 10. The interface between the masked and coated areas showing the scratch that produced the surface defect

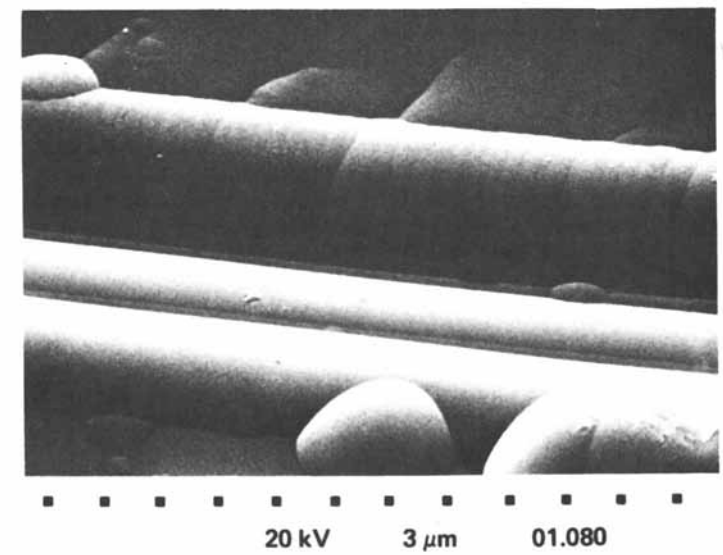

Figure 11. A cylindrical sector defect in a fluorocarbon film grown over a scratched glass surface

In Plasma Polymerization; Shen, M., et al.;
ACS Symposium Series; American Chemical Society: Washington, DC, 1979.

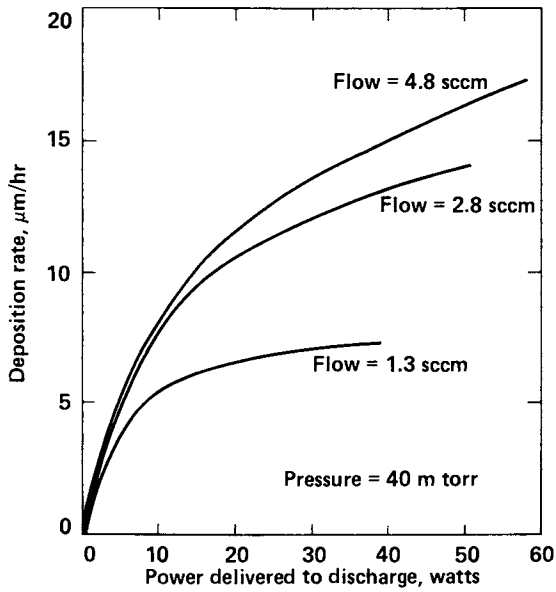

Figure 12. Deposition rate of plasma polymerized perfluoro-2-butene vs. power for a helical resonator at 10.17 MHz

Summary

Plasma polymerization has been adapted for coating hollow glass microsphere laser fusion targets. For this application, coatings must be concentric, smooth, and match the density of glass. Uniform coatings were achieved through continuous random exposure to the plasma by means of a vibrating pan. Coatings of perfluoro-2-butene were first deposited using a parallel plate apparatus which resulted in undesirably rough surface finishes. In our efforts to improve smoothness, a helical resonator discharge source was developed which provided a higher coating rate and an electrodeless, reproducible discharge with a fixed geometry. Use of a microwave discharge resulted in coatings with unusually low density. Coating rate was measured as a function of discharge power, pressure, and flow rate. Increased power and flow rate both produced higher coating rates. Coating rates as high as 15 μm/hr were measured at 50 watts power, 2.5 SCCM flow, and 200 millitorrs pressure.

Surface finish of the coatings was improved by pulsing the plasma, by ion bombardment, and by periodic injection of chain transfer gases. Coatings up to 20 μm thick can now be reliably prepared with defects less than 0.03 μm high. Imperfections on the glass substrate were shown to result in coating defects.

Literature Cited

1. Holland, L., "Vacuum Deposition of Thin Films," Chapman and Hall, London, 1970.
2. Chopra, K. L., "Thin Film Phenomena," McGraw-Hill, New York, 1969.
3. Linder, E. G., and Davis, A. P., J. Phys. Chem. (1931), 35, 3649.
4. Niinomi, M. Kobayashi, H., Bell, A. T., and Shen, M., J. Appl. Phys. (1973), 44, 4317.
5. Jesch, K, Bloor, J. E., and Kronick, P. L., J. Poly. Sci.: Part A-1 (1966), 4, 1487.
6. Wydeven, T., and Kubacki, R., Applied Optics (1976), 15, 132.
7. Yasuda, H., and Hsu, T. S., J. Poly. Sci. (1977), 15, 2411.
8. Gazicki, M., Wrobel, A. M., and Kryszewski, M., J. Appl. Poly. Sci. (1977), 21, 2013.
9. Hollahan, J. R., and Bell, A. T., Eds., "Techniques and Applications of Plasma Chemistry," Wiley, New York, 1974.
10. Harkins, W. D., and Gans, D. M., J. Amer. Chem. Soc. (1930), 52, 5165.
11. Thompson, L. F., and Mayhan, K. G., J. Appl. Poly. Sci. (1972), 16, 2291.
12. Yasuda, H., and Lamaze, C. E., J. Appl. Poly. Sci., (1971), 15, 2277.

In Plasma Polymerization; Shen, M., et al.;
ACS Symposium Series; American Chemical Society: Washington, DC, 1979.

13. Jolly, W. L., "Synthetic Inorganic Chemistry," Prentice-Hall, Inc., Englewood Cliffs, New Jersy, 1960.
14. Kirk, R. W., in "Techniques and Applications of Plasma Chemistry," Hollahan, J. R., and Bell, A. T., eds., Wiley, New York, 1974.
15. Weinstein, B. W., J. Appl. Phys. (1975), 46, 5305.
16. Kobayashi, H., Bell, A. T., and Shen, M., J. Appl. Poly. Sci. (1973), 17, 885.
17. Lowe, A. T., Fries, R. J., Inertial Confinement Fusion, Technical Digest, Optical Society of America, Washington, D.C., 1977.
18. Kobayashi, H., Shen, M., and Bell, A. T., Macromol. Sci. - Chem. (1974), 48, 373.
19. Tibbitt, J. M., Jensen, R., Bell, A. T., and Shen, M., Macromolecules (1977), 10, 647.

Work performed under the auspices of the U.S. Department of Energy by the Lawrence Livermore Laboratory under contract number W-7405-ENG-48.

RECEIVED March 29, 1979.

INDEX

In Plasma Polymerization; Shen, M., et al.;
ACS Symposium Series; American Chemical Society: Washington, DC, 1979.

In Plasma Polymerization; Shen, M., et al.;
ACS Symposium Series; American Chemical Society: Washington, DC, 1979.

In Plasma Polymerization; Shen, M., et al.;
ACS Symposium Series; American Chemical Society: Washington, DC, 1979.

In Plasma Polymerization; Shen, M., et al.;
ACS Symposium Series; American Chemical Society: Washington, DC, 1979.

In Plasma Polymerization; Shen, M., et al.;
ACS Symposium Series; American Chemical Society: Washington, DC, 1979.

In Plasma Polymerization; Shen, M., et al.;
ACS Symposium Series; American Chemical Society: Washington, DC, 1979.

In Plasma Polymerization; Shen, M., et al.;
ACS Symposium Series; American Chemical Society: Washington, DC, 1979.

N

O

In Plasma Polymerization; Shen, M., et al.;
ACS Symposium Series; American Chemical Society: Washington, DC, 1979.

In Plasma Polymerization; Shen, M., et al.;
ACS Symposium Series; American Chemical Society: Washington, DC, 1979.

In Plasma Polymerization; Shen, M., et al.;
ACS Symposium Series; American Chemical Society: Washington, DC, 1979.

In Plasma Polymerization; Shen, M., et al.;
ACS Symposium Series; American Chemical Society: Washington, DC, 1979.

Q

R

S

In Plasma Polymerization; Shen, M., et al.;
ACS Symposium Series; American Chemical Society: Washington, DC, 1979.

T

In Plasma Polymerization; Shen, M., et al.;
ACS Symposium Series; American Chemical Society: Washington, DC, 1979.

In Plasma Polymerization; Shen, M., et al.;
ACS Symposium Series; American Chemical Society: Washington, DC, 1979.